DEVELOPMENT OF RHODIUM(III)-CATALYZED ARYLATION AND CYCLOADDITION OF BENZOHYDROXAMIC ACIDS AND SEMICARBAZONES FOR REGIOSELECTIVE C-N AND C-C BOND FORMATION

LAM HON WAH

Ph.D

The Hong Kong Polytechnic University

2016

The Hong Kong Polytechnic University

Department of Applied Biology and Chemical Technology

Development of Rhodium(III)-Catalyzed Arylation and Cycloaddition of Benzohydroxamic Acids and Semicarbazones for Regioselective C-N and C-C Bond Formation

LAM Hon Wah

A thesis submitted in partial fulfillment

of the requirement for the degree of

Doctor of Philosophy

August 2015

CERTIFICATION OF ORIGINALITY

I hereby declare that this thesis is my own work and that, to the best of my knowledge and belief, it reproduces no material previously published or written, nor material that has been accepted for the award of any other degree or diploma, except where due acknowledgement has been made in the text.

LAM Hon Wah

ABSTRACT

Abstract of the thesis entitled

Development of Rhodium(III)-Catalyzed Arylation and Cycloaddition of Benzohydroxamic Acids and Semicarbazones for Regioselective C-N and C-C bond Formation

Submitted by LAM Hon Wah

for the degree of Doctor of Philosophy

at The Hong Kong Polytechnic University in 2015

Transition metal-catalyzed electrophilic amination with carbon-nucleophiles is a promising approach for carbon-nitrogen bond formation. In this research, we explored the rhodium(III)-catalyzed cross-coupling reactions of organoboronic acids and hydroxylamines derivatives. Furthermore, catalytic cycloaddition reactions of benzohydroxamic acids / semicarbazones with diazo compounds / alkynes were also accomplished.

The arylation of *N*-alkylhydroxylamines with arylboronic acids was first examined by treating *O*-benzoyl-*N*-isopropylhydroxylamine with

6-methoxy-2-naphthaleneboronic acid and [Cp*Rh(OAc)$_2$] (Cp* = pentamethylcyclopentadiene, OAc = acetate) (0.25 mol%) in MeOH at room temperature for 2 h, and the desired amine **7a** was obtained in 90% yield.

Likewise, *N*,*N*-dialkylhydroxylamines and benzohydroxamic acids are effective substrates for the C-N coupling reactions with the corresponding tertiary amines and amides being formed in 47 – 97% yields. Aliphatic cyclic and acyclic hydroxylamines containing benzyl and heterocyclic moieties were tolerated.

[Cp*Rh(Ph)Cl(PPh$_3$)] was prepared to examine the mechanism of the C-N coupling reaction. Upon reacting phenylrhodium(III) complex with *O*-benzoyl-*N*-cyclohexylhydroxylamine and **2a**, *N*-cyclohexylaniline (< 20%) and **7j** (80%) were obtained. This finding supports the involvement of the [Ar-Rh] complex as active species.

Inspired by our previous finding on the rhodium(III)-catalyzed arene C–H coupling reactions with diazomalonates, we envisioned that a transformation involving formal [4 + 1] cycloaddition of diazo compounds with *O*-acetyl benzohydroxamic acids should give oxisoindoles as products via reductive elimination of the σ-allylrhodacycle. Treating *O*-acetyl benzohydroxamic acid **3a** with diazomalonate and [Cp*Rh(OAc)$_2$] (5 mol%) in THF, oxisoindole **9a** was

produced in 89% yield. Substituents such as -OMe, -Me, -NO_2 and -CF_3 were tolerated and the corresponding oxisoindoles were formed in 76 – 93% yields. Diazo compounds having esters, phenylsulfone, cyano and phosphonate groups are good coupling partners, and their reactions with benzohydroxamic acids gave the corresponding oxisoindoles in up to 90% yields. Notably, alkyl diazoacetates with β-hydrogen atom were good partners for the cycloaddition reaction. The possible β-hydride elimination did not seem to compete effectively with the reductive elimination.

To ascertain that the reaction should go through chelation-assisted C–H/N–H deprotonation of *O*-acetyl benzohydroxamic acid, we reacted **3a** (0.12 mmol) with [Cp*Rh$(OAc)_2$] (0.1 mmol) in THF at 60 ^oC for 2 h under a N_2 atmosphere. A dinuclear arylrhodium(III)-amide complex was obtained and characterized by X-ray crystallography. This dinuclear arylrhodium(III) complex was catalytically inactive for the cycloaddition reaction. The observed inertness is attributed to the stability of the aza-rhodacyclic complex, which should be difficult to dissociate for diazo coordination.

Isoindoles are important scaffolds in materials science. We anticipated that isoindoles could be prepared by the formal [4 + 1] cycloaddition of *O*-carboxylates oximes with diazo compounds. However, this reaction was

unsuccessful in our initial trials due to relative instability of the N-O bond in the reaction conditions. We envisioned that the analogous N-N bond should be more stable, and yet it should serve as an isoelectronic replacement for the N-O bond. In this work, semicarbazones containing a *tert*-butyl carbazate moiety was examined for the rhodium(III)-catalyzed cycloaddition reaction with alkynes. The *tert*-butyl carbazate group should serve a leaving group to effect reductive elimination of the rhodacyclic intermediate. By treating semicarbazone **5a** with 1-phenyl-1-propyne (**6a**), $[Cp^*RhCl_2]_2$ (5 mol%), CsOAc (25 mol%) and HOAc (1.2 equiv) in MeOH at 120 ℃ for 16 h, the desired product isoquinolone **10a** was obtained in 93% yield. However, the Rh(III)-catalyzed cycloaddition reaction between semicabazone **5a** and diazomalonate (**4a**) is still under investigation.

PUBLICATIONS AND CONFERENCE

Publications

Lam, H.-W.; Lau, Y.-F.; Yu, W.-Y. "Rhodium(III)-Catalyzed Electrophilic Amination of Arylboronic Acids with *O*-Carboxyl Hydroxyamines/amides', manuscript in preparation.

Lam, H.-W.; Chan, C.-M.; Yu, W.-Y. "Rhodium(III)-Catalyzed Formal Oxidative [4 + 2] Cycloaddition of Benzosemicarbazones and Alkynes", manuscript in preparation.

Lam, H.-W.; Man, K.-Y.; Chan, W.-W.; Zhou, Z.; Yu, W.-Y. "Rhodium(III)-Catalyzed Formal Oxidative [4 + 1] Cycloaddition of Benzohydroxamic Acids and α-Diazoesters. A Facile Synthesis of Functionalized Benzolactams", *Organic & Biomolecular Chemistry*, **2014**, 12, 4112

CONFERENCE

Lam, H.-W.; Lau, Y.-F.; Yu, W.-Y. "Rh(III)-Catalyzed Arylation of O-Acetly Hydroxamic Acids with Aryl/Vinyl Boronic Acids", 11th International Symposium on Organic Free Radicals, Berne, Swiss, 1-5 July, 2012

SYMPOSIUMS

Lam, H.-W.; Man, K.-Y.; Chan, W.-W.; Zhou, Z.; Yu, W.-Y. "Rh(III)-Catalyzed Oxidative [4+1] Cycloaddition of *O*-Acetyl Hydroxamic Acids with –Diazoesters", The 21th Symposium on Chemistry Postgraduate Research in Hong Kong, 12 April, 2014

Lam, H.-W.; Lau, Y.-F.; Yu, W.-Y. "Rh(III)-Catalyzed Arylation of O-Acetly Hydroxamic Acids with Aryl/Vinyl Boronic Acids", The The 20th Symposium on Chemistry Postgraduate Research in Hong Kong, 23 April, 2013

ACKNOWLEDGEMENTS

I would like to thank my supervisor Dr. Michael Wing-Yiu Yu for his dedicated advice throughout the course of my study. Under his guidance, I trained up rational mind-set, start seeing negative experimental result as part of the problem solving skill training. This unforgettable experience could not be gained elsewhere but only from Dr Michael Yu's group.

I would also like to thank my ex-chief supervisor Prof. Chak Po Lau for bringing me into graduate school. All the wonderful memories, friendships and achievements in the past few years would only be dream if Prof. Lau didn't kindly open the gate for me. I am so grateful for being your last postgraduate student. I hereby express my greatest respect and appreciation to Prof. Lau.

Two heads are better than one. I couldn't have accomplished all the targets during the time without help from the others and I am a very lucky guy that senior researchers from both Prof Lau's group and Dr Yu's group have been willing to share their experience to me. I would like to thank Dr Hung-Wai Cheung, Dr Chau-Ming So, Dr Ting-Yan Lee, Dr Chi-On Chan, Dr. Chung-Wing Leung, Dr Wing-Nga Sit, Dr Yuk-Tai Tsoi, Dr Chun-Wo Chan, Dr Wai-Wing Chan and Dr Ka-Ho Ng for their unselfish sharing and assistance. Extra respect and appreciation are credited to Dr

Wing-Nga Sit and Dr Yuk-Tai Tsoi for not only offering me help but also care at my hard time.

I am thankful to the valuable discussion and help from Mr. Yan-Fung Lau, Ms. Ka-Yi Man, Mr. Chun-Ming Chan, Mr. Fo-Ning Ng, Ms. Pui-Yiu Lee, Mr Wing-Yin Keung and Mr. Siu-Fung Lo. I wish all of you the best in your own research.

The technical support from the Department of Applied Biology and Chemical Technology are crucial throughout the course of my study. Especially, I would like to thank Prof. Zhongyuan Zhou for his experienced X-ray crystallographic studies and Mr. Wing-Kong Kwan and Dr. Kenneth Siu-Cheong Yan for their NMR support and lab safety advice.

I would like to thank Dr. Gary Kwong-Chak Cheung individually. You are the best teacher, adviser, brother and friend in my life. I am so grateful and lucky to have you being with me in my every single hard time.

Furthermore, I would like to thank my friend Mr Ka-Kit Poon and Ms Fionie Hoi-Man Chow. For some reasons they are not with me anymore but the time and memory from both of you helped me to pass through hard times and made me be a better person. I would also like to thank Ms Hing Lau and especially to Mr Chun-Yuen Lau, for his ever patient comfort and support. With your words, I know I can do much better in every aspect than I imagined.

Expressing my deepest love to all of my family members would be the last but not least thing to do. My mother: Ms. Ka-Fung Ma, My father: Mr. Hing-Sui Lam and my sister Ms. Yuk-Yin Lam, without your unconditional love and support I wouldn’t have walked so far. All of you are the most important reason for me not to giving up. Finally, one sentence would be more than excellent to express my love and appreciation to my girlfriend: Ms Erica Lai-Tung Chan, you are my glucose and oxygen in my life.

TABLE OF CONTENTS

ABBREVIATIONS AND SYMBOLS

Ac	Acetyl
AcOH	Acetic acid
Ar	Aryl
Å	Anstom
BDE	Bond dissociation energy
Bn	Benzoyl
Boc	*tert*-Butoxy carbonyl
Bz	Benzyl
cod	1,5-Cyclooctadiene
Cp*	Pentamethylcyclopentadienyl
dba	Dibenzylideneacetone
DCE	1,2-Dichloroethane
DCM	Dichloromethane
DMF	*N*,*N*-Dimethylformamide
DMSO	Dimethyl sulfoxide
EtOAc	Ethyl acetate
GC-MS	Gas chromatography-mass spectrometry

KIE	Kinetic isotope effect
LiO*t*Bu	Lithium *tert*-butoxide
MeCN	Acetonitrile
NEt_3	Triethylamine
NMR	Nuclear magnetic resonance
phen	1,10-Phenanthroline
Piv	2,2,2-Trimethylacetyl
PPh_3	Triphenylphosphine
OAc	Acetate
OPiv	2,2,2-Trimethylacetate
OTf	Trifluoromethanesulfonate
rt	Room temperature
THF	Tetrahydrofuran
TLC	Thin layer chromatography
s	Singlet
d	Doublet
t	Triplet
q	Quartet
m	Multiplet

δ	Chemical shift in NMR
J	Coupling constant

LIST OF FIGURES

LIST OF TABLES

LIST OF SCHEMES

Chapter 1

Introduction

1.1 General Background

Carbon-nitrogen (C-N) bond formations are important in synthetic organic chemistry because C-N bonds are important structures commonly found in many pharmaceuticals, agrochemicals and electronic materials.[1] Conventionally, *N*-alkylation of amines with alkyl halides is used to furnish C-N bond. Despite its simplicity, the synthetic value of this reaction is very limited due to overalkylation, which leads to a mixture of primary, secondary, tertiary and quaternary products.[2]

In the last two decades, the palladium-catalyzed cross coupling reactions of arylhalides with anilines which also known as the Buchward-Hartwig amination served as a powerful tool for synthesis of arylamines.[1,3] A generally accepted mechanism, which involves palladium(0) as the active catalyst is depicted in scheme 1.1.

Scheme 1.1 Proposed mechanism for Buchward-Hartwig type amination

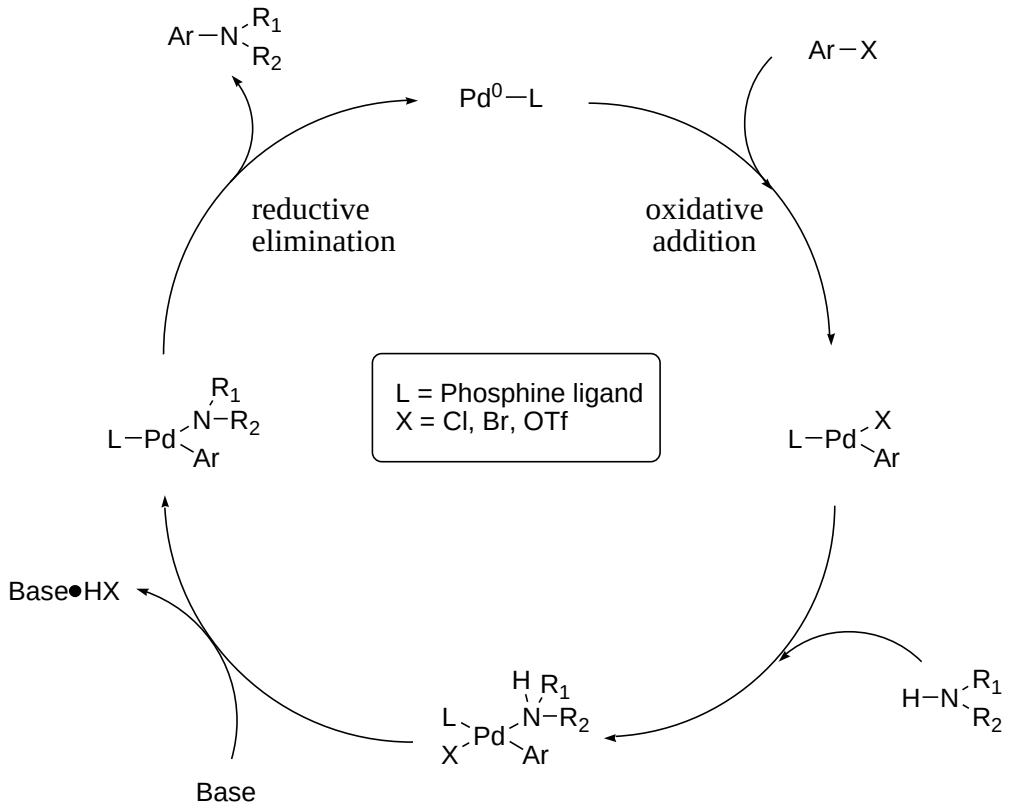

Despite the advancement in the scope of reaction and regioselectivity, this reaction usually employs a strongly basic environment and halogenated arenes as substrates. Halogen-substituents are usually not tolerated due to its reactivity towards low-valent palladium species. For higher atom-economy and synthetic efficiency, direct amination of unactivated arenes (C-H bond) which operates under milder reaction conditions and exhibits board functional group tolerance is highly desirable.

1.2 C-N Bond Formation via C-H Bond Activation

1.2.1 The Challenges of C-H Bond Functionalization

Direct C-H bond functionalization has been a subject of extensive investigation over the past decades.[4] To utilize C-H bonds in cross-coupling reactions, some challenges have to be overcome.[4c,5] Bond weakening or bond breaking is the first step for most of the organic reactions. C-H bond is a strong covalent bond compared to other C-X bonds (X refers to halogen and oxygen atoms) (Table 1.1)[6]. Thus, C-H bond cleavage requires to overcome larger kinetic energy barrier compared to C-X bond cleavage.

Table 1.1 Experimental bond dissociation energy (BDE) based on radical heats of formation [RX → R • + H •]

bond	BDE (kcal mol^{-1})	bond	BDE (kcal mol^{-1})
C_6H_5-I	67	CH_3-H	105
C_6H_5-Br	84	C_6H_5-H	112
C_6H_5-Cl	97	$C_6H_5CH_2$-H	97

Besides, C-H bond has an extremely low pKa value (45 – 60) that renders heterolytic cleavage by strong bases unfeasible.[7]

For chemoselectivity, over oxidation of C-H bond to C-O bond under strongly oxidizing reaction conditions is common. Moreover, preservation of functional groups which contain a relatively weak C-X bond is important in synthetic organic chemistry. Furthermore, regioselectivity of C-H bond functionalization is very challenging as the chemical reactivity of each different C-H bond is similar.

1.2.2 Transition Metal-Mediated C-H Activation

Inner-sphere and outer-sphere are the two major pathways for transition metal-mediated C-H activation.[4c,8] (Scheme 1.2)

Scheme 1.2 The two major pathways for transition metal-mediated C-H activation

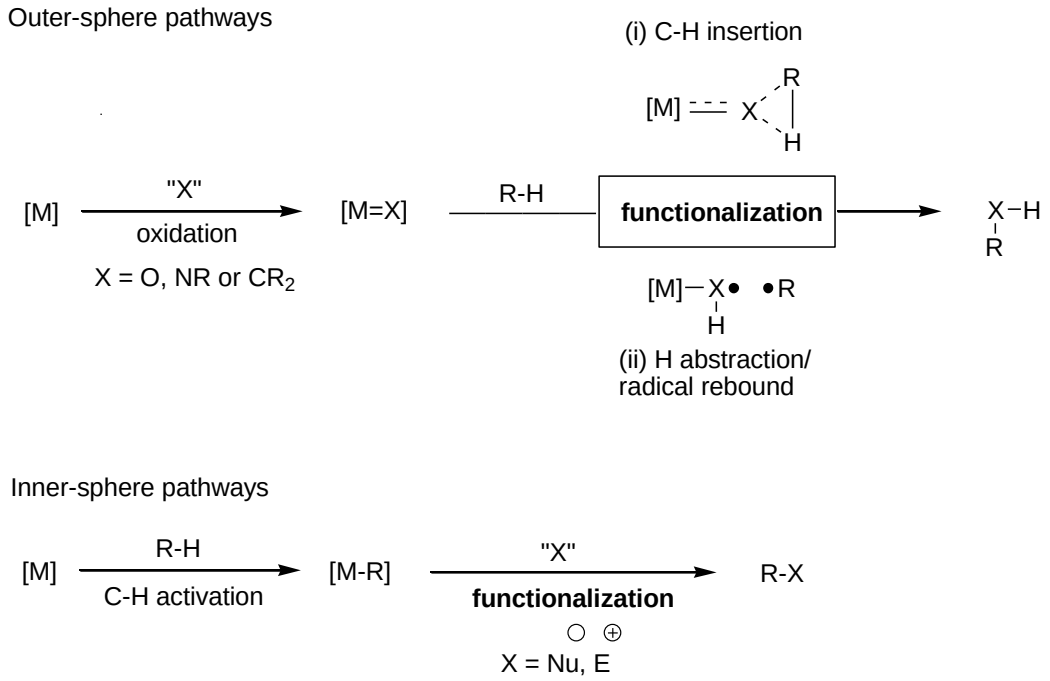

In outer-sphere pathways, the transition metal [M] would be activated by an oxo (O), nitrenoid (NR) or carbene (CR) species to give a highly reactive [M=X]. This [M=X] species would then interact with the C-H bond via either a direct C-H bond insertion or hydrogen atom abstraction/ radical rebound to furnish the C-H functionalization product.

For inner-sphere pathways, the C-H bond would be first cleaved by transition metal to give organometallic species [M-R]. Oxidative addition, electrophilic C-H activation, σ-bond metathesis and agostic interaction followed

by deprotonation are the possible mechanisms for the C-H bond cleavage. [M-R] would then be functionalized by either an electrophiles or nucleophiles.

1.3 Electrophilic (Umpolung) Amination

1.3.1 Reaction Background of Electrophilic Amination

In a conventional *N*-alkylation reaction between alkyl halides (R-X, with X= halides) and amines, alkyl halides are considered as $R^{\delta+}$ supplier with amines being nucleophiles for the reaction. Electrophilic (umpolung) amination offers an alternative synthetic route for C-N bond construction which involves an inversion of polarity in the amines species, allowing the change of its reaction partners from electrophilic alkyl halides to nucleophilic species such as organolithium reagents and Grignard reagents. [9, 10a] (Scheme 1.3)

Scheme 1.3 Inversion of polarity in electrophilic amination

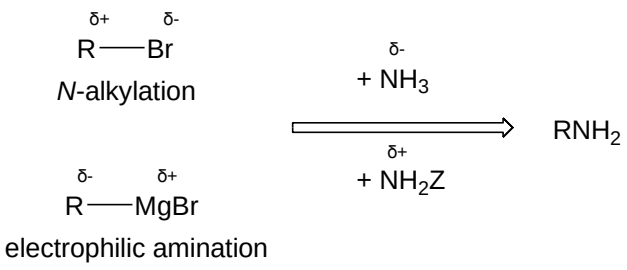

Electrophilic amination reactions can be classified as either substitutions or additions.[11] The electrophilic aminating reagents used in substitution reactions are chloramines, hydroxylamines, hydrazines, and oxaziridines. These reagents contain an electron-withdrawing group, which can be displaced by nucleophile easily. In contrast, imines, oximes, azides and azo compounds are used in addition reactions.

1.3.2 Early Work on Electrophilic Amination Reactions

1.3.2.1 Electrophilic Amination Using *N*-Chloroamines

Chloroamines is a common substrate for the electrophilic amination of organometalic reagents such as Grignard reagents.[12] By employing suitable haloamines and organometalic reagents, primary and secondary amines could be obtained. (Scheme 1.4 eq 1 and 2) It was also found that the use of dialkylmagnesium could optimize the yield of the desired product. (Scheme 1.4 eq 3)

Scheme 1.4 Electrophilic amination using *N*-chloroamines

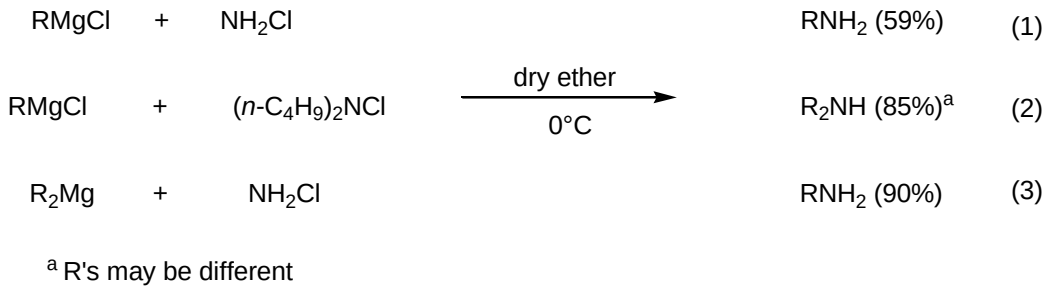

However, when phenyl Grignard reagents were used for the preparation of anilines, only very low yields of desired anilines were obtained. It was proposed that the low yield may due to the ambident character of "NH_2" of the chloroamine.[13] (Scheme 1.5)

Scheme 1.5 Ambident character of "NH_2"

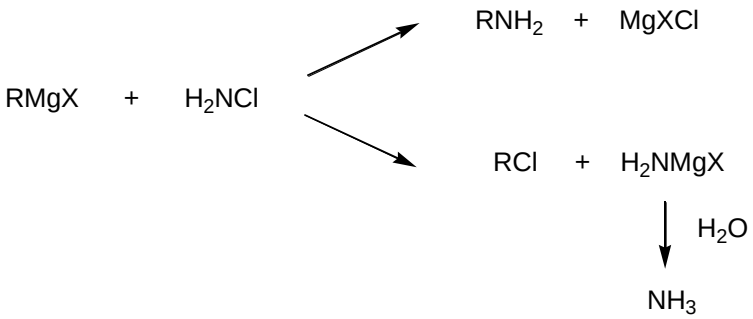

1.3.2.2 Electrophilic Amination Using *O*-Alkylhydroxylamines

The amination of carbanion with methoxyamine is also known as the Schverdina-Kotscheschkow amination. Hydrochloride salt of the desired amine can be obtained from the reaction between the corresponding *O*-alkylhydroxylamines and Grignard reagents followed by hydrolysis. Notably, phenyllithium was also effective for the reaction, and the desired anilines were obtained in 63% yield. However, excess organolithium reagents (2 to 3 equiv) or additional stoichiometric amount of methyllithium is needed for the deprotonation of the *O*-alkylhydroxylamines as the amination reactions were proved to be not a direct displacement by the cabanion at the free amino group but more likely involve *N*-mono and *N*,*N*-dilithioaniline species.[9] (Scheme 1.6)

Scheme 1.6 Proposed mechanism for electrophilic amination using *O*-alkylhydroxylamines

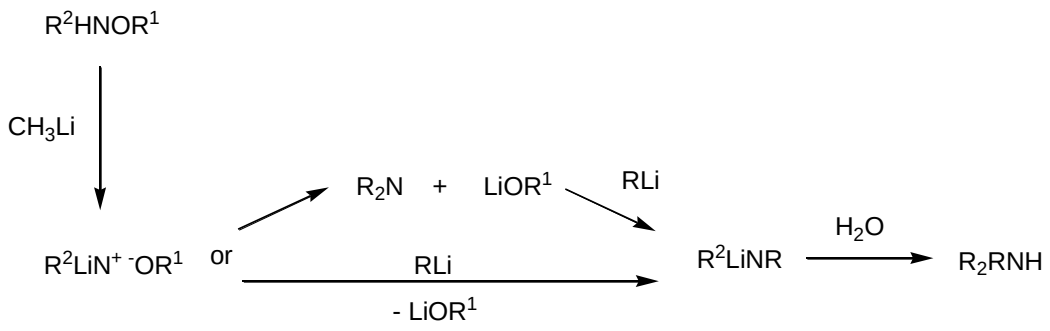

1.3.2.3 Electrophilic Amination Using *O*-Arylhydroxylamines and *O*-Acylhydroxylamines

Sheradsky and co-workers discovered that *O*-arylhydroxylamines and *O*-acylhydroxylamines were useful reagents for amination of various ester enolates.[14] It was found that *O*-(2,4-dinitrophenyl)-hydroxylamine (DPH) was exceptionally useful for the synthesis of amino esters. (Scheme 1.7) However, these reagents became less effective when the basicity of the ester enolate increases due to decomposition of DPH under strongly basic medium.

Scheme 1.7 Electrophilic amination using DPH for the synthesis of amino esters

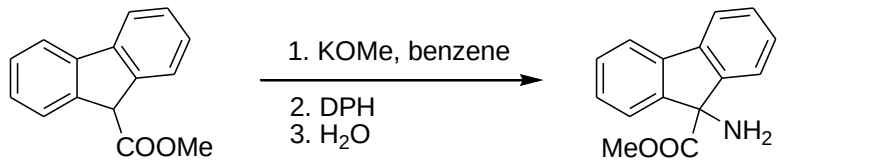

50%

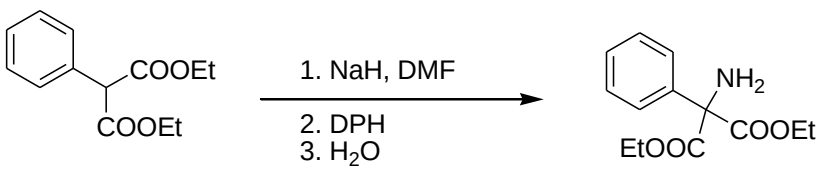

53%

DPH = *O*-(2,4-dinitrophenyl)-hydroxylamine

1.3.2.4 Electrophilic Amination Using *O*-Sulfonylhydroxylamines

The scope of the enolate amination was broadened by the use of *O*-(mesitysulfonyl)hydroxylamine (MSH) and its derivatives. Methyl diethylphosphonacetate[15] and malonodinitrile[16] were successfully aminated by MSH. (Scheme 1.8) The use of MSH was not limited to the amination of ester enolate but also for the transformation of alkyl-, alkenyl- and aryllithium compounds to its corresponding tertiary amines in good yield.[17] Notably, 1-alkynylcuprates could also be aminated with the derivatives of MSH in good yields.[18]

Scheme 1.8 Electrophilic amination using *O*-sulfonylhydroxylamines

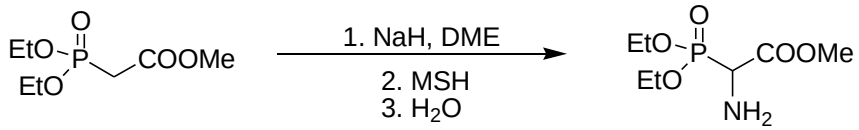

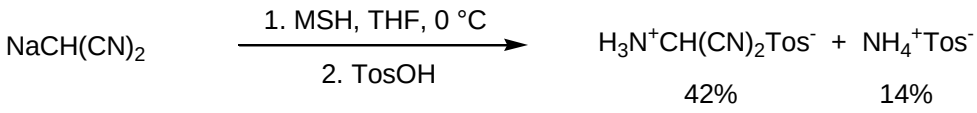

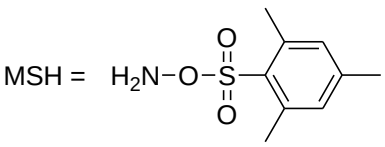

1.3.2.5 Electrophilic Amination Using *O*-Phosphinylhydroxylamines

O-Phosphinylhydroxylamines is a even better aminating agent than *O*-sulfonylhydroxylamines as it is a relatively more stable compound which can be stored indefinitely at -20°*C*.[9] *O*-(diphenylphosphinyl)hydroxylamine and its derivatives (Scheme 1.9) were useful in the aminating of ester enloates, Grignard reagents such as phenyl- and alkylmagnesium bromides,[19] (Scheme 1.10) organolithium derivatives such as lithium enolates and alkynyllithium cuprates.[20] (Scheme 1.11)

Scheme 1.9 *O*-(Diphenylphosphiny)hydroxylamine and its derivatives

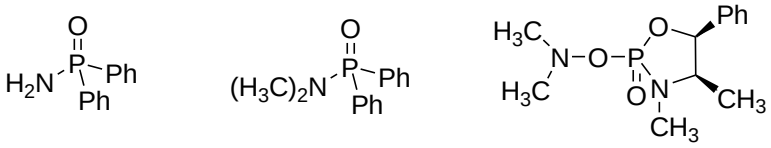

Scheme 1.10 Aminating of ester enloates and phenyl- and alkylmagnesium bromides using *O*-(diphenylphosphiny)hydroxylamine

Colvin and co-workers

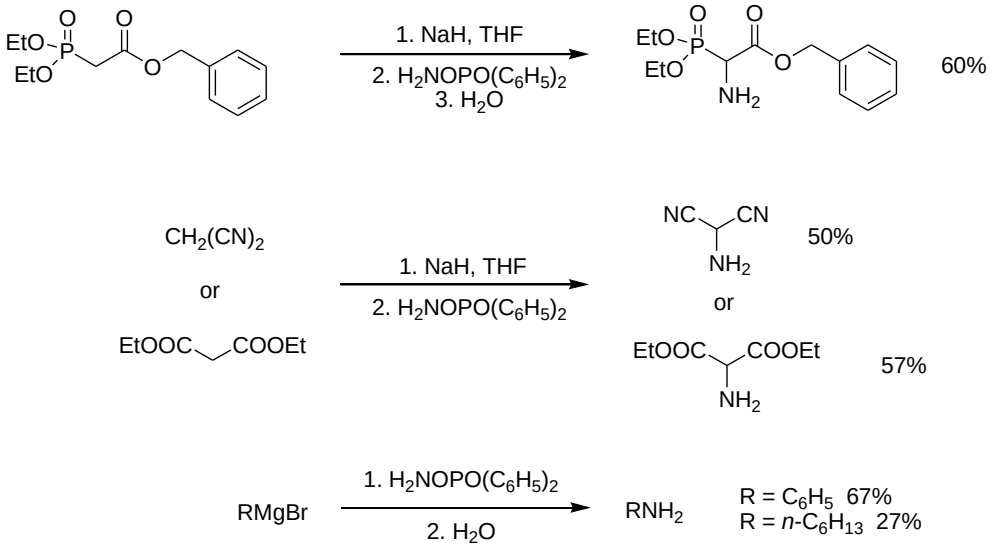

Scheme 1.11 Aminating of lithium enolates and alkynyllithium cuprates

Boche and co-worker

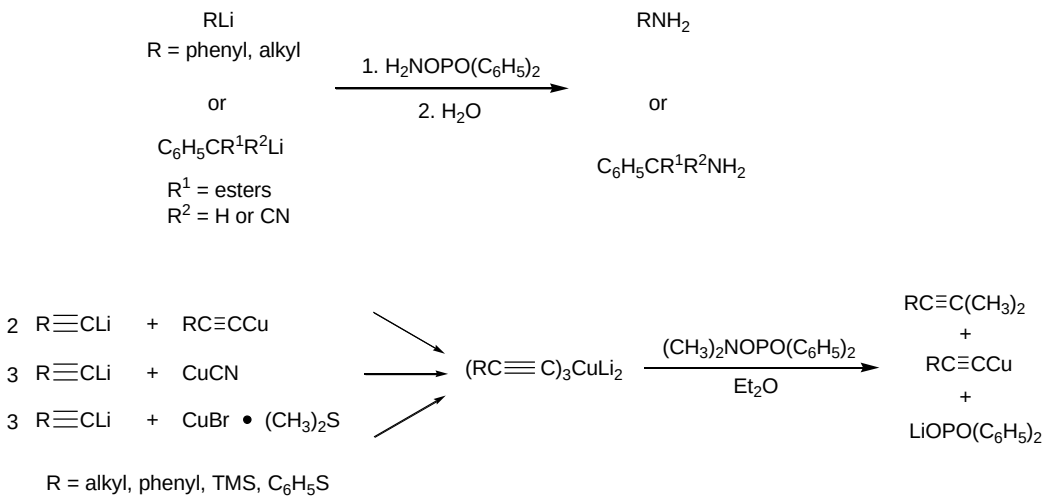

O-(Trimethylsilyl)cyanohydrin anions can be generated by reacting aldehydes with lithium diisopropylamide (LDA). Amination of

O-(trimethylsilyl)cyanohydrin anions can be accomplished by using *O*-(diphenylphosphinyl)hydroxylamine. Upon hydrolysis of the resulting amines, amides can be obtained.[21] (Scheme 1.12)

Scheme 1.12 Synthesis of amides using aldehydes and *O*-(diphenylphosphinyl)hydroxylamine

Boche and co-worker

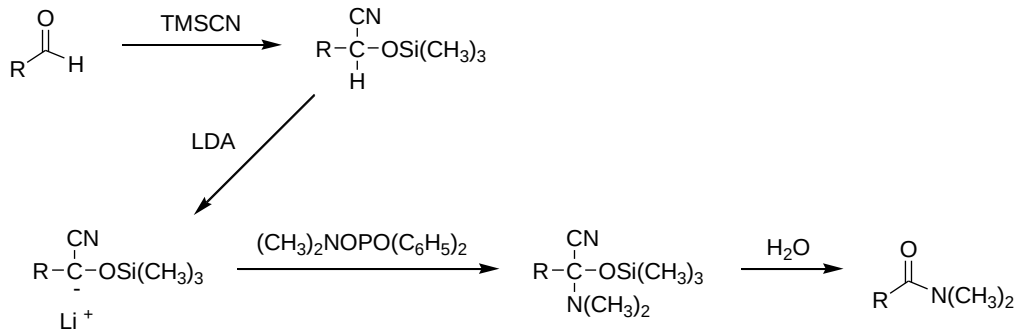

The synthesis of chiral amines can also be accomplished by using chiral *O*-(diphenylphosphinyl)hydroxylamine derivatives.[22] (Scheme 1.13)

Scheme 1.13 Synthesis of chiral amines using chiral *O*-(diphenylphosphiny)hydroxylamine

Boche and co-worker

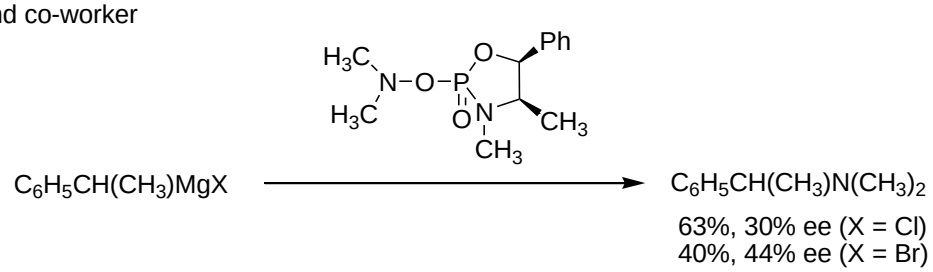

1.3.2.6 Electrophilic Amination Using Azides

The synthesis of anilines was known to proceed via the reaction between azides and Grignard reagents or organolithium compounds followed by hydrolytic work-up. The reaction scopes were further extended to the *ortho*-amination of certain aromatic compounds.[23] (Scheme 1.14)

Scheme 1.14 *ortho*-Amination of aromatic compounds using azides

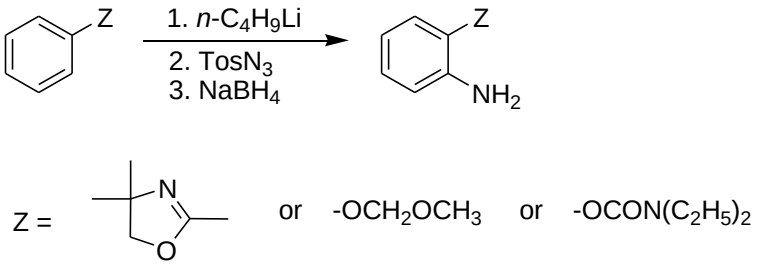

1.3.2.7 Electrophilic Amination Using Oximes

Amines can be synthesized from the addition reaction between oximes and Grignard regents or organolithium compounds followed by reduction using BH_3 as reducing agent.[24] (Scheme 1.15)

Scheme 1.15 Electrophilic amination using oximes

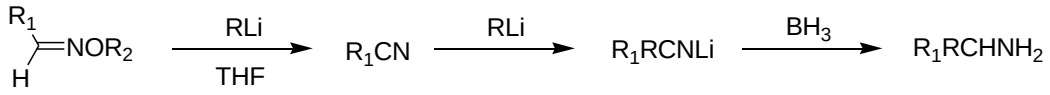

1.4 Transition Metal-Catalyzed Electrophilic Amination Reactions

1.4.1 Copper-Catalyzed Electrophilic Amination Reactions

The oxidative coupling of lithium alkyl copper amide, which is formed in situ from lithium dialkylcuprates and amines, was first reported by Yamamoto and co-workers in 1980.[25] (Scheme 1.16) It was found that alkylation of amines could be accomplished by the reaction between lithium dialkylcuprates and amines with molecular oxygen bubbling into the reaction mixture.

Scheme 1.16 Oxidative coupling of lithium alkyl copper amide

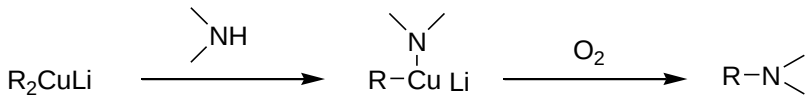

Following Yamamoto's work, there were several reports on the application of amination of lithium dialkylcuprates.[26] However, a stoichiometric amount of copper (I) salt was needed for transmetalation. Until 1997, Narasaka and co-workers reported the first transition metal catalyzed amination reaction using electrophilic amination source. They reported the copper(I)-catalyzed amination of alkyl Grignard reagents with sulfonyloxime.[27a] They later also reported the copper-catalyzed reaction of γ, δ-unsaturated ketone *O*-methoxycarbonyloximes with lithium bromide to provide 2-(bromomethyl)-3,4-dihydro-2*H*-pyrroles.[27d] (Scheme 1.17) For the synthesis of 2-(bromomethyl)-3,4-dihydro-2*H*-pyrroles, it was proposed that the reaction should go through a single electron transfer from CuBr to the γ, δ-unsaturated ketone *O*-methoxycarbonyloximes. Radical cyclization of the resulting compound furnished the desired product. The active CuBr was regenerated by ion-exchange with lithium bromide.

Scheme 1.17 Precedent examples of copper(I)-catalyzed electrophilic amination of organometallic reagents

Narasaka and co-workers

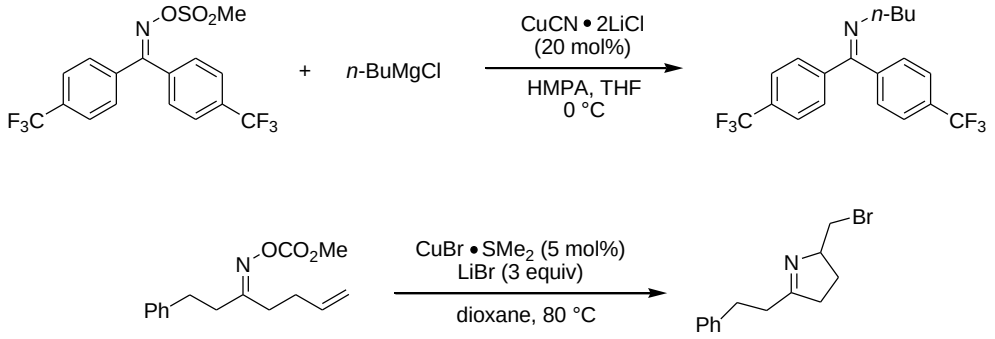

In 2004, Berman and Johnson reported the first copper-catalyzed electrophilic amination of diorganozinc reagents using *O*-benzoylhydroxylamine (sp^3 nitrogen source) as an electrophilic aminating reagent.[28a] The scope of the *O*-benzoylhydroxylamines and organozinc reagents were broadened with fine modification of reaction conditions.[28b,c] Grignard reagents were first found to be ineffective reagents for the reaction due to the Grignard addition to the carbonyl of the *O*-benzoylhydroxylamines. This problem was later overcome by slow addition of the Grignard reagent.[28d] (Scheme 1.18)

Scheme 1.18 Amination of organozinc reagents using *O*-benzoylhydroxylamine

Berman and Johnson

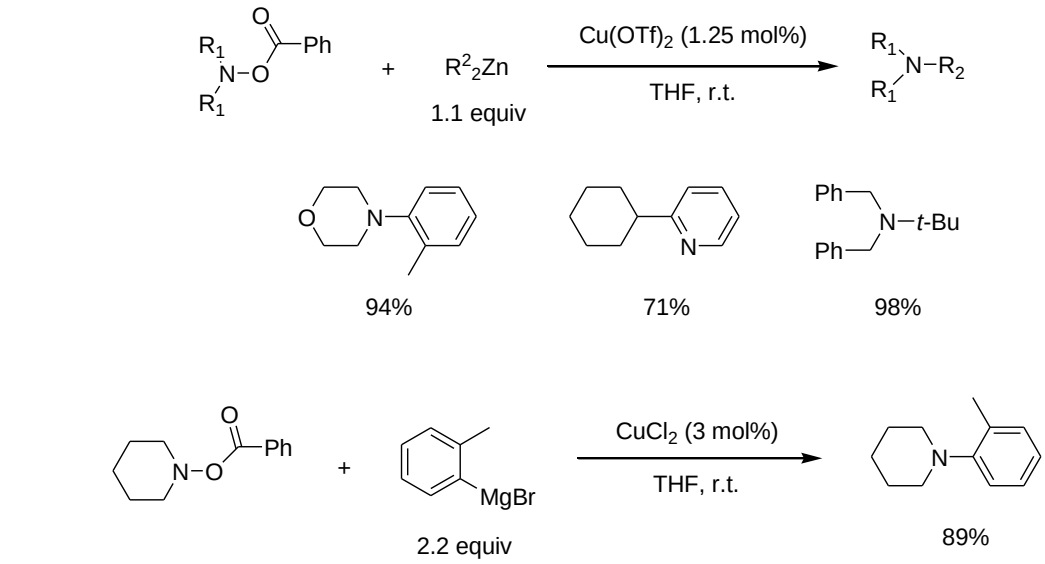

Regarding to the reaction mechanism, chirality of product was found to be retained when a chiral organozinc reagent (which is in situ generated from the reaction of $ZnCl_2$ and a chiral Grignard reagent) was employed for the reaction. This result suggested that the reaction should go through a polar mechanism rather than a radical mechanism.[28d] An endocyclic competition experiment was also performed to differentiate whether the reaction go through an S_N2 displacement at nitrogen or non-S_N2 oxidative addition/reductive elimination of the N-O/C-N. (Scheme 1.19) **A** and **A-*d*$_{14}$** were prepared as precursors of organocopper. If the reaction proceeds through an intramolecular S_N2 mechanism, no desired product **B** would be obtained due to the strained transition state **X** in

an intramolecular S_N2 pathway. In contrast, if the reaction goes through a non-S_N2 oxidative process, desired product **B** would be obtained as the transition state **Y** is attainable. A near statistical mixture of B ($d_0/d_4/d_{10}/d_{14}$) were obtained indicates the reaction should go through an S_N2 intermolecular pathway.

Scheme 1.19 Mechanistic studies of the copper catalyzed electrophilic amination of orgnaozinc using *O*-benzoylhydroxylamine

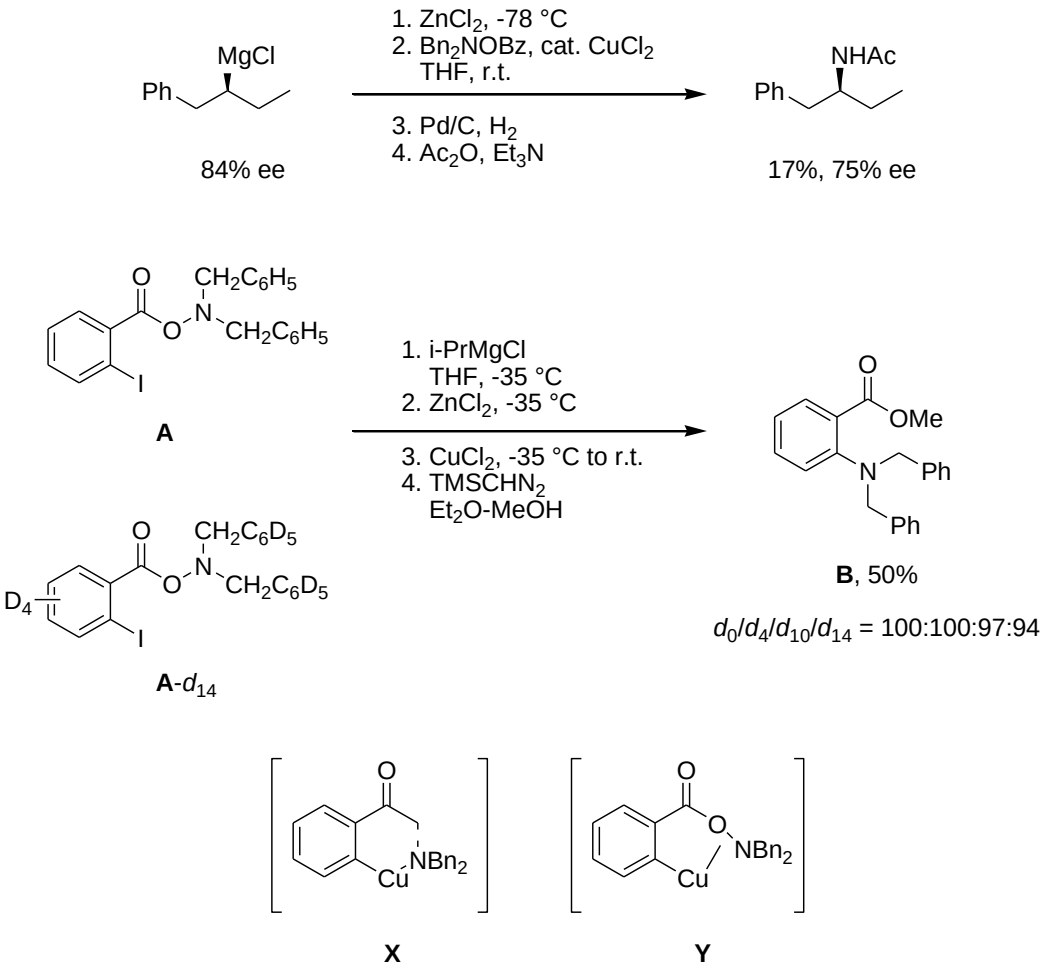

In 2002, Göttlich and co-workers studied the use of nitrogen-chlorine bond in copper-catalyzed amination reaction.[29a,b] Similar to the mechanism proposed by Narasaka in 1997, they suggested that single electron transfer from Cu(I) to *N*-chloro-*N*-pentenylamines, followed by a series of radical rearrangement to give 3-chloropiperidine as product. (Scheme 1.20)

Scheme 1.20 Mechanism of Cu(I)-catalyzed cyclization of *N*-chloro-*N*-pentenylamines

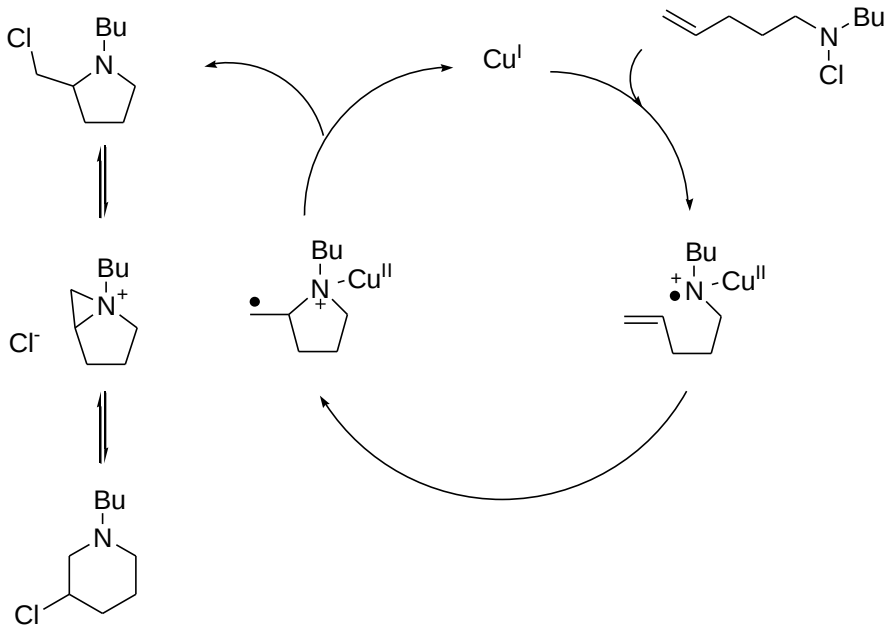

Organoboranes are considered carbanion-equivalent. Due to strong covalent B-C bond, organoboranes are relatively more stable than organolithium, organozinc and Grignard reagents. In 2007, Liebeskind and co-workers reported

the Cu-catalyzed *N*-imination of arylboronic acids or organostannanes. It was proposed that N-O bond of ketoxime was oxidatively added to the Cu(I); the carboxylate ligand provides the driving force for the transmetalation with arylboronic acids. Reductive elimination of the resulting species should furnish the desired product. The same strategy was employed later for the synthesis of pyridine from the coupling reaction between α,β-unsaturated ketoxime *O*-pentafluorobenzoates and vinylboronic acids. (Scheme 1.21)

Scheme 1.21 Cu-catalyzed *N*-imination of arylboronic acids and vinylboronic acids

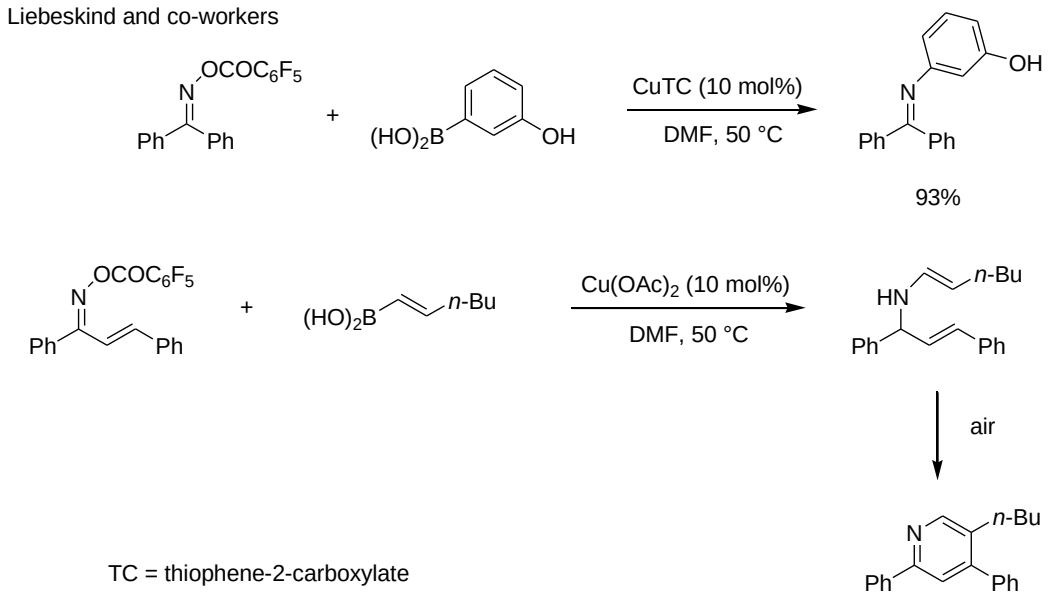

In 2008, Lei and co-workers reported the first electrophilic amidation of arylboronic acids. In the presence of 10 mol% CuCl and 3 equiv of Na_2CO_3 , arylboronic acids were amidated by *N*-chloroamides under room temperature.[31] (Scheme 1.22)

Scheme 1.22 Cu(I)-catalyzed amidation of arylboronic acids using *N*-chloroamides

Lei and co-workers

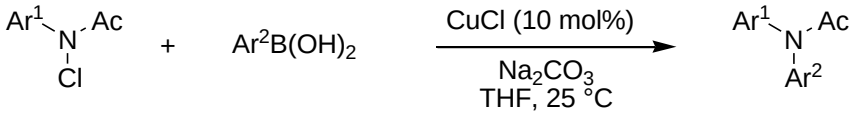

1.4.2 Palladium-Catalyzed Electrophilic Amination Reactions

To improve the generality of the cyclization of γ, δ-unsaturated ketone oximes, Narasaka and co-workerss employed $Pd(PPh_3)_4$ as catalyst and transformed γ,δ-unsaturated ketone oximes into pyrrole successfully in two steps.[27b] Differed from the radical mechanism suggested in Leibeskind's copper-catalyzed reaction, it was proposed that the N-O bond was oxidatively added to the Pd(0), and the Pd-N bond would then undergo migratory insertion

and β-hydride elimination to give the desired imine. A chlorotrimethylsilane-mediated cyclization of the resulting imine would furnish the corresponding pyrrole.[27e] (Scheme 1.23)

Scheme 1.23 Palladium(0)-catalyzed cyclization of γ,δ-unsaturated ketone oximes for the synthesis of pyrroles

Narasaka and co-workers

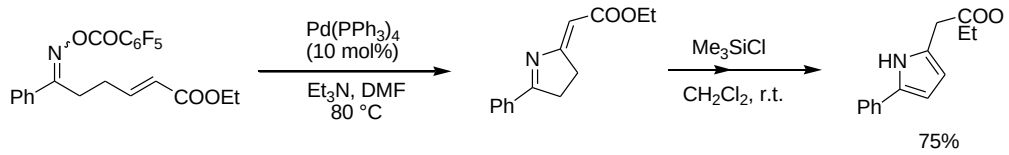

The cleavage of N-O bond by low-valent Pd species was supported by the reaction between 4,4'-bis(trifluoromethyl)benzophenone *O*-methylsulfonyloxime and $Pd(PPh_3)_4$, and 4,4'-bis(trifluoromethylphenyl)methylideneamine was obtained as crude product after quenching with buffer solution at pH 9. The crude product was then hydrolyzed into benzophenone by acid treatment.[27e] (Scheme 1.24)

Scheme 1.24 Cleavage of N-O bond by Pd(0)

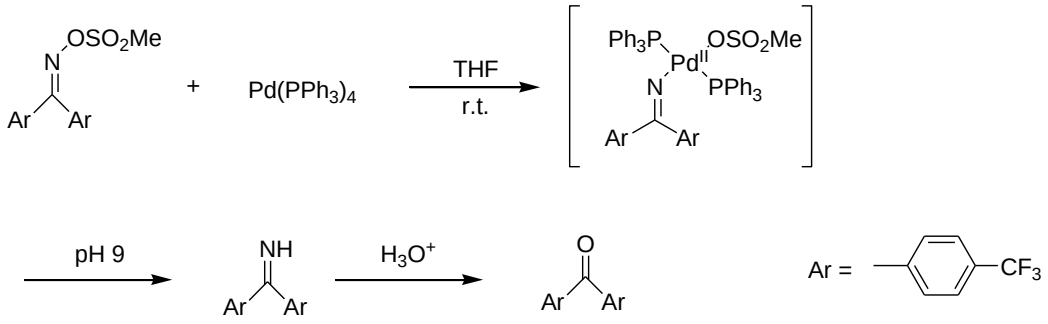

The alkylideneaminopalladium(II) species was not being isolated. However, the oxidative addition N-O bond to low-valent transition metal complex was confirmed by Pombeiro and co-workerss who prepared an aminorhenium(III) complex by reacting acetone oxime with rhenium(I) complex.[32] (Scheme 1.25)

Scheme 1.25 Preparation of aminorhenium(III) complex

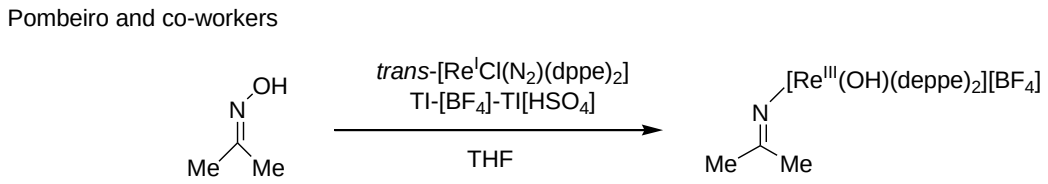

This amino-Heck reaction strategy has been further explored for the synthesis of pyridines and isoquinolines. Narasaka and co-workers discovered that a β-methoxy-substituted γ, δ-unsaturated ketone oximes would be cyclized to give pyridines in the presence of $Pd(PPh_3)_4$ with $(n\text{-}Bu)_4NCl$ and Et_3N as additives. A methoxy group on the *β*-position is essential since coordination to

the Pd^{II} center should help direct the cyclization to 6-*endo* mode.[27c] (Scheme 1.26)

Scheme 1.26 Palladium(0)-catalyzed cyclization of γ,δ-unsaturated ketone oximes for the synthesis of pyridines

Narasaka and co-workers

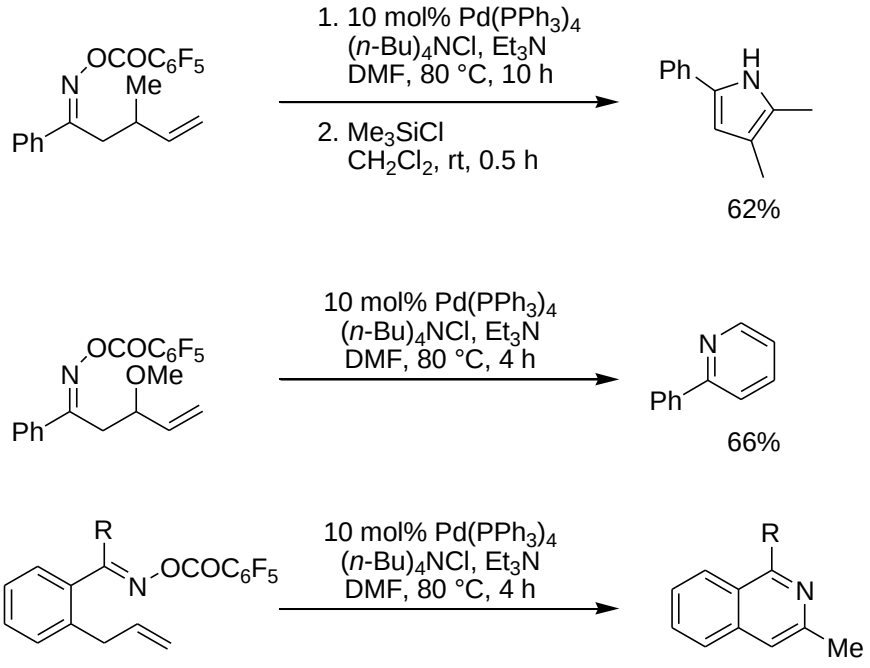

In 2005, Abell and co-workers employed *O*-pentafluorobenzoylamidoximes as substrate for the palladium(0)-catalyzed amino-Heck reaction to synthesize imidazoles.[33a] They later discovered that *O*-acyloximes with a pendant alkyne could be an effective substrate for the synthesis of pyrroles.[33b] The vinylpalladium intermediate was trapped successfully with carbon monoxide and ethanol to give product B as well as the reduced product A. (Scheme 1.27) This

demonstrated that further coupling reactions with this vinylpalladium species are possible. (Scheme 1.27)

Scheme 1.27 Palladium(0)-catalyzed amino-Heck reaction for the synthesis of imidazoles and pyrroles

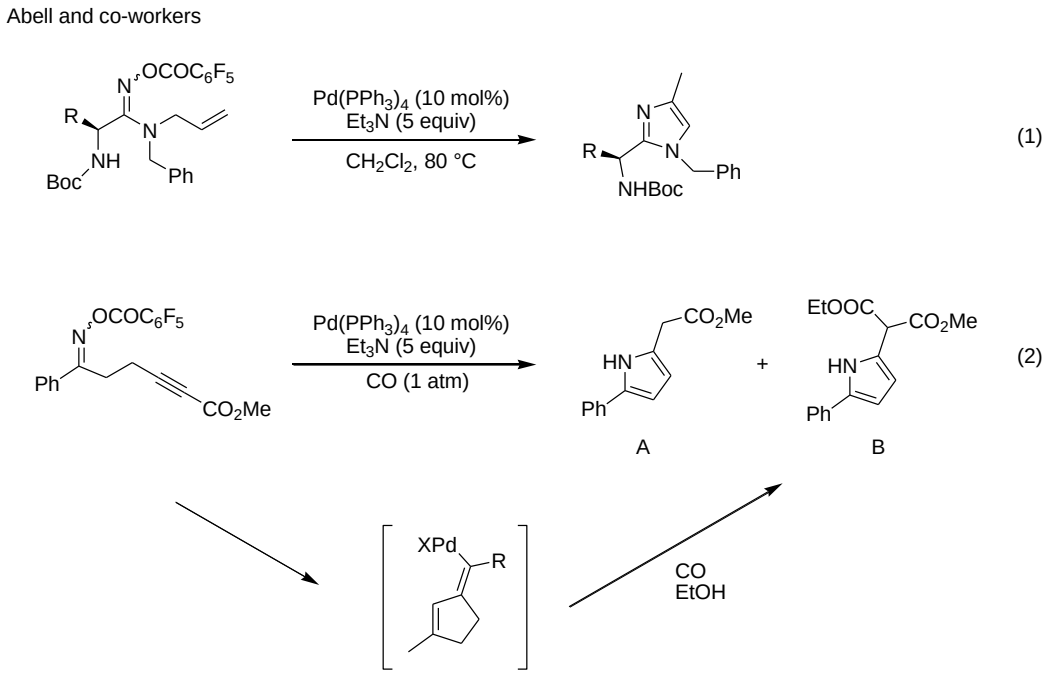

The palladium-catalyzed cross coupling reaction between *O*-acylbenzophenone oximes and benzyne to give phenanthridines was reported by Zhu and co-workers. It was proposed that after the oxidative addition of Pd(0) species into the N-O bond of the oximes, the oxime moiety would direct the σ-C-H bond for C-H activation to form a palladacycle, which would undergo further coupling reaction with benzyne.[34] (Scheme 1.28)

Scheme 1.28 Palladium-catalyzed cross coupling reaction between *O*-acylbenzophenone oximes and benzyne to give phenanthridines and its proposed mechanism

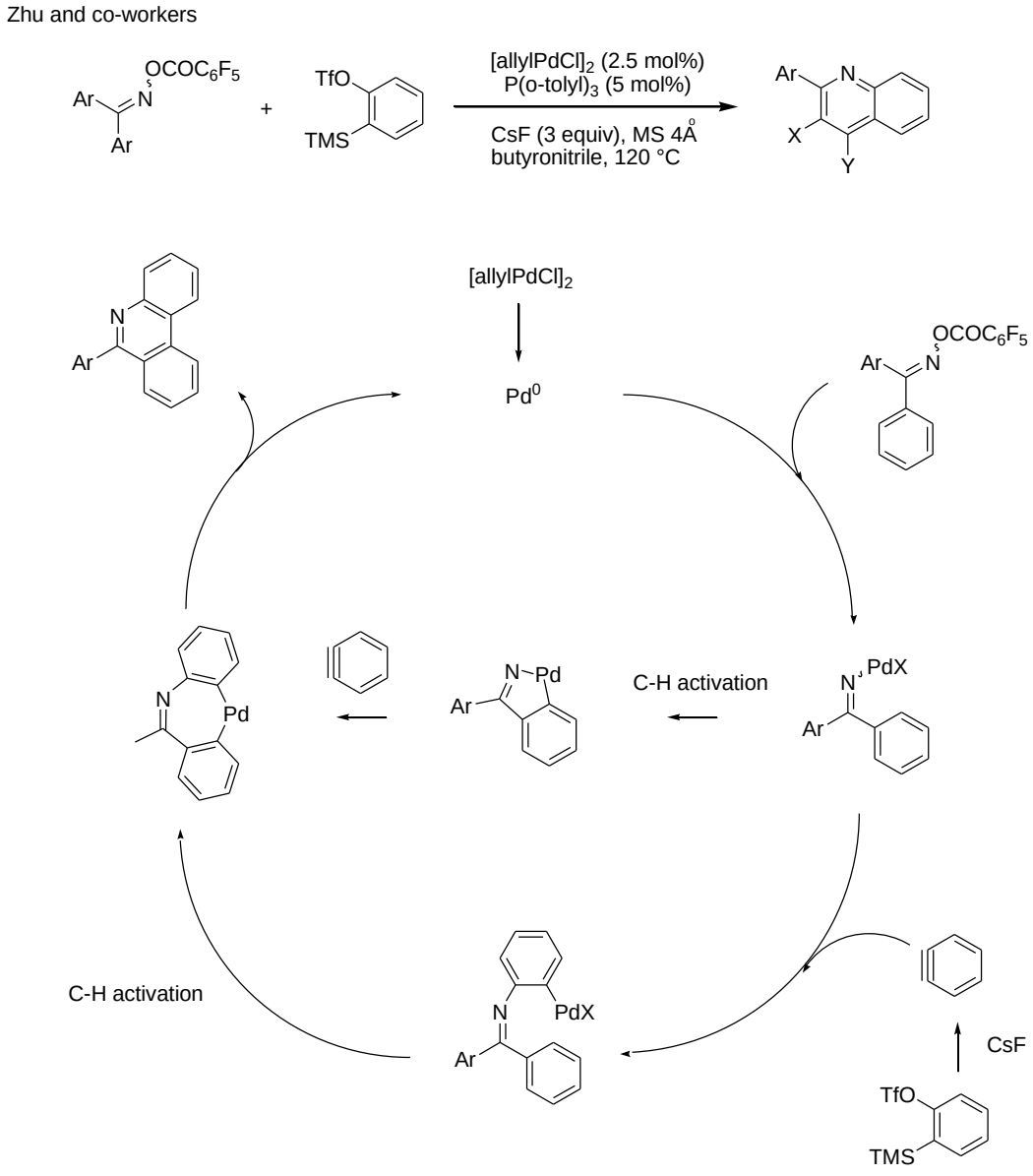

1.4.3 Other Transition Metal-Catalyzed Electrophilic Amination Reactions

Apart from copper and palladium, other transition metals such as nickel and rhodium have also been examined for the catalytic electrophilic amination reactions.

1.4.3.1 Nickel-Catalyzed Electrophilic Amination Reactions

In 2005, Johnson and co-workers reported that nickel(0) is catalytically active towards the reactions between organozinc and *O*-benzoyl hydroxylamines. The desired amines could be obtained in high yield under very mild conditions.[35] (Scheme 1.29)

Scheme 1.29 Nickel-catalyzed electrophilic amination of organozinc halides using *O*-benzoyl hydroxylamines

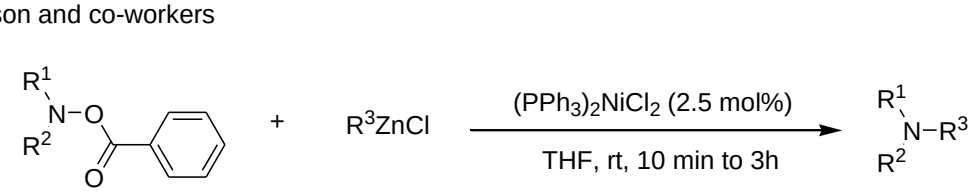

Jarvo and co-workers also reported the nickel-catalyzed electrophilic amination of diorganozinc reagents with *N*,*N*-dialkyl-*N*-chloroamines.[36a] (Scheme 1.30) It was proposed that the reaction would start with the oxidative addition of nickel catalyst into the N-Cl bond by a single electron transfer mechanism followed by transmetalation of organozinc reagents and reductive elimination which furnish the desired products. An alternative S_N2 attack of aryl-nickel complex on *N*-chloroamine was also proposed.

Scheme 1.30 Nickel-catalyzed electrophilic amination of organozinc halides using *N*,*N*-dialkyl-*N*-chloroamines

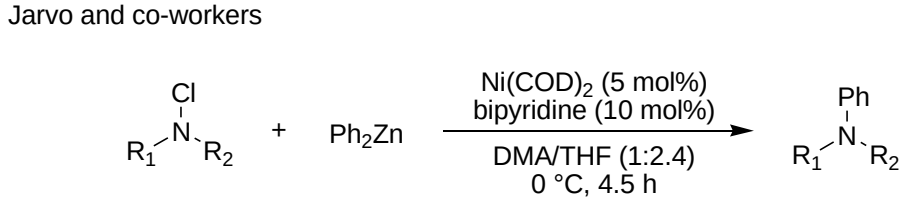

1.4.3.2 Rhodium-Catalyzed Electrophilic Amidation Reactions

Enamides are synthetically useful in organic chemistry and they are important building blocks of many natural compounds and pharmaceuticals. In

2014, Loh and co-workers reported that alkenylboronic acids could be amidated in the presence of 1.25 mol% $[Cp^*RhCl_2]_2$ and 1.5 equiv of NaOAc.[37] (Scheme 1.31) It was proposed that Rh complex II would be formed from the transmetalation between alkenylboronic acids and Rh(III) complex and base assisted coordination of *N*-pivaloyloxyl amide to the Rh(III) complex. A redox neutral pivalate assisted 1,2-migration from Rh to N of the Rh complex II would be followed and give Rh complex III. Protonation of the complex III would furnish the desired enamides and regenerate the active Rh^{III} catalyst.

Scheme 1.31 Rhodium(III)-catalyzed cross-coupling of alkenylboronic acids and *N*-pivaloyloxylamides for the synthesis of enamides

Loh and co-workers

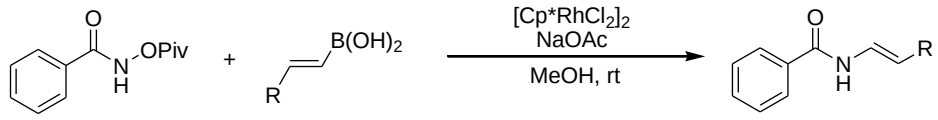

R = alkyl, aryl

Proposed mechanism

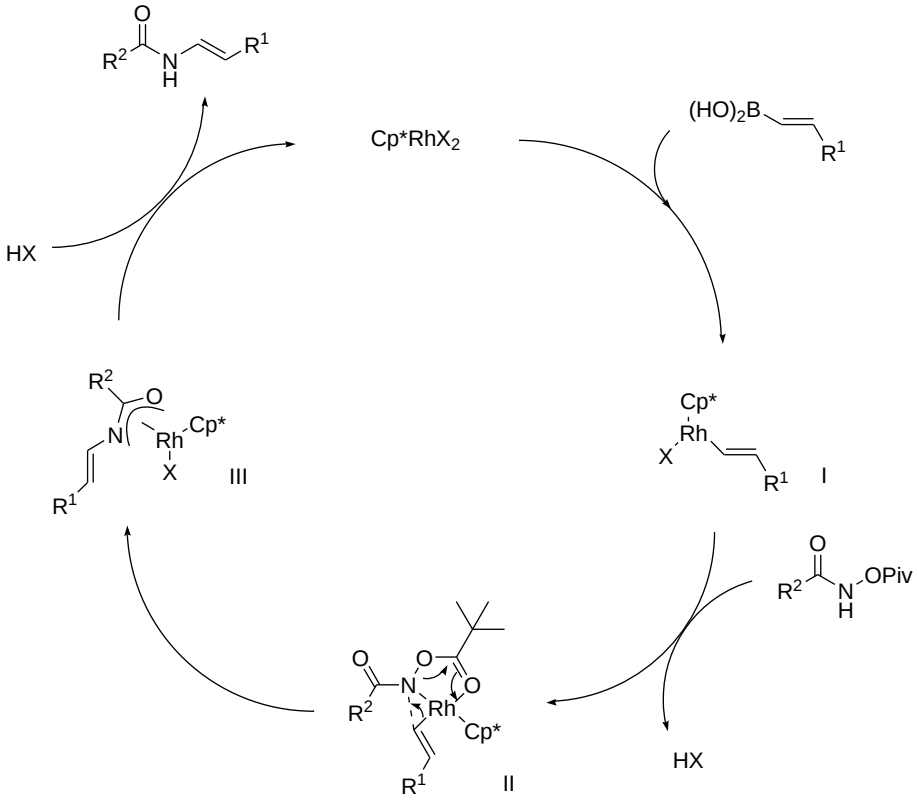

X = OPiv or OAc

1.5 Transition Metal-Catalyzed Amination/ Amidation of Aromatic C-H Bond

The synthesis of amines and amides through amination/amidation of Grignard reagents, organozinc, -lithium reagents and organoboranes are established and well documented C-N bond construction methods. However, in the view of atom economy and synthetic simplicity, direct amination/amidation of C-H bond is an even better synthetic route as C-H bond is common in organic molecules.

1.5.1 Challenges for Transition Metal-Catalyzed Amination/Amidation of Aromatic C-H Bond

Transition metal mediated C-H bond activation is usually performed under acidic conditions. The reaction route involves a metalated intermediate which processes pseudo-nucleophilic character.[38] While in conventional C-N bond construction process, a nucleophilic nitrogen moiety is involved by reacting amines in basic condition. As a result, changing the polarity of nitrogen source by using electrophilic aminating agents in the direct C-H bond amination is a

reasonable strategy which facilitates the coupling reaction between a nucleophilic C-M center and an electrophilic nitrogen source.

1.5.2 Copper-Catalyzed Electrophilic Amination of Aromatic C-H Bond

Miura and co-workerss were the first to report a copper-catalyzed electrophilic amination of oxadiazoles and benzoxazoles under very mild reaction conditions using *N*-chloroamines.[39a] They later further explored the scope of reaction to other electron deficient arenes such as fluorinated benzenes with hydroxylamines as aminating reagents.[39b] (Scheme 1.32)

Scheme 1.32 Copper-catalyzed electrophilic amination of electron deficient arenes

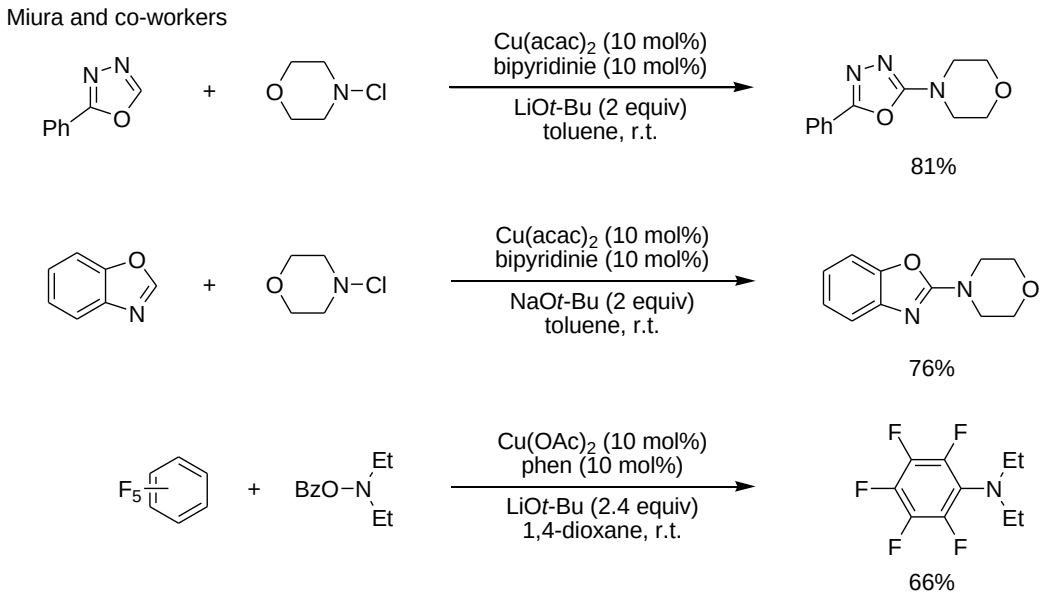

1.5.3 Palladium-Catalyzed Electrophilic Amination of Aromatic C-H Bond

Not long later, Hartwig and co-workers reported the palladium-catalyzed cyclization of *O*-acylbenzoximes for the synthesis of indoles through electrophilic amination approach.[40] It was proposed that the mechanistic cycle begins with the oxidative addition of N-O bond to Pd(0), after tautomerization of the resulting complex, σ-C-H bond of the oxime will be activated and give a cyclopalladated complex. Reductive elimination of the cyclopalladated complex

will give the desired indoles and regenerate the active Pd(0) compelx. The oxidative addition of N-O bond to Pd(0) was confirmed by the isolation of Pd(II) imido complex from the reaction between $Pd(PCy_3)_2$ and an oxime ester containing a pentafluorobenzoyl group. (Scheme 1.33)

Scheme 1.33 Palladium-catalyzed cyclization of *O*-acylbenzoximes for the synthesis of indoles

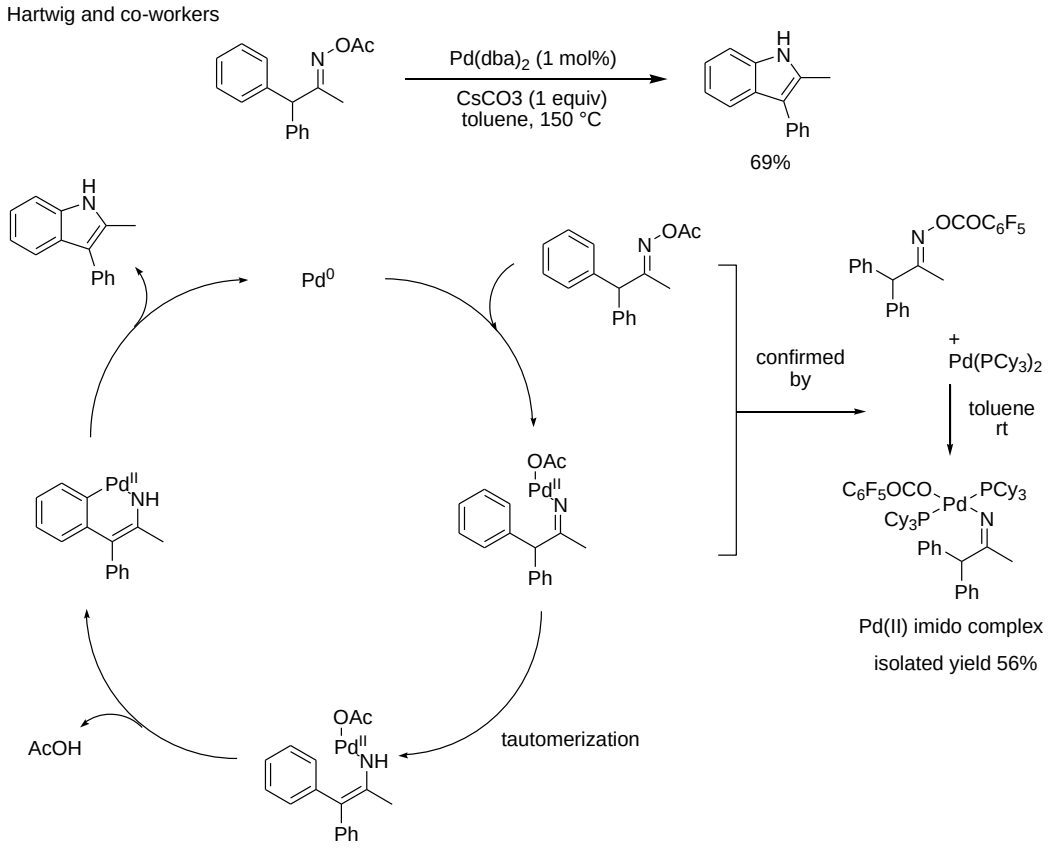

Yu and co-workers reported the electrophilic C-H amination of benzamide using hydroxylamines through a Pd/Ag system. A protocol that involved the in-situ generation of hydroxylamines was also reported.[41] (Scheme 1.34)

Scheme 1.34 Palladium catalyzed electrophilic C-H amination of benzamide

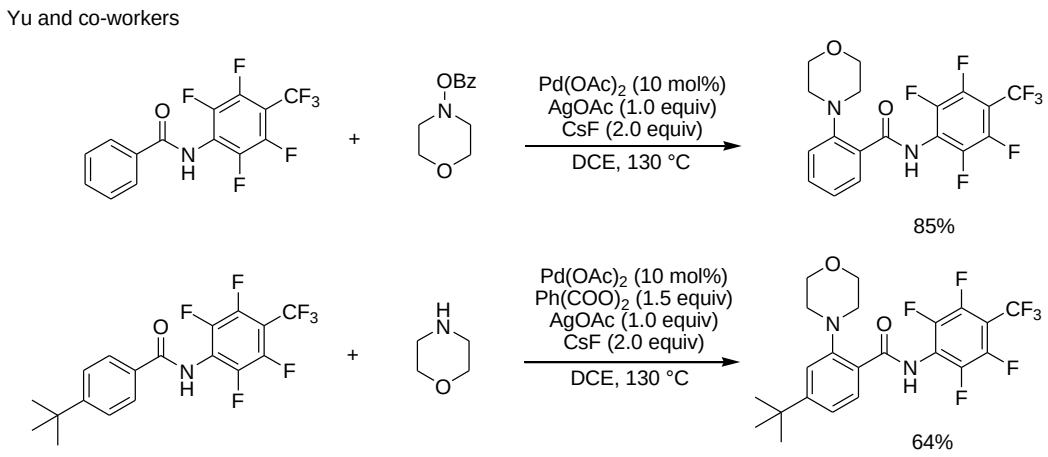

Other electrophilic aminating reagents were also examined. In 2001, Zhang and co-workers reported the palladium-catalyzed electrophilic amination of acetanilides using *N*-fluorobenzenesulfonimide (NFSI). Using 10 mol% $Pd(OAc)_2$ and 2 equiv of $NaHCO_3$, acetanilides could be aminated by NFSI in high yields. *Para* position of the acetanilides must be blocked for *ortho* C-H activation.[42] (Scheme 1.35)

Scheme 1.35 Palladium-catalyzed electrophilic amination of acetanilides using *N*-fluorobenzenesulfonimide

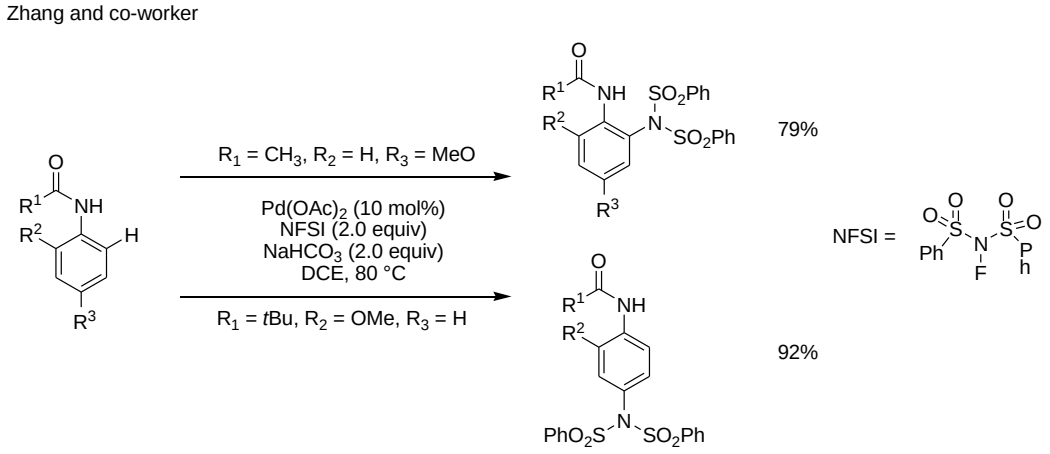

Beside employing oximes and amides as directing group for regioselective C-H functionalization, benzamides and carboxylic acids were also examined. Yu and co-workers reported the palladium-catalyzed σ-C-H amidation of benzamides and benzoic acids. A mechanism which involved the generation of nitrene and migratory insertion into Pd-C bond was proposed.[43] (Scheme 1.36)

Scheme 1.36 Palladium-catalyzed *σ*-C-H amidation of benzoic acids

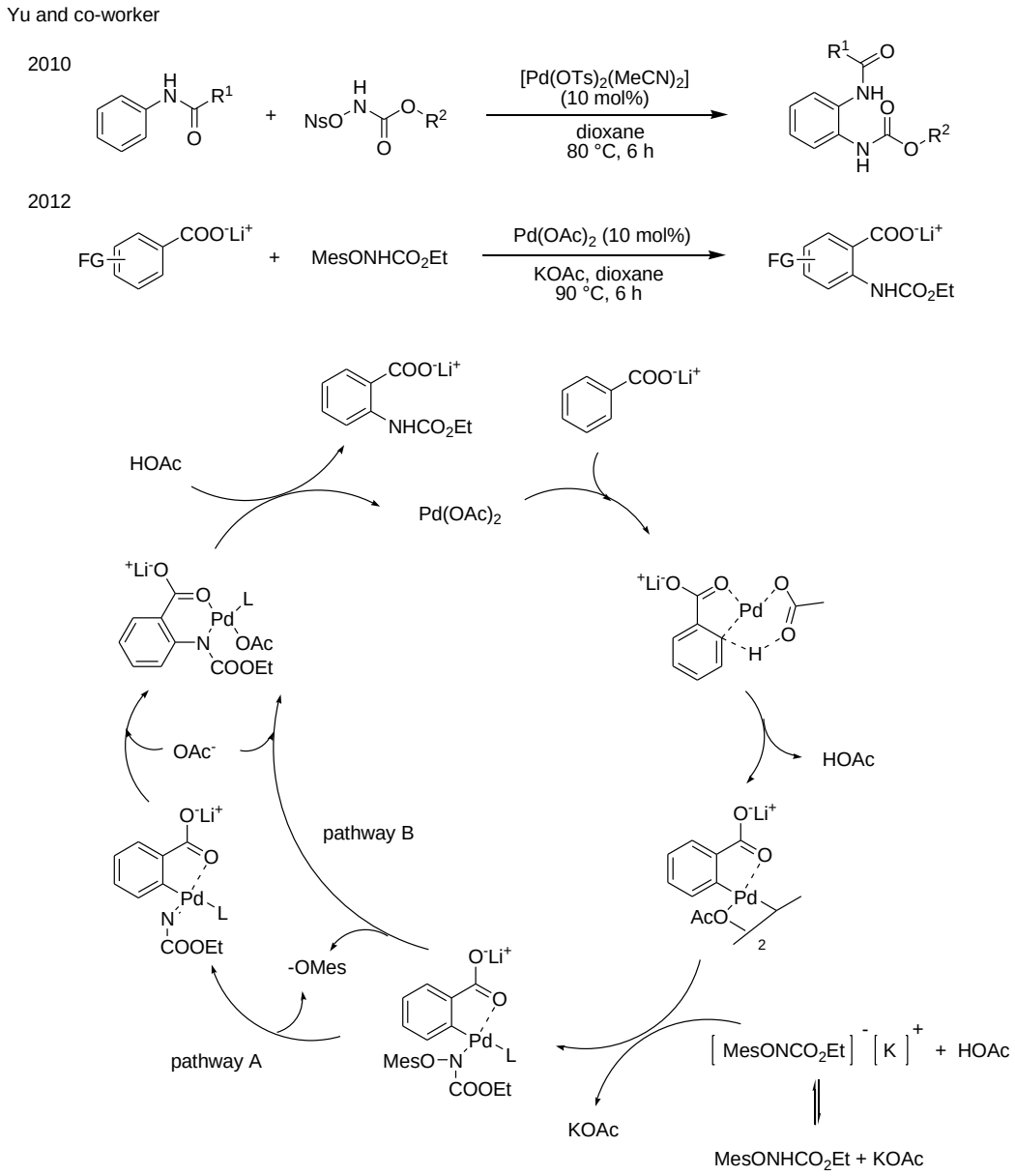

1.5.4 Rhodium-Catalyzed Electrophilic Amination of Aromatic C-H Bonds

1.5.4.1 Early Examples of Rhodium-Catalyzed Electrophilic Amination of Arenes

A pioneering work on Rh-catalyzed electrophilic amination of aromatic C-H bond was reported Yu and Glorius.

Yu and co-workers reported the amination of oxime ethers with secondary amines[44a] and later primary amines[44b] using *N*-chloramines. A cationic Rh species was generated from $[Cp^*RhCl_2]_2$ and $AgSbF_6$, with different amount of CsOAc as base (30 mol% to 1.3 equiv), benzoximes could be aminated by primary and secondary amines. (Scheme 1.37)

Scheme 1.37 Rhodium(III)-catalyzed amination of oxime ethers with secondary amines and primary amines using *N*-chloramines

Yu and co-workers

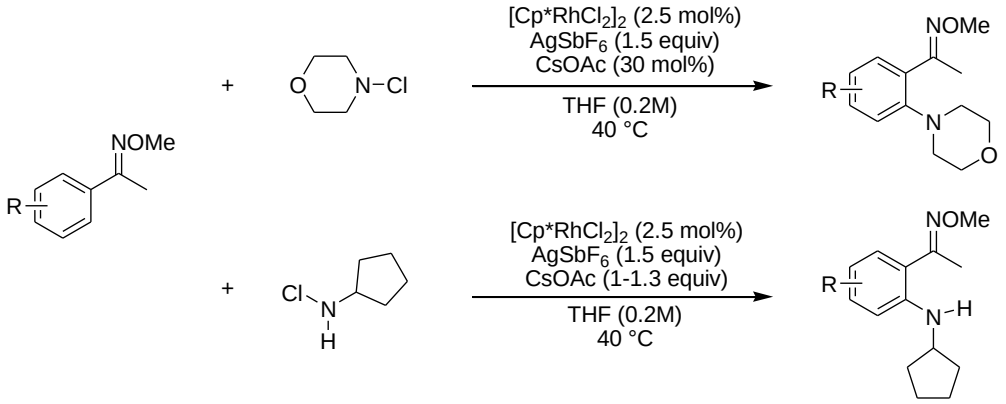

Likewise, Glorius and co-workers reported the amination of oxime ether with *N*-chloramines[45a] and carboxylate-NHBoc derivatives[45b] with the Cp*Rh catalytic system. (Scheme 1.38)

Scheme 1.38 Glorius's work on the Rh(III)-catalyzed electrophilic amination of aromatic C-H bonds

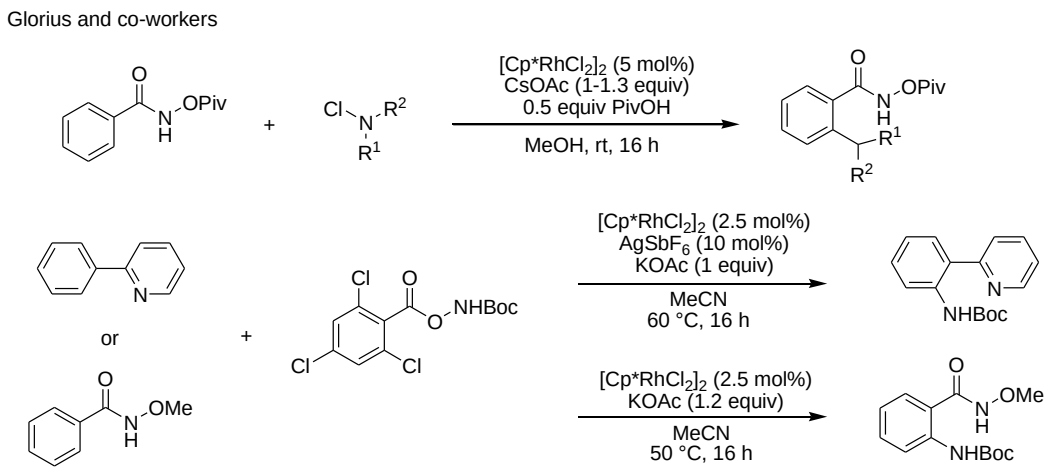

As noted earlier, azides were used as aminating agents for the amination of Grignard reagents and organolithium compounds. In 2012, Chang and co-workers were the first to report the rhodium(III)-catalyzed condensation reaction between benzamides and sulfonyl azide[46a] or aryl azide.[46b] (Scheme 1.39) They later expanded the scope of azides to benzyl and alkyl azides.[46c]

Scheme 1.39 Rhodium(III)-catalyzed condensation reaction between benzamides and sulfonyl azide and aryl azide

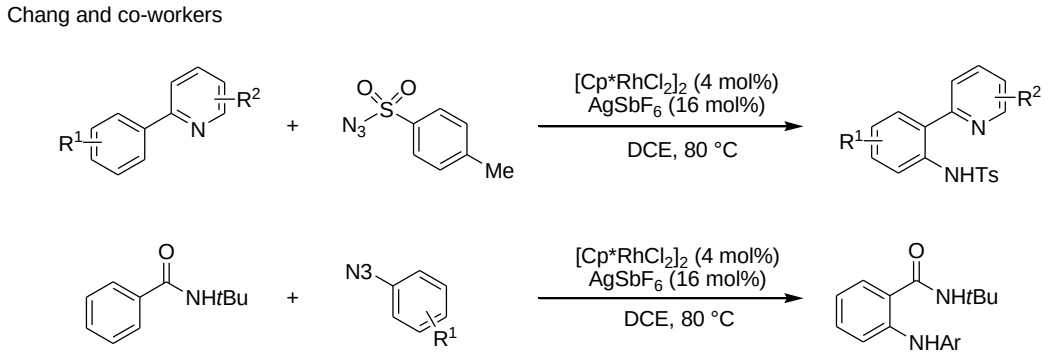

1.5.4.1 Rhodium-Catalyzed Cyclization of Electrophilic Aminating Agents

Previously, Fagnou and coworkers developed the alkyne cycloaddition with benzohydroxamic acids synthesis of isoquinolones.[47] Not long later, Glorius and co-workers achieved the cycloaddition of benzohydroxamic acids with olefins to afford tetrahydroisoquinolinone.[48] It was proposed that the reaction should involve sequential N-H/ C-H deprotonation of the benzohydroxamic acids to give a rhodacycle, followed alkyne migratory insertion. The resulting Rh complex would undergo C-N bond formation via reductive elimination to furnish the cycloaddition product. (Scheme 1.40)

Scheme 1.40 Rhodium-catalyzed cyclization of benzohydroxamic acids with alkynes/alkenes

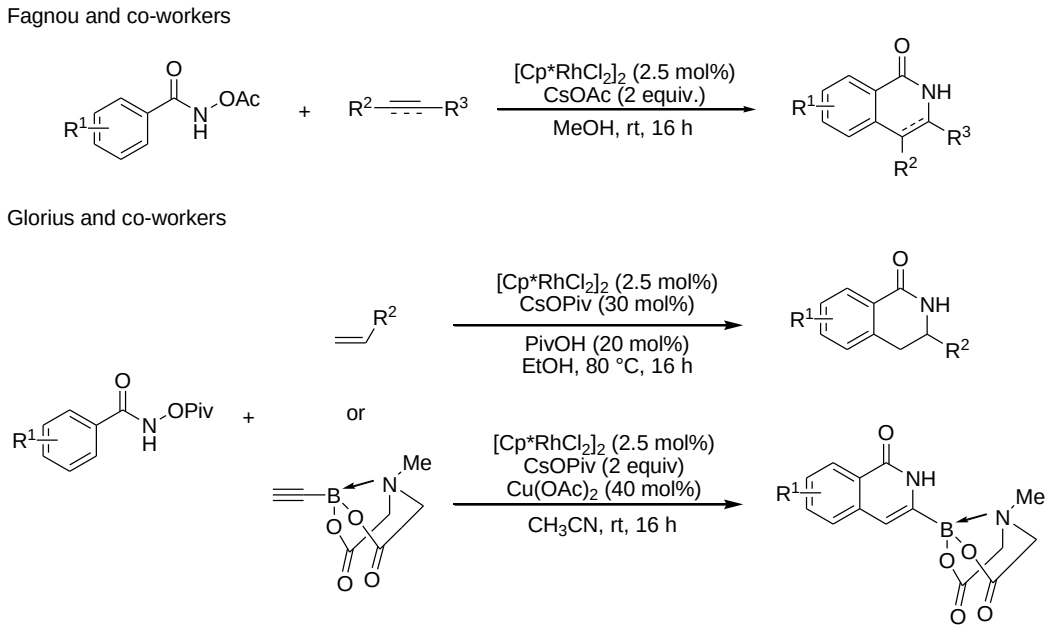

Glorius also reported the cyclization of arylimidates with organoazides through a Rh/Cu catalytic system. It was proposed that the reaction should first initiated by the Rh^{III}-catalyzed amidation of arylimidates. The *σ*-amidated arylimidates should then undergo a Cu^{II}-catalyzed cyclization to give the desired 1*H*-indazoles.[49] (Scheme 1.41)

Scheme 1.41 Rh/Cu catalyzed cyclization of arylimidates for the synthesis of 1*H*-indazoles

Glorius and co-workers

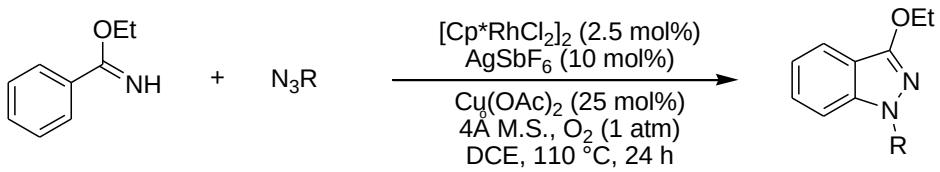

Rovis and co-workers further expanded the scope the cyclization of benzohydroxamic acids. By employing 1 mol% $[Cp^*RhCl_2]_2$ and 20 mol% CsOAc, *O*-pivaloyl benzhydroxamic can be cyclized with diazo compounds to give γ-lactams under very mild conditions.[50] DFT study suggested that the mechanism should go through a sequential N-H/ C-H deprotonation of the benzohydroxamic acids to give a five-membered ring rhodacycle. The electrophilicity of the Rh^{III} center should be enhanced and promote the elimination of di-nitrogen from diazo compound and give a Rh-carbene species. Carbenoid insertion should then be followed. While reductive elimination of such species should not be favorable, instead, a pivalate migration from N to Rh should give raise to a Rh^{V}-nitrenoid intermediates. The C-N bond formation should be followed and give the desired γ-lactams.[51] (Scheme 1.42)

Scheme 1.42 Proposed mechanism for the Rh^{III} catalyzed cyclization of benzohydroxamic acids with diazo compounds to give γ-lactams

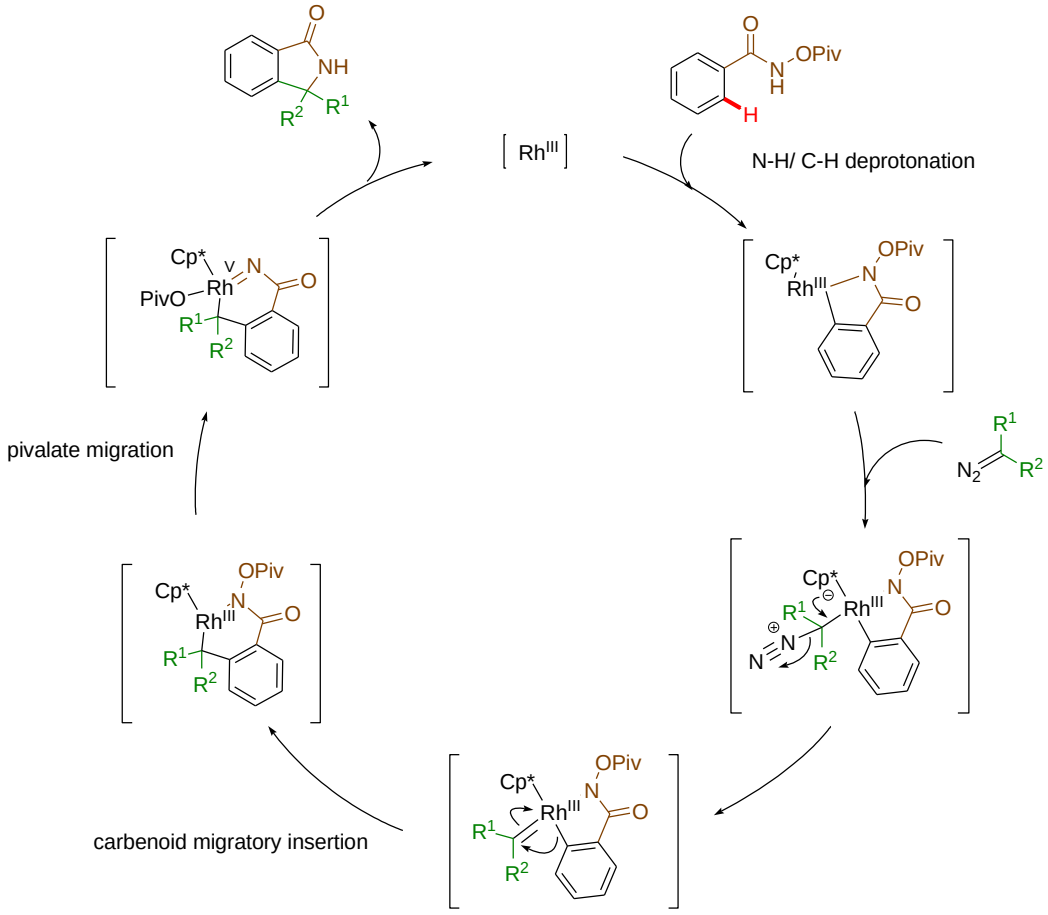

1.5.5 Other Transition Metal-Catalyzed Electrophilic Amination of Aromatic C-H Bond

1.5.5.1 Ruthenium-Catalyzed Electrophilic Amination of Aromatic C-H Bond

In 2013, Ackermann and co-workers reported the ruthenium-catalyzed C-H amidations of heteroaryl arenes using azides. $[RuCl_2(p\text{-cymene})]_2$ (5 mol%) and $AgSbF_6$ (20 mol%) were used for the generation of a cationic ruthenium species which display high catalytic activity for the transformations.[52] At the same year, Yu (JQ) and co-workers reported ruthenium-catalyzed *ortho*-C-H amination of arenes and heteroarenes using hydroxylamines. By employing 10 mol% $[RuCl_2(p\text{-cymene})]_2$ and 2 equiv of K_2CO_3, benzamides could be amidated up to 98% yield under room temperature.[53] (Scheme 1.43)

Scheme 1.43 Ruthenium-catalyzed electrophilic amination of C-H bond

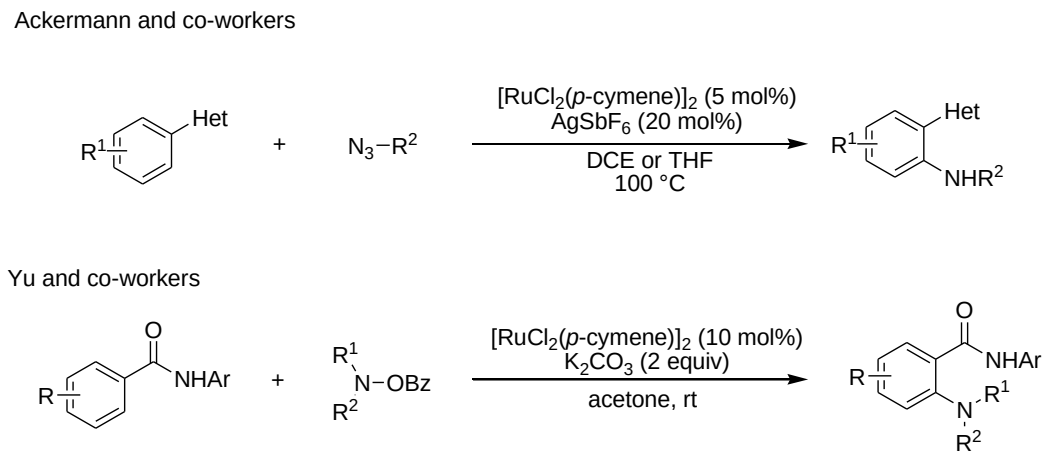

1.5.5.2 Iridium-Catalyzed Electrophilic Amination of Aromatic C-H Bond

Iridium-catalyzed C-H bond functionalization has been gaining great interest due to its high reactivity towards C-H bond. Chang and co-workers demonstrated a Cp*Ir catalytic system could catalyze the C-H amination benzamides. Using 2 mol% $[Cp^*IrCl_2]_2$ and 8 mol% $AgNTF_2$, benzamides could be aminated under room temperature in high yield. Alkenic sp^2 C-H bonds were also aminated under elevated temperature. Notably, an iridacyclic intermediate, which was synthesized from the reaction *2*-phenylpyridine and $[Cp^*IrCl_2]_2$, was employed as catalyst for the reaction between *N*-*t*-butylbenzamides and benzoyl azides in the presence of 4 mol% $AgNTF_2$. The desired product was obtained in

52 % yield, and an cationic Cp*Ir species was believed to be the active species.[54]

(Scheme 1.44)

Scheme 1.44 Iridium-catalyzed C-H amination using benzoyl azides

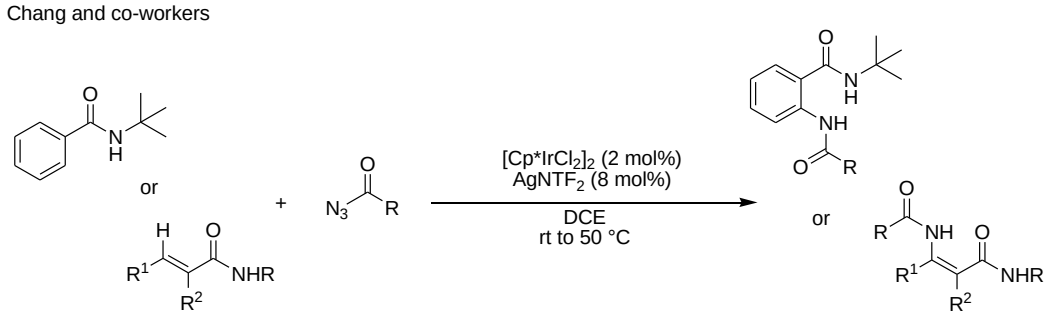

1.6 Aims and Objectives

Formation of C-N bonds is a significant issue in synthetic organic chemistry. In this research, we aim to develop transition metal catalyzed amination/amidation reactions based on the reactivity of electrophilic aminating/amidating reagents.

Conventional C-N bond construction methods such as *N*-alkylation were extensively explored; however, their synthetic value was limited to harsh reaction conditions and over-alkylation. Our initial attention is directed to Rh-catalyzed C-N bond construction using hydroxylamines and benzohydramic acids. The first part of the research is to achieve the synthesis of *N*-alkylanilines and *N*,*N*-dialkylanilines via a Rh^{III}-catalyzed electrophilic amination of arylboronic acids using hydroxylamines. We will explore the electrophilic amidation of arylboronic acids.

From literature report, benzohydroxamic acids could serve as a directing group for *ortho*-selective C-H functionalization and the carboxylate group is an excellent leaving group. Formation of two new bonds in one-pot is challenging in synthetic chemistry. In the second part of our research, we will explore the coupling reaction between benzohydroxamic acids and diazo compounds. It is

anticipated that one new C-C bond and one new C-N bond will be formed and give oxisoindoles as desired product. The reaction mechanism will also be investigated by synthesizing potential reaction intermediates.

In the last part of our research, we will further explore the synthesis of isoindoles via Rh^{III}-catalyzed cyclization reaction. Semicabazones with suitable coordinating strength and good leaving group property will be designed. The reactivity of this newly designed semicabazones will be tested through the Rh^{III}-catalyzed cyclization reaction with alkynes.

Chapter 2

Rhodium(III)-Catalyzed Electrophilic Amination of Arylboronic Acids with O-Carboxyl Hydroxyamines/amides

2.1 Introduction

Aromatic secondary amines are important scaffolds in biologically active compounds, and they are known to serves as antioxidants for rubber manufacturing as well as useful additives for gasoline.[2b] Notably, aromatic secondary amines are important building blocks for synthesis of numerous pharmaceutical compounds (Figure 2.1).[55]

Figure 2.1 Examples of important pharmaceutical compounds

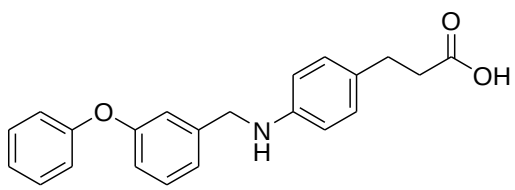

GPR120 Agonists
GW9508

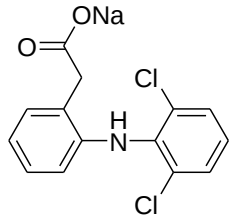

Voltaren

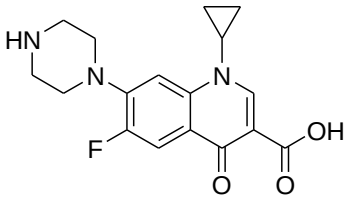

Ciproxin

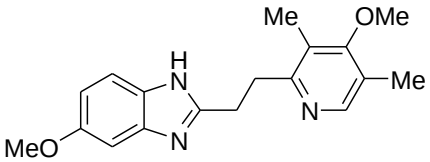

Prilosec

N-Alkylation of anilines is the most common method for synthesizing aromatic secondary amines. In the presence of a base, anilines would react with alkyl halides by nucleophilic displacement to form *N*-alkylanilines. However, over-alkylation remains a major drawback for this transformation.

Buchward and Hartwig have developed a series of Pd catalysts for the synthesis of anilines derivatives.[1,3] These are elegant works but halide functional groups are often not tolerated due to the reactivity of the low-valent palladium species towards halogen groups. Therefore, a general system which is highly efficient, tolerant to a broad spectrum of functional groups and substrate scopes under mild reaction conditions is highly desirable.

Electrophilic (umpolung) amination has been gaining increasing attention for arylamines synthesis under mild conditions.[9] Various aminating reagents such as haloamines and hydroxyamines derivatives were known to be effective reagents for transferring substituted amino groups to nucleophilic organometallics such as organolithium, -magnesium [9-24] and –boranes[59]. Transition metal-catalyzed/mediated electrophilic amination involving aryl boronic acids as nucleophiles under mild conditions are sparse in the literature.[60]

In this chapter, we describe the Cp*Rh(III)-catalyzed cross coupling of arylboronic acids with *O*-benzoyl hydroxylamines for the synthesis of secondary amines.[61] This protocol can also be applied for the synthesis of tertiary amines and amides.

2.2 Results and Discussion

2.2.1 Rhodium-Catalyzed Cross-Coupling Reaction of Arylboronic Acids with *O*-Benzoyl Hydroxylamines for the Synthesis of Secondary Anilines

To begin, *O*-benzoyl-*N*-isopropylhydroxylamine (**1a**) was treated with 6-methoxy-2-naphthaleneboronic acid (**2a**) and [Cp*Rh(OAc)$_2$] (1 mol% Rh) in THF at room temperature for 2 h (Scheme 2.1); the secondary amine **7a** was obtained in 80% yield by ^{1}H NMR analysis of the crude mixture using dibromomethane as internal standard.

Scheme 2.1 Preliminary study

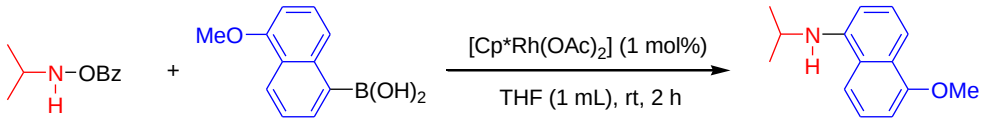

1a (1 equiv) **2a** (1.2 equiv) **7a** (80%)

2.2.1.1 Reaction Optimization

With this encouraging result, we turned to optimize the reaction conditions. The solvent effect was first examined.

Table 2.1 Effect of solvents

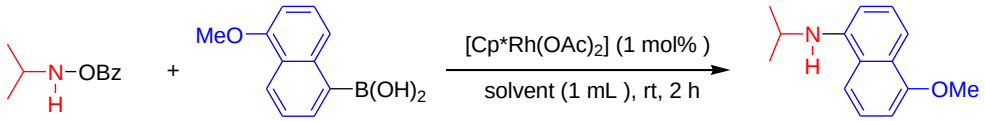

1a **2a** **7a**

entry	solvent	**7a** (%)[a]
1	THF	80
2	DMF	84
3	DCE	45
4	toluene	38
5	MeOH	90
6	1,4-dioxane	85

Reaction conditions: **1a** (0.2 mmol), **2a** (0.24 mmol), $[Cp^*Rh(OAc)_2]$ (1 mol%), solvent (1 mL).
[a]Yields were based on ^1H NMR using dibromomethane as internal standard.

With donor solvents such as tetrahydrofuran, dimethylformamide, methanol and 1,4-dioxane, excellent results were obtained (Table 2.1 entries 1, 2, 5, 6). However, when weakly coordinating solvents such as DCE and toluene were employed, only moderate **7a** formation was obtained (entries 3 and 4). We later found that methanol gave the best result and became the solvent of choice.

Table 2.2 Effect of temperature and catalyst loading

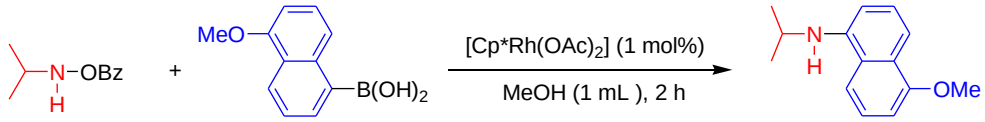

1a **2a** **7a**

entry	catalyst loading (%)	temperature (°C)	**7a** (%)[a]
1	1	rt	90
2	1	40	55
3	0.25	rt	88

Reaction conditions: **1a** (0.2 mmol), **2a** (0.24 mmol), [Cp*Rh(OAc)$_2$] (1 mol%). [a]Yield based on ^{1}H NMR using dibromomethane as internal standard.

When the reaction temperature was raised to 40 °C, the product yield diminished to 55% (Table 2.2 entry 2). This may probably be attributed to the decomposition of **1a**. Lowering the catalyst loading to 0.25 mol% did not adversely affect the product yield (entry 3). Having the optimized reaction conditions (Table 2.2 entry 3), we proceeded to examine the substrate scope of the reaction.

2.2.1.2 Scope and Limitation

Table 2.3 Substrate scope of arylboronic acids

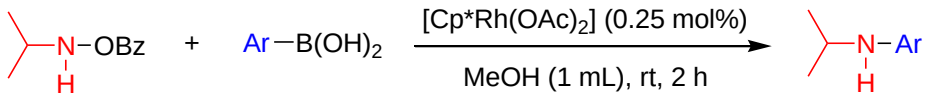

1a **2** **7**

entry	**1**	**2**	yield (%)[a]
1	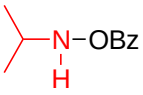 **1a**	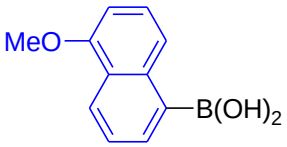 **2a**	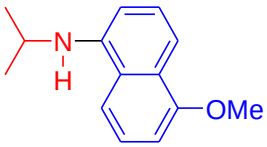 **7a**, 90
2	**1a**	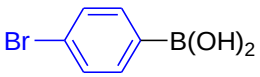 **2b**	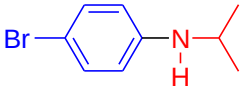 **7b**, 86
3	**1a**	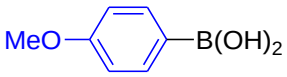 **2c**	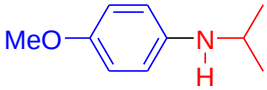 **7c**, 42
4	**1a**	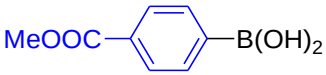 **2d**	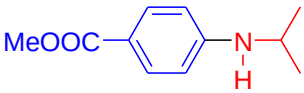 **7d**, 75
5	**1a**	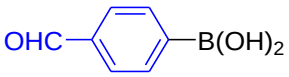 **2e**	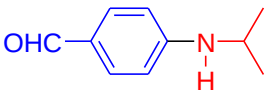 **7e**, 90
6	**1a**	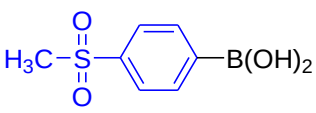 **2f**	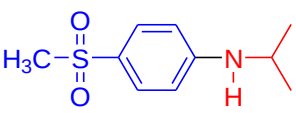 **7f**, 44

7	**1a**	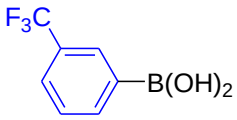 **2g**	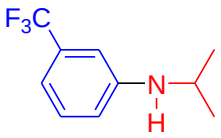 **7g**, 56
8	**1a**	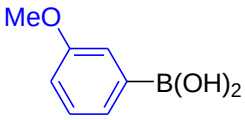 **2h**	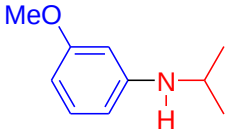 **7h**, 60
9	**1a**	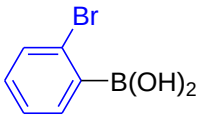 **2i**	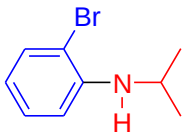 **7i**, 30

Reaction conditions: **1a** (0.2 mmol), **2** (0.24 mmol), [Cp*Rh(OAc)$_2$] (0.25 mol%). [a]Isolated yield.

Table 2.3 shows the scope of arylboronic acids for the Rh(III)-catalyzed amination reaction. Electron-releasing and -withdrawing substituents on the arylboronic acids (-OMe, -Br, -CF_3) were well tolerated, and their reaction with **1a** gave the corresponding secondary anilines in 30% - 86% yields (Table 2.3, entries 2, 3 7, 8 and 9). Other functional groups such as esters, aldehydes and methylsulfones were also well tolerated and the arylboronic acid reacted with *O*-benzoyl-*N*-isopropylhydroxylamine (**1a**) to furnish the desired secondary anilines in 44% to 90% yields (entries 4 – 6). Sterically hindered 2-bromophenylboronic acid (**2i**) was a less effective substrate, yet **7i** can be obtained in 30% yield.

Table 2.4 Substrate scope of *N*-alkylhydroxylamines

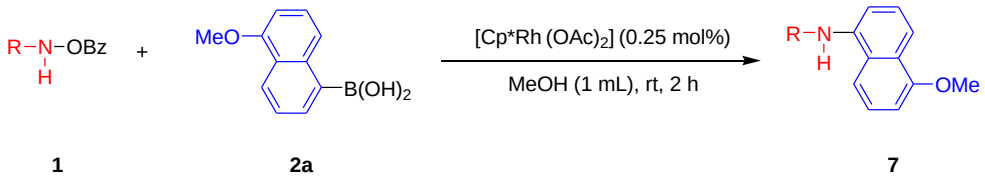

1 **2a** **7**

entry	**1**	**2**	yield (%)[a]
1	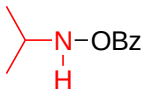 **1a**	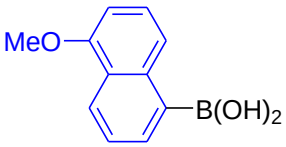 **2a**	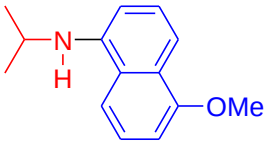 **7a**. 90
2	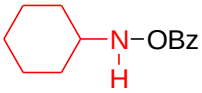 **1b**	**2a**	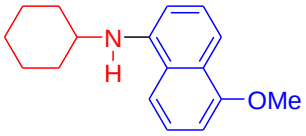 **7j**, 85
3	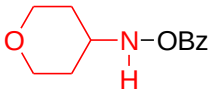 **1c**	**2a**	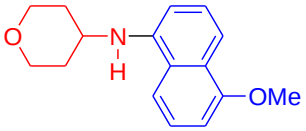 **7k**, 78
4	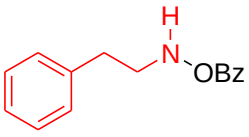 **1d**	**2a**	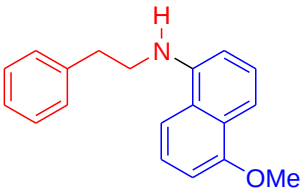 **7l**, 40

5	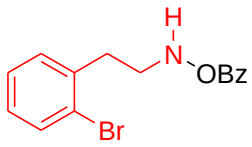 **1e**	**2a**	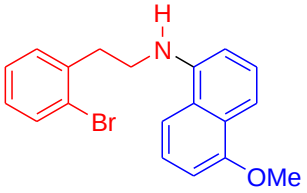 **7m**, 60
6	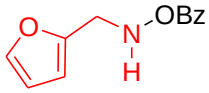 **1f**	**2a**	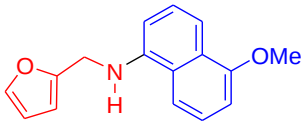 **7n**, 85

Reaction conditions: **1** (0.2 mmol), **2a** (0.24 mmol), [Cp*Rh(OAc)$_2$] (0.25 mol%). [a]Isolated yield.

The scope of the *O*-benzoylhydroxylamines is depicted in Table 2.4. Aliphatic acyclic and cyclic *O*-benzoylalkylhydroxylamines (**1a** and **1b**) reacted smoothly with **2a** to afford the corresponding amines in 85% - 90% yields (Table 2.4 entries 1 and 2). *O*-Benzoylhydroxylamine (**1c**) containing a cyclic ether moiety is a good substrate for reacting with **2a** to furnish the amine product in 78% yield (entry 3). Fused heterocycles compounds such as indolines are important building blocks for pharmaceutical and natural products.[56] Indolines can be synthesized by intramolecular amination of 2-phenethylamine derivatives.[57] Reacting *O*-benzoyl-*N*-2-bromophenethylhydroxylamine (**1e**) with **2a** afforded **7m** in 60% yield. In this work, when **7m** was further subjected to the Pd-catalyzed Buchward-Hartwig amination reaction, the indoline products **7v** was obtained in 85% yield (Scheme 2.2). *O*-Benzoylhydroxylamine with a furan

moiety (**1f**) was also effective substrate and gave the corresponding amine **7n** in 85% yield.

Scheme 2.2 Buchward-Hartwig amination of **7m**

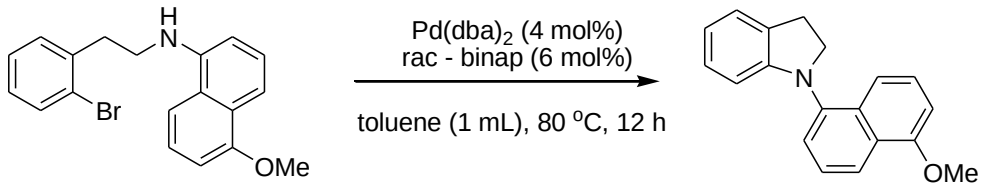

7m **7v**

85%

2.2.2 Rhodium-Catalyzed Cross-Coupling Reaction of Arylboronic Acids with *O*-Benzoyl Hydroxylamines for the Synthesis of *N*,*N*-Dialkyl Anilines

Apart from the arylation of *N*-alkylhydroxylamines, *N*,*N*-dialkylhydroxylamines were also tested as substrates for this Rh-catalyzed amination. Table 2.5 shows the scope of Rh(III)-catalyzed arylation of *N*, *N*-dialkylhydroxylamines.

Table 2.5 Scope of *N*, *N*-dialkylhydroxylamines

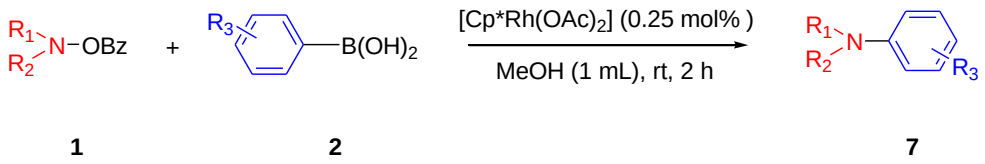

1 **2** **7**

entry	**1**	**2**	yield (%)[a]
1	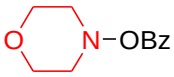 **1g**	**2b**	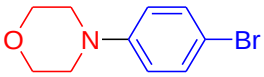 **7o**, 86
2	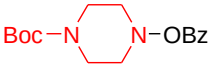 **1h**	**2b**	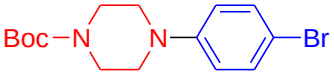 **7p**, 80
3	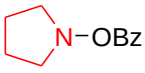 **1i**	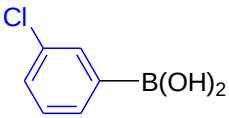 **2j**	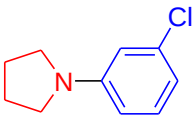 **7q**, 71
4	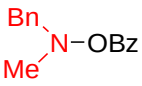 **1j**	**2b**	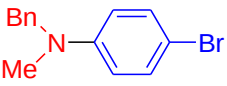 **7r**, 72

5	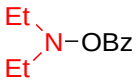 **1k**	**2b**	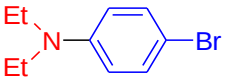 **7s**, 47
6	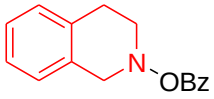 **1l**	 **2k**	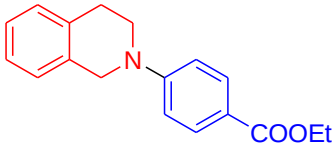 **7t**, 75
7	**1l**	**2b**	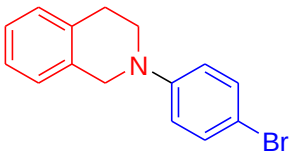 **7u**, 84

Reaction conditions: **1** (0.2 mmol), **2** (0.24 mmol), [Cp*Rh(OAc)$_2$] (0.25 mol%).

[a]Isolated yield.

With [Cp*Rh(OAc)$_2$] (0.25 mol%) as catalyst and **2** as coupling partner, *N*,*N*-dialkylhydroxylamines (**1g** – **1l**) reacted smoothly to give the corresponding tertiary amines in 47% - 86% yields (Table 2.5). These results are comparable to the Cu-catalyzed arylation of *N*, *N*-dialkylhydroxylamines.

2.2.3 Rhodium-Catalyzed Cross-Coupling Reaction of Arylboronic Acids with *O*-Acetyl Hydroxamic Acids for the Synthesis of Secondary Benzamides

Following the successful coupling reactions of arylboronic acids with *N*,*N*-dialkylhydroxylamines and *N*-alkylhydroxylamines, we further explored the coupling reaction between arylboronic acids with *O*-acetyl hydroxamic acids. In our initial attempts, *O*-acetyl benzohydroxamic acid (**3a**) was treated with phenylboronic acid (**2k**) in the presence of [Cp*Rh(OAc)$_2$] (5 mol%) in methanol at room temperature for 4 h. Benzanilide (**8a**) was obtained in 17% yield (Scheme 2.3). The product was characterized by ^{1}H NMR with reference to the literature data.

Scheme 2.3 Preliminary study

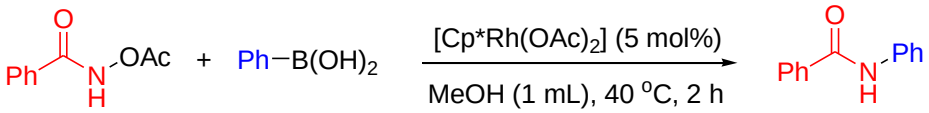

3a **2k** **8a**

17%

2.2.3.1 Reaction Optimization

With this preliminary finding, we proceed to optimization reaction.

Table 2.6 Solvent effect

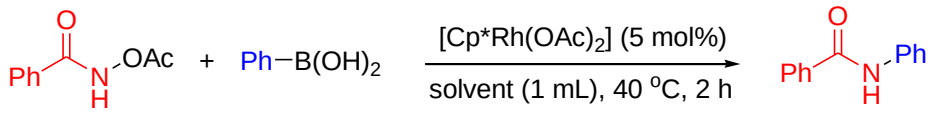

3a **2k** **8a**

entry	solvent	**8a** (%)[a]
1	MeOH	17
2	1,4-dioxane	82
3	toluene	30
4	THF	87
5	DMF	0
6	DCM	0

Reaction conditions: **3a** (0.2 mmol), **2k** (0.3 mmol), [Cp*Rh(OAc)$_2$] (5 mol%), solvent (1 mL). [a]Yields were based on ^{1}H NMR using dibromomethane as internal standard.

Table 2.6 shows the solvent effect for the Rh-catalyzed reaction between *O*-acetyl benzohydroxamic acid (**3a**) and phenylboronic acid (**2k**). Excellent yields of **8a** were obtained with 1,4-dioxane and THF as solvent. (Table 2.6, entries 2 and 4) The use of methanol and toluene as solvent resulted in moderate product yields (entries 1 and 3). However, when DMF and DCM were employed, no desirable product (**8a**) was observed.

Table 2.7 Leaving group effect

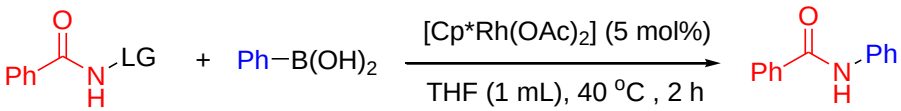

3 **2k** **8a**

entry	leaving group	**8a** (%)[a]
1	-OAc	87
2	-OPiv	80
3	-OMe	60

Reaction conditions: **3** (0.2 mmol), **2k** (0.3 mmol), [Cp*Rh(OAc)$_2$] (5 mol%).

[a]Yields were based on ^{1}H NMR using dibromomethane as internal standard.

The effect of the leaving group on the benzohydroxamic acid was also studied. Carboxylate-type leaving groups such as –OAc and –OPiv (Table 2.7, entries 1 and 2) gave **8a** in excellent yield. *N*-Methoxybenzamide also reacted with **2k** to give the desired product. However, only 60% yield of **8a** was obtained. Based on these findings, -OAc was chosen as the leaving group on the benzohydroxamic acid.

Table 2.8 Effect of the loading of arylboronic acid

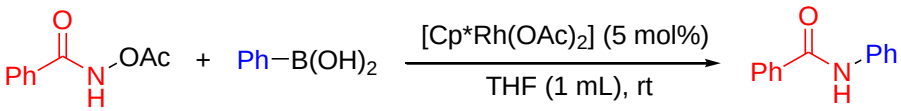

3a **2k** **8a**

entry	loading of **2k** (equiv)	time	**8a**[a] (%)
1	1.5	2	87
2	1.1	18	59
3	1.1	24	62

Reaction conditions: **3a** (0.2 mmol), **2k**, [Cp*Rh(OAc)$_2$] (5 mol%).

[a]Yields were based on ^{1}H NMR using dibromomethane as internal standard.

At the beginning of the screening study, 1.5 equiv of **2k** were used to ensure complete consumption of the starting material **3a** (Table 2.8 entry 1). Hoping to develop a more economical protocol, we employed 1.1 equiv of **2k** for the coupling reaction (entries 2 and 3). However, only 62% yield of **8a** yields were obtained even after 24 h reaction.

Table 2.9 Effect of catalyst loading and temperature

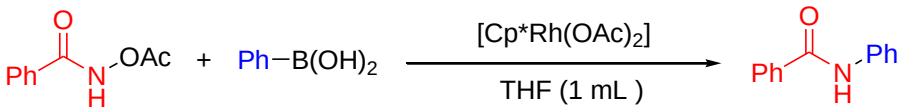

3a **2k** **8a**

entry	catalyst loading (%)	temp (^{o}C)	time	**8a** (%)[a]
1	5	40	2	87
2	5	rt	2	80
3	1	40	4	88
4	1	rt	4	70
5	1	rt	18	73

Reaction conditions: **3a** (0.2 mmol), **2k** (0.3 mmol), [Cp*Rh(OAc)$_2$] (5 mol%).

[a]Yields were based on ^{1}H NMR using dibromomethane as internal standard.

To our delight, lowering the catalyst loading to 1 mol% still produced comparable product yields if a longer reaction time (14 h) was employed (Table 2.9, entries 1 and 3). The reaction can be run at room temperature with 5 mol% Rh catalyst, and **8a** was produced in 80% yield (entry 2). However, when the analogous reaction was performed with 1 mol% Rh catalyst at room temperature, only 70% of **8a** was obtained. No further improvement was achieved even running the reaction for 18 h (entry 5).

2.2.3.2 Scope and Limitation

Table 2.10 Substrate scope of arylboronic acids

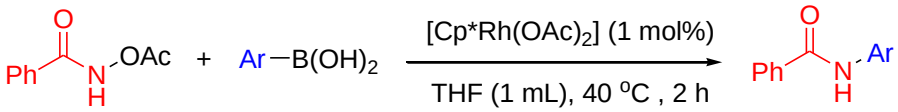

3a **2** **8**

entry	**3**	**2**	yield (%)[a]
1	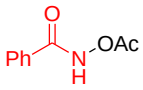 **3a**	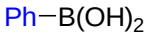 **2k**	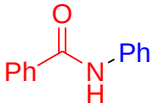 **8a**, 82
2	**3a**	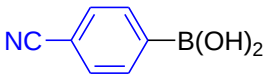 **2l**	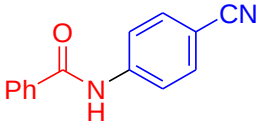 **8b**, 85
3	**3a**	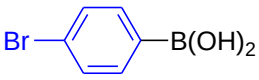 **2b**	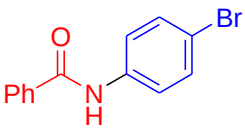 **8c**, 95
4	**3a**	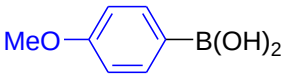 **2c**	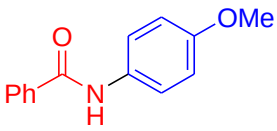 **8d**, 90
5	**3a**	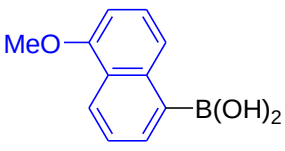 **2a**	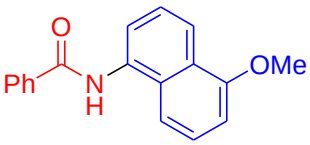 **8e**, 68

6	**3a**	 **2d**	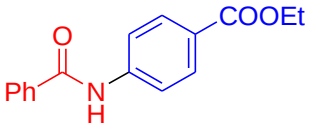 **8f**, 97
7	**3a**	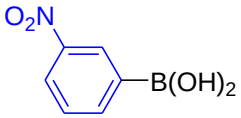 **2m**	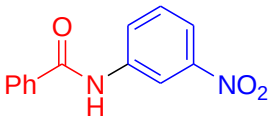 **8g**, 76
8	**3a**	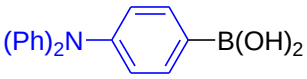 **2n**	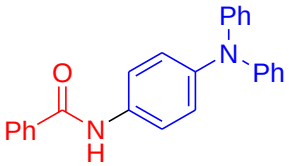 **8h**, 76
9	**3a**	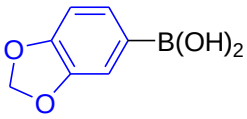 **2o**	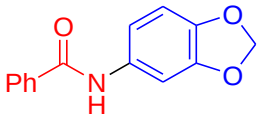 **8i**, 90
10	**3a**	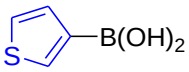 **2p**	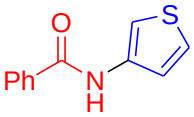 **8j**, 75
11	**3a**	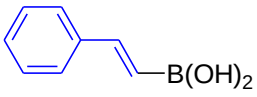 **2q**	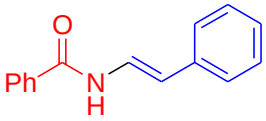 **8k**, 52[b]

Reaction conditions: **3a** (0.2 mmol), **2** (0.3 mmol), [Cp*Rh(OAc)$_2$] (1 mol%). [a]Isolated yield. [b]5 mol% [Cp*Rh(OAc)$_2$] was employed.

Table 2.10 depicts the substrate scope of arylboronic acids for the Rh(III)-catalyzed amidation reaction. Electron-releasing and -withdrawing

substituents on the arylboronic acids (-OMe, -CN, -Br, -COOEt) were well tolerated, and the corresponding amides were formed in 85% – 97% yields (Table 10, entries 2 – 4 and 6). Sterically bulky 6-methoxy-2-naphthaleneboronic acid (**2a**) reacted under the Rh-catalyzed amidation to give **8e** in 68% yield. Arylboronic acids containing substituents such as nitro (**2m**), methylenedioxy (**2n**) and diphenylamino (**2o**) are effective coupling partners, which were transformed to give the corresponding amides in 76% - 90% yields. Notably, heterocyclic arylboronic acid **2p** was also effective coupling partner for the reaction. The corresponding amide **8j** was obtained in 75% yield. Synthetically useful enamide can also be synthesized by this protocol. When trans-2-phenylvinylboronic acid (**2q**) was allowed to react with **3a**, *N*-styrylbenzamide (**8k**) was formed in 52% yield.

Table 2.11 Substrate scope of *O*-acetyl hydroxamic acids

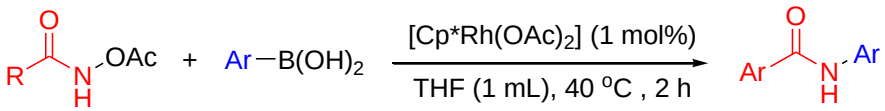

3 **2** **8**

entry	**3**	**2**	yield (%)[a]
1	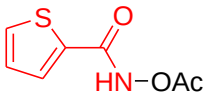 **3b**	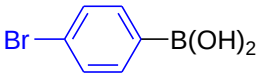 **2b**	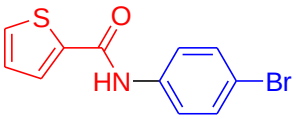 **8l**, 75
2	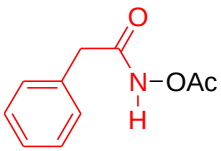 **3c**	**2b**	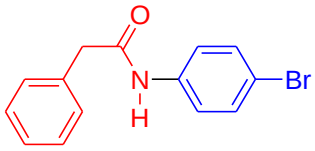 **8m**, 89
3	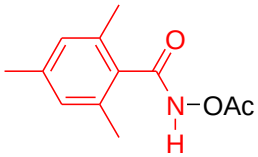 **3d**	**2b**	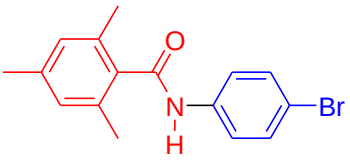 **8n**, 85

Reaction conditions: **3a** (0.2 mmol), **2** (0.3 mmol), [Cp*Rh(OAc)$_2$] (1 mol%). [a]Isolated yield.

The substrate scope of *O*-acetyl hydroxamic acids was shown in Table 2.10. *O*-Acetyl hydroxylamide bearing a heterocylic moiety such as thiophene was a good substrate for the reaction. Substrate **3b** reacted with 4-bromophenylboronic acid (**2b**) to give the corresponding amide (**8l**) in 75% yield. *N*-(acetyloxy)-benzeneacetamide (**3c**) which contains an alkyl chain also reacted

smoothly with **2b** to give **8m** in 89% yield. Sterically hindered substrate did not present a challenge in this reaction. Substrate **3d** reacted with **2b** to give **8n** in 85% yield.

2.2.4 Proposed Mechanism

We proposed that this reaction should begin with the transmetallation of with arylboronic acids to Cp*Rh(OAc)$_2$ to form an arylrhodium complex A (Scheme 2.4). Hydroxylamines should then undergo ligand exchange and coordinate to the rhodium complex to give complex **B**. Aryl migration to the nitrogen atom of hydroxylamines should give the desired product. The benzoyl group of the hydroxylamines should assist trasmetallation of another arylboronic acid to regenerate the reactive arylrhodium complex **A**.

Scheme 2.4 Proposed mechanism

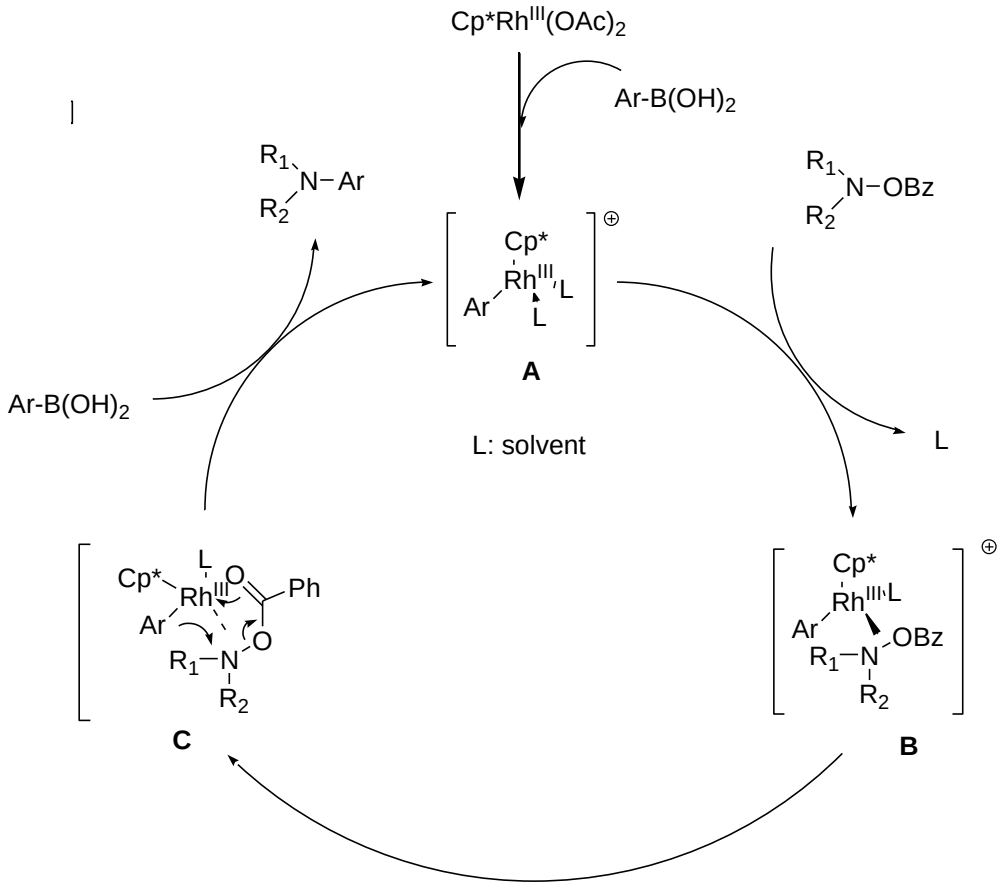

To test this hypothesis, we synthesized Cp*Rh(Ph)Cl(PPh_3) by reacting one equivalent of Cp*$RhCl_2$(PPh_3) with five equivalents of phenylboronic acids in NEt_3 and THF. The reaction mixture was purified by flash column chromatography.[58]

Cp*$RhCl_2$(PPh_3) was employed to catalyze the coupling reaction between **1b** and **2a** in the presence of silver acetate (Scheme 2.5). The desired product **7j** was obtained in 80% yield. This result demonstrates that the triphenylphosphine

will not hinder the catalytic cycle.

Scheme 2.5 Cp*$RhCl_2(PPh_3)$ catalyzed coupling reaction of **1b** with **2a**

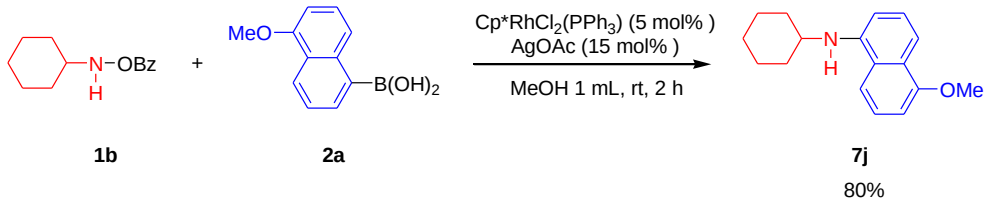

1b **2a** **7j**

80%

The coupling reaction between **1b** and **2a** by employing Cp*Rh(Ph)Cl(PPh_3) as catalyst was conducted. Consistent with our hypothesis, *N*-cyclohexylaniline was obtained in catalytic amount which was observed by GMCS and 80% of **7j** was obtained (Scheme 2.6).

Scheme 2.6 Cp*Rh(Ph)Cl(PPh_3) catalyzed coupling reaction of **1b** with **2a**

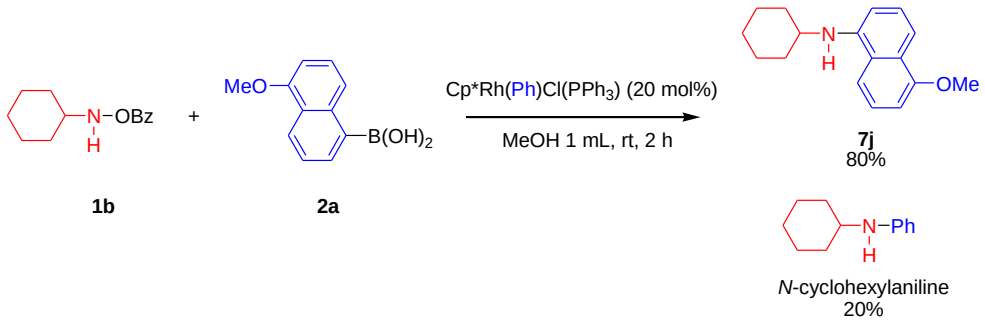

1b **2a** **7j**

80%

N-cyclohexylaniline

20%

2.3 Concluding Summary

In conclusion, we accomplished the Rh(III)-catalyzed amination and amidation of arylboronic acids using hydroxylamines and benzohydroxamic acids for the synthesis of anilines and amides.

For the amination of arylboronic acids using *N*-alkylhydroxylamines, functional groups such as halogens, methoxy, sulfonyl, aldehydes, ketones and esters were well tolerated, and the corresponding anilines were obtained in good yields. Apart from *N*-alkylhydroxylamines, *N*, *N*-dialkylhydroxylamines can be coupled with arylboronic acids to give the corresponding amines in good yields.

For the amidation of arylboronic acids using benzohydroxamic acids, both electron-releasing and –withdrawing substituents and some problematic substituents such as amino, nitro groups on the arylboronic acids were well tolerated and gave the desired amides in good yields. Alkenylboronic acids and heterocyclic arylboronic acids were effective coupling partners for the reaction.

The reaction were proposed to be initiated by the transmetallation of arylboronic acids to $Cp^*Rh(OAc)_2$ to form an arylrhodium complex. Hydroxylamines should then coordinate to this resulting arylrhodium complex. Subsequence aryl migration to the nitrogen atom of hydroxylamines should give the desired product.

$Cp^*Rh(Ph)Cl(PPh_3)$ was synthesized to test the catalytic activity of an arylrhodium complex. It was found that 20 mol% of $Cp^*Rh(Ph)Cl(PPh_3)$ successfully catalyzed the coupling reaction between **1b** and **2a** to give the desired **7j** in 80% yield.

2.4 Experimental Section

2.4.1 General Experimental

All the arylboronic acids were obtained from commercial sources and used without purification. All the solvents used were obtained from commercial sources and were distillated according to literature method. *O*-Benzoylhydroxylamines were prepared from its corresponding amines and benzoyl peroxide following a literature procedure with modification. *O*-Acetylbenzohydroxamic acids were synthesized according to the literature method. Cp*Rh$(OAc)_2$ was synthesized by literature procedure.

Thin layer chromatography was performed on silica gel plates. Silica gel (Merck, 230 - 400 mesh) was used for flash column chromatography. ^{1}H and ^{13}C NMR spectra were recorded on a Brüker (400 MHz) NMR spectrometer. The chemical shift (δ) values are given in parts per million (ppm) with multiplicity (s = singlet, d = doublet, t = triplet, q = quartet, m = multiplet, td = triplet of doublets) and are referenced to residual solvent peaks. Coupling constants (J) were reported in Hertz (Hz). Melting points were measured on a Büchi Melting Point B - 545 machine. Mass spectra and high resolution mass spectra (HRMS)

were obtained on a VG MICROMASS Fison VG platform, a Finnigan Model Mat 95 ST instrument, or a Brüker APEX 47e FT - ICR mass spectrometer.

2.4.2 Experimental Procedures and Physical Characterization

2.4.2.1 Preparation of *O*-Benzoylhydroxylamines

Benzoyl peroxide (10 mmol, 1 equiv) was dissolved in dichloromethane (25 mL). Buffer solution (25 mL) at pH 10.5 (from sodium hydrogencarbonate and sodium hydroxide) was added to form a biphasic solution. The corresponding amine (10 mmol, 1 equiv) was then added. The resulting reaction mixture was then stirred at room temperature and was monitored by TLC. Upon complete consumption of the starting material, the reaction mixture was extracted by DCM (3 x 10 mL). After washing with saturated brine solution (3 x 10 mL), the combined organic extracts were dried over $MgSO_4$ and concentrated by rotary evaporation. The residue was purified by flash chromatography to afford the *O*-benzoylhydroxylamines.

_O_-Benzoyl-_N_-isopropylhydroxylamine (1a)

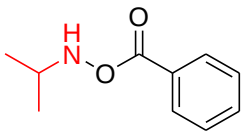

Eluant: *n*-hexane – ethyl acetate (9:1 v/v) The product was obtained as a colorless liquid (85 % yield). ^{1}H NMR (400 MHz, $CDCl_3$): δ_H 8.03 (d, *J* = 7.2 Hz, 2H), 7.69 (bs, 1H), 7.59 (t, *J* = 7.4 Hz, 1H), 7.46 (t, *J* = 7.6 Hz, 2H), 3.41 – 3.35 (m, 1H), 1.20 (d, *J* = 6.4 Hz, 6H) ^{13}C NMR (100 MHz, $CDCl_3$): δ_C 166.9, 133.3, 129.3, 128.5, 52.4, 20.0

_O_-Benzoyl-_N_-cyclohexylhydroxylamine (1b)

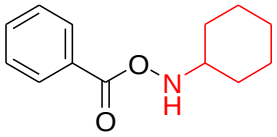

Eluant: *n*-hexane – ethyl acetate (9:1 v/v) The product was obtained as a colorless liquid (85 % yield). ^{1}H NMR (400 MHz, $CDCl_3$): δ_H 8.02 (d, *J* = 7.2 Hz, 2H), 7.73 (bs, 1H), 7.58 (t, *J* = 7.4 Hz, 1H), 7.45 (t, *J* = 7.6 Hz, 2H), 3.05 (m, 1H), 1.98 – 1.96 (m, 2H), 1.81 – 1.79 (m, 2H), 1.66 – 1.63 (m, 2H), 1.36 – 1.18 (m, 4H) ^{13}C NMR (100 MHz, $CDCl_3$): δ_C 167.0, 133.3, 129.3, 128.54, 128.51, 59.9, 30.3, 25.8, 24.5

_O_-Benzoyl-_N_-tetrahydropyranylhydroxylamine (1c)

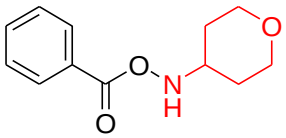

Eluant: *n*-hexane – ethyl acetate (9:1 v/v) The product was obtained as a colorless liquid (75 % yield). ^{1}H NMR (400 MHz, $CDCl_3$): δ_H 8.02 (d, *J* = 7.2 Hz, 2H), 7.59 (t, *J* = 6.8 Hz, 1H), 7.46 (t, *J* = 7.8 Hz, 2H), 4.05 – 4.00 (dt, *J* = 11.6 Hz, 2H), 3.48 – 3.41 (m, 2H), 3.35 – 3.27 (m, 1H), 1.93 – 1.89 (dd, *J* = 12.4, 2H), 1.69 – 1.59 (m, 2H) ^{13}C NMR (100 MHz, $CDCl_3$): δ_C 166.9, 133.5, 129.4, 128.6, 128.2, 66.2, 57.0, 30.5

_O_-Benzoyl-_N_-phenethylhydroxylamine (1d)

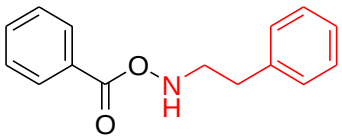

Eluant: *n*-hexane – ethyl acetate (9:1 v/v) The product was obtained as a colorless liquid (70 % yield). ^{1}H NMR (400 MHz, $CDCl_3$): δ_H 8.01 (d, *J* = 7.6Hz, 2H), 7.59 (t, *J* = 7.4 Hz, 1H), 7.46 (t, *J* = 7.6 Hz, 2H), 7.32 (t, *J* = 7.4 Hz, 2H), 7.25 (d, *J* = 7.6 Hz, 3H), 3.44 (t, *J* = 7.2 Hz, 2H), 2.97 (t, *J* = 7.2 Hz, 2H) ^{13}C NMR (100 MHz, $CDCl_3$): δ_C 166.9, 138.9, 133.5, 129.5, 128.9, 128.8, 128.7, 128.6, 126.7, 53.8, 34.0

_O_-Benzoyl-_N_-2-bromophenethylhydroxylamine (1e)

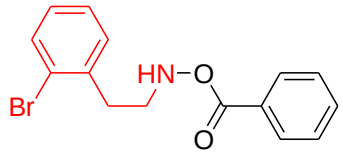

Eluant: *n*-hexane – ethyl acetate (9:1 v/v) The product was obtained as a colorless liquid (62 % yield). ^{1}H NMR (400 MHz, $CDCl_3$): δ_H 8.02 (d, *J* = 7.2 Hz, 2H), 7.885 (bs, 1H) 7.61 – 7.55 (m, 2H), 7.46 (t, *J* = 7.8 Hz, 2H), 7.30 – 7.24 (m, 2H), 7.12 – 7.08 (m, 1H), 3.44 (t, *J* = 7.0 Hz, 2H) 3.11 (t, *J* = 7.2 Hz, 2H) ^{13}C NMR (100 MHz, $CDCl_3$): δ_C 166.7, 138.2, 133.4, 133.1, 131.0, 129.4, 128.5, 128.4, 128.3, 127.6, 124.6, 52.0, 34.4

_O_-Benzoyl-_N_-furfurylhydroxylamine (1f)

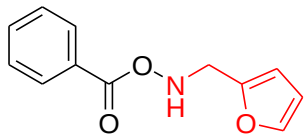

Eluant: *n*-hexane – ethyl acetate (9:1 v/v) The product was obtained as a pale yellow liquid (62 % yield). ^{1}H NMR (400 MHz, $CDCl_3$): δ_H 7.98 (d, *J* = 7.2 Hz, 3H), 7.56 (t, *J* = 7 Hz, 1H), 7.43 (t, *J* = 7.8 Hz, 2H), 7.38 – 7.38 (m, 1H), 6.30 (s, 2H), 4.28 (s, 2H) ^{13}C NMR (100 MHz, $CDCl_3$): δ_C 166.6, 150.0, 142.7, 133.4, 129.4, 128.5, 128.2, 110.5, 109.1, 49.1

2.4.2.2 Preparation of *O*-Benzoylhydroxylamines from Secondary Amines

A reported procedure from literature was followed. A 250 mL round bottomed flask was charged with benzoyl peroxide (10 mmol), dipotassium hydrogen phosphate (15 mmol) and *N*,*N*-dimethylformamide (50 mL). The mixture was stirred and the corresponding secondary amine (12 mmol) was added in one batch. The resulting mixture was stirred at room temperature and was monitored by TLC. Upon complete consumption of the starting material, deionized water (50 mL) was added and the suspension was stirred for 5 mins. The solution was then transferred to a separating funnel and was extracted with (3 x 30 mL) DCM. After washing with saturated brine solution (3 x 20 mL), the combined organic extracts were dried over $MgSO_4$ and concentrated by rotary evaporation. The residue was purified by flash chromatography to afford the *O*-benzoylhydroxylamines.

_N_-(Benzoyloxy)morpholine (1g).

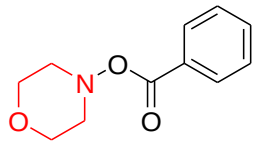

Eluant: *n*-hexane – ethyl acetate (9:1 v/v) The product was obtained as a pale yellow solid (78 % yield). ^{1}H NMR (400 MHz, $CDCl_3$): δ_H 8.00 (d, *J* = 7.3 Hz, 2H), 7.56 (t, *J* = 7.4 Hz, 1H), 7.43 (t, *J* = 7.6 Hz, 2H), 3.96 – 3.83 (m, 4H), 3.44 (bd, *J* = 9.2 Hz, 2H), 3.05 – 3.03 (m, 2H). ^{13}C NMR (100 MHz, $CDCl_3$): δ_C 164.6, 133.2, 129.4, 129.2, 128.4, 65.8, 57.0

tert-Butyl 4-(benzoyloxy)piperazine-1-carboxylate (1h).

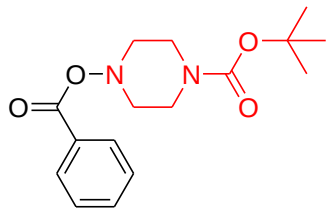

Eluant: *n*-hexane – ethyl acetate (9:1 v/v) The product was obtained as a white solid (80 % yield). ^{1}H NMR (400 MHz, $CDCl_3$): δ_H 8.00 (d, *J* = 8.0 Hz, 2H), 7.57 (t, *J* = 7.2 Hz, 1H), 7.44 (t, *J* = 7.6 Hz, 2H), 4.02 (m, 2H), 3.43 – 3.31 (m, 4H), 2.91 (m, 2H), 1.47 (s, 9H). ^{13}C NMR (100 MHz, $CDCl_3$): δ_C 164.6, 154.5, 133.2, 129.4, 129.1, 128.5, 80.2, 55.9, 28.4

***N*-(Benzoyloxy)pyrrolidine (1i).**

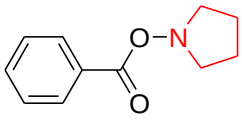

Eluant: *n*-hexane – ethyl acetate (9:1 v/v) The product was obtained as a white solid (80 % yield). ^{1}H NMR (400 MHz, $CDCl_3$): δ_H 7.96 (d, *J* = 7.2 Hz, 2H), 7.54 (t, *J* = 7.4 Hz, 1H), 7.42 (t, *J* = 7.8 Hz, 2H), 3.31 (m, 4H), 1.96 (m, 4H). ^{13}C NMR (100 MHz, $CDCl_3$): δ_C 165.2, 132.9, 129.6, 129.4, 128.4, 57.7, 22.2

***N*-(Benzoyloxy)benzylmethylamine (1j).**

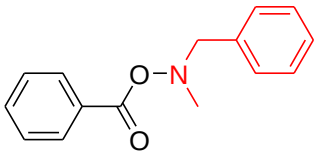

Eluant: *n*-hexane – ethyl acetate (9:1 v/v) The product was obtained as a colorless liquid (65 % yield). ^{1}H NMR (400 MHz, $CDCl_3$): δ_H 7.90 (d, *J* = 7.6 Hz, 2H), 7.51 (t, *J* = 7.4 Hz, 1H), 7.43 – 7.23 (m, 7H), 4.16 (s, 2H), 2.93 (s, 3H). ^{13}C NMR (100 MHz, $CDCl_3$): δ_C 165.0, 135.7, 133.0, 129.42, 129.35, 128.39, 128.35, 127.8, 65.1, 46.1

***N*-(Benzoyloxy)diethylamine (1k).**

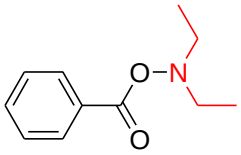

Eluant: *n*-hexane – ethyl acetate (9:1 v/v) The product was obtained as a colorless liquid (72 % yield). ^{1}H NMR (400 MHz, $CDCl_3$): δ_H 8.04 (d, *J* = 7.6 Hz, 2H), 7.57 (t, *J* = 7.4 Hz, 1H), 7.44 (t, *J* = 7.6 Hz, 2H), 3.05 (q, *J* = 7.1 Hz, 4H), 1.18 (t, *J* = 7.0 Hz, 6H). ^{13}C NMR (100 MHz, $CDCl_3$): δ_C 165.9, 133.0, 129.5, 129.2, 128.4, 53.5, 11.9

***N*-(Benzoyloxy)-1,2,3,4-tetrahydroisoquinoline (1l).**

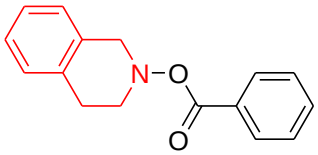

Eluant: *n*-hexane – ethyl acetate (9:1 v/v) The product was obtained as a white solid (82 % yield). ^{1}H NMR (400 MHz, $CDCl_3$): δ_H 8.00 (d, *J* = 8.0 Hz, 2H), 7.56 (t, *J* = 7.4 Hz, 1H), 7.43 (t, *J* = 7.6 Hz, 2H), 7.22 – 7.14 (m, 3H), 7.06 (d, *J* = 6.4 Hz, 1H), 4.43 (bs, 2H), 3.55 (bs, 2H), 3.12 (t, *J* = 6.0 Hz, 2H). ^{13}C NMR (100 MHz, $CDCl_3$): δ_C 164.9, 133.1, 132.9, 132.3, 129.5, 129.3, 128.4, 128.4, 126.9, 126.8, 126.2, 58.1, 53.4, 26.7

2.4.2.3 Preparation of *O*-Acetyl hydroxylamide

A reported procedure from the literature was followed. Hydroxylamine hydrochloride (20 mmol) and NaOH (25 mmol) were dissolved in a 40 mL water and THF mixture (1:1). The corresponding benzoyl chloride (5 mmol) was then added into the suspension via syringe. The mixture was stirred at room temperature overnight and then 1 M HCl was added to acidify the solution until the pH is 1. EtOAc (10 mL) was added and the organic layer was washed with brine and dried over $MgSO_4$. The solvent was evaporated to give a light orange solid. It was then dissolved in THF (30 mL). After purging with nitrogen, acetyl chloride (2.9 mmol) and Et_3N (2.9 mmol) were added subsequently via a syringe. The suspension was stirred overnight at room temperature. The solid formed was filtered off and EtOAc (20 mL) was added to the filtrate. The filtrate was then washed with water, brine and dried over $MgSO_4$. A white solid was obtained after evaporation of the solvent. Pure product was obtained by flash column chromatography using hexane/EtOAc 8:2 as eluent.

***N*-Hydroxybenzamide acetate (3a).**

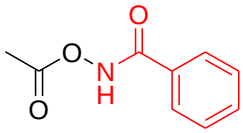

Eluant: *n*-hexane – ethyl acetate (9:1 v/v) The product was obtained as a white solid (85 % yield). ^{1}H NMR (400 MHz, $CDCl_3$): δ_H 9.47 (bs, 1H), 7.82 (d, *J* = 7.6 Hz, 2H), 7.58 (t, *J* = 7.4 Hz, 1H), 7.47 (t, *J* = 7.6 Hz, 2H), 2.30 (s, 3H). ^{13}C NMR (100 MHz, $CDCl_3$): δ_C 169.2, 166.4, 132.8, 130.7, 128.9, 127.5, 18.4

***N*-Hydroxy-2-thiophenecarboxamide acetate (3b).**

Eluant: *n*-hexane – ethyl acetate (9:1 v/v) The product was obtained as a white solid (65 % yield). ^{1}H NMR (400 MHz, $CDCl_3$): δ_H 9.35 (bs, 1H), 7.68 (d, *J* = 4.0 Hz, 1H), 7.59 (d, *J* = 5.29 Hz, 1H), 7.13 (t, *J* = 4.4 Hz, 1H), 2.29 (s, 3H). ^{13}C NMR (100 MHz, $CDCl_3$): δ_C 169.2, 161.5, 133.5, 131.8, 130.5, 127.9, 18.3

***N*-(acetyloxy)-benzeneacetamide (3c).**

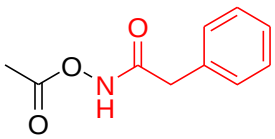

Eluant: *n*-hexane – ethyl acetate (9:1 v/v) The product was obtained as a white solid (77 % yield). ^{1}H NMR (400 MHz, $CDCl_3$): δ_H 8.74 (bs, 1H), 7.40 – 7.31 (m, 5H), 3.66 (s, 2H), 2.19 (s, 3H). ^{13}C NMR (100 MHz, $CDCl_3$): δ_C 170.4, 168.7, 132.9, 129.3, 129.1, 127.7, 40.8, 18.2

***N*-(Acetyloxy)-2,4,6-trimethylbenzamide (3d).**

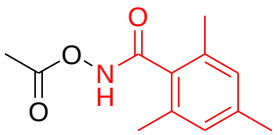

Eluant: *n*-hexane – ethyl acetate (9:1 v/v) The product was obtained as a white solid (67 % yield). ^{1}H NMR (400 MHz, $CDCl_3$): δ_H 8.99 (bs, 1H), 6.86 (s, 2H), 2.33 (s, 6H), 2.28 (s, 6H). ^{13}C NMR (100 MHz, $CDCl_3$): δ_C 168.8, 139.9, 135.8, 129.7, 128.4, 21.1, 19.1, 18.4

2.4.3 A General Procedure for the Rh-Catalyzed Cross Coupling Reaction of *O*-Benzoylhydroxylamines with Arylboronic Acids

O-Benzoylhydroxylamines (0.2 mmol) was dissolved in MeOH (1 mL) in a 8 mL-vial with magnetic stirrer. Arylboronic acids (0.24 mmol) and Cp*Rh$(OAc)_2$ (0.25 mol% in stock solution) were then added subsequently. The reaction vial was then allowed to stir in a water bath at room temperature for 2 h. The reaction mixture was filtered through a plug of Celite and the filtrate was concentrated by rotary evaporator. The mixture was then purified by flash column chromatography on a silica gel to give the desired product.

_N_-Isopropyl-5-methoxynaphthalen-1-amine (7a).

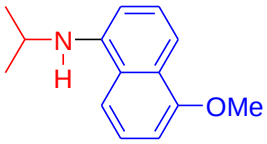

Eluant: *n*-hexane – ethyl acetate (9:1 v/v) The product was obtained as a colorless liquid (90 % yield). ^{1}H NMR (400 MHz, $CDCl_3$): δ_H 7.55 – 7.51 (m, 2H), 7.07 – 7.05 (m, 1H), 7.03 – 7.02 (m, 1H), 6.88 – 6.85 (m, 1H), 6.821 – 6.816 (m, 1H), 3.88 (s, 3H), 3.78 – 3.68 (m, 1H), 1.27 (d, *J* = 6.4 Hz, 6H) ^{13}C NMR (100 MHz, $CDCl_3$): δ_C 155.2, 143.5, 130.7, 128.2, 127.9, 127.6, 119.0, 118.9, 55.5, 44.9, 23.1

4-Bromo-_N_-isopropylbenzenamine (7b).

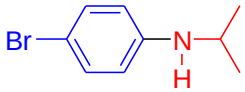

Eluant: *n*-hexane – ethyl acetate (9:1 v/v) The product was obtained as a colorless liquid (86 % yield). ^{1}H NMR (400 MHz, $CDCl_3$): δ_H 7.23 (d, *J* = 8.8 Hz, 2H), 6.46 (d, *J* = 8.8 Hz, 2H), 3.62 – 3.53 (m, 1H), 1.20 (d, *J* = 6Hz, 6H) ^{13}C NMR (100 MHz, $CDCl_3$): δ_C 146.6, 132.1, 115.0, 108.6, 44.5, 23.0

_N_-Isopropyl-4-methoxybenzenamine (7c).

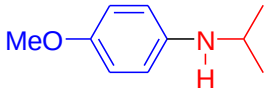

Eluant: *n*-hexane – ethyl acetate (9:1 v/v) The product was obtained as a colorless liquid (42 % yield). ^{1}H NMR (400 MHz, $CDCl_3$): δ_H 6.78 (d, *J* = 9.2 Hz, 2H), 6.58 (d, *J* = 9.2 Hz, 2H), 3.75 (s, 3H), 3.59 – 3.50 (m, 1H), 1.18 (d, *J* = 6 Hz, 6H) ^{13}C NMR (100 MHz, $CDCl_3$): δ_C 152.1, 141.9, 115.13, 115.07, 56.0, 45.4, 23.3

Methyl 4-(isopropylamino)benzoate (7d).

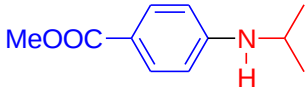

Eluant: *n*-hexane – ethyl acetate (9:1 v/v) The product was obtained as a colorless liquid (75 % yield). ^{1}H NMR (400 MHz, $CDCl_3$): δ_H 7.84 (d, *J* = 8.8 Hz, 2H), 6.52 (d, *J* = 8.8 Hz, 2H), 3.84 (s, 3H), 3.72 – 3.66 (m, 1H), 1.23 (d, *J* = 6.4 Hz, 6H) ^{13}C NMR (100 MHz, $CDCl_3$): δ_C 167.5, 151.2, 131.8, 118.1, 111.9, 51.6, 44.2, 22.9

4-(Isopropylamino)benzaldehyde (7e).

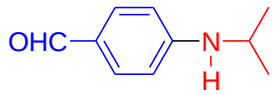

Eluant: *n*-hexane – ethyl acetate (9:1 v/v) The product was obtained as a colorless liquid (90 % yield). ^{1}H NMR (400 MHz, $CDCl_3$): δ_H 9.70 (s, 1H), 7.68 (d, *J* = 8.8 Hz, 2H), 6.58 (d, *J* = 8.8 Hz, 2H), 3.78 – 3.68 (m, 1H), 1.26 (d, *J* = 6 Hz 6H) ^{13}C NMR (100 MHz, $CDCl_3$): δ_C 190.3, 152.5, 132.5, 126.4, 112.3, 44.3, 22.8

***N*-Isopropyl-4-(methylsulfonyl)benzenamine (7f).**

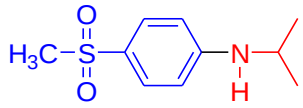

Eluant: *n*-hexane – ethyl acetate (9:1 v/v) The product was obtained as a colorless liquid (44 % yield). ^{1}H NMR (400 MHz, $CDCl_3$): δ_H 7.66 (d, *J* = 8.8 Hz, 2H), 6.57 (d, *J* = 8.8 Hz, 2H), 4.20 (bs, 1H), 3.71 – 3.65 (m, 1H), 2.99 (s, 3H), 1.23 (d, *J* = 6 Hz, 6H) ^{13}C NMR (100 MHz, $CDCl_3$): δ_C 151.7, 129.6, 126.8, 112.1, 45.2, 44.2, 22.8

3-(Trifluoromethyl)-*N*-isopropylbenzenamine (7g).

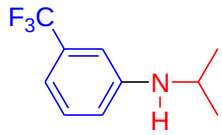

Eluant: *n*-hexane – ethyl acetate (9:1 v/v) The product was obtained as a colorless liquid (56 % yield). ^{1}H NMR (400 MHz, $CDCl_3$): δ_H 7.24 (t, *J* = 8.4 Hz, 1H), 6.90 (d, *J* = 7.6 Hz, 1H), 6.78 (s, 1H), 6.71 (d, *J* = 8Hz, 1H), 3.70 – 3.61 (m, 1H), 1.23 (d, *J* = 6.4 Hz, 6H) ^{13}C NMR (100 MHz, $CDCl_3$): δ_C 147.7, 129.8, 125.9, 123.2, 116.3, 113.4, 109.4, 44.4, 22.9 ^{19}F NMR (100 MHz, $CDCl_3$): δ_F 62.9

***N*-Isopropyl-3-methoxybenzenamine (7h).**

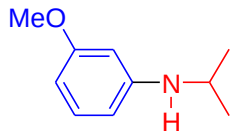

Eluant: *n*-hexane – ethyl acetate (9:1 v/v) The product was obtained as a colorless liquid (60 % yield). ^{1}H NMR (400 MHz, $CDCl_3$): δ_H 7.07 (t, *J* = 8Hz, 1H), 6.26 – 6.19 (m, 2H), 6.15 – 6.14 (m, 1H), 3.77 (s, 3H), 3.64 – 3.58 (m, 1H), 1.21 (d, *J* = 6 Hz, 6H) ^{13}C NMR (100 MHz, $CDCl_3$): δ_C 161.0, 149.1, 130.1, 106.6, 102.1, 99.3, 55.2, 44.4, 23.2

2-Bromo-*N*-isopropylbenzenamine (7i).

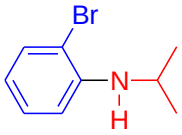

Eluant: *n*-hexane – ethyl acetate (9:1 v/v) The product was obtained as a colorless liquid (30 % yield). ^{1}H NMR (400 MHz, $CDCl_3$): δ_H 7.43 – 7.40 (m, 1H), 7.19 – 7.14 (m, 1H), 6.66 (d, *J* = 8Hz, 1H), 6.56 – 6.52 (m, 1H), 3.71 – 3.62 (m, 1H), 1.26 (d, *J* = 6.4 Hz, 6H) ^{13}C NMR (100 MHz, $CDCl_3$): δ_C 144.2, 132.7, 128.6, 117.6, 112.2, 110.1, 44.7, 23.0

***N*-Cyclohexyl-5-methoxynaphthalen-1-amine (7j).**

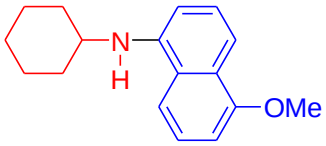

Eluant: *n*-hexane – ethyl acetate (9:1 v/v) The product was obtained as a colorless liquid (85 % yield). ^{1}H NMR (400 MHz, $CDCl_3$): δ_H 7.54 – 7.50 (m, 2H), 7.07 – 7.02 (m, 2H), 6.87 – 6.80 (m, 2H), 3.87 (s, 3H), 3.40 – 3.33 (m, 1H), 2.14 – 2.11 (m, 2H), 1.82 – 1.77 (m, 2H), 1.70 – 1.66 (m, 1H), 1.47 – 1.28 (m, 5H) ^{13}C NMR (100 MHz, $CDCl_3$): δ_C 155.1, 143.7, 130.7, 128.0, 127.9, 127.5, 118.9, 106.4, 105.9, 55.5, 52.1, 33.6, 26.2, 25.2

Tetrahydro-*N*-(1-methoxynaphthalen-5-yl)-2H-pyran-4-amine (7k).

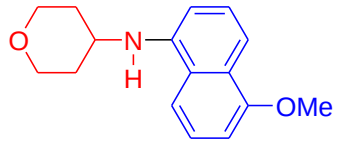

Eluant: *n*-hexane – ethyl acetate (9:1 v/v) The product was obtained as a colorless liquid (78 % yield). ^{1}H NMR (400 MHz, $CDCl_3$): δ_H 7.56 – 7.51 (m, 1H), 7.08 – 7.03 (m, 2H), 6.89 – 6.86 (m, 1H), 6.822 – 6.819 (m, 1H), 4.05 – 4.02 (m, 2H), 3.88 (s, 3H), 3.64 – 3.53 (m, 3H), 2.11 (d, *J* = 12.8Hz, 2H), 1.57 – 1.47 (m, 2H) ^{13}C NMR (100 MHz, $CDCl_3$): δ_C 155.4, 142.9, 130.6, 128.4, 128.1, 127.5, 119.0, 118.8, 106.4, 106.3, 67.1, 55.5, 49.6, 33.7

5- Methoxy-*N*-phenethylnaphthalen-1-amine (7l).

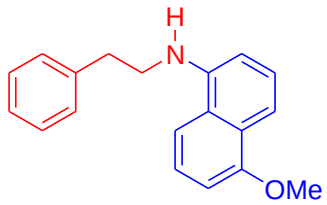

Eluant: *n*-hexane – ethyl acetate (9:1 v/v) The product was obtained as a colorless liquid (40 % yield). ^{1}H NMR (400 MHz, $CDCl_3$): δ_H 7.55 (d, *J* = 8.8 Hz, 2H), 7.34 (t, *J* = 7.4 Hz, 2H), 7.27 – 7.25 (m, 3H), 7.09 – 7.04 (m, 2H), 6.87 – 6.85 (m, 2H), 3.89 (s, 3H), 3.50 (t, *J* = 7 Hz, 2H), 2.99 (t, *J* = 7 Hz, 2H) ^{13}C NMR (100 MHz, $CDCl_3$): δ_C 155.3, 144.3, 139.5, 130.7, 129.0, 128.8, 128.4, 127.9, 127.6, 126.6, 118.9, 118.7, 106.5, 105.7, 55.5, 45.5, 35.6

***N*-(2-Bromophenethyl)-5-methoxynaphthalen-1-amine (7m).**

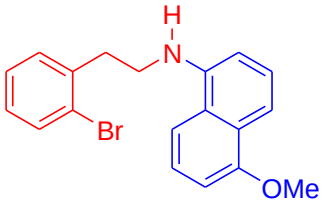

Eluant: *n*-hexane – ethyl acetate (9:1 v/v) The product was obtained as a colorless liquid (60 % yield). ^{1}H NMR (400 MHz, $CDCl_3$): δ_H 7.60 – 7.55 (m, 3H), 7.27 – 7.26 (m, 2H), 7.14 – 7.05 (m, 3H), 6.89 – 6.87 (m, 2H), 3.89 (s, 3H), 3.52 (t, *J* = 7.2 Hz, 2H), 3.13 (t, *J* = 6.8 Hz, 2H) ^{13}C NMR (100 MHz, $CDCl_3$): δ_C 155.3, 144.2, 139.0, 133.2, 131.1, 130.7, 128.4, 128.0, 127.7, 127.6, 124.8, 118.9, 118.6, 106.5, 105.6, 55.5, 44.0, 36.0

***N*-((Furan-2-yl)methyl)-5-methoxynaphthalen-1-amine (7n).**

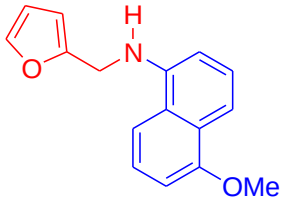

Eluant: *n*-hexane – ethyl acetate (9:1 v/v) The product was obtained as a colorless liquid (85 % yield). ^{1}H NMR (400 MHz, $CDCl_3$): δ_H 7.58 – 7.55 (m, 2H), 7.395 – 7.393 (m, 1H), 7.10 – 7.05 (m, 2H), 6.95 – 6.90 (m, 2H), 6.35 – 6.28 (m, 2H), 4.41 (s, 2H), 3.89 (s, 3H) ^{13}C NMR (100 MHz, $CDCl_3$): δ_C 155.5, 152.9, 143.9, 142.1, 130.5, 128.7, 127.9, 127.8, 119.0, 118.6, 110.6, 107.3, 106.4, 106.1, 55.5, 41.9

4-(4-Bromophenyl)morpholine (7o).

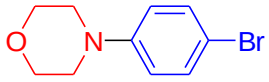

Eluant: *n*-hexane – ethyl acetate (9:1 v/v) The product was obtained as a colorless liquid (86 % yield). ^{1}H NMR (400 MHz, $CDCl_3$): δ_H 7.36 (d, *J* = 8.8 Hz, 2H), 6.78 (d, *J* = 8.8 Hz, 2H), 3.85 (t, *J* = 4.6 Hz, 4H), 3.12 (t, *J* = 4.6 Hz, 4H) ^{13}C NMR (100 MHz, $CDCl_3$): δ_C 150.3, 131.6, 117.3, 112.2, 66.8, 49.2

***tert*-Butyl 4-(4-bromophenyl)piperazine-1-carboxylate (7p).**

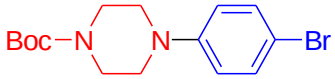

Eluant: *n*-hexane – ethyl acetate (9:1 v/v) The product was obtained as a white solid (80 % yield). ^{1}H NMR (400 MHz, $CDCl_3$): δ_H 7.34 (d, *J* = 8.0 Hz, 2H), 6.78 (d, *J* = 8.0 Hz, 2H), 3.56 (t, *J* = 4.0 Hz, 4H), 3.09 (t, *J* = 6.0 Hz, 4H), 1.48 (s, 9H) ^{13}C NMR (100 MHz, $CDCl_3$) : δ_C 154.7, 150.3, 132.0, 118.2, 112.4, 80.0, 49.2, 28.4

1-(3-Chlorophenyl)pyrrolidine (7q).

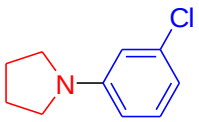

Eluant: *n*-hexane – ethyl acetate (9:1 v/v) The product was obtained as a colorless liquid (71 % yield). ^{1}H NMR (400 MHz, $CDCl_3$): δ_H 7.12 (t, *J* = 8.0 Hz, 1H), 6.62 (d, *J* = 8.0 Hz, 1H), 6.53 (s, 1H), 6.43 (m, 1H), 3.27 (t, *J* = 6.6 Hz, 4H), 2.03 – 2.00 (m, 4H). ^{13}C NMR (100 MHz, $CDCl_3$): δ_C 149.0, 135.1, 130.2, 115.3, 111.6, 110.0 , 47.8, 25.6

***N*-Benzyl-4-bromo-*N*-methylbenzenamine (7r).**

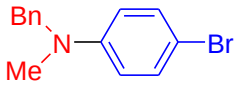

Eluant: *n*-hexane – ethyl acetate (9:1 v/v) The product was obtained as a colorless liquid (72 % yield). ^{1}H NMR (400 MHz, $CDCl_3$): δ_H 7.37 – 7.26 (m, 5H), 7.22 (d, *J* = 8.0 Hz, 2H), 6.63 (d, *J* = 8.0 Hz, 2H), 4.53 (s, 2H), 3.03 (s, 3H). ^{13}C NMR (100 MHz, $CDCl_3$): δ_C 148.6, 138.4, 131.8, 128.7, 127.1, 126.7 , 114.0, 108.5, 56.6, 38.8

4-Bromo-*N*,*N*-diethylbenzenamine (7s).

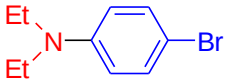

Eluant: *n*-hexane – ethyl acetate (9:1 v/v) The product was obtained as a colorless liquid (72 % yield). ^{1}H NMR (400 MHz, $CDCl_3$): δ_H 7.27 (d, *J* = 8.0 Hz, 2H), 6.55 (d, *J* = 12.0 Hz, 2H), 3.32 (q, *J* = 7.1 Hz, 4H), 1.15 (t, *J* = 8.0 Hz, 6H). ^{13}C NMR (100 MHz, $CDCl_3$): δ_C 146.8, 131.9, 113.5, 107.0, 44.5, 12.4

Ethyl 4-(3,4-dihydroisoquinolin-2(1H)-yl)benzoate (7t).

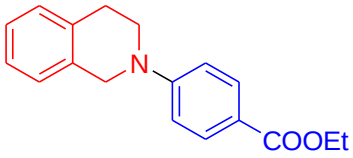

Eluant: *n*-hexane – ethyl acetate (9:1 v/v) The product was obtained as a white solid (75 % yield). ^{1}H NMR (400 MHz, $CDCl_3$): δ_H 7.96 (d, *J* = 8.8 Hz, 2H), 7.23– 7.17 (m, 4H), 6.88 (d, *J* = 9.2 Hz, 2H), 4.52 (s, 2H), 4.34 (q, *J* = 7.1 Hz, 2H), 3.66 (t, *J* = 6.0 Hz, 2H), 3.00 (t, *J* = 5.8 Hz, 2H), 1.38 (t, *J* = 7.2 Hz, 3H). ^{13}C NMR (100 MHz, $CDCl_3$): δ_C 167.0, 153.1, 135.2, 134.0, 131.5, 128.4, 126.9, 126.7, 126.5, 118.9, 112.3, 60.4, 49.3, 45.1, 29.2, 14.6

2-(4-Bromophenyl)-1,2,3,4-tetrahydroisoquinoline (7u).

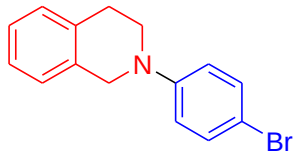

Eluant: *n*-hexane – ethyl acetate (9:1 v/v) The product was obtained as a white solid (84 % yield). ^{1}H NMR (400 MHz, $CDCl_3$): δ_H 7.36 (d, *J* = 8.8 Hz, 2H), 7.21 – 7.15 (m, 4H), 6.85 (d, *J* = 8.8 Hz, 2H), 4.39 (s, 2H), 3.54 (t, *J* = 5.8 Hz, 2H), 2.99 (t, *J* = 5.8 Hz, 2H). ^{13}C NMR (100 MHz, $CDCl_3$): δ_C 149.5, 134.8, 134.1, 132.08, 132.07, 128.7, 126.68, 126.65, 126.3, 116.7, 50.7, 46.6, 29.0

1-(1-Methoxynaphthalen-5-yl)indoline (7v).

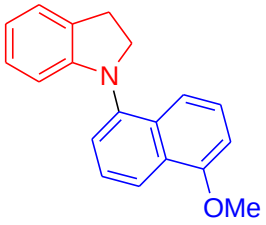

Eluant: *n*-hexane – ethyl acetate (9:1 v/v) The product was obtained as a white solid (85 % yield). ^{1}H NMR (400 MHz, $CDCl_3$): δ_H 7.71 (d, *J* = 9.2 Hz, 1H), 7.64 (d, *J* = 8.8 Hz, 1H), 7.55 – 7.52 (m, 1H), 7.442 – 7.437 (m, 1H), 7.20 – 7.06 (m, 6H), 6.76 (t, *J* = 7.2 Hz, 1H), 4.04 (t, *J* = 8.4 Hz, 2H), 3.92 (s, 3H), 3.17 (t, *J* = 8.4 Hz, 2H) ^{13}C NMR (100 MHz, $CDCl_3$): δ_C 156.6, 147.7, 140.4, 131.4, 130.3, 130.0, 128.4, 127.7, 127.3, 125.2, 120.4, 119.3, 118.9, 113.9, 108.1, 106.1, 55.5, 52.8, 28.4

2.4.4 A General Procedure for the Rh-Catalyzed Cross Coupling Reaction of *O*-Acetyl Hydroxylamide with Arylboronic Acids

O-Acetyl hydroxylamide (0.2 mmol), arylboronic acids (0.3 mmol) and [Cp*Rh(OAc)$_2$] (1 mol %) were charged in a 8 mL vial with a magnetic stirrer. THF (1 mL) was then added and the reaction mixture was allowed to stir in an oil bath at 40 ^{o}C for 2 h. The reaction mixture was filtered through a plug of Celite and the filtrate was concentrated by rotary evaporator. The mixture was then purified by flash column chromatography on a silica gel to give the desired product.

_N_-Phenylbenzamide (8a).

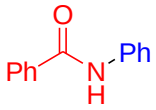

Eluant: *n*-hexane – ethyl acetate (8:2 v/v) The product was obtained as a white solid (82 % yield). ^{1}H NMR (400 MHz, $CDCl_3$): δ_H 7.88 (d, *J* = 7.4 Hz, 2H), 7.81 (bs, 1H), 7.65 (d, *J* = 7.8 Hz, 2H), 7.56 (t, *J* = 7 Hz, 1H), 7.50 (t, *J* = 7.3 Hz, 2H), 7.38 (t, *J* = 7.8 Hz, 2H), 7.16 (t, *J* = 7.4 Hz, 1H). ^{13}C NMR (100 MHz, $CDCl_3$): δ_C 165.9, 138.1, 135.2, 132.0, 129.2, 128.9, 127.18, 124.7, 120.4

***N*-(4-Cyanophenyl)benzamide (8b).**

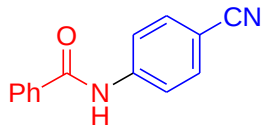

Eluant: *n*-hexane – ethyl acetate (8:2 v/v) The product was obtained as a white solid (85 % yield). ^{1}H NMR (400 MHz, $CDCl_3$): δ_H 8.07 (bs, 1H), 7.87 (d, *J* = 7.6 Hz, 2H), 7.80 (d, *J* = 8.4 Hz, 2H), 7.65 (d, *J* = 8.4 Hz, 2H), 7.60 (t, *J* = 7.2 Hz, 1H), 7.51 (t, *J* = 7.6 Hz, 2H). ^{13}C NMR (100 MHz, $CDCl_3$): δ_C 165.9, 142.0, 134.1, 133.4, 132.5, 129.0, 127.1, 119.9, 118, 107.4

***N*-(4-Bromophenyl)benzamide (8c).**

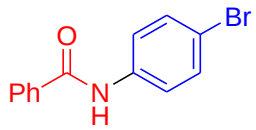

Eluant: *n*-hexane – ethyl acetate (8:2 v/v) The product was obtained as a white solid (95 % yield). ^{1}H NMR (400 MHz, $CDCl_3$): δ_H 7.76 (d, *J* = 7.6 Hz, 2H), 7.47 (d, *J* = 8.8 Hz, 2H), 7.41 (t, *J* = 7.4 Hz, 1H), 7.36 – 7.31 (m, 4H). ^{13}C NMR (100 MHz, $CDCl_3$): δ_C 167.1, 137.5, 134.6, 131.8, 131.7, 128.5, 127.3, 122.3, 117.0

_N_-(4-Methoxyphenyl)benzamide (8d).

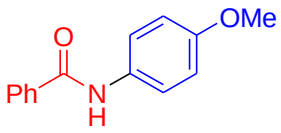

Eluant: *n*-hexane – ethyl acetate (8:2 v/v) The product was obtained as a white solid (90 % yield). ^{1}H NMR (400 MHz, $CDCl_3$): δ_H 7.87 (d, *J* = 7.6 Hz, 2H), 7.71 (bs, 1H), 7.56 – 7.47 (m, 5H), 6.92 (d, *J* = 8.8 Hz, 2H), 3.82 (s, 3H). ^{13}C NMR (100 MHz, $CDCl_3$): δ_C 165.8, 156.8, 135.2, 131.8, 131.2, 128.9, 127.1, 122.3, 114.4, 55.7

_N_-(1-Methoxynaphthalen-5-yl)benzamide (8e).

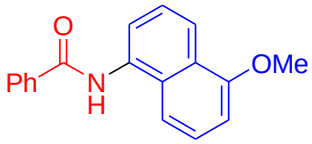

Eluant: *n*-hexane – ethyl acetate (8:2 v/v) The product was obtained as a white solid (68 % yield). ^{1}H NMR (400 MHz, $CDCl_3$): δ_H 8.25 (s, 1H), 7.92 (d, *J* = 7.6 Hz, 3H), 7.50 – 7.74 (m, 2H), 7.73 – 7.50 (m, 6H), 7.18 – 7.13 (m, *2*H), 3.93 (s, 3H). ^{13}C NMR (100 MHz, $CDCl_3$): δ_C 165.8, 157.3, 135.1, 133.5, 131.9, 131.8, 129.2, 129.2, 128.8, 127.6, 127.0, 120.7, 119.4, 117.4, 105.8, 55.3

Ethyl-4-(benzamido)benzoate (8f).

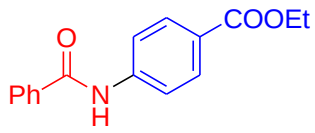

Eluant: *n*-hexane – ethyl acetate (8:2 v/v) The product was obtained as a white solid (97 % yield). ^{1}H NMR (400 MHz, $CDCl_3$): δ_H 8.07 (d, *J* = 8.4 Hz, 2H), 7.92 (bs, 1H), 7.89 (d, *J* = 7.6 Hz, 2H), 7.74 (d, *J* = 8.4 Hz, 2H), 7.59 (t, *J* = 7.2 Hz, 1H), 7.52 (t, *J* = 7.4 Hz, 2H), 4.38 (q, *J* = 7.1 Hz, 2H), 1.40 (t, *J* = 7.2 Hz, 3H). ^{13}C NMR (100 MHz, $CDCl_3$): δ_C 166.3, 165.9, 142.2, 134.7, 132.4, 131.0, 129.1, 127.2, 126.4, 119.3, 61.1, 14.5

***N*-(3-Nitrophenyl)benzamide (8g).**

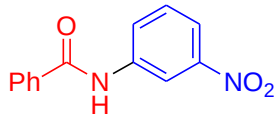

Eluant: *n*-hexane – ethyl acetate (8:2 v/v) The product was obtained as a white solid (76 % yield). ^{1}H NMR (400 MHz, $CDCl_3$): δ_H 8.61 (s, 1H), 8.18 (bs, 1H), 8.01 (m, 2H), 7.91 (d, *J* = 7.6 Hz, 2H), 7.65 – 7.53 (m, 4H). ^{13}C NMR (100 MHz, $CDCl_3$): δ_C 165.9, 148.8, 139.4, 134.3, 132.5, 130.0, 129.1, 127.2, 125.8, 119.0, 115.0

***N*-(4-(Diphenylamino)phenyl)benzamide (8h).**

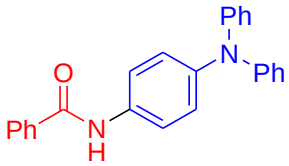

Eluant: *n*-hexane – ethyl acetate (8:2 v/v) The product was obtained as a white solid (76 % yield). ^{1}H NMR (400 MHz, $CDCl_3$): δ_H 7.86 (d, *J* = 6.8 Hz, 3H), 7.54 – 7.46 (m, 5H), 7.25 (t, *J* = 7.6 Hz, 4H), 7.10 (t, *J* = 7.2 Hz, 6H), 7.00 (t, *J* = 7.2 Hz, 2H). ^{13}C NMR (100 MHz, $CDCl_3$): δ_C 165.7, 147.8, 144.5, 135.0, 132.9, 131.8, 129.2, 128.8, 127.0, 125.0, 123.9, 122.6, 121.5

***N*-(Benzo[d][1,3]dioxol-6-yl)benzamide (8i).**

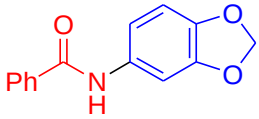

Eluant: *n*-hexane – ethyl acetate (8:2 v/v) The product was obtained as a white solid (90 % yield). ^{1}H NMR (400 MHz, $CDCl_3$): δ_H 7.98 (s, 1H), 7.83 (d, *J* = 7.6Hz, 2H), 7.52 (t, *J* = 7.4 Hz, 1H), 7.43 (t, *J* = 7.4 Hz, 2H), 7.32 (m, 1H), 6.92 – 6.90 (m, 1H), 6.75 (d, *J* = 8.4 Hz, 1H), 5.95 (s, 2H). ^{13}C NMR (100 MHz, $CDCl_3$): δ_C 165.8, 147.9, 144.5, 134.9, 132.2, 131.7, 128.7, 127.0, 113.8, 108.1, 103.3, 101.3

***N*-(Thiophen-3-yl)benzamide (8j).**

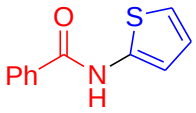

Eluant: *n*-hexane – ethyl acetate (8:2 v/v) The product was obtained as a white solid (75 % yield). ^{1}H NMR (400 MHz, $CDCl_3$): δ_H 8.12 (bs, 1H), 7.86 (d, *J* = 7.6 Hz, 2H), 7.733 – 7.727 (m, 1H), 7.55 (t, *J* = 7 Hz, 1H), 7.48 (t, *J* = 7.4 Hz, 2H), 7.29 – 7.27 (m, 1H), 7.12 (d, *J* = 4.8 Hz, 1H). ^{13}C NMR (100 MHz, $CDCl_3$): δ_C 165.2, 135.8, 134.6, 132.0, 128.9, 127.1, 124.8, 121.5, 110.9

***N*-Styrylbenzamide (8k).**

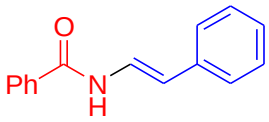

Eluant: *n*-hexane – ethyl acetate (8:2 v/v) The product was obtained as a white solid (52 % yield). ^{1}H NMR (400 MHz, $CDCl_3$): δ_H 8.00 (bs, 1H), 7.86 (d, J = 7.6 Hz, 2H), 7.78 – 7,71 (m, 1H), 7.56 (t, *J* = 7Hz, 1H), 7.48 (t, *J* = 7.6 Hz, 2H), 7.36 (d, *J* = 7.6 Hz, 2H), 7.31 (t, *J* =7.6 Hz, 2H), 7.21 (t, *J* = 7.2 Hz, 1H), 6.27 (d, *J* = 14.8Hz, 1H). ^{13}C NMR (100 MHz, $CDCl_3$): δ_C 164.6, 136.2, 133.6, 132.3, 129.0, 128.9, 127.3, 127.0, 125.8, 123.2, 113.8

***N*-(4-Bromophenyl)thiophene-2-carboxamide (8l).**

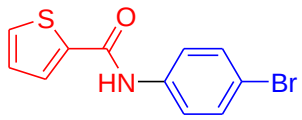

Eluant: *n*-hexane – ethyl acetate (8:2 v/v) The product was obtained as a white solid (75 % yield). ^{1}H NMR (400 MHz, *d* - acetone): δ_H 7.89 (d, *J* = 3.7 Hz, 1H), 7.79 – 7.72 (m, 3H), 7.50 (d, *J* = 8.8 Hz, 2H), 7.17 (t, *J* = 4.4 Hz, 1H). ^{13}C NMR (100 MHz, *d* - acetone): δ_C 160.1, 140.3, 138.6, 131.7, 131.7, 128.7, 128.0, 122.0, 115.8

***N* -(4-Bromophenyl)-2-phenylacetamide (8m).**

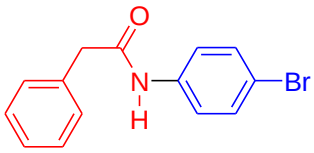

Eluant: *n*-hexane – ethyl acetate (8:2 v/v) The product was obtained as a white solid (89 % yield). ^{1}H NMR (400 MHz, $CDCl_3$): δ_H 7.46 – 7.28 (m, 9H), 7.00 (bd, 1H), 3.74 (s, 2H). ^{13}C NMR (100 MHz, $CDCl_3$): δ_C 169.2, 136.8, 134.3, 132.1, 129.7, 129.5, 128.0, 121.5, 117.2, 45.0

***N*-(4-Bromophenyl)-2,4,6-trimethylbenzamide (8n).**

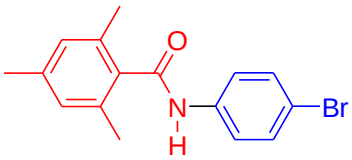

Eluant: *n*-hexane – ethyl acetate (8:2 v/v) The product was obtained as a white solid (89 % yield). ^{1}H NMR (400 MHz, $CDCl_3$): δ_H 7.47 (q, J = 8.9 Hz, 5H), 6.87 (s, 2H), 2.31 (s, 6H), 2.30 (s, 3H). ^{13}C NMR (100 MHz, $CDCl_3$): δ_C 169.0, 139.2, 137.1, 134.4, 132.2, 128.6, 121.5, 117.3, 21.3, 19.3

Chapter 3

Rhodium(III)-Catalyzed Formal Oxidative [4+1] Cycloaddition of Benzohydroxamic Acids and α-Diazoesters

3.1 Introduction

In Chapter 2, we achieved the Rh-catalyzed cross coupling reaction of *O*-acetyl benzohydroxamic acids with arylboronic acids for aryl benzamide synthesis. We postulated that the carboxylate group on the *O*-acetyl benzohydroxamic acids should serve as a good leaving group for C-N bond formation.

Not long ago, our group developed the *ortho*-selective arene C-H coupling reactions with *α*-diazomalonates; acetophenone oximes, arylpyridines, benzoic acids and benzylamines are effective substrates for this transformation.[62] An alkylrhodacyclic complex was structurally characterized. It was believed that protonolysis of this alkylrhodacyclic(III) complex should furnish the necessary C – H bond for the product formation. Motivated by the characterization of the

alkylrhodacyclic complex, we anticipated that reductive elimination rather than protonolysis should bring about a formal [4+1] cycloaddition.

Oxidative C–H coupling reactions with alkynes to give six-membered heterocycles have been extensively investigated;[63-65] analogous studies on carbenoid cycloadditions to afford five-membered heterocycles are sparse in the literature.[66,67] In this chapter, we describe Rh(III)-catalyzed formal [4+1] cycloaddition of diazomalonates with O-acetyl benzohydroxamic acids to afford oxisoindoles.

3.2 Results and Discussion

3.2.1 Rhodium(III)-Catalyzed Formal Oxidative [4+1] Cycloaddition of Benzohydroxamic Acids and α-Diazoesters

We first examined the reaction of *O*-acetyl benzohydroxamic acid (**3a**) with diazomalonate (**4a**) in the presence of [Cp*Rh(OAc)$_2$] (5 mol% Rh) in toluene (2 mL) at 60 ℃ for 4 h, and the desired oxisoindole was obtained in 64% yield (Scheme 3.1). The product oxisoindoles **9a** was confirmed by $^{1}H/^{13}C$ NMR spectroscopy and X-ray crystallography (Figure 3.1).

Scheme 3.1 Preliminary study

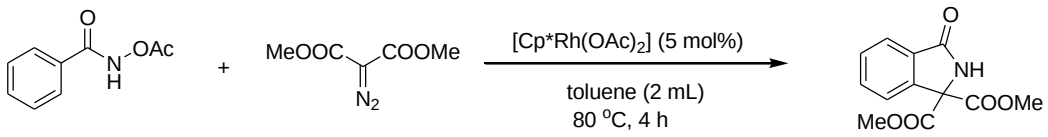

3a **4a** **9a**

Figure 3.1 Molecular structure of dimethyl 3-oxoisoindoline-1,1-dicarboxylate (**9a**)

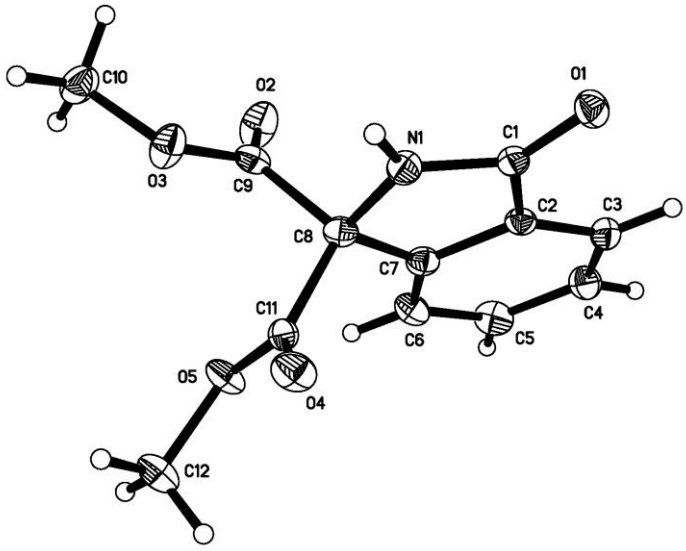

Table 3.1 Selected bond distances [Å] and angles [°]

Bond distances	
C(8)-C(9)	1.555(6)
C(8)-C(11)	1.538(5)
N(1)-C(8)	1.443(4)
C(7)-C(8)	1.506(5)
Bond angles	
C(11)-C(8)-C(9)	107.6(3)
N(1)-C(8)-C(7)	102.9(3)
N(1)-C(8)-C(9)	109.0(3)
C(7)-C(8)-C(11)	112.0(3)

Table 3.2 Crystal data and structure refinement for **9a**

Empirical formula	C_{12} H_{11} N O_5
Formula weight	249.22
Temperature	296(2) K
Wavelength	0.71073 Å
Crystal system	Triclinic
Space group	P-1
Unit cell dimensions	a = 8.2884(3) Å = 86.047(2)°.
	b = 8.7403(3) Å = 79.510(2)°.
	c = 8.8266(3) Å = 71.615(2)°.
Volume	596.60(4) $Å^3$
Z	2
Density (calculated)	1.387 Mg/m^3
Absorption coefficient	0.110 mm^{-1}
F(000)	260
Crystal size	0.42 x 0.40 x 0.38 mm^3
Theta range for data collection	2.35 to 27.50°.
Index ranges	-10<=h<=7, -11<=k<=11,
	-11<=l<=11
Reflections collected	4618
Independent reflections	1765 [R(int) = 0.0490]
Completeness to theta = 27.50°	64.3%
Absorption correction	None
Max. and min. transmission	0.7456 and 0.4133
Refinement method	Full-matrix least-squares on F^2
Data / restraints / parameters	1765 / 0 / 163
Goodness-of-fit on F^2	1.002
Final R indices [I>2sigma(I)]	R1 = 0.0915, wR2 = 0.2531
R indices (all data)	R1 = 0.1350, wR2 = 0.2625
Largest diff. peak and hole	0.341 and -0.316 e.$Å^{-3}$

3.2.2 Optimization of Reaction Conditions

With this initial success, we proceeded to reaction optimization. The solvent effect was first examined.

Table 3.3 Effect of solvent

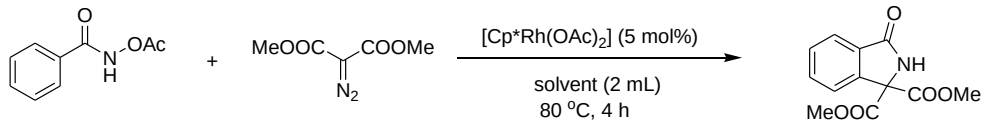

3a **4a** **9a**

entry	solvent	**9a** (%)[a]
1	toluene	64
2	MeOH	0[b]
3	DMF	95
4	MeCN	82
5	ethyl acetate	85
6	DCE	84
7	1,4-dioxane	93
8	THF	93

Reaction conditions: **3a** (0.2 mmol), **4a** (0.24 mmol, 1.2 equiv). [a] Yields were determined by ^{1}H NMR using dibromoethane as internal standard. [b] No detectable product formation.

Excellent yields (>90%) were obtained when dimethylformamide, acetonitrile, ethyl acetate 1,2-dichloroethane, 1,4-dioxane and tetrahydrofuran were employed as solvent (Table 3.3, entries 3-8). Lower product yield (64%) was obtained when toluene was used as solvent. Notably, no detectable **9a**

formation was observed when methanol was used as solvent. For easier work-up, tetrahydrofuran was chosen as solvent for the carbenoid cycloaddition reaction.

Table 3.4 Effect of leaving group of benzohydroxamic acid

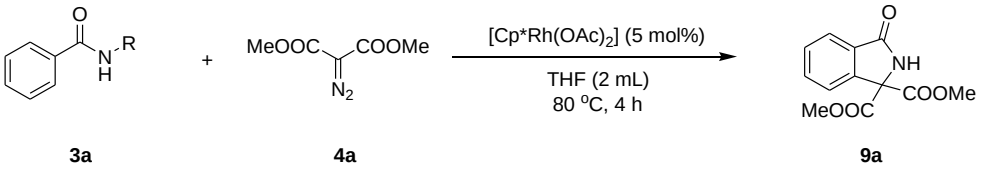

3a **4a** **9a**

entry	leaving group	**9a** (%)[a]
1	-OH	0[b]
2	-OMe	0[b]
3	-OPiv	98
4	-OAc	99
5	-OBz	86

Reaction conditions: **3a** (0.2 mmol), **4a** (0.24 mmol, 1.2 equiv). [a] Yields were determined by ^{1}H NMR using dibromoethane as internal standard. [b] No detectable product formation.

For effect of the leaving group of the benzohydroxamic acid, substrates with *N*-hydroxy and *N*-methoxy groups did not give any detectable oxisoindoles product (Table 3.4, entries 1-2). While carboxylate-type leaving groups were able to produce the desired oxisoindoles product in 86% - 99% yields (Table 3.4, entries 3-5). Acetate and pivalate groups were found to give slightly better results than benzoate. Thus, acetate becomes the leaving group of choice for the transformation.

Table 3.5 Catalytic activities of selected Rh complexes

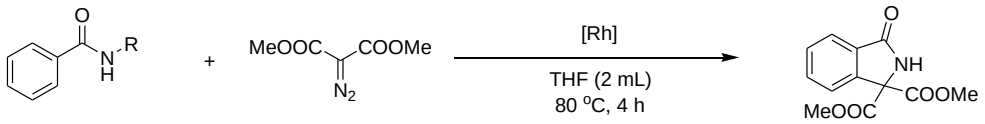

3a **4a** **9a**

entry	Rh complexes (5 mol%)	**9a** (%)[a]
1	$[(COD)RhCl]_2$	0[b]
2	$(Ph_3P)_3RhCl$	0[b]
3	$[Cp^*Rh(OAc)_2]$	99
4	-	0[b]

Reaction conditions: **3a** (0.2 mmol), **4a** (0.24 mmol, 1.2 equiv). [a] Yields were determined by ^1H NMR using dibromoethane as internal standard. [b] No detectable product formation.

Employing other Rh complexes such as $[(COD)RhCl]_2$ and $[(Ph_3P)_3RhCl]$ as catalyst did not give any detectable oxisoindoles product (Table 3.5 entries 1-2). In this study, $[Cp^*Rh(OAc)_2]$ was found to be the best Rh catalyst for the carbenoid cycloaddition (entry 3).

Table 3.6 Effect of temperature and catalyst loading

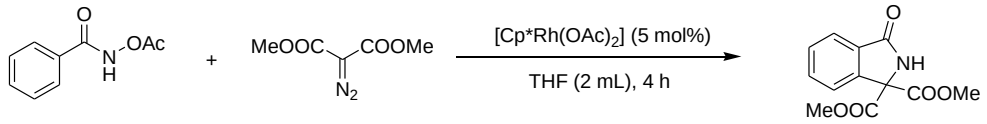

3a **4a** **9a**

entry	temperature (℃)	catalyst loading (mol%)	**9a** (%)[a]
1	40	5	74
2	60	5	99
3	80	5	93
4	100	5	90
5	60	1	68
6	60	2.5	75
7	60	1	91[b]

Reaction conditions: **3a** (0.2 mmol), **4a** (0.24 mmol, 1.2 equiv). [a] Yields were determined by ^{1}H NMR using dibromoethane as internal standard. [b]Reaction time was 16 h.

At 60 ℃, lowering the catalyst loading from 2.5 mol% to 1 mol% resulted in diminished product yield (Table 3.6, entries 5 and 6). Similarly, lowering the temperature also diminished the product yield (entry 1). However, the product yield was improved to 91% when the reaction time was prolonged to 16 h while keeping the reaction temperature at 60 ℃ (entry 7). With this optimized conditions, we turned to examine the substrate scope of the reaction.

3.2.3 Scope and Limitation

Table 3.7 Scope of benzohydroxamic acids

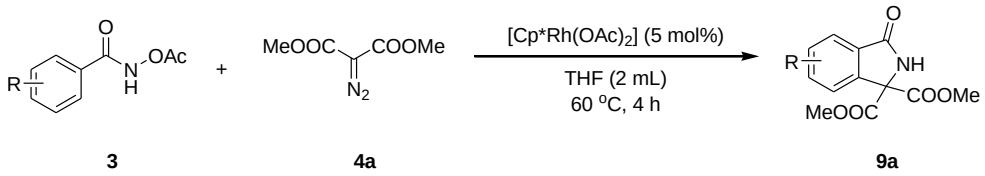

3 **4a** **9a**

entry[a]	**3**	**2**	yield (%)[b]
1	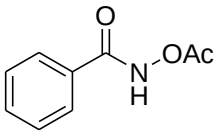 **3a**	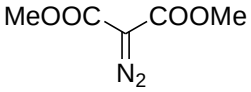 **4a**	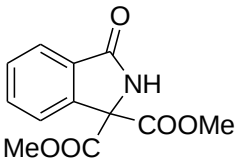 **9a**, 89
2	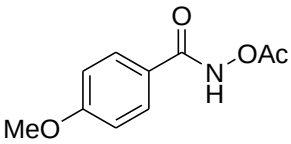 **3e**	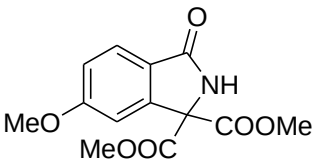 **4a**	**9b**, 90
3	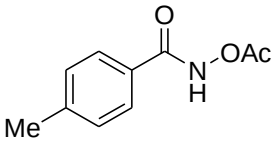 **3f**	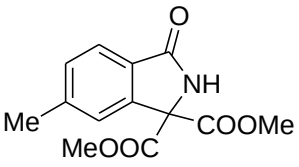 **4a**	**9c**, 82
4	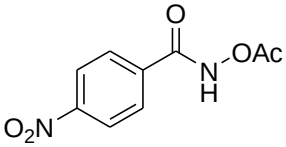 **3g**	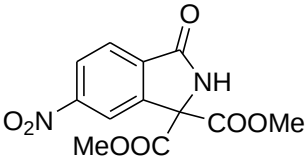 **4a**	**9d**, 76

5	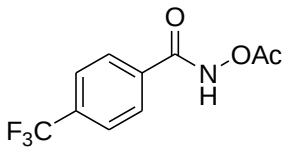 **3h**	**4a**	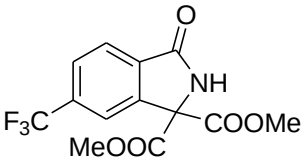 **9e**, 93
6	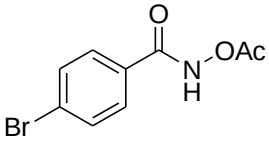 **3i**	**4a**	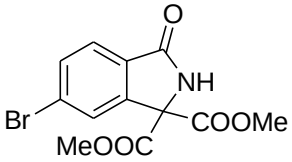 **9f**, 82
7	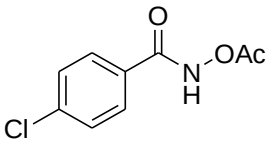 **3j**	**4a**	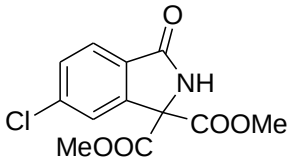 **9g**, 77
8	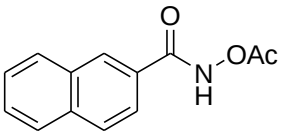 **3k**	**4a**	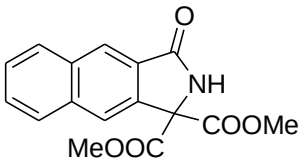 **9h**, 73
9	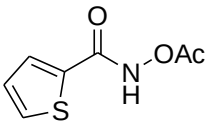 **3b**	**4a**	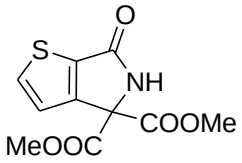 **9i**, 63

10	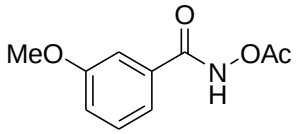 **3i**	**4a**	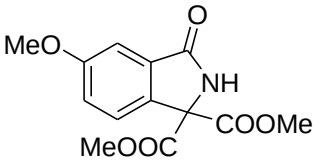 **9j**, 39	
			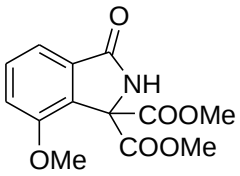 **9j'**, 9	

[a]Reaction conditions: **3** (0.2 mmol), **4a** (0.24 mmol, 1.2 equiv), [Cp*Rh(OAc)$_2$] (5 mol%), THF (2 mL), 60 ℃ for 4 h. [b] Isolated yields.

Table 3.7 depicts the reaction scope study of the benzohydroxamic acids. Electron-releasing and -withdrawing substituents (-OMe, -Me, -NO_2, -CF_3) were well tolerated and the corresponding oxisoindoles products were obtained in 76% - 93% yields (Table 3.7, entries 1 – 5). Benzohydroxamic acids with chloro- and bromo- substituents also reacted smoothly with **4a** to give **9f** and **9g** in 77% and 82% yield respectively (entries 6 – 7). The *ortho*-C-H bond was regioselectively functionalized with the assistance of the amide group on the benzohydroxamic acid. The less hindered *ortho*-C-H bond of disubstituted benzohydroxamic acid **3k** was functionalized exclusively to give **9h** in 73% yield (entry 8). However, when *meta*-substituted benzohydroxamic acid **3i** was employed, a mixture of regiomeric products (**9j** and **9j'**) were obtained in 48% combined yields (entry 10). Consistent with other reported findings, less hindered *ortho*-C-H bond was

functionalized preferentially. It is well known that rhodium-carbenoids would react with oxygen, nitrogen and sulphur atoms to give reactive ylides. When *N*-(thiophen-3-yl)benzamide (**3b**) was reacted with **3a, 9i** was obtained in 63% yield and no ylide-mediated reaction was observed.

Table 3.8 Substrate scope (diazo)

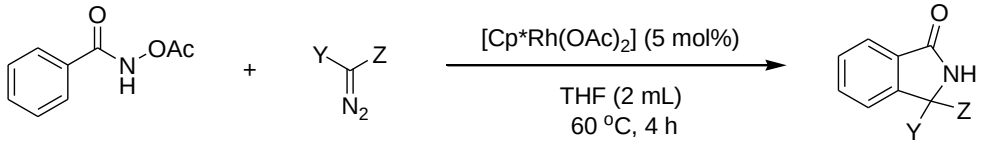

3a **4** **9**

entry[a]	**3a**	**2**	yield (%)[b]
1	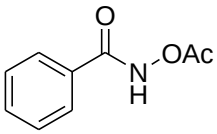	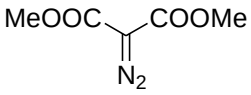	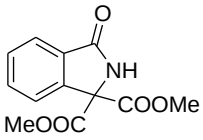
	3a	**4a**	**9a**, 89
2	**3a**	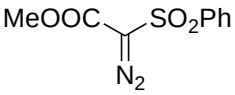	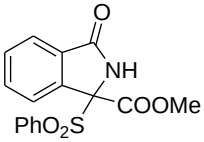
		4b	**9k**, 77
3	**3a**	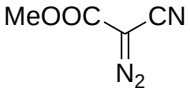	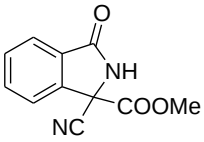
		4c	**9l**, 72
4	**3a**	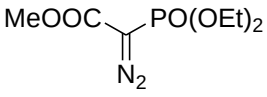	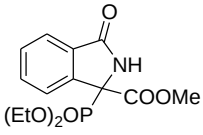
		4d	**9m**, 30

5	**3a**	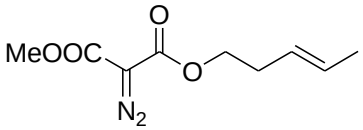 **4e**	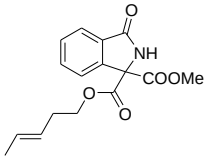 **9n**, 86
6	**3a**	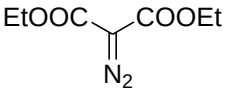 **4f**	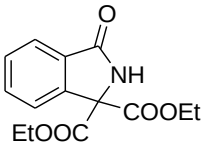 **9o**, 80
7	**3a**	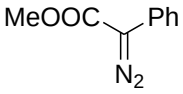 **4g**	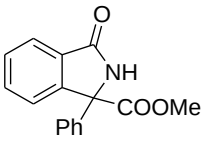 **9p**, 83
8	**3a**	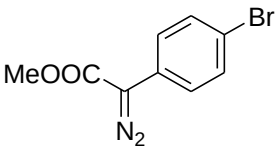 **4h**	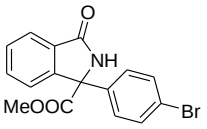 **9q**, 90
9	**3a**	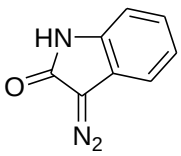 **4i**	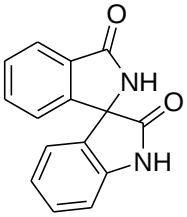 **9r**, 75
10	**3a**	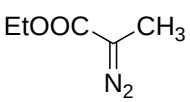 **4j**	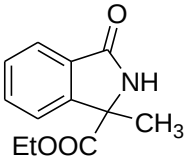 **9s**, 32

11	**3a**	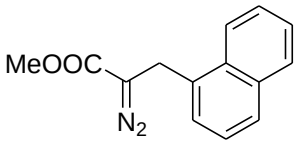 **4k**	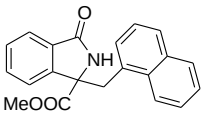 **9t**, 62
12	**3a**	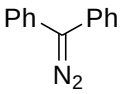 **4l**	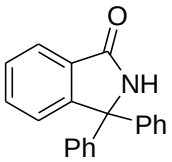 **9u**, 82

[a]Reaction conditions: **3** (0.2 mmol), **4** (0.24 mmol), [Cp*Rh(OAc)$_2$] (5 mol%), THF (2 mL), 60 °C for 4 h. [b] Isolated yields.

Table 3.8 shows the substrate scope of the diazo reagents. Acceptor – acceptor type diazo reagents coupled effectively with **3a** under the optimized reaction conditions to produce the corresponding oxisoindoles products in 30% – 89% yields (Table 3.8, entries 1 – 6). Functional groups such as esters, phenylsulfone (entry 2), cyano (entry 3) and diethyl phosphonate (entry 4) were well tolerated. It is known that alkene moieties would undergo cyclopropanation with Rh-carbenoid species.[68] In this work, an internal alkene moiety was found to be tolerated in the Rh-catalyzed cycloaddition reaction. For example, the reaction of **3a** with **4e** produced **9n** in 86% yield (entry 5). No cyclopropanation products were obtained. Apart from acceptor – acceptor type diazo reagents, donor – acceptor and donor – donor type diazo reagents were also effective coupling partners. For example, treating methyl α-phenyldiazoacetate (**4g**) and methyl

α-(4-bromophenyldiazoacetate) (**4h**) with **3a** under the standard reaction conditions furnished the corresponding products **9p** and **9q** in 83% and 90% respectively (entries 7 - 8). Cyclic diazo reagents such as diazooxindole (**4i**) reacted smoothly to give the bicyclic product **9r** in 75% yield. Alkyl diazoacetates with *β*-hydrogen atom are challenging reagents for the cycloaddition reaction; competitive *β*-hydride elimination of the alkylrhodium complex would terminate the catalytic cycle by forming inactive rhodium-hydride species.[69] In this work, alkyldiazoacetates **4j** and **4k** coupled with **3a** to give the corresponding oxisoindoles in 32% and 62% yield respectively (entries 10 – 11). Donor–donor type diazo reagents such as diphenyldiazomethane (**4l**) was found to couple effectively with **3a,** and **9u** was obtained in 82% yield.

3.2.4 Proposed Mechanism

Previously, Yu and co-workers reported the Rh(III)- catalyzed direct carbenoid cross-couplings with arene C−H bonds, and a *σ*-alkyl−Rh(III) complex was isolated and characterized. It is plausible that the alkylrhodium(III) complex was formed via migratory carbene insertion to the Rh-aryl bond (Scheme 3.2).[63b,70]

Scheme 3.2 Preparation of alklrhodium(III) complex

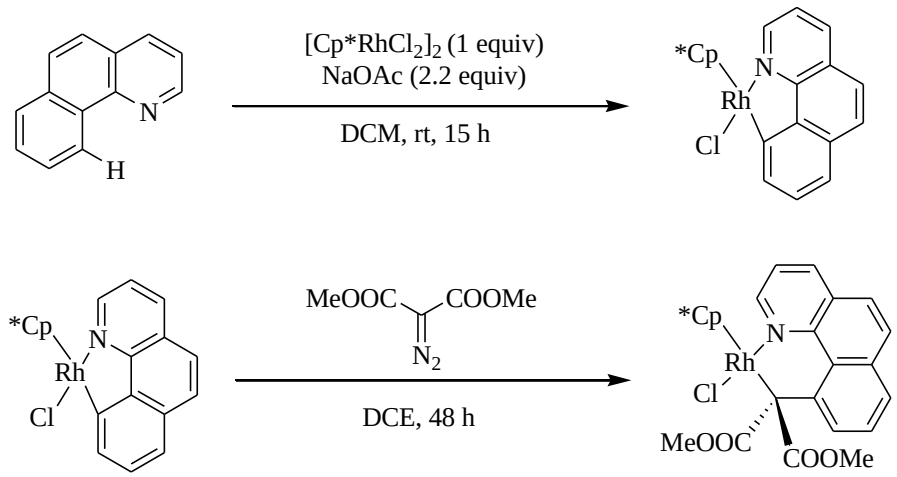

Assuming that the Rh(III)-catalyzed formal oxidative [4+1] cycloaddition of benzohydroxamic acids and diazoesters proceed via a similar pathway, we reacted *O*-acetyl benzohydroxamic acids (**3a**, 0.12 mmol) with [Cp*Rh(OAc)$_2$] (0.1 mmol) in THF at room temperature for 2 h under a N_2 atmosphere. The

crude reaction mixture was then filtered by Celite® ; ^{1}H NMR analysis of the mixture revealed a complicated spectrum. By column chromatography over alumina with dichloromethane as the eluent, the first orange band was collected and removal of the dichloromethane gave a dark orange solid. ^{1}H NMR spectrum of the purified sample showed four sets of aromatic signals (δ_H 7.78, d, J = 7.6 Hz, 1H; δ_H 7.69, d, J = 7.2 Hz, 1H; δ_H 7.36, t, J = 7.6 Hz, 1H; δ_H 7.21, J = 7.4 Hz, 1H). This suggested that the *ortho*-C-H bond of *O*-acetyl benzohydroxamic acid has been cleaved. However, the equivalent –CH_3 signal of the Cp* was split into five distinct absorption peaks (δ_H 1.94, s, 3H; δ_H 1.26, s, 3H; δ_H 1.18, s, 3H; δ_H 1.16, s, 3H; δ_H 0.97, s, 3H). An unknown multiplet signal was found in the region between 4.16 – 4.01 ppm, which was assigned to 2 H atoms. To obtain further insight into the structure of the complex, we prepared a single crystal of this complex for X-ray diffraction study.

To this end, the reaction temperature was raised to 60 ^{o}C and the mixture was allowed to react for 2 h. The sample was purified by column chromatography and it was then dissolved in a minimum amount of dichloromethane. Diethyl ether was then carefully added. A dark red crystal (5% yield) was obtained after standing for 3 days. By means of X-ray crystallography,

the molecular structure was established to be a dinuclear arylrhodium(III) complex (Figure 3.2).

Figure 3.2 Molecular structure of dinuclear arylrhodium(III) complex **$[Rh(C_{19}H_{21}NO_3)]_2$**

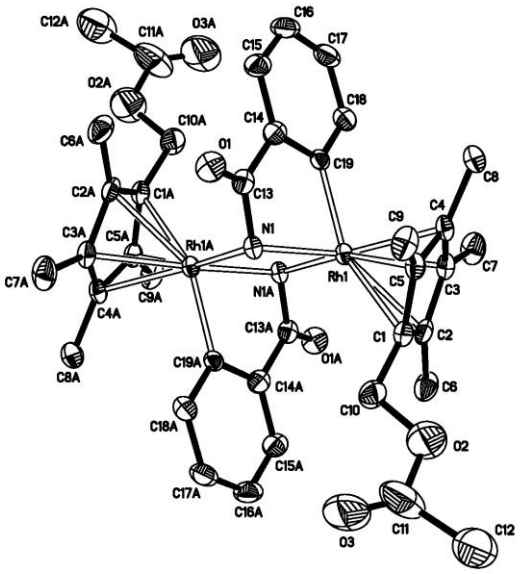

Table 3.9 Selected bond distances [Å] and angles [°]

Bond distances	
Rh(1)-C(19)	2.024(3)
Rh(1)–N(1)	2.111(3)
Rh(1)–N(1A)	2.169(3)
C(10)–O(2)	1.397
Bond angles	
N(1)-Rh(1)-N(1A)	81.24(13)
C(11)-O(2)-C(10)	110.7(6)
N(1)-C(13)-C(14)	111.4(3)
C(14)-C(19)-Rh(1)	114.3(3)

Table 3.10 Crystal data and structure refinement for dinuclear arylrhodium(III) complex

Empirical formula	**$[Rh(C_{19}H_{21}NO_3)]_2$**
Formula weight	828.56
Temperature	296(2) K
Wavelength	0.71073 Å
Crystal system	Rhombohedral
Space group	R-3
Unit cell dimensions	a = 34.5934(6) Å = 90°.
	b = 34.5934(6) Å = 90°.
	c = 8.2566(3) Å = 120°.
Volume	8556.9(4) $Å^3$
Z	9
Density (calculated)	1.447 Mg/m^3
Absorption coefficient	0.913 mm^{-1}
F(000)	3798
Crystal size	0.42 x 0.24 x 0.24 mm^3
Theta range for data collection	2.04 to 27.48°.
Index ranges	-44<=h<=44, -44<=k<=44,
	-10<=l<=10
Reflections collected	30007
Independent reflections	4313 [R(int) = 0.0472]
Completeness to theta = 27.48°	98.9%
Absorption correction	Semi-empirical from equivalents
Max. and min. transmission	0.7456 and 0.6128
Refinement method	Full-matrix least-squares on F^2
Data / restraints / parameters	4313 / 3 / 212
Goodness-of-fit on F^2	1.004
Final R indices [I>2sigma(I)]	R1 = 0.0649, wR2 = 0.1959
R indices (all data)	R1 = 0.0885, wR2 = 0.2312
Extinction coefficient	0.00012(4)
Largest diff. peak and hole	1.250 and -1.203 $e.Å^{-3}$

The complex features a five-membered cyclic structure with the measured Rh(1)–C(19) distance to be 2.024(3) Å.[71] The four membered aza-rhodium cycle was characterized by the measured Rh(1)–N(1) and Rh(1)–N(1A) distances of 2.111(3) Å and 2.169(3) Å, respectively. As expected, the two Cp rings adopt an anti-conformation. Notably, a methyl group on the Cp rings was acetoxylated with the C(10)–O(2) distance being 1.397 Å. This explained why equivalent $–CH_3$ signals of the Cp* was split into five different peaks and the appearance of the multiplet signal between 4.16 – 4.01 ppm. When the dinuclear arylrhodium(III) complex was reacted with diazomalonate (**4a**) in THF at 60 ℃, no desired product formation was observed. The dinuclear arylrhodium(III) complex was fully recovered. The observed poor reactivity is attributed to the strong aza-rhodium cycle, which should be difficult to dissociate for diazo coordination.

Kinetic isotopic effect (KIE) study was also performed. **3a** and **3a-d_5** (0.2 mmol, 1 equiv) were reacted with **4a** (0.2 mmol, 1 equiv) at 40 ^oC for 20 minutes in two parallel experiments. (Scheme 3.3)

Scheme 3.3 Kinetic isotopic effect (KIE) study

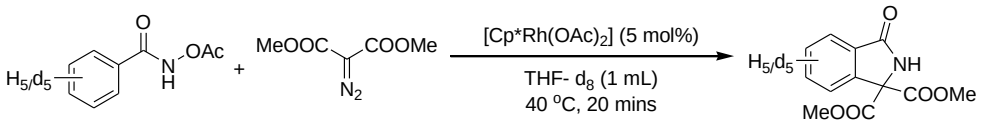

3a/3a-d$_5$ **4a** **9a/9a-d$_4$**

The reactions were quenched by immersing the reaction vials in ice water. The reaction mixture was filtered and the desired product (**9a**/**9a-d$_4$**) was obtained by flash column chromatography. The KIE values were calculated by the ratio of product formation of **9a** and **9a-d$_4$**. The KIE experiment was repeated three times. (Table 3.11)

Table 3.11 Experiemtnal results on the KIE experiment

run	yield of **9a**	yield of **9a-d$_4$**	KIE values
1	13	13	1
2	11	10	1.1
3	11	11	1
average	-	-	1.03

It is known that KIE values > 2 were observed in many [Cp*Rh^{III}]-catalyzed C–H coupling reactions. For example, the k_H/k_D of the Rh(III)-catalyzed cycloaddition of *O*-pivalate hydroxamic acids with alkyne is 15 ± 1. In this work, a k_H/k_d of 1.03 was observed, suggesting that the C–H activation is not the turnover-limiting step.

On the basis of the previous report of our group[62], literature[51,72] and the mechanistic study that performed, a plausible mechanism for this Rh-catalyzed cycloaddition reaction is proposed and was shown on scheme. It is postulated that the electrophilic [Cp*Rh$(OAc)_2$] would initially undergo a chelation-assisted C–H/N–H deprotonation of *O*-acetyl benzohydroxamic acids to form a five-membered rhodacycle with elimination of acetic acid. We proposed that coordination of the diazo compound with **A** may form the diazonium intermediate **B**. Extrusion of N_2 from **B** would afford the Rh-carbene **C**, which subsequently undergoes migratory insertion to give **D**. Further C–N bond formation via reductive elimination would furnish the desired product and the N-OAc moiety may act as an internal oxidant to regenerate the active Rh catalyst (Scheme 3.4).

Scheme 3.4 Proposed mechanistic cycle

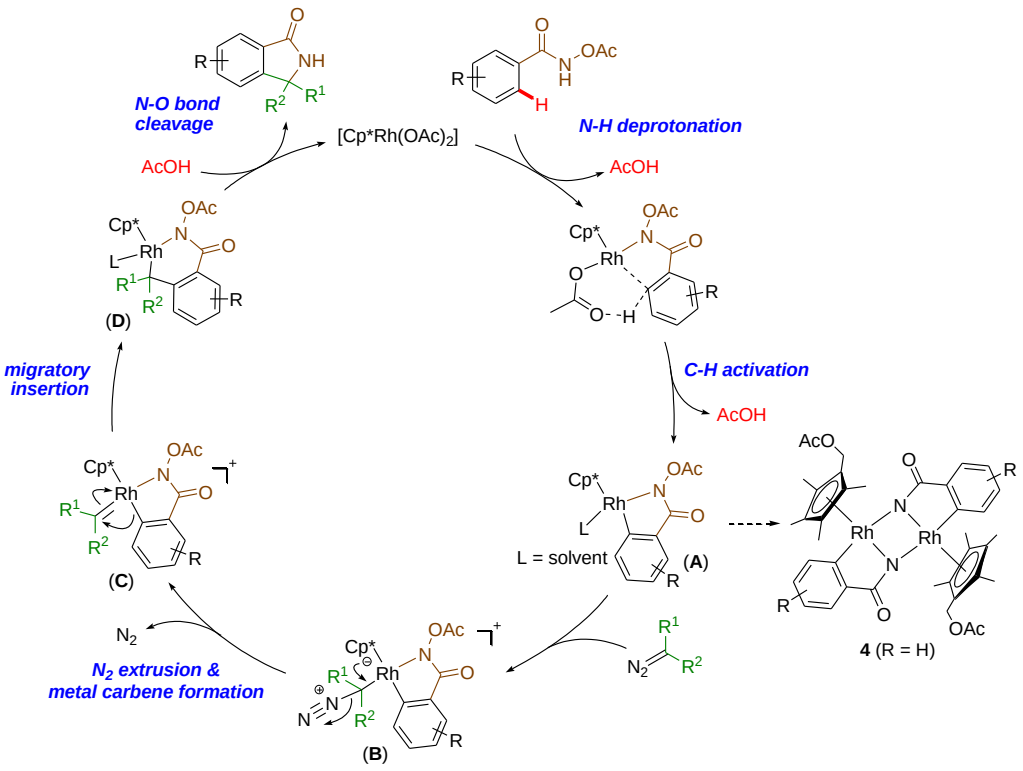

3.3 Concluding Summary

In conclusion, we have developed a mild rhodium(III)-catalyzed formal oxidative [4+1] cycloaddition of benzohydroxamic acids and α-diazoesters. Electron-releasing and –withdrawing substituents on the benzohydroxamic acids were well tolerated and gave the corresponding oxisoindoles in good yields.

Donor-acceptor, acceptor-acceptor and donor-donor type diazo compounds were effective reagents for the cycloaddition reaction. Alkyl diazoacetates with *β*-hydrogen atom which may deactivate the Rh catalyst due to *β*-hydride elimination were good partners for the cycloaddition reaction. Diazo compounds with alkene moiety were successfully coupled with benzohydroxamic acids to give the desired oxisoindoles despite potential competitive cyclopropanation between alkene moieties and Rh-carbenoid species.

A dinuclear aryl-aza-rhodium(III) complex was successfully isolated. However, this complex is inactive for catalyzing the cycloaddition reaction and it may due to the strong aza-rhodium cycle which hinder diazo coordination.

3.4 Experimental Section

3.4.1 General Experimental

All the reagents were obtained from commercial sources and used without purification. All the solvents used were obtained from commercial sources and were distillated according to the literature procedures. All catalytic reactions were carried out under a nitrogen atmosphere. Benzohydroxamic acids were prepared from benzoic acids and benzoyl chlorides following a modified procedure. *O*-Acetyl-benzohydroxamic acids, *O*-pivaloylbenzohydroxamic acids, *O*-enzoylbenzohydroxamic acid and *O*-methoxylbenzohydroxamic acid were synthesized according to the literature methods. $[Cp^*Rh(OAc)_2]$, $[Rh(cod)Cl]_2$ and diazo compounds were synthesized following the literature procedures.

Thin layer chromatography was performed on silica gel plates. Silica gel (Merck, 230 - 400 mesh) was used for flash column chromatography. ^{1}H and ^{13}C NMR spectra were recorded on a Brüker (400 MHz) NMR spectrometer. The chemical shift (δ) values are given in parts per million (ppm) with multiplicity (s= singlet, d= doublet, t= triplet, q= quartet, m= multiplet, td= triplet of doublets) and are referenced to residual solvent peaks. Coupling constants (J) were reported in Hertz (Hz). Melting points were measured on a Büchi Melting Point

B - 545 machine. Mass spectra and high resolution mass spectra (HRMS) were obtained on a VG MICROMASS Fison VG platform, a Finnigan Model Mat 95 ST instrument, or a Brüker APEX 47e FT - ICR mass spectrometer.

3.4.2 Experimental Procedures and Physical Characterization for Substrate Synthesis

General procedure A for the synthesis of benzohydroxamic acids from benzoyl chloride

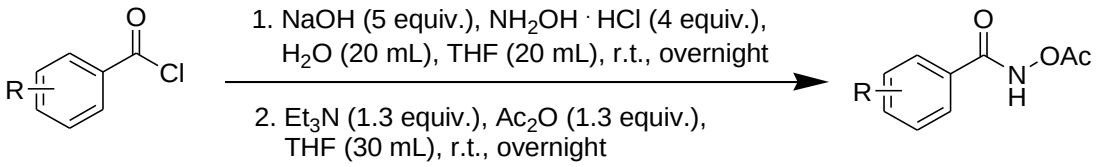

Hydroxylamine hydrochloride (2.78 g, 40 mmol) and NaOH pellets (2 g, 50 mmol) was dissolved in water (20 mL) and then stirred for 5 minutes in a 100 mL-rounded bottom flask equipped with a magnetic stirrer. Then, benzoyl chloride (10 mmol) dissolved in THF (20 mL) was added via a syringe. After stirring the reaction mixture at room temperature overnight, 2 M HCl was added to acidify the solution to pH 1. The organic layer was collected and the aqueous

layer was extracted with EtOAc (3 x 10 mL). The combined organic layer was washed by water and then brine. After drying the organic layer over $MgSO_4$, it was then concentrated under reduced pressure to afford crude *N* -hydroxybenzamide solid.

N-Hydroxybenzamide dissolved in THF (15 mL) was stirred in a 100 mL-rounded bottom flask equipped with a magnetic stirrer. 1.3 equiv acetyl acetate was then added and 1.3 eqiuv. Et_3N was added in dropwise manner. The reaction was monitored by TLC. Upon complete consumption of the starting materials, the organic layer was collected, washed with water and brine and then dried over $MgSO_4$. The solution was concentrated under reduced pressure to afford crude benzohydroxamic acids as a solid. Recrystallization of the solid from hexanes/EtOAc gave the desired product.

General procedure B for the synthesis of benzohydroxamic acids from benzoyl chloride

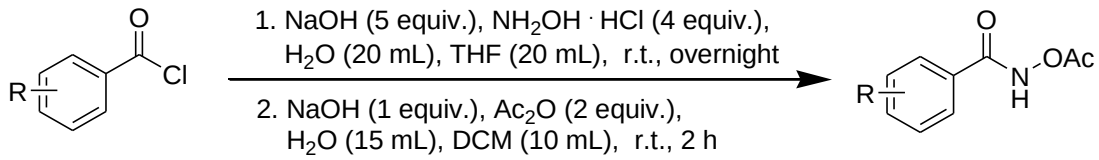

Hydroxylamine hydrochloride (2.78 g, 40 mmol) and NaOH pellets (2 g, 50 mmol) was dissolved in water (20 mL) and then stirred for 5 minutes in a 100 mL-rounded bottom flask equipped with a magnetic stirrer. Then, benzoyl chloride (10 mmol) dissolved in THF (20 mL) was added via a syringe. After stirring the reaction mixture at room temperature overnight, 2 M HCl was added to acidify the solution to pH 1. The organic layer was collected and the aqueous layer was extracted with EtOAc (3 x 10 mL). The combined organic layer was washed by water and then brine. After drying the organic layer over $MgSO_4$, it was then concentrated under reduced pressure to afford crude *N* -hydroxybenzamide solid.

NaOH pellets (1 equiv.) in water (0.5 M) and *N*-hydroxybenzamide in DCM (15 mL) were stirred for 5 minutes in a 100 mL rounded bottom flask equipped with a magnetic stirrer. Acetyl acetate diluted with THF (5 mL) was added

dropwise over 30 minutes. The reaction was monitored by TLC. Upon complete consumption of the starting material, the organic layer was collected, washed with water and then brine and dried over $MgSO_4$. It was then concentrated under reduced pressure to afford crude benzohydroxamic acids as a solid. Recrystallization from hexanes/EtOAc gave the desired product.

3.4.3 General Procedure for Rh(III)-Catalyzed [4+1] Cycloaddition of Benzohydroxamic Acids with Diazo Compounds

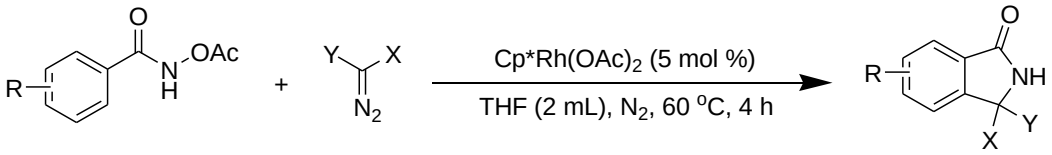

A 8 mL-vial equipped with a magnetic stirrer was charged with *O*-acetyl benzohydroxamic acid (0.2 mmol) and [Cp*Rh(OAc)$_2$] (5 mol %). 0.5 mL THF was then added via syringe. Diazo compound was diluted with 1.5 mL THF and was added in one pot. The reaction vial was allowed to stir for 4 h in a 60 ℃ oil bath. Upon complete reaction, the crude mixture was filtered through Celite® and concentrated under reduced pressure. The residue was then purified by flash column chromatography to give the desired product.

Dimethyl 3-oxoisoindoline-1,1-dicarboxylate (9a).

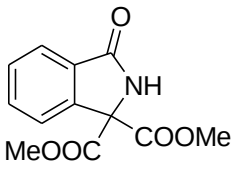

Eluent: 50% n-hexane / 50% ethyl acetate. The product was obtained as an off-white solid (89% isolated yield), ^{1}H NMR (400 MHz, $CDCl_3$): δ_H 7.86 - 7.82 (t, 2H, , *J* = 8.0 Hz), 7.67 - 7.63 (t, 1H, *J* = 7.2 Hz), 7.59 - 7.55 (t, 1H, *J* = 7.6 Hz), 6.87 (s, 1H), 3.83 (s, 6H). ^{13}C NMR (100 MHz, $CDCl_3$): δ_C 169.9, 167.0, 140.1, 133.1, 131.0, 130.5, 125.7, 124.3, 70.7, 54.3. HRMS (ESI): calcd. for C12H12NO5: 250.0715 , found: 250.0712.

Dimethyl 6-methoxy-3-oxoisoindoline-1,1-dicarboxylate (9b).

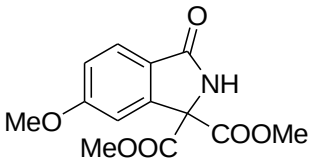

Eluent: 40% n-hexane / 60% ethyl acetate. The product was obtained as a white solid (90% isolated yield). ^{1}H NMR (400 MHz, $CDCl_3$): δ_H 7.75 - 7.72(d, 1H, *J* = 8.8 Hz), 7.312 - 7.307 (d, 1H, *J* = 2.0 Hz), 7.08 - 7.06 (dd, 1H), 6.60(s, 1H), 3.91 (s, 3H), 3.83(s, 6H). ^{13}C NMR (100 MHz, $CDCl_3$): δ_C 169.7, 167.0, 163.9, 142.4, 125.7, 123.3, 117.1, 110.6, 56.35, 54.35. HRMS (ESI): calcd. for C13H13NO6Na : 302.0641 , found: 302.0630.

Dimethyl 6-methyl-3-oxoisoindoline-1,1-dicarboxylate (9c).

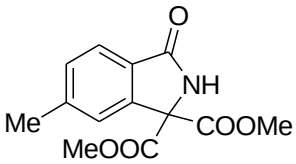

Eluent: 50% n-hexane / 50% ethyl acetate. The product was obtained as a white solid (82% isolated yield). ^{1}H NMR (400 MHz, $CDCl_3$): δ_H 7.72-7.70 (d, 1H, *J* = 8 Hz), 7.63 (s, 1H), 7.37 - 7.35 (d, 1H, *J* = 7.6 Hz), 7.04 (s, 1H) 3.82 (s, 6H), 2.49 (s, 3H). ^{13}C NMR (100 MHz, $CDCl_3$): δ_C 169.9, 166.9, 143.9, 140.3, 131.4, 128.2, 125.8, 123.9, 70.4, 54.1, 22.2. HRMS (ESI): calcd. for C13H14NO5: 264.0872, found: 264.0861.

Dimethyl 6-nitro-3-oxoisoindoline-1,1-dicarboxylate (9d).

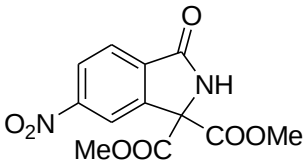

Eluent: 40% n-hexane / 60% ethyl acetate. The product was obtained as a white solid (93% isolated yield). ^{1}H NMR (400 MHz, $CDCl_3$): δ_H 8.692 – 8.688 (d, 1H, *J* = 1.6 Hz), 8.46 – 8.43 (dd, 1H), 8.008 – 7.988 (d, 1H, *J* = 8.0 Hz), 7.80 (s, 1H), 3.88(s, 6H). ^{13}C NMR (100 MHz, $CDCl_3$): δ_C 167.6, 165.9, 151.2, 141.2, 136.2, 126.1, 125.5, 121.7, 70.7, 54.9. calcd. for C12H10N2O7Na: 317.0386, found: 317.0374.

Dimethyl 6-(trifluoromethyl)-3-oxoisoindoline-1,1-dicarboxylate (9e).

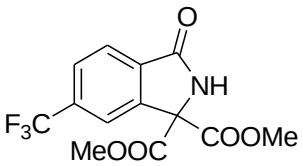

Eluent: 50% n-hexane / 50% ethyl acetate. The product was obtained as a white solid (93% isolated yield). ^{1}H NMR (400 MHz, $CDCl_3$): δ_H 8.12 (s, 1H), 8.00 – 7.95 (d, 1H, *J* = 8.0 Hz), 7.85 – 7.83 (d, 1H, *J* = 8.0 Hz), 3.86 (s, 6H). ^{13}C NMR (100 MHz, $CDCl_3$): δ_C 168.6, 166.2, 140.3, 134.9, 134.3, 127.9, 125.0, 123.2, 123.1, 70.8, 54.7. HRMS (ESI): calcd. for C13H11NO5F3: 318.0589, found: 318.0594.

Dimethyl 6-bromo-3-oxoisoindoline-1,1-dicarboxylate (9f).

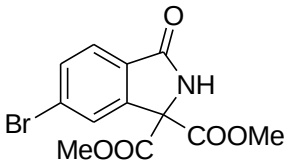

Eluent: 50% n-hexane / 50% ethyl acetate. The product was obtained as a white solid (77% isolated yield). ^{1}H NMR (400 MHz, $CDCl_3$): δ_H 8.00 (s, 1H), 7.70 - 7.67 (dd, 2H), 7.32 (s, 1H), 3.85 (s, 6H). ^{13}C NMR (100 MHz, $CDCl_3$): δ_C 169.0, 166.4, 141.7, 134.1, 130.0, 129.1, 127.8, 125.6, 70.4, 54.6. HRMS (ESI): calcd. for C12H11NO5Br: 327.9821, found: 327.9805.

Dimethyl 6-chloro-3-oxoisoindoline-1,1-dicarboxylate (9g).

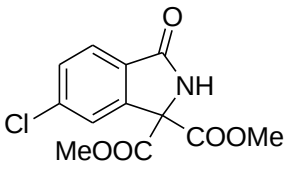

Eluent: 50% n-hexane / 50% ethyl acetate. The product was obtained as a white solid (82% isolated yield). ^{1}H NMR (400 MHz, $CDCl_3$): δ_H 7.84 - 7.83 (d, 1H, *J* = 1.6 Hz), 7.76 - 7.74 (d, 1H, *J* = 8.0 Hz), 7.55 - 7.53 (dd, 1H), 7.22(s, 1H), 3.85 (s, 6H). ^{13}C NMR (100 MHz, $CDCl_3$): δ_C 168.8, 166.4, 141.6, 139.5, 131.2, 129.5, 126.2, 125.5, 70.4, 54.5. HRMS (ESI): calcd. for C12H11NO5Cl: 284.0326, found: 284.0327.

Methy**l 3-oxo-1-phenyl-2,3-di**hy**dro-1H-benzo[f]isoindole-1-carboxylate (9h).**

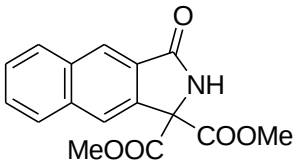

Eluent: 50% n-hexane / 50% ethyl acetate. The product was obtained as a white solid (73% isolated yield). 1H NMR (400 MHz, $CDCl_3$): δ_H 8.34 - 8.31(d, 2H, *J* = 24.4 Hz), 8.04 - 8.00 (t, 2H, *J* = 7.6 Hz), 7.66 - 7.59 (m, 2H), 6.97 (s, 1H), 3.86(s, 6H). 13C NMR (100 MHz, $CDCl_3$): δ_C 169.6, 167.3, 139.8, 134.7, 134.1, 130.0, 129.2, 128.7, 128.0, 127.8, 125.5, 125.1, 70.5, 54.4. HRMS (ESI): calcd. for C16H14N2O5: 300.0872, found: 300.0870.

Dimethy**l 5, 6-di**hy**dro-6-oxothieno[3,2-c]pyrrole-4,4-dicarboxylate (9i).**

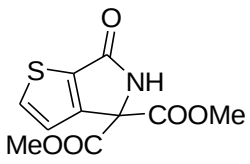

Eluent: 50% n-hexane / 50% ethyl acetate. The

product was obtained as a white solid (63% isolated yield). ^{1}H NMR (400 MHz, $CDCl_3$): δ_H 7.72 – 7.71 (q, 1H, *J* = 0.8 Hz), 7.28 – 7.27 (d, 1H, *J* = 4.8 Hz), 6.96 (s, 1H), 3.83(s, 6H). 13C NMR (100 MHz, $CDCl_3$): δ_C 166.0, 165.0, 150.6, 136.7, 135.3, 122.8, 69.7, 54.2. HRMS (ESI): calcd. for C10H9NO5NaS: 278.0099, found: 278.0108.

Dimethyl 5-methoxy-3-oxoisoindoline-1,1-dicarboxylate(9j).

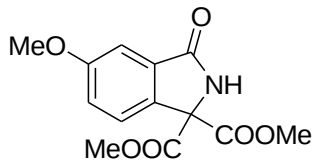

Eluent: 50% n-hexane / 50% ethyl acetate. The product was obtained as a white solid. ^{1}H NMR (400 MHz, $CDCl_3$): 7.73 – 7.71 (d, 1H, *J* = 8.4 Hz), 7.30 – 7.29 (d, 1H, *J* = 2.4 Hz), 7.19 – 7.17 (q, 1H, *J* = 2.4 Hz), 6.82 (s, 1H), 3.87 (s, 3H), 3.82 (d, 3H). 13C NMR (100 MHz, $CDCl_3$): δ_C 169.6, 167.0, 161.7, 132.3, 132.1, 126.4, 121.0, 106.9, 70.1, 56.0 , 54.0. HRMS (ESI): calcd. for C13H14NO6: 280.0821, found: 280.0830.

Dimethyl 7-methoxy-3-oxoisoindoline-1,1-dicarboxylate (9j').

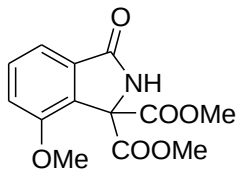

Eluent: 50% n-hexane / 50% ethyl acetate. The product was obtained as a white solid.^{1}H NMR (400 MHz, $CDCl_3$): 7.55 – 7.51 (t, 1H, *J* = 7.6 Hz), 7.45 – 7.43 (d, 1H, *J* = 7.6 Hz), 7.15 – 7.13 (d, 1H, *J* = 8.0 Hz), 6.91 (s, 1H), 3.92 (s, 3H), 3.79 (d, 3H). 13C NMR (100 MHz, $CDCl_3$): δ_C 170.3, 167.0, 156.3, 133.0, 132.4, 128.5, 116.5, 116.1, 70.1, 56.5, 53.9. HRMS (ESI): calcd. for C13H14NO6: 280.0821, found: 280.0830.

Methyl 3-oxo-1-(phenylsulfonyl)isoindoline-1-carboxylate (9k).

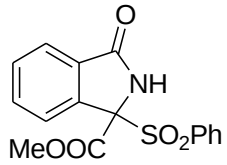

Eluent: 50% n-hexane / 50% ethyl acetate. The product was obtained as an off-white solid (84% isolated yield). ^{1}H NMR (400 MHz, $CDCl_3$): δ_H 8.17 - 8.15(d, 1H, *J* = 8 Hz), 7.71 - 7.67 (m, 1H), 7.57 - 7.48 (m, 5H), 7.35 - 7.31 (t, 2H, *J* = 7.6 Hz), 7.20 (s, 1H), 3.99(s, 3H). ^{13}C NMR (100 MHz, $CDCl_3$): δ_C 168.6, 163.4, 136.8, 135.3, 133.3, 132.6, 131.6, 131.4, 130.8, 129.1, 126.6, 124.3, 85.0, 54.9. HRMS (ESI): calcd. for $C16H13NO5Na^{+}$: 354.0412, found: 354.0405.

Methyl 1-cyano-3-oxoisoindoline-1-carboxylate (9l).

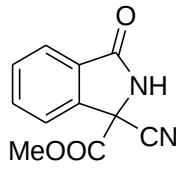

Eluent: 50% n-hexane / 50% ethyl acetate. The product was obtained as a white solid (72% isolated yield). ^{1}H NMR (400 MHz, $CDCl_3$): δ_H 7.93 - 7.90 (d, 1H, *J* = 7.6 Hz), 7.84 - 7.83 (d, 1H, *J* = 7.6 Hz), 7.76 - 7.72 (td, 1H), 7.70 - 7.66 (td, 1H), 7.46 (s, 1H), 3.93(s, 3H). ^{13}C NMR (100 MHz, $CDCl_3$): δ_C 169.7, 164.7, 139.4, 134.3, 131.8, 129.9, 125.3, 123.9, 115.2, 59.7, 55.5. HRMS (ESI): calcd. for $C_{11}H_9N_2O_3$: 217.0613, found 217.0618.

Methyl 1-(ethoxyphosphono)-3-oxoisoindoline-1-carboxylate (9m)

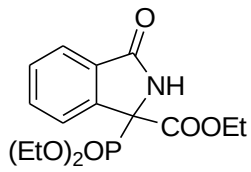

Eluent: 50% n-hexane / 50% ethyl acetate. The product was obtained as a light yellow solid (30% isolated yield). ^{1}H NMR (400 MHz, $CDCl_3$): δ_H 7.99 – 7.97 (d, 1H, *J* = 7.6 Hz), 7.86 – 7.84 (d, 1H, *J* = 7.2 Hz), 7.66 – 7.63 (t, 1H, *J* = 7.4 Hz), 7.58 – 7.54 (t, 1H, *J* = 7.6 Hz), 6.86 (s, 1H), 4.33 – 4.28 (q, 2H, *J* = 6.8 Hz), 4.15 – 4.10 (q, 2H, *J* = 7.2Hz), 4.08 – 3.99 (m, 1H), 3.89 – 3.79 (m, 1H), 1.34 – 1.31 (t, 3H, *J* = 7Hz), 1.25 – 1.21 (t, 3H, *J* = 7 Hz), 1.14 – 1.11 (t, 3H, 7.2 Hz). ^{13}C NMR (100 MHz, $CDCl_3$): δ_C 169.5, 165.8, 139.4, 139.3, 132.64, 132.62, 131.23, 131.19, 129.9, 125.62, 125.59, 124.1, 68.4, 66.9, 65.1, 65.09, 65.02, 64.8, 64.7, 63.4, 16.47, 16.41, 16.35, 16.29, 14.12. ^{31}P NMR (100 MHz, H_3PO_4): 13.6, 13.52, 13.46, 13.42, 13.37. HRMS (ESI): calcd. for C15H21NO6P: 342.1107, found: 342.1100.

1-methyl 1-(E)-pent-3-enyl 3-oxoisoindoline-1,1-dicarboxylate (9n).

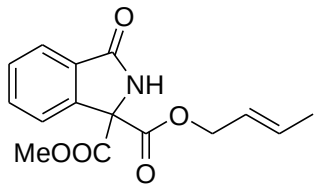

Eluent: 50% n-hexane / 50% ethyl acetate. The product was obtained as a white solid (86% isolated yield), ^{1}H NMR (400 MHz, $CDCl_3$): 7.86 – 7.84 (d, 1H, *J* = 7.6 Hz), 7.84 – 7.82 (d, 1H, *J* = 7.6 Hz), 7.67 – 7.63 (m, 1H), 7.58 – 7.55 (m, 1H), 6.85 (s, 1H), 5.85 – 5.76 (m, 1H), 5.57 – 5.50 (m, 1H), 4.64 – 4.62 (m, 2H), 3.83 (s, 1H), 1.72-1.70 (d, 3H, J = 6.4 Hz). ^{13}C NMR (100 MHz, $CDCl_3$): δ_C 169.6, 166.8, 166.0, 140.0, 133.3, 132.8, 130.8, 130.3, 125.6, 124.1, 123.7, 70.6, 68.0, 54.0, 17.9. HRMS (ESI): calcd. for C15H15NO5Na: 312.0848, found: 312.0838.

Diethyl 3-oxoisoindoline-1,1-dicarboxylate (9o).

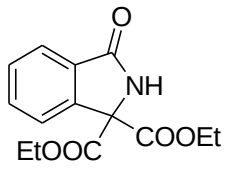

Eluent: 50% n-hexane / 50% ethyl acetate. The product was obtained as a white solid (80% isolated yield). ^{1}H NMR (400 MHz, $CDCl_3$): δ_H 7.85 - 7.81(t, 2H, *J* = 8.0 Hz), 7.65 - 7.61 (t, 1H, *J* = 7.6 Hz), 7.57 - 7.53 (t, 1H, *J* = 7.6 Hz), 7.23 (s, 1H), 4.30 - 4.25 (dd, 4H, *J* = 7.2 Hz), 1.30 - 1.26 (t, 6H, *J* = 7.2 Hz). ^{13}C NMR (100 MHz, $CDCl_3$): δ_C 170.1, 166.5, 140.3, 133.0, 131.1, 130.4, 125.7, 124.3, 70.9, 63.6, 14.3. HRMS (ESI): calcd. for C14H16NO5: 278.1028, found: 278.1021.

Methyl 3-oxo-1-phenylisoindoline-1-carboxylate (9p).

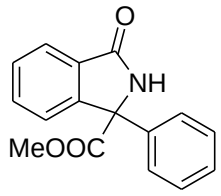

Eluent: 50% n-hexane / 50% ethyl acetate. The product was obtained as a white solid (83% isolated yield), mp 168 – 169 ^{o}C. ^{1}H NMR (400 MHz, $CDCl_3$): δ_H 7.86 - 7.84 (d, 1H, *J* = 7.2 Hz), 7.71 - 7.69 (d, 1H, *J* = 7.6 Hz), 7.61 - 7.57 (td, 1H), 7.54 - 7.50 (t, 1H, *J* = 7.6 Hz), 7.37 - 7.33 (m, 5H), 7.02 (s, 1H), 3.84(s, 3H) ^{13}C NMR (100 MHz, $CDCl_3$): δ_C 170.4, 170.2, 145.6, 138.7, 132.9, 131.0, 129.7, 129.5, 129.1, 125.8, 125.7, 124.2, 71.1, 53.8 . HRMS (ESI): calcd. for C16H14NO3: 268.0974, found: 268.0971.

Methyl 1-(4-bromophenyl)-3-oxoisoindoline-1-carboxylate (9q).

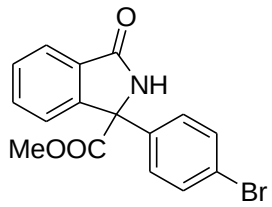

Eluent: 50% n-hexane / 50% ethyl acetate. The product was obtained as an off-white solid (90% isolated yield). ^{1}H NMR (400 MHz, $CDCl_3$): δ_H 8.06 (s, 1H), 7.85 - 7.83 (d, 1H, *J* = 7.6 Hz), 7.70 - 7.68 (d, 1H, *J* = 7.6 Hz), 7.61 - 7.57 (t, 1H, *J* = 7.2 Hz), 7.54 - 7.50 (t, 1H, *J* = 7.6 Hz), 7.47 - 7.44 (d, 2H, *J* = 8.6 Hz), 7.30 - 7.28 (d, 2H, *J* = 8.8 Hz), 3.83 (s, 3H). ^{13}C NMR (100 MHz, $CDCl_3$): δ_C 169.95, 169.87, 145.3, 137.8, 133.1, 132.6, 130.7, 129.9, 127.6, 125.5, 124.4, 123.4, 70.5, 53.9. HRMS (ESI): calcd. for C16H13NO3Br: 346.0079, found: 346.0085.

Spiro[indoline-3,1'-isoindoline]-2,3'-dione (9r).

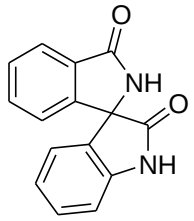

Eluent: 50% n-hexane / 50% ethyl acetate. The product was obtained as a white solid (75% isolated yield). ^{1}H NMR (400 MHz, *d*6-DMSO): δ_H 10.9 (s, 1H), 9.03 (s, 1H), 7.75 - 7.73 (m, 1H), 7.55 – 7.49 (m, 2H), 7.33 - 7.29 (m, 1H), 7.02 - 6.90 (m, 4H). δC 13C NMR (100 MHz, *d*6-DMSO): δ_C 175.8, 170.9, 146.2, 143.2, 133.2, 132.3, 130.7, 129.7, 128.5, 124.7, 123.9, 123.2, 111.1, 67.7. HRMS (ESI): calcd. for C15H10N2O2Na : 273.0640, found: 273.0627.

Ethyl 1-methyl-3-oxoisoindoline-1-carboxylate (9s).

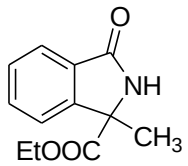

Eluent: 50% n-hexane / 50% ethyl acetate. The product was obtained as an orange solid (32% isolated yield). ^{1}H NMR (400 MHz, $CDCl_3$): δ_H 7.82 - 7.80(d, 1H, *J* = 7.2 Hz), 7.68 - 7.66 (d, 1H, *J* = 7.6 Hz),7.61 - 7.57 (t, 1H, *J* = 7.6 Hz), 7.52 - 7.48 (t, 1H, *J* = 7.6 Hz), 7.03 (s, 1H), 4.21 - 4.16 (q, 2H), 1.80 (s, 3H), 1.26 - 1.23 (t, 3H, *J* = 8.4 Hz). ^{13}C NMR (100 MHz, $CDCl_3$): δC 13C NMR (100 MHz, $CDCl_3$): δ_C 170.5, 170.2, 136.8, 135.3, 133.3, 132.6, 131.6, 131.4, 64.9, 62.7, 25.7, 14.3. HRMS (ESI): calcd. for C12H14NO3: 220.0974, found: 220.0967.

Methyl 1-((naphthalen-2-yl)methyl)-3-oxoisoindoline-1-carboxylate (9t).

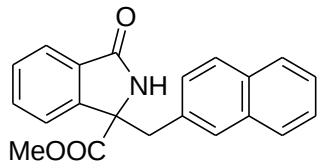

Eluent: 50% n-hexane / 50% ethyl acetate. The product was obtained as a white solid (62% isolated yield). ^{1}H NMR (400 MHz, $CDCl_3$): δ_H 7.89 – 7.87 (m, 1H), 7.78 – 7.76 (m, 4H), 7.69 - 7.64 (m, 2H), 7.56 – 7.50 (m, 1H), 7.49 – 7.46 (m, 2H), 7.27 - 7.25 (m, 1H), 6.42 (s, 1H), 3.97 – 3.93 (d, 1H, *J* = 13.6 Hz), 3.69 (s, 3H), 3.10 – 3.06 (d, 1H, *J* = 13.2 Hz), ^{13}C NMR (100 MHz, $CDCl_3$): δ_C 170.8, 169.6, 145.2, 133.5, 132.9, 132.7, 132.3, 131.0, 129.7, 129.0, 128.6, 127.9, 127.8, 127.6, 126.4, 126.3, 124.2, 123.5, 69.0, 53.2, 45.5. HRMS (ESI): calcd. for C21H18NO3: 332.1287, found: 332.1284.

3,3-diphenylisoindolin-1-one (9u).

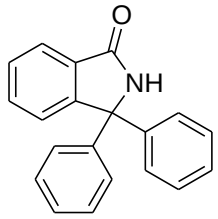

Eluent: 50% n-hexane / 50% ethyl acetate. The product was obtained as a white solid (82% isolated yield), mp 216 – 217 ^{o}C. ^{1}H NMR (400 MHz, $CDCl_3$): δ_H 7. 89 - 7.87(d, 1H, *J* = 7.6 Hz), 7.58 - 7.54(td, 1H), 7.50 - 7.43 (m, 2H), 7.32 - 7.26 (m, 10H), 7.11 (s, 1H). ^{13}C NMR (100 MHz, $CDCl_3$): δ_C 170.3, 150.5, 143.1, 132.6, 131.1, 129.0, 128.8, 128.3, 127.5, 124.9, 124.7, 71.4. HRMS (ESI): calcd. for C20H16NO: 286.1232, found: 286.1226.

Chapter 4

Rhodium(III)-Catalyzed Cycloaddition of Semicarbazones with Alkynes for the Synthesis of Isoquinoline and Initial Investigaion on the Cycloaddition of Semicarbazones with Diazo Compounds

4.1 Introduction

Employing functional groups as both directing group and internal oxidant are of current interest for catalytic C-H bond functionalizations.[73] For example, Hartwig and co-workers pioneered the use of oxime esters for Pd-catalyzed intermolecular aromatic C-H aminations.[40] The oxime moiety served as both the directing group and the internal oxidant for regenerating the active Pd(0) catalyst. Later, Fagnou and Glorius independently developed the rhodium(III)-catalyzed cycloaddition of benzohydroxamic acids with alkynes[47] and alkenes[48] to form isoquinolines and isoquinolones respectively (Scheme 4.1). The active Cp*Rh(III) catalyst was probably regenerated via N-OAc bond cleavage.

Scheme 4.1 Selected examples for functional groups acting as both directing group and internal oxidant for C-H bond functionalization

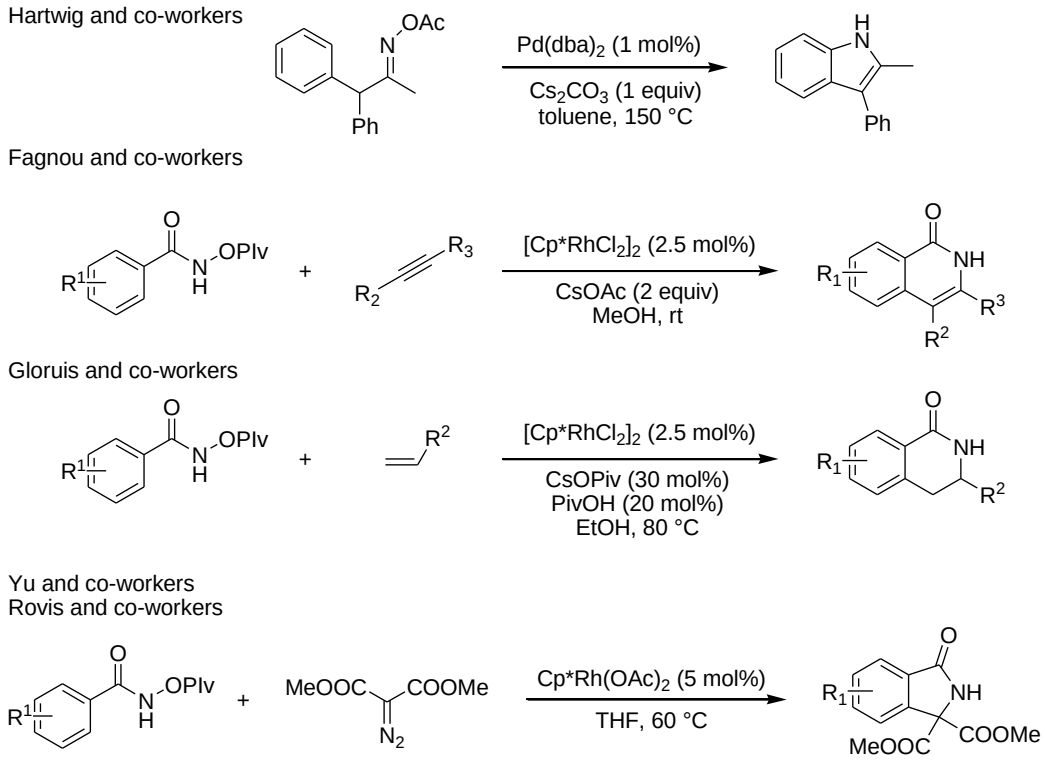

Literature reports on the functionalization of isoindoles are sparse due to their unstable *ortho*-quinoid structures.[77] Prompted by our earlier success in Rh-catalyzed [4+1] cycloaddition of benzohydroxamic acids with diazoesters to yield benzolactams, we anticipated the analogous synthesis of isoindoles by the Rh-catalyzed cycloaddition. To assess the feasibility of this synthetic route, we reacted *O*-acetyl acetophenone oximes (0.2 mmol) with diazomalonate (0.22 mmol) with Cp*Rh(OAc)$_2$ (5 mol%) in 1,4-dioxane at 60 ℃ for 16 h, and the

desired isoindole was not obtained with the starting oximes almost completely decomposed. Despite several trials, no significant improvement was achieved. (Table 4.1)

Table 4.1 Initial screening study on the rhodium(III)-catalyzed cycloaddition of *O*-acetyl acetophenone oximes with diazomalonate

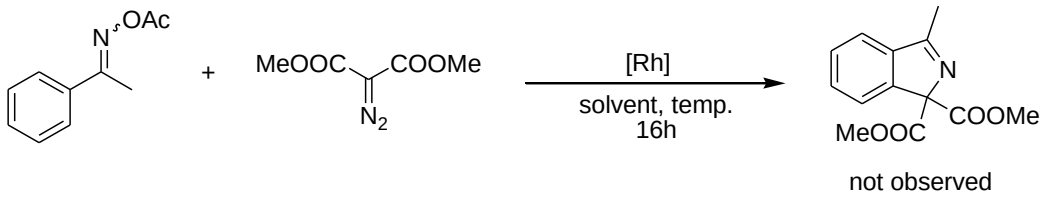

entry	[Rh] (5 mol% Rh)	solvent	temperature (℃)	yield
1	$[Cp^*Rh(OAc)_2]$	1,4-dioxane	60	0
2	$[Cp^*Rh(OAc)_2]$	THF	60	0
3	$[Cp^*Rh(OAc)_2]$	DCE	60	0
4	$[Cp^*Rh(OAc)_2]$	DMF	60	0
5	$[Cp^*RhCl_2]_2$ + 20 mol% NaOAc	1,4-dioxane	60	0
6	$[Cp^*RhCl_2]_2$ + 20 mol% NaOAc	THF	60	0
7	$[Cp^*RhCl_2]_2$ + 20 mol% NaOAc	DCE	60	0
8	$[Cp^*RhCl_2]_2$ + 20 mol% NaOAc	DMF	60	0

Reaction conditions: 0.2 mmol of *N*-acetylbenzoxime and 0.22 mmol **4a** were employed.

Noted the relative instability of the *O*-acetyl oximes, we envisioned that a more stable N-N bond could serve as an isoelectronic replacement for the N-O bond for catalyst regeneration. In this chapter, we examined the Rh(III)-catalyzed cycloaddition of acetophenone semicarbazones with alkynes to give isoquinolones. Further exploration of the analogous cycloaddition with diazoesters will be discussed. (Scheme 4.2) Literature reports on N-N bond as internal oxidant is relatively sparse.[74-75] Scheme 4.3 depicts selected examples on C-H bond functionalization using N-N bond as internal oxidant in Rh, Ru and Pd catalytic system.

Scheme 4.2 Condensation reaction between acetophenone and *tert*-butyl carbazate for the synthesize of semicarbazones

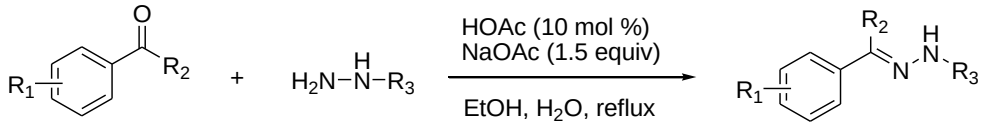

1.0 equiv 1.5 equiv **5**

Scheme 4.3 Selected examples on C-H bond cycloaddition using N-N bond as internal oxidant in Rh and Ru catalytic system

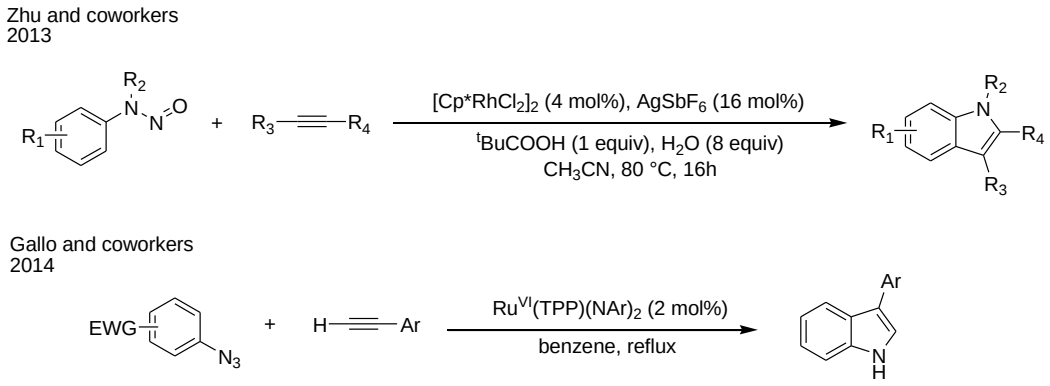

4.2 Results and Discussion

4.2.1 Rhodium(III)-Catalyzed Cycloaddition of Semicarbazones with Alkynes for the Synthesis of Isoquinolines

Acetophenone semicarbazones were prepared by condensation of acetophenone (1 equiv) with acetohydrazide (1.5 equiv) in the presence of HOAc (10 mol%) and NaOAc (1.5 equiv) in a EtOH-H_2O (2:1 v/v) mixture, and the semicarbazone product was obtained in 75% yield. (Scheme 4.5) To begin, (*E*)-*N*'-(1-*p*-tolylethylidene)acetohydrazide was treated with 1-phenyl-1-propyne (**6a**), $[Cp^*RhCl_2]_2$ (5 mol% Rh), CsOAc (25 mol%) and HOAc (3 equiv) in

CH_3CN at 120 ℃ for 16 h and isoquinolones (**10a**) was obtained in 30% yield (Scheme 4.4). The structure of **10a** was confirmed by ^{1}H and ^{13}C NMR.

Scheme 4.4 Preparation of acetophenone semicarbazones and preliminary study on the Rh^{III} catalyzed cycloaddition of acetophenone semicarbazones with alkynes

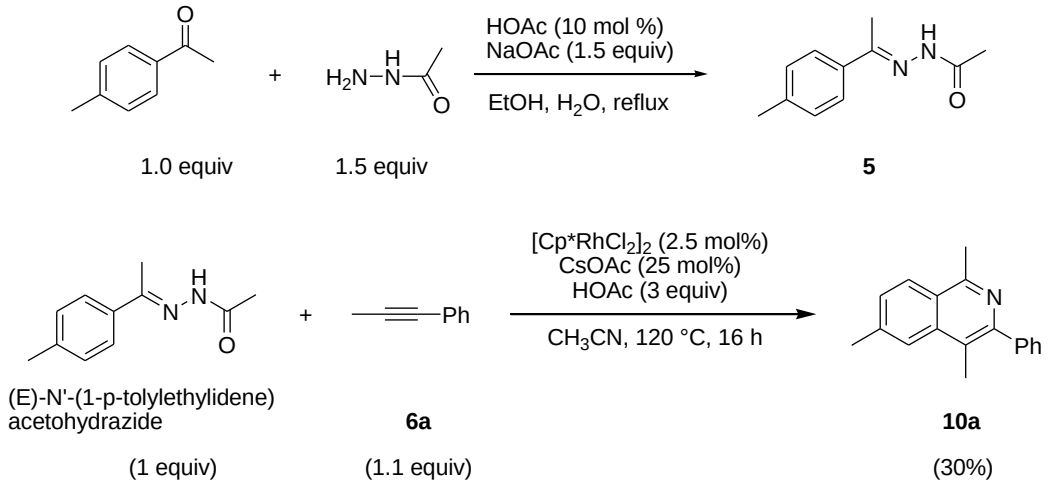

4.2.1.1 Optimization of Reaction Conditions

For reaction optimization, we first examined the effect of the amide leaving group.

Table 4.2 Effect of leaving group

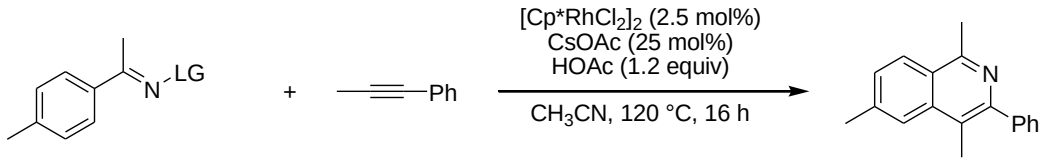

5 **6a** **10a**

entry	substrate	yield of **10a** (%)[a]
1	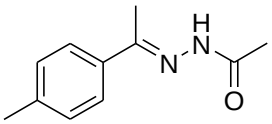 **5**	30
2	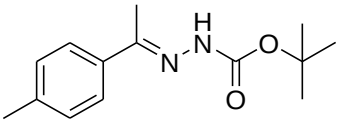 **5a**	80

Reaction conditions: **5** (0.2 mmol), **6a** (0.22 mmol), $[Cp^*RhCl_2]_2$ (2.5 mol%), CH_3CN (2.5 mL).
[a]Yields were based on ^1H NMR using dibromomethane as internal standard.

We hypothesized that a better amide leaving group such as carbamate on the substrate would facilitate effective coupling reaction. Thus, when **5a** bearing a *t*-butyl carbamate leaving group was reacted with 1-phenyl-1-propyne **6a** in the presence of $[Cp^*RhCl_2]_2$ (2.5 mol%), isoquinolone **10a** was formed in 80% yield. (Table 4.2, entry 2) Compound **10a** was isolated as the only regioisomer and the structure was characterized by ^1H and ^{13}C NMR with reference to the reported spectroscopic data.

Table 4.3 Effect of solvents

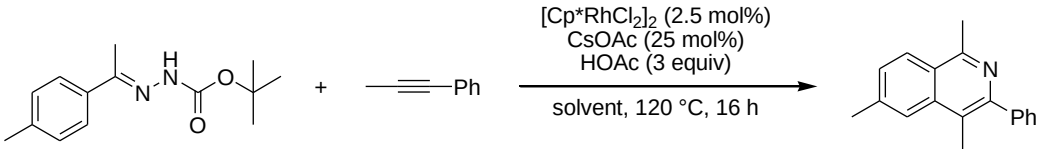

5a **6a** **10a**

entry	solvent	yield of **10a** (%)
1	CH_3CN	80
2	DMF	45
3	1,4-dioxane	35
4	toluene	19
5	DCE	34

Reaction conditions: **5a** (0.2 mmol), **6a** (0.22 mmol), $[Cp^*RhCl_2]_2$ (2.5 mol%), solvent (2.5 mL).
[a]Yields were based on ^{1}H NMR using dibromomethane as internal standard.

Using other coordinating solvents such as DMF and dioxane led to lower product yields (Table 4.3, entries 2 and 3). Non-polar (toluene) and weakly polar non-coordinating solvents (DCE) were inferior in terms of product yields (entries 4 and 5). In all cases studied in this work, high regioselectivity was observed with **10a** was isolated as the major product.

Table 4.4 Effect of temperature

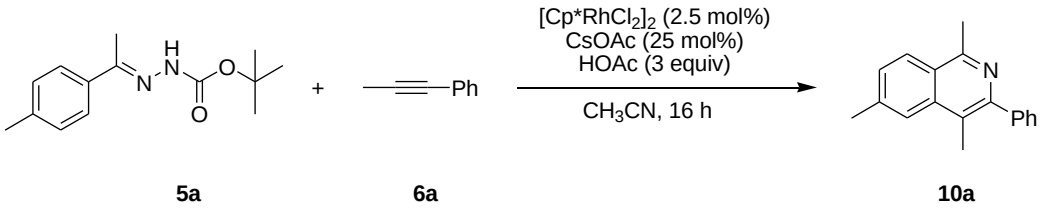

5a **6a** **10a**

entry	temperature (℃)	yield of **10a** (%)
1	60	30
2	80	40
3	100	45
4	120	80

Reaction conditions: **5a** (0.2 mmol), **6a** (0.22 mmol), $[Cp^*RhCl_2]_2$ (2.5 mol%), CH_3CN (2.5 mL).
[a]Yields were based on ^1H NMR using dibromomethane as internal standard.

The reaction was performed at 60 ℃ (Table 4.4, entry 1), and only 30% of **10a** was obtained. Little improvement of the product yields (40%) were achieved when performing the reaction at 80 ℃ and 100 ℃ (entries 2-3). The best result was attained at the reaction temperature of 120 ℃.

Table 4.5 Effect of catalyst and additives

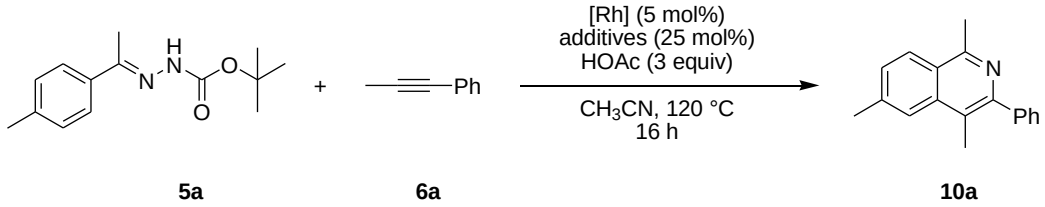

5a **6a** **10a**

entry	catalyst	additives (25 mol%)	acid (1.2 equiv)	yield of **10a** (%)
1	$[Cp^*RhCl_2]_2$	CsOAc	HOAc	80
2	$[Cp^*RhCl_2]_2$	-	-	13
3	$[Cp^*RhCl_2]_2$	-	HOAc	10
4	$[Cp^*RhCl_2]_2$	CsOAc	-	11
5	$[Cp^*IrCl_2]_2$	CsOAc	HOAc	48
6	$[(Cymene)RuCl_2]_2$	CsOAc	HOAc	10
7	$Pd(OAc)_2$	-	HOAc	0
8	$[Cp^*Co(CO)I_2]$	CsOAc	HOAc	0

Reaction conditions: **5a** (0.2 mmol), **6a** (0.22 mmol), catalyst (5 mol% per metal), CH_3CN (2.5 mL). [a]Yields were based on ^1H NMR using dibromomethane as internal standard.

When other d^6 metal complexes such as $[Cp^*IrCl_2]_2$ and $[Ru(cymene)Cl_2]_2$ were tested as catalyst, only 48% and 10% of **10a** were obtained respectively (entries 5 and 6, Table 4.5). Other metal complexes such as $Pd(OAc)_2$ and $[Cp^*Co(CO)I_2]$ did not give any **10a** formation under the optimized reaction conditions (entries 7 and 8). Notably, 1,2-bis(1-*p*-tolylethylidene)hydrazine was obtained in 40% yield with $[Cp^*Co(CO)I_2]$ as catalyst, (Scheme 4.6). Apparently, the hydrazine was formed by homo-coupling of **5a**.

Scheme 4.6 **[**Cp*Co(CO)I_2]-catalyzed homo-coupling of **10a**

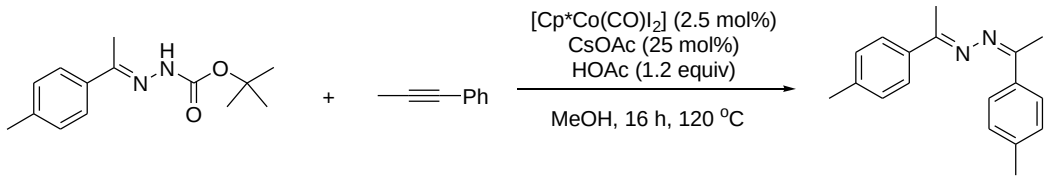

5a **6a** 40%

We found that CsOAc and acetic acid together were crucial for this transformation. Without either CsOAc or acetic acid as additives, the yield of **10a** dropped dramatically to around 10% (entries 2-3).

4.2.1.2 Scope and Limitation

Table 4.6 Scope of semicarbazones

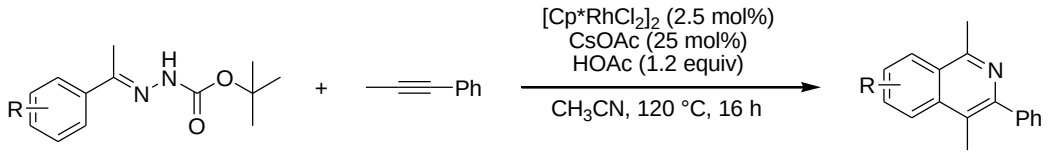

5 **6a** **10**

entry	**5**	**6a**	yield (%)[a]
1	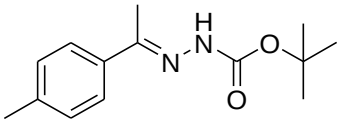 **5a**	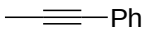 **6a**	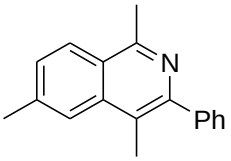 **10a**, 80
2	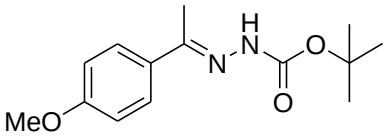 **5b**	**6a**	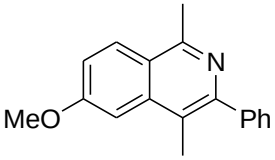 **10b**, 93
3	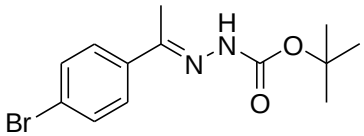 **5c**	**6a**	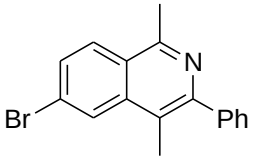 **10c**, 45
4	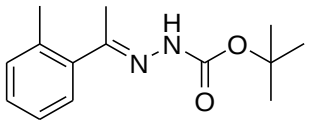 **5d**	**6a**	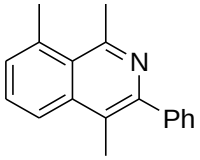 **10d**, 5
5	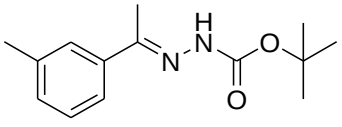 **5e**	**6a**	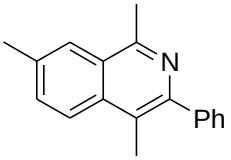 **10e**, 67

6	**5a**	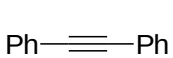 **6b**	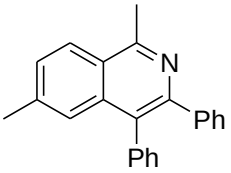 **10f**, 80

Reaction conditions: **5** (0.2 mmol), **6a** (0.22 mmol), $[Cp^*RhCl_2]_2$ (2.5 mol%), CH_3CN (2.5 mL). [a]Isolated yield.

Employing 1-phenyl-1-propyne as coupling partner, the reaction scope study of the semicarbazones was examined (Table 4.6). Electron-releasing substituents such as –OMe group was well tolerated, and the reaction with **6a** gave the desired product **10b** in 93% yield (Table 4.6, entry 2). Substrates with electron-withdrawing substituents such as –Br reacted with **6a** to give **10c** in 45% yield (entry 3). Sterically hindered 2-methyl benzosemicarbazone **5d** was an ineffective substrate for the reaction. The reaction of **5d** with **6a** gave **10d** in only 5% yield. Less bulky 3-methyl benzosemicarbazone **5e** reacted with **6a** to produce **10e** in 67% yield. It was worth noting that only one regioisomer **10e** was produced. The less bulky *ortho* C-H bond was activated to give **10e** as a single product (Scheme 4.7). Sterically hindered diphenylaceylene **6b** was also a good coupling partner for this reaction and was reacted with **5a** to give the corresponding isoquinolines **10f** in 80% yield.

Scheme 4.7 Cp*Rh(III) catalyzed cycloaddition of **5e** with **6a**

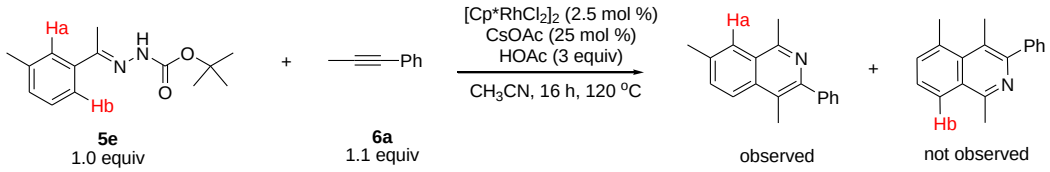

4.2.2 Rhodium(III)-Catalyzed Cycloaddition of Semicarbazones with Diazomalonate for the Synthesis of Isoindoles

We postulated that the alkyne cycloaddition with semicarbazones should start with *ortho*-C-H bond activation of the semicarbazones to form rhodacycle **A**. (Scheme 4.8) Alkynes would then coordinate to complex **A**, followed by migratory insertion to form a 7-membered rhodacycle D. The isoquinolones would then be formed via cleavage of the N-N bond. On the basis of the alkyne cycloaddition reactions, we proceeded to examine the analogous diazo coupling with semicarbazones.

Scheme 4.8 Proposed mechanism for the rhodium(III)-catalyzed cycloaddition of semicarbazone with alkynes for the synthesis of isoquinolones

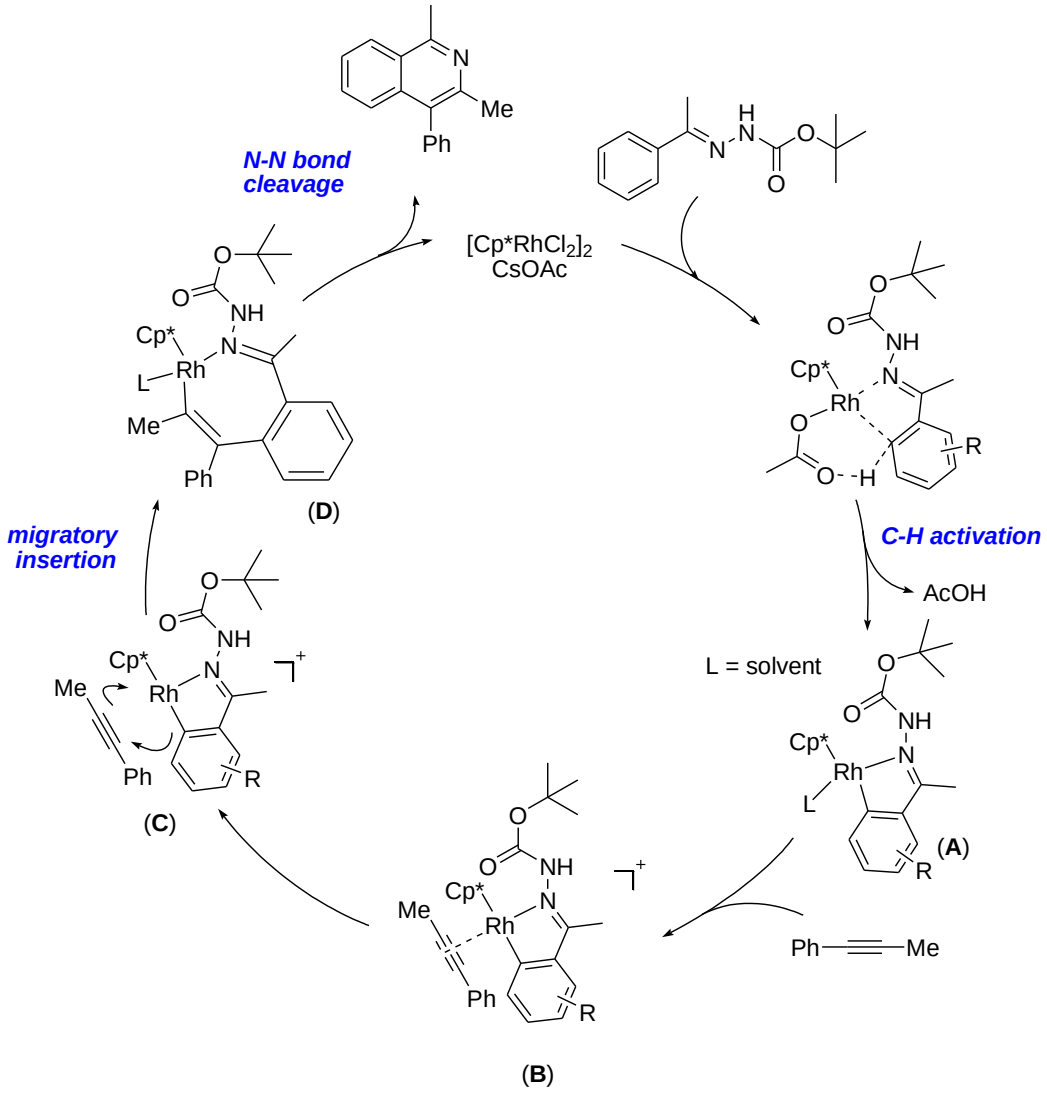

4.2.2.1 Investigation of the rhodium(III)-catalyzed cycloaddition of semicarbazone with diazomalonate

We reacted **5a** with diazomalonate **4a** in the presence of $[Cp^*RhCl_2]_2$ (5 mol% Rh), CsOAc (25 mol%) and HOAc (3 equiv) in CH_3CN at 100 ℃ for 16 h. However, the desired isoindole was not observed by NMR and GC-MS analysis of the crude reaction mixture. Thin layer chromatography analysis revealed that **4a** was completely consumed with formation of some unidentified compounds. Notably, 70% of the semicarbazone **5a** was recovered. The reaction temperature was probably too high, resulting in decomposition of the diazomalonates. Thus, we turned to examining the effect of temperature for the diazo reaction.

Table 4.7 Effect of temperature

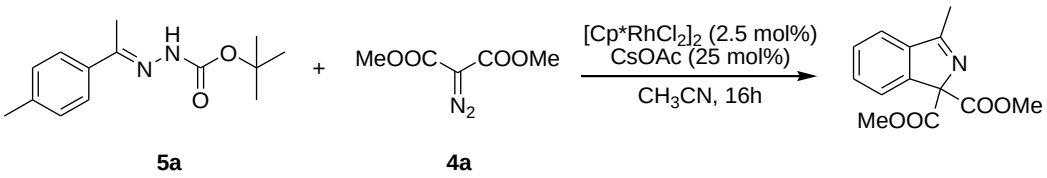

5a **4a**

entry	temperature (℃)	yield (%)
1	60	0
2	80	0
3	100	0

Reaction conditions: **5a** (0.2 mmol), **4a** (0.22 mmol), $[Cp^*Rh(Cl)_2]_2$ (5 mol% per metal), CH_3CN (2 mL).

With $[Cp^*RhCl_2]_2$ (2.5 mol%) as catalyst and CsOAc (25 mol%) as additives in CH_3CN, the diazo coupling reaction was performed at 60 ℃ and 80 ℃. At 80 ℃ (Table 4.7, entry 2), only a trace quantity of diazomalonate **4a** was recovered without any product formation. When the reaction temperature was lowered to 60 ℃ (entry 1), no desired product formation was observed with 60% recovery of **4a**.

Considering the successful development of the Rh(III)-catalyzed cycloaddition reaction between semicarbazones and alkynes, the *ortho*-C-H bond of semicarbazones should be activated and the cyclometallated rhodium complex should be reactive under the reaction conditions. Thus, we postulated that the

coordination of the diazo compounds to the metallocyclic rhodium (III) would be the bottle neck of the reaction.

Table 4.8 Effect of solvent

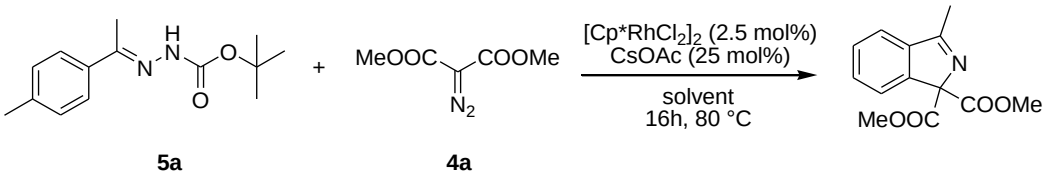

5a **4a**

entry	solvent	yield (%)
1	DCE	0
2	toluene	0
3	MeOH	0

Reaction conditions: **5a** (0.2 mmol), **4a** (0.22 mmol), 5 mol% [Rh], solvent (2 mL).

To allow a facile coordination of the diazomalonates, some less coordinating solvent were evaluated for the coupling reaction between **5a** and **4a**. To our surprise, employing solvents such as DCE, toluene and MeOH failed to result any formation of the desired isoindoles (Table 4.8, entries 1-3). Again, about 70% of the semicarbazone **5a** remained uncomsumed with only a trace amount of **4a** being recovered.

Table 4.9 Catalytic activities of selected Rh complex

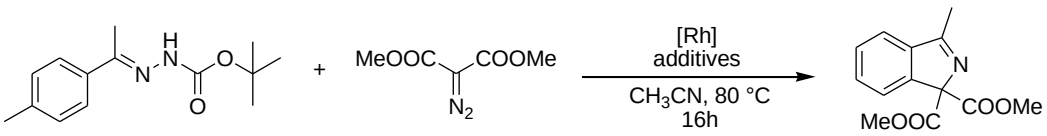

5a **4a**

entry	Rh complexes (5 mol% Rh)	additives (25 mol%)	yield (%)
1	$[Cp^*Rh(CH_3CN)_3](SbF_6)_2$	CsOAc	0
2	$[Cp^*Rh(CH_3CN)_3](SbF_6)_2$	NaOAc	0
3	$[Cp^*Rh(CH_3CN)_3](SbF_6)_2$	AgOAc	0

Reaction conditions: **5a** (0.2 mmol), **4a** (0.22 mmol), 5 mol% [Rh], CH_3CN (2 mL).

We turned to examine cationic $[Cp^*Rh(CH_3CN)_3](SbF_6)_2$ complex as catalyst. We hypothesized that cationic rhodium(III) complexes should favor faster substrate binding and electrophilic C-H cleavage, and thereby should exhibit higher reactivity.

In this work, $[Cp^*Rh(CH_3CN)_3](SbF_6)_2$ was prepared by reacting $[Cp^*RhCl_2]_2$ with $AgSbF_6$ in CH_3CN. To perform the catalysis, $[Cp^*Rh(CH_3CN)_3](SbF_6)_2$ with 25 mol% acetate salt was then treated with **5a** (0.2 mmol) and **4a** (0.22 mmol) in CH_3CN at 80 ℃ for 16h (Table 4.9). Complete conversion of both **5a** and **4a** was observed; however, the desired isodinole was not obtained. Instead, from the crude reaction mixture, we isolated a mixture of compounds after flash column chromatography. ^{1}H NMR analysis of the mixture showed six sets of aromatic signals: δ_H 7.44, s, 1H; δ_H 7.25, d, J = 7.6 Hz, 1H; δ_H 7.21, d, J = 8.0 Hz, 0.6H; δ_H 7.21, s, 0.6H; δ_H 7.12, d, J = 8.0 Hz, 0.6H, δ_H 6.99, d, J = 7.6 Hz, 1H. Comparing the ^{1}H NMR spectrum of the mixture to that of **5a** (which contains two sets of aromatic doublet signals), the *ortho*-C-H bond of **5a** were conspicuously absent in ^{1}H NMR of the mixture (Scheme 4.9). This finding suggests that the *ortho*-C-H bond has been functionalized. Consistent with this notion, two singlet aromatic signals (δ_H 7.44, s and δ_H 7.21, s) assignable to H_b of the semicarbazone were observed (Scheme 4.10).

Scheme 4.9 ^{1}H NMR spectrum of **5a** (aromatic region)

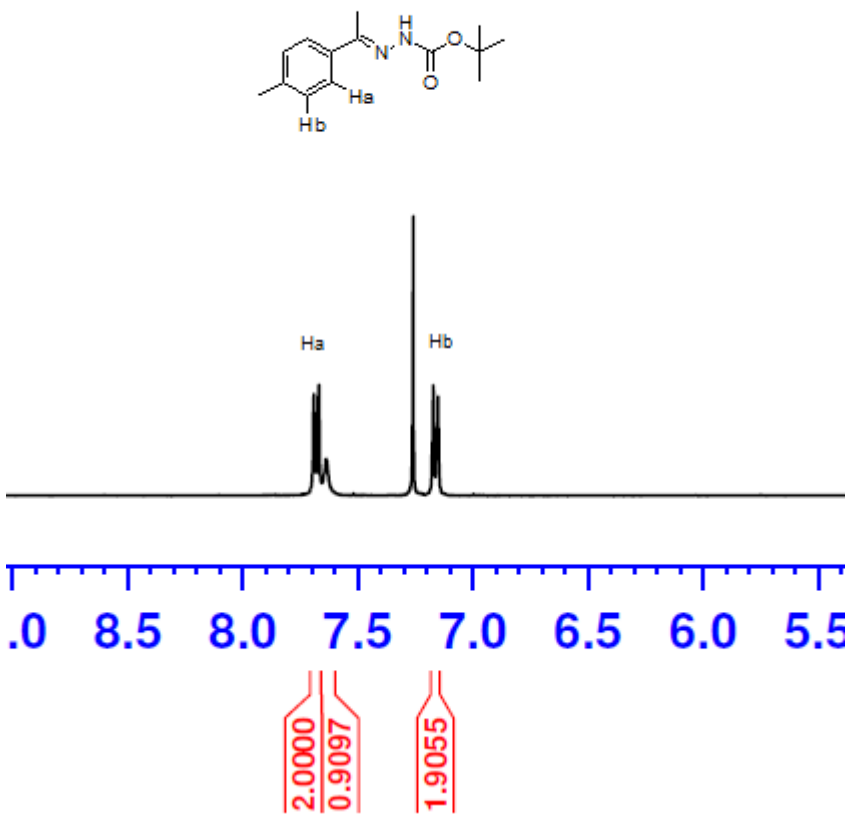

Scheme 4.10 ^{1}H NMR spectrum analysis of the isolated impure compounds (aromatic region)

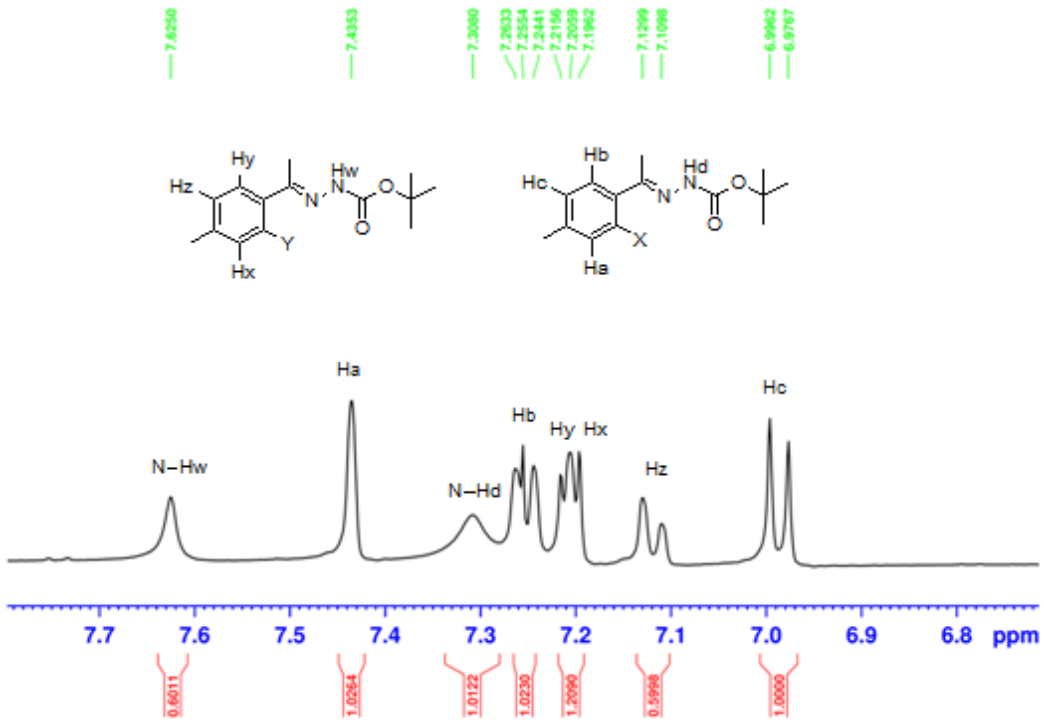

We also conducted a stoichiometric reaction study. In this study, **5a** (0.05 mmol) and **4a** (0.055 mmol) was reacted in the presence of $[Cp^*Rh(CH_3CN)_3](SbF_6)_2$ (0.05 mmol) and NaOAc (0.05 mmol) in CH_3CN at 80 ℃ for 2h (Scheme 4.11). However, the desired product was not observed. Instead, we isolated a rhodium complex after flash column chromatography.

Scheme 4.11 Stoichiometric reaction between **5a** and **4a** in the presence of $[Cp^*Rh(CH_3CN)_3](SbF_6)_2$

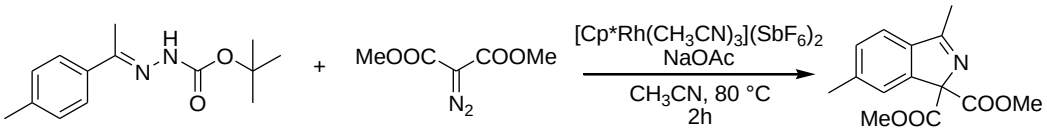

5a **4a**

^{1}H NMR analysis of this rhodium complex shows three aromatic signals (δ_H 7.56, s, 1H; δ_H 7.31, d, 1H, J = 8 Hz; δ_H 6.84, d, 1H, J = 8 Hz). By spectrum comparison of these signals to that of the starting **5a**, **5a** was likely to be cyclometallated with $[Cp^*Rh(CH_3CN)_3](SbF_6)_2$. For the ^{1}H NMR spectrum of the isolated rhodium complex, the upfield region features four singlet signals assignable to the two methyl groups on **5a** (δ_H 2.40, s, 3H; δ_H 2.37, s, 3H), the *tert*-butyl group on **5a** (δ_H 1.54, s, 9H) and the five methyl signals on the Cp*(δ_H 1.64, s, 15H). (Scheme 4.12)

Scheme 4.12 ^{1}H NMR analysis of the resulting rhodium complex from the stoichiometric reaction between **5a** and **4a** in the presence of $[Cp^*Rh(CH_3CN)_3](SbF_6)_2$

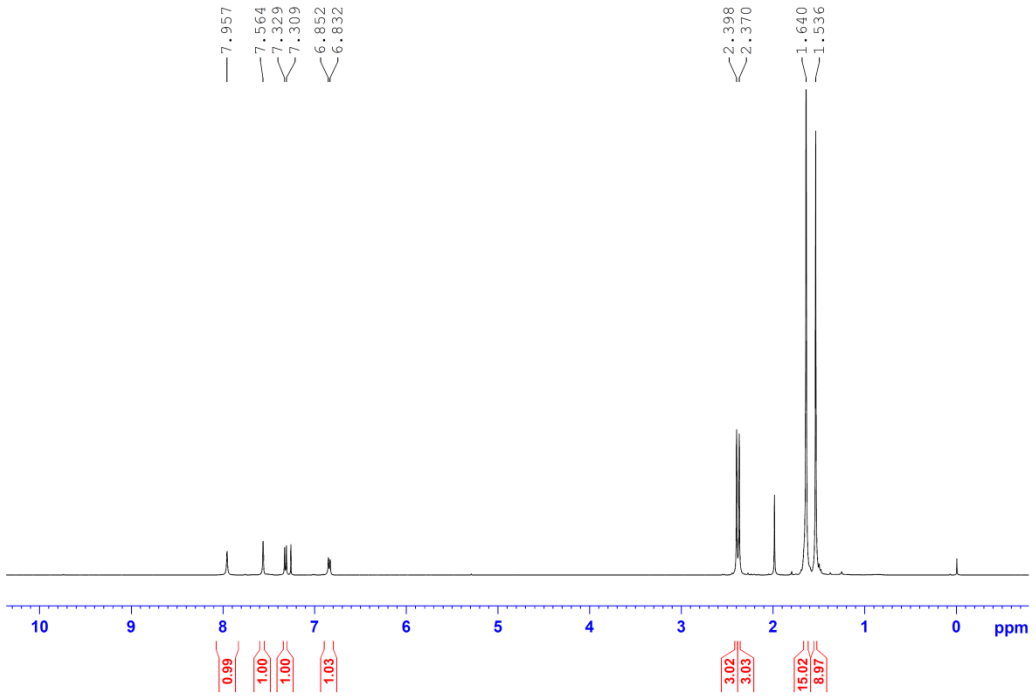

This complex was then successfully synthesized by reacting $[Cp^*RhCl_2]_2$ (1 mmol) with **5a** (1 mmol) in the presence of NaOAc (2 mmol) in CH_3CN (20 mL) at 60 ℃ for 1 day. The resulting reaction mixture was then filtered by Celite® . An excess amount of lithium chloride was then added to the filtrate, and the insoluble solid was filtered by Celite® . The desired complex was then isolated by column chromaograhy using DCM/acetone 95:5 as eluent. The sample was purified by dissolving it in minimum amount of DCM and layered carefully with

n-hexane. A dark red crystal was obtained in 70% yield after standing for 3 days. As LiCl was added for exchanging the counter ion, we proposed the identity of the complex is [Cp*Rh($C_{14}H_{19}N_2O_2$)Cl] (Scheme4.13)

Scheme4.13 Synthesis of cyclorhodated complex from $[Cp^*RhCl_2]_2$ and **5a**

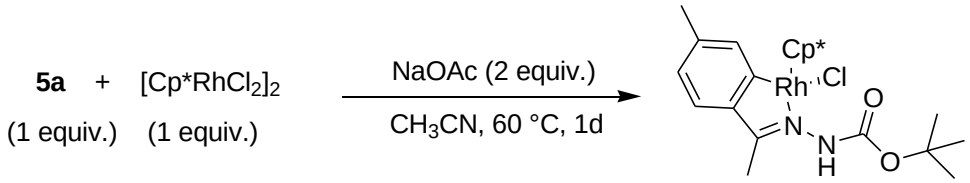

6

The feasibility of the cycloaddition of **5a** with diazomalonate **4a** was re-examined. In this regard, cyclorhodated complex **6** was reacted with five equivalent of **4a** in CH_3CN at 60 ℃ for 16 h. However, despite the complete consumption of the cyclorhodated complex, no desired isoindole was observed. Instead, an unknown compound with molecular weight 349.27 was observed in ESIMS.

4.3 Concluding Summary

In conclusion, we have developed a Rh(III)-catalyzed cycloaddition of semicarbazones with alkynes for the synthesis of isoquinolines. Substituents such as –methoxy and –bromide on the semicarbazones were well tolerated and gave the corresponding isoquinoline in good yields. The mechanism should involve *ortho* C-H bond activation by the Rh^{III} center to give a five-membered cyclorhodated complex. Upon the coordination and insertion of alkynes, a seven-membered ring cyclorhodated complex was probably formed. A Rh^{V}-nirenoid intermediate could then be generated by carbamate migration from N to Rh and undergo the C-N bond formation to give the desired isoquinoline .

We have employed this newly synthesized compound as substrate for the synthesis of isoindoles through Rh(III)-catalyzed cycloaddition reaction with diazomalonate. However, formation of the desired isoindole was not observed.

4.4 Experimental Section

4.4.1 General Experimental

All the reagents were obtained from commercial sources and used without purification. All the solvents used were obtained from commercial sources and were distillated according to literature methods. Semicabazones were prepared from its corresponding ketones and hydrazines following the modification synthetic route of literature procedures. Diazo compounds were synthesized according to the literature method. The Rh catalysts, [Cp*Rh$(OAc)_2$] and Cp*Rh$(CH_3CN)_3(SbF_6)_2$ was synthesized following the literature procedures.

Thin layer chromatography was performed on silica gel plates. Silica gel (Merck, 230 - 400 mesh) was used for flash column chromatography. ^{1}H and ^{13}C NMR spectra were recorded on a Brüker (400 MHz) NMR spectrometer. The chemical shift (δ) values are given in parts per million (ppm) with multiplicity (s = singlet, d = doublet, t = triplet, q = quartet, m = multiplet, td = triplet of doublets) and are referenced to residual solvent peaks. Coupling constants (J) were reported in Hertz (Hz). Melting points were measured on a Büchi Melting Point B - 545 machine. Mass spectra and High resolution mass spectra (HRMS)

were obtained on a VG MICROMASS Fison VG platform, a Finnigan Model Mat 95 ST instrument, or a Brüker APEX 47e FT - ICR mass spectrometer.

4.4.2 Experimental Procedures and Physical Characterization for Substrate Synthesis

General procedure for the synthesis of semicarbazones from ketones

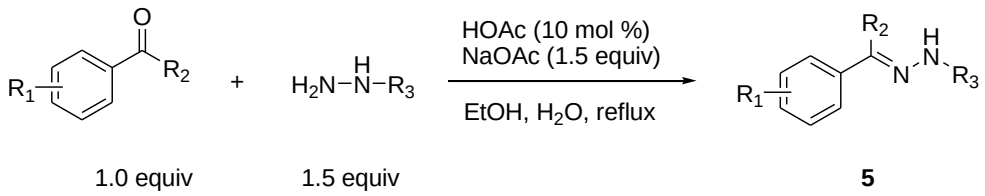

1.0 equiv 1.5 equiv **5**

NaOAc (0.62 g, 1.5 equiv) was dissolved in water (5 mL) in a 50 mL two-necked flask equipped with a magnetic stirrer. The corresponding ketone (5 mmol) was then added. Ethanol (10 mL) was added to the resulting solution to lower the turbidity. 10 mol % of acetic acid was then added as catalyst. The corresponding hydrazine (7.5 mmol) was dissolved in ethanol (10 mL) and transfer to a dropping funnel. The two-necked flask equipped with this dropping funnel was allowed to heat until reflux at 110 ^{o}C. The hydrazine solution in the dropping funnel was then allowed to drop slowly.

The resulting reaction mixture was then allowed to heat under reflux overnight and then cooled to room temperature. It was concentrated under reduced pressure and the desired semicarbazone would precipitate out and can be obtained by suction filtration. Cold water (2 x 10 mL) and ethanol (2 x 10 mL) were used to wash the product and the product can be used without further purification.

(E)-N'-(1-p-tolylethylidene)acetohydrazide.

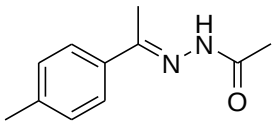

The product was obtained as an white solid (75% isolated yield), ^{1}H NMR (400 MHz, $CDCl_3$): δ_H 7.81 (d, 2H, , *J* = 8.0 Hz), 7.24 (d, 2H, *J* = 14.4 Hz), 2.40 (s, 3H), 2.31 (s, 3H). ^{13}C NMR (100 MHz, $CDCl_3$): δ_C 157.7, 139.7, 135.8, 129.0, 126.6, 21.3, 15.0.

4-methylbenzosemicarbazone (5a).

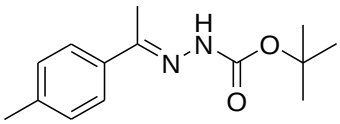

The product was obtained as an white solid (70% isolated yield), ^{1}H NMR (400 MHz, $CDCl_3$): δ_H 7.68 (d, 2H , *J* = 8.2 Hz), 7.64 (bs, 1H), 7.16 (d, 2H, *J* = 8.1 Hz), 2.35 (s, 3H), 2.17 (s, 3H), 1.55 (s, 9H). ^{13}C NMR (100 MHz, $CDCl_3$): δ_C 160.4, 152.8, 130.7, 127.6, 113.6, 81.2, 55.3, 28.3, 12.5.

4-methoxybenzosemicarbazone (5b).

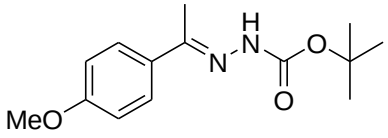

The product was obtained as an white solid (77% isolated yield), ^{1}H NMR (400 MHz, $CDCl_3$): δ_H 7.74 (d, 2H , *J* = 8.8 Hz), 7.66 (bs, 1H), 6.88 (d, 2H, *J* = 8.8 Hz), 3.82 (s, 3H), 2.16 (s, 3H), 1.55 (s, 9H). ^{13}C NMR (100 MHz, $CDCl_3$): δ_C 160.4, 152.8, 130.7, 127.6, 113.6, 81.2, 55.3, 28.3, 12.5.

4-bromobenzosemicarbazone (5c).

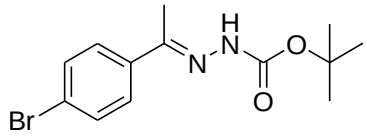

The product was obtained as an white solid (80% isolated yield), ^{1}H NMR (400 MHz, $CDCl_3$): δ_H 7.88 (bs, 1H), 7.67 (d, 2H, *J* = 8.4 Hz), 7.49 (d, 2H, *J* = 8.4 Hz), 2.18 (s, 3H), 1.57 (s, 9H). ^{13}C NMR (100 MHz, $CDCl_3$): δ_C 146.1, 136.9, 131.4, 127.8, 123.3, 81.5, 28.3, 12.5.

2-methylbenzosemicarbazone (5d).

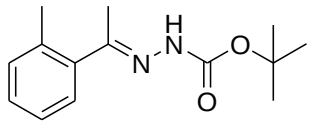

The product was obtained as an white solid (65% isolated yield), ^{1}H NMR (400 MHz, $CDCl_3$): δ_H 7.31 (bs, 1H), 7.29-7.18 (m, 4H), 2.41 (s, 3H), 2.18 (s, 3H), 1.57 (s, 9H). ^{13}C NMR (100 MHz, $CDCl_3$): δ_C 139.5, 135.7, 130.7, 128.28, 128.26, 125.6, 81.2, 28.3, 20.6, 16.6.

3-methylbenzosemicarbazone (5e).

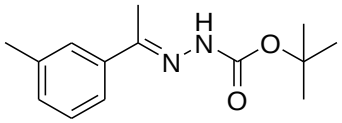

The product was obtained as an white solid (73% isolated yield), ^{1}H NMR (400 MHz, $CDCl_3$): δ_H 7.77 (bs, 1H), 7.65 (s, 1H), 7.52 (d, 2H, *J* = 7.6 Hz), 7.23 (d, 1H, *J* = 7.6 Hz), 7.15 (d, 1H, *J* = 7.2 Hz), 2.36 (s, 3H), 2.17 (s, 3H), 1.55 (s, 9H). ^{13}C NMR (100 MHz, $CDCl_3$): δ_C 138.0, 137.9, 129.9, 128.1, 126.8, 123.4, 81.3, 28.3, 21.4, 12.7.

4.4.3 A General Procedures for the Rh(III)-Catalyzed Formal Oxidative [4+2] Cycloaddition of Benzosemicarbazone with Alkyne:

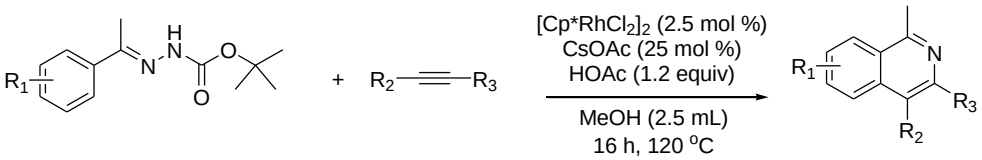

5 1.0 equiv + **6** 1.1 equiv → **10**

A 8 mL glass vial equipped with a magnetic stirrer was charged with benzosemicarbazone **5** (0.20 mmol, 1.0 equiv), $[Cp^*RhCl_2]_2$ (2.5 mol %), CsOAc (25 mol %), MeOH (2.5 mL) and HOAc (1.2 equiv). The reaction vial was

allowed to stir for 15 minutes at room temperature. Alkynes **6** (0.22 mmol, 1.1 equiv) was then added and the reaction mixture was heated and stirred at 120 ^{o}C.

The reaction mixture was filtered through a plug of Celite and the filtrate was concentrated by a rotary evaporator. It was then purified by flash column chromatography on a silica gel to give the desired product.

4.4.4 Experimental Procedures for the Synthesis of Cyclorhodated Complex Formed from **5a** and $[Cp^*RhCl_2]_2$

A 8 mL glass vial equipped with a magnetic stirrer was charged with benzosemicarbazone **5a** (1 mmol, 1.0 equiv), $[Cp^*RhCl_2]_2$ (1 mmol, 1.0 equiv) and NaOAc (2 mmol, 2.0 equiv). CH3CN (20 mL) was added as solvent. The reaction vial was warmed to 60 ^{o}C and was allowed to stir for 1 day under a N_2 atmosphere. The resulting reaction mixture was then filtered by Celite® . Excess amount of lithim chloride was then added to the filtrate and the insoluble solid was then filtered by celite. The desired complex was then isolated by column chromaograhy using DCM/acetone 95:5 as eluent. The sample was purified by dissolving it in minimum amount of DCM and *n*-hexane was then carefully

added. A dark red crystal was obtained after standing for 3 days.

Cyclorhodated complex from $[Cp^*RhCl_2]_2$ and 5a (6)

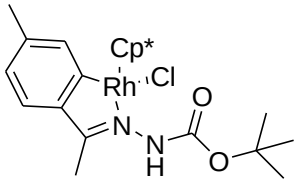

The product was obtained as an red solid (70% isolated yield), ^{1}H NMR (400 MHz, $CDCl_3$): δ_H 7.86 (bs, 1H), 7.56 (s, 1H), 7.31 (d, 1H, *J* = 8.0 Hz), 6.84 (d, 1H, *J* = 8.0 Hz), 2.40 (s, 3H), 2.37 (s, 3H), 1.64 (s, 15H), 1.54 (s, 9H). ^{13}C NMR (100 MHz, $CDCl_3$): δ_C 152.9, 141.4, 140.8, 136.9, 127.5, 123.7, 96.7, 96.6, 81.4, 28.3, 21.9, 15.4

Chapter 5

Conclusion

Rhodium-catalyzed arylation and cycloaddition of various electrophilic aminating/amidation reagents for regioselective C-N and C-C bond formation has been developed. In our study, hydroxylamines were found to be transformed to synthetic useful anilines and benzohydroxamic acids/ semicarbazones were transformed to important heterocyclic compounds oxisoindoles and isoquinoline.

In *Chapter 2*, we developed the Rh(III)-catalyzed amination and amidation of arylboronic acids using hydroxylamines and benzohydroxamic acids. The desired anilines and amides were obtained in up to 97% yields. Functional groups on the arylboronic acids such as –methoxy, -halogens, -heterocyclic moiety, -aldehydes, -ketones, esters, -nitro and amines were well tolerated. Both *N*-alkylhydroxylamines and *N*, *N*-dialkylhydroxylamines were effective reagents for this transformation. Alphatic and benzo hydroxamic acids coupled smoothly with arylboronic acids to give the corresponding amides in good yields. Moreover, we demonstrated that a [Ar-Rh] complex is the active catalyst for this transformation. [Cp*Rh(Ph)Cl(PPh_3)] was synthesized and employed as catalyst

for the coupling reaction between **1b** and **2a**. The desired amines **7j** was obtained in 80% yield which proven the catalytic activity of a [Ar-Rh] species.

The coupling reaction between the *ortho*-selective arene C-H of various arenes and α-diazomalonates for carbene insertion product was reported by our group previously. In *Chapter 3*, we developed the rhodium(III)-catalyzed cycloaddition of benzohydroxamic acids with α-diazomalonates. We postulated that the N-O bond of benzohydroxamic acids could serve as an internal oxidant for the regeneration of the active Rh catalyst. The Rh-catalyzed coupling reaction exhibits excellent *ortho*-selectivity. Notably, donor-acceptor, acceptor-acceptor and donor-donor type diazo compounds were effective reagents for the cycloaddition reaction. Problematic diazo reagents such as alkyl diazoacetates and diazo compounds with alkene moiety coupled smoothly with benzohydroxamic acids to give the corresponding oxisoindoles in good yields and no major side reaction product (from β-hydride elimination and cyclopropanation) was observed. To have a better understanding on the mechanism of the reaction, we tried to synthesize the cyclic rhodium complex by reacting [Cp*Rh$(OAc)_2$] with benzohydroxamic acids **3a**. A dinuclear aryl-aza-rhodium(III) complex was isolated and characterized by X-ray crystallography. However, this dinuclear aryl-aza-rhodium(III) complex was

catalytically inactive towards the cycloaddition between **3a** and **4a** possibly due to the strong aza-rhodium cycle which hinders the diazo coordination.

To accomplish the synthesis of isoindoles through a cycloaddition reaction strategy, semicarbazones which contain a relatively stable N-N bond was synthesized and was considered as an isoelectronic replacement for *O*-carboxylates oximes which contain a relatively less stable N-O bond. In *Chapter 4*, we reported the Rh(III)-catalyzed cycloaddition of semicarbazones with alkynes for the synthesis of isoquinoline. This reaction served as a model reaction for studying the potential coupling reaction between semicarbazones and diazo compounds. When $[Cp^*Rh(CH_3CN)_3](SbF_6)_2$ was employed as catalyst for the coupling reaction between semicarbazones **5b** and diazo malonate **4a**, an *ortho*-selective C-H carbene insertion product was observed. The cycloaddition of semicarbazones with diazo compounds for the synthesis of isoindoles is still under investigation.

Appendices

Figure A.1 ^{1}H NMR spectrum of **1a**

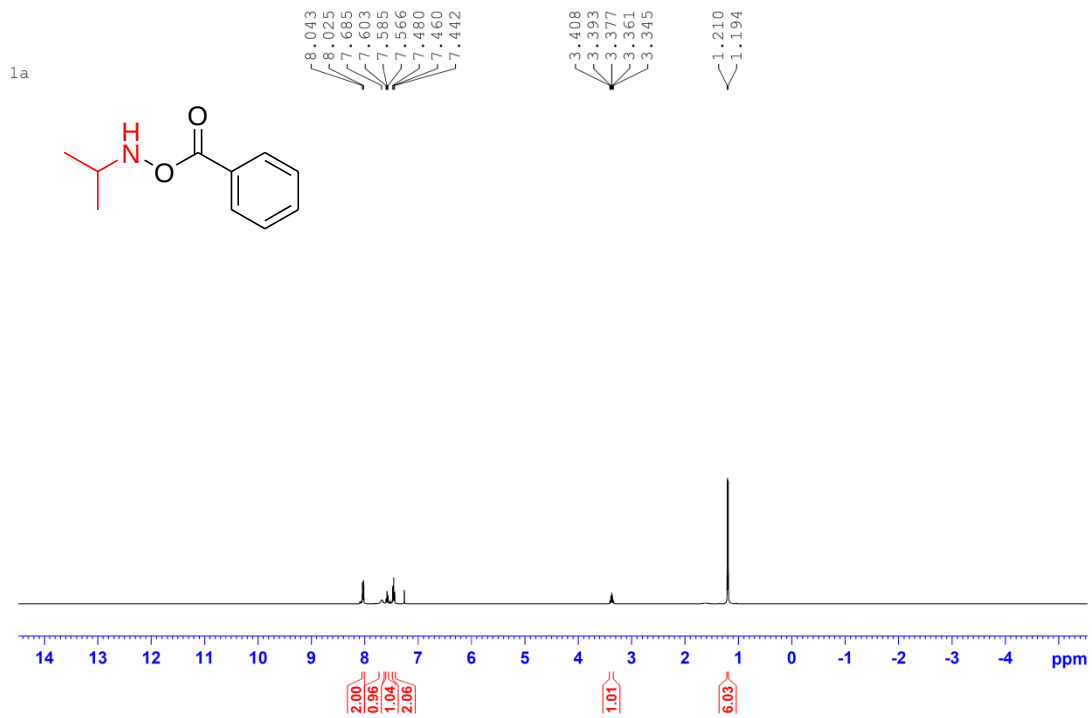

Figure A.2 ^{13}C NMR spectrum of **1a**

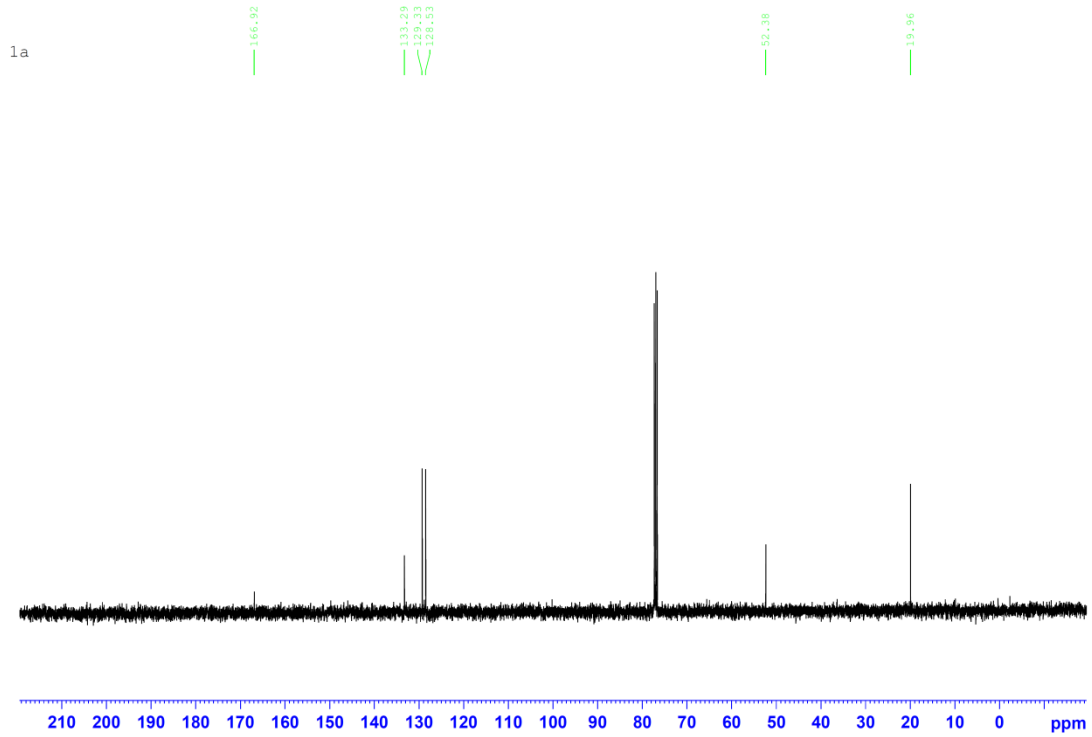

Figure A.3 ^{1}H NMR spectrum of **1b**

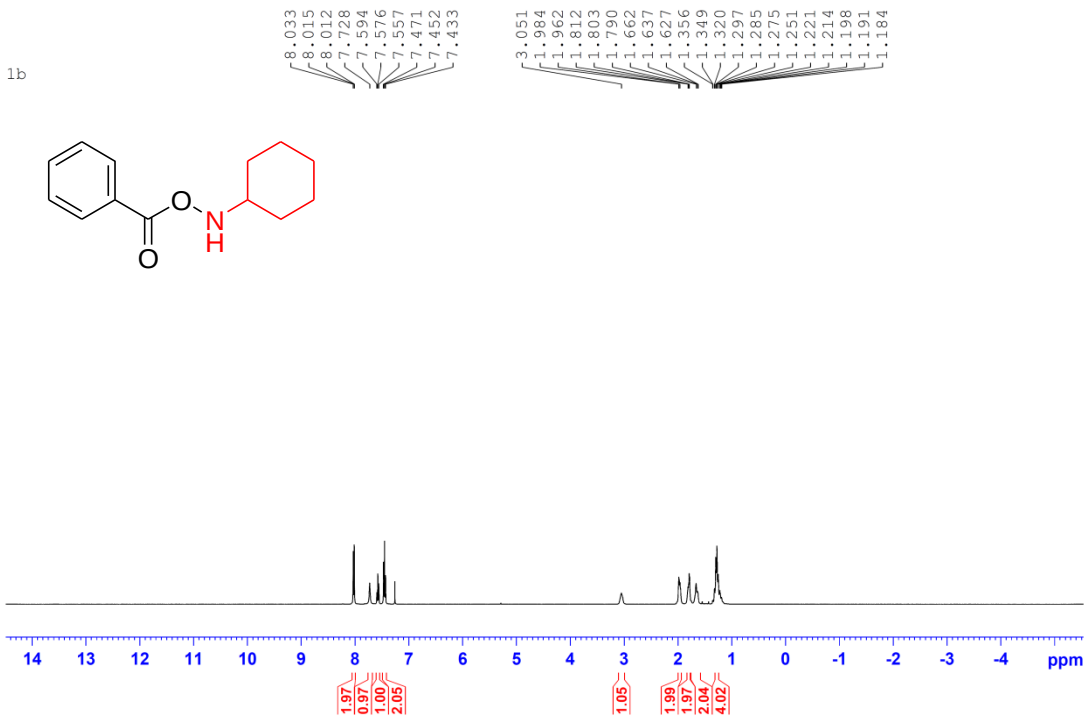

Figure A.4 ^{13}C NMR spectrum of **1b**

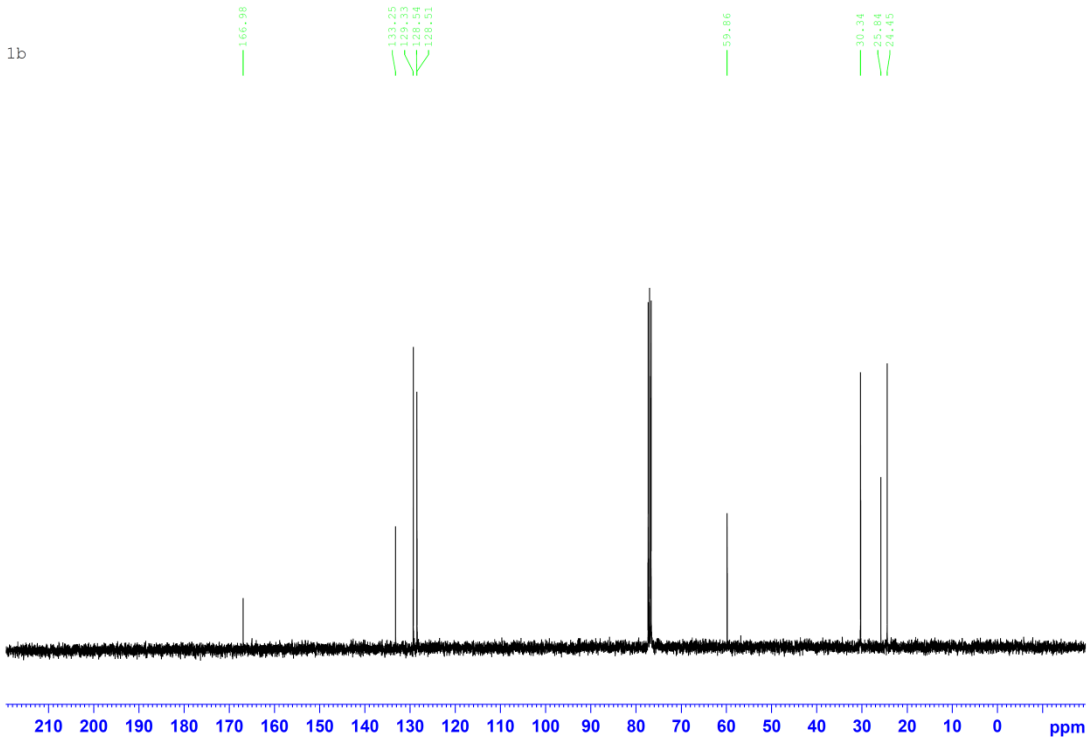

Figure A.5 ^{1}H NMR spectrum of **1c**

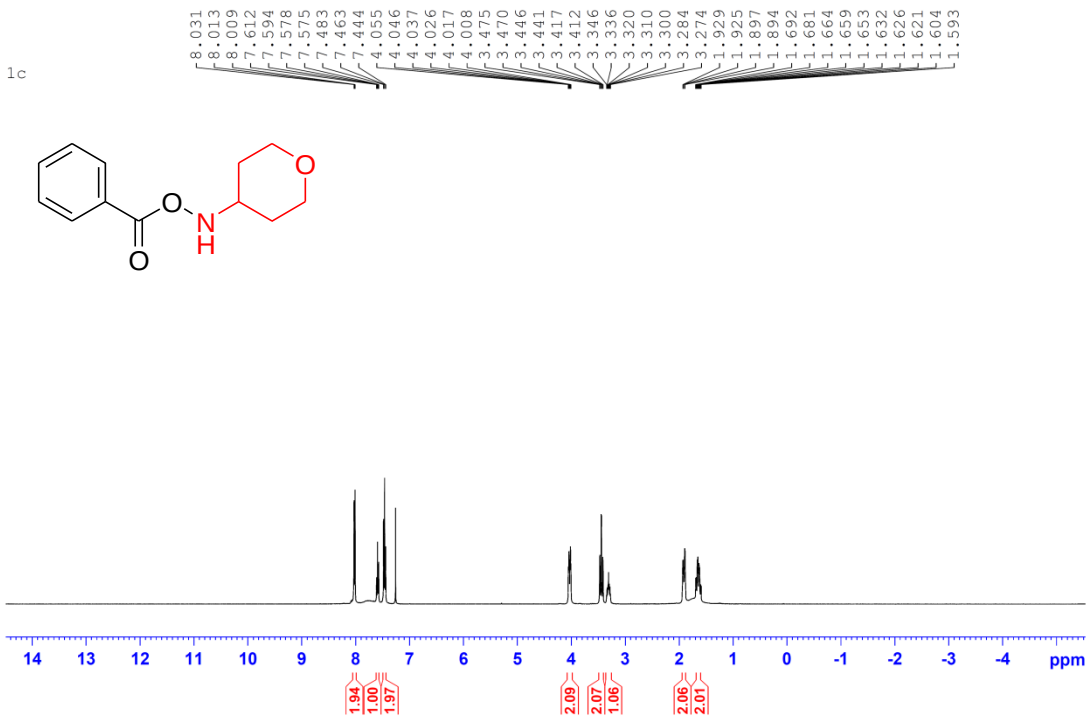

Figure A.6 ^{13}C NMR spectrum of **1c**

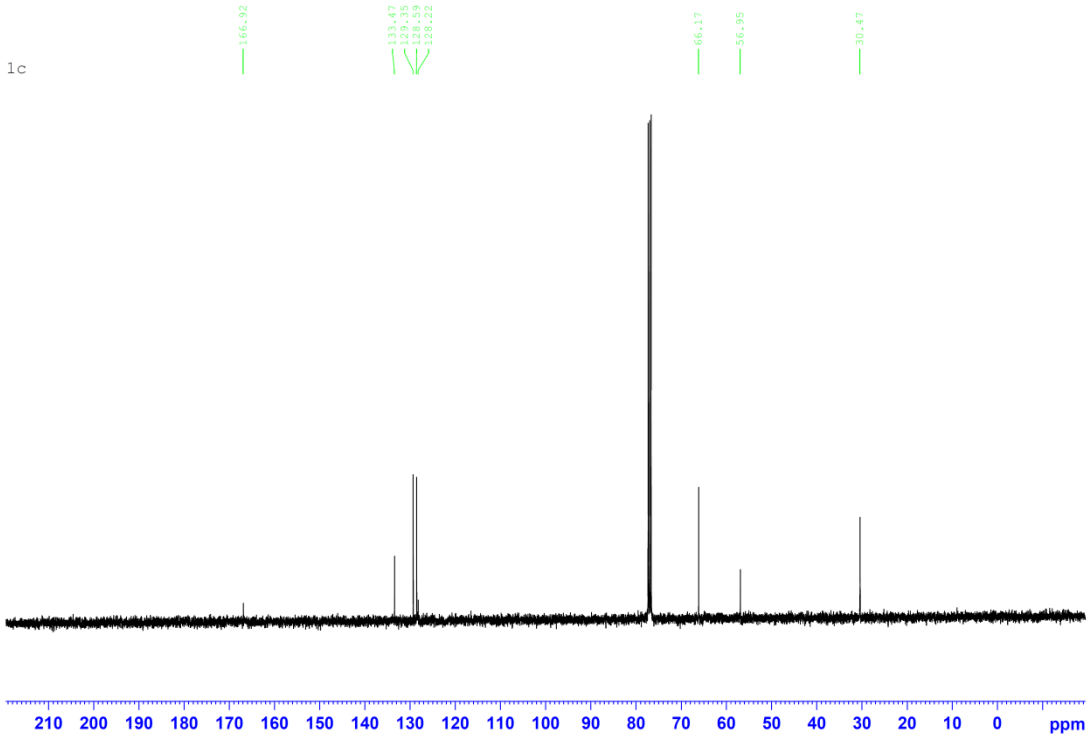

Figure A.7 ^{1}H NMR spectrum of **1d**

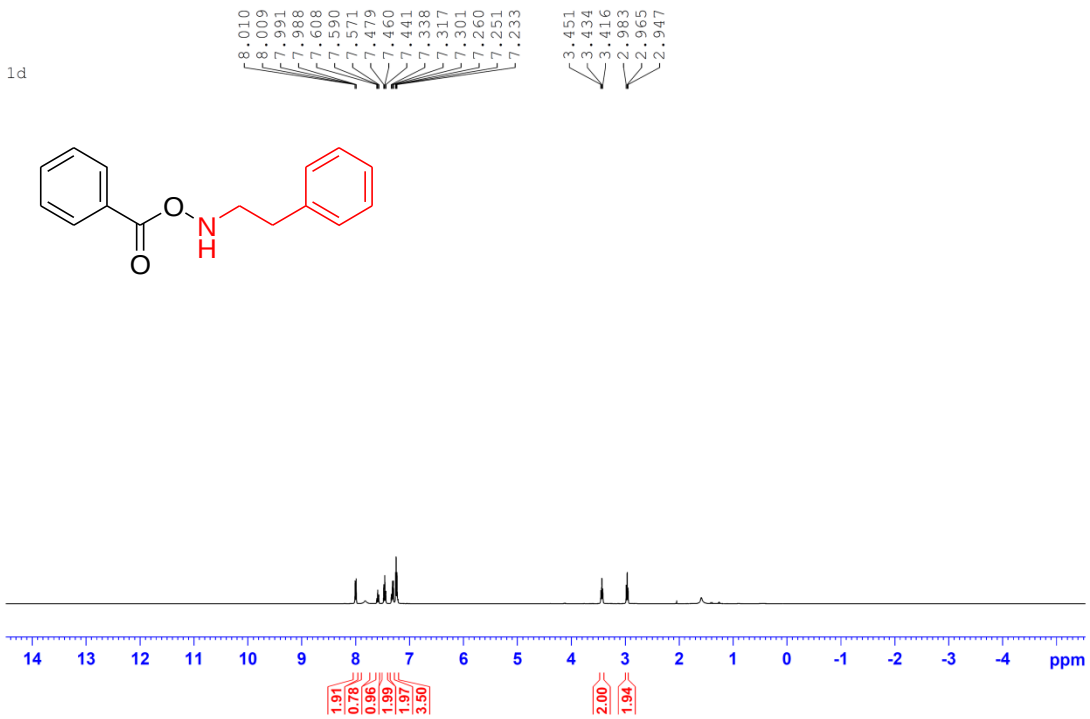

Figure A.8 ^{13}C NMR spectrum of **1d**

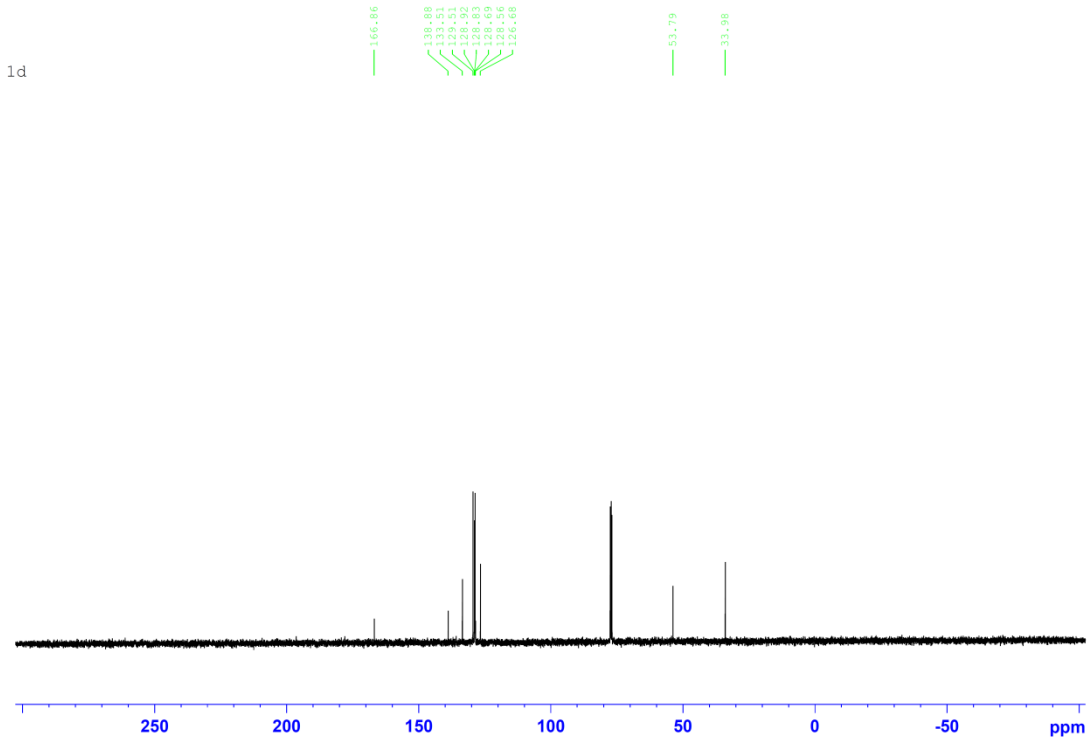

Figure A.9 ^{1}H NMR spectrum of **1e**

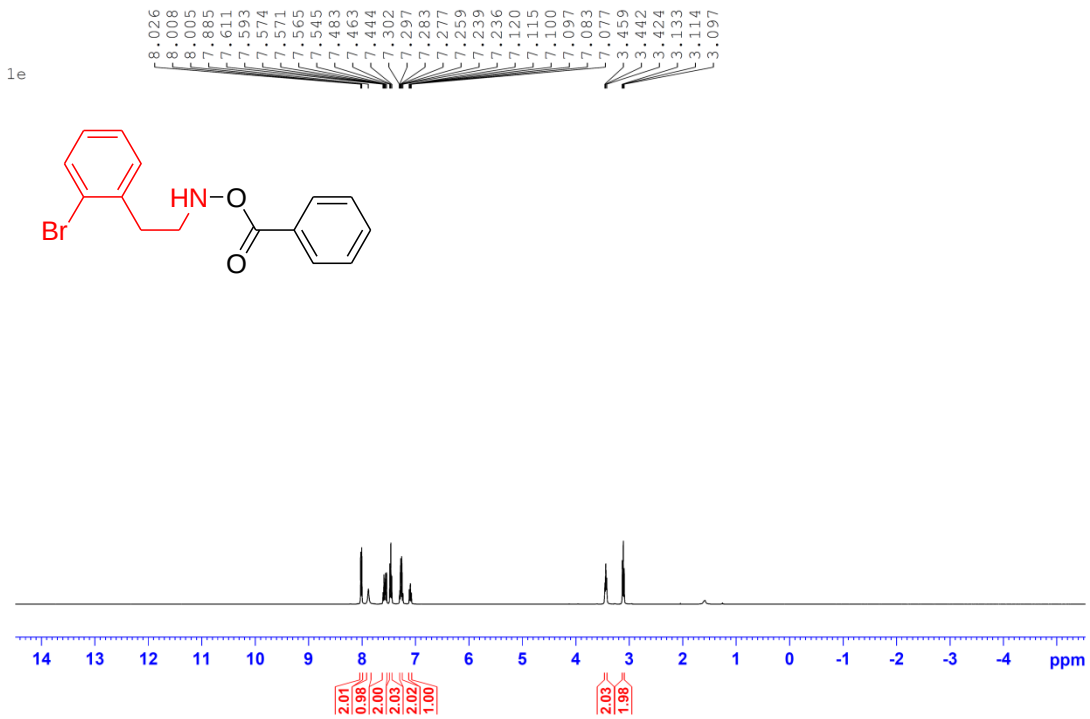

Figure A.10 ^{13}C NMR spectrum of **1e**

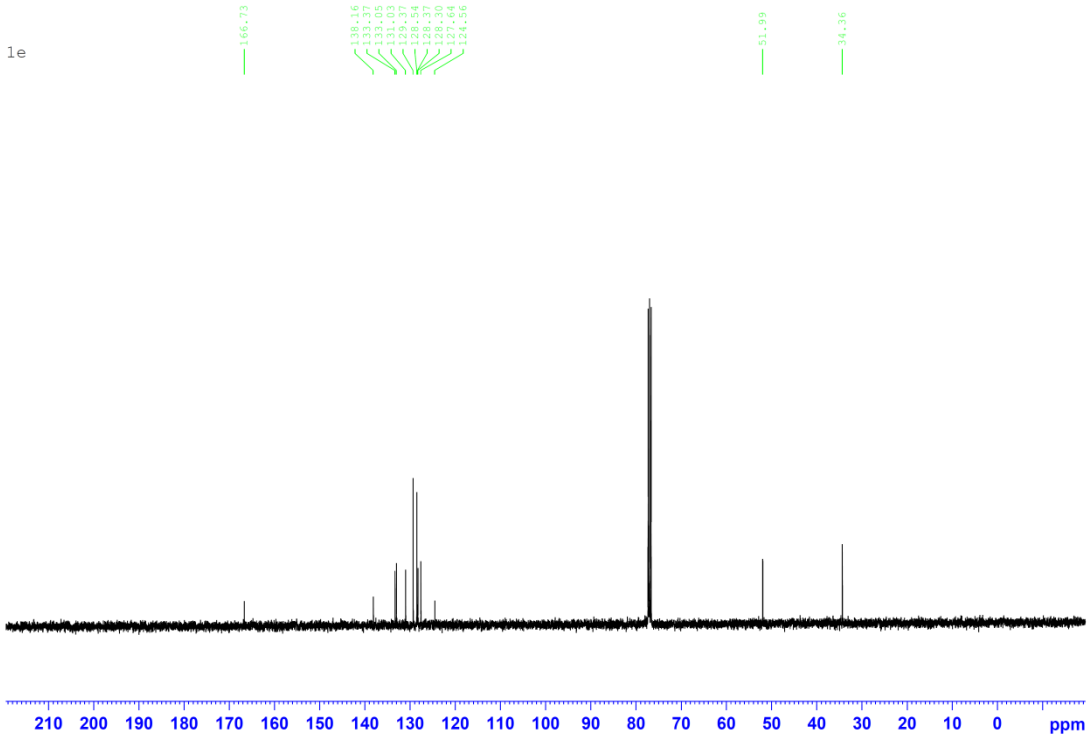

Figure A.11 ^{1}H NMR spectrum of **1f**

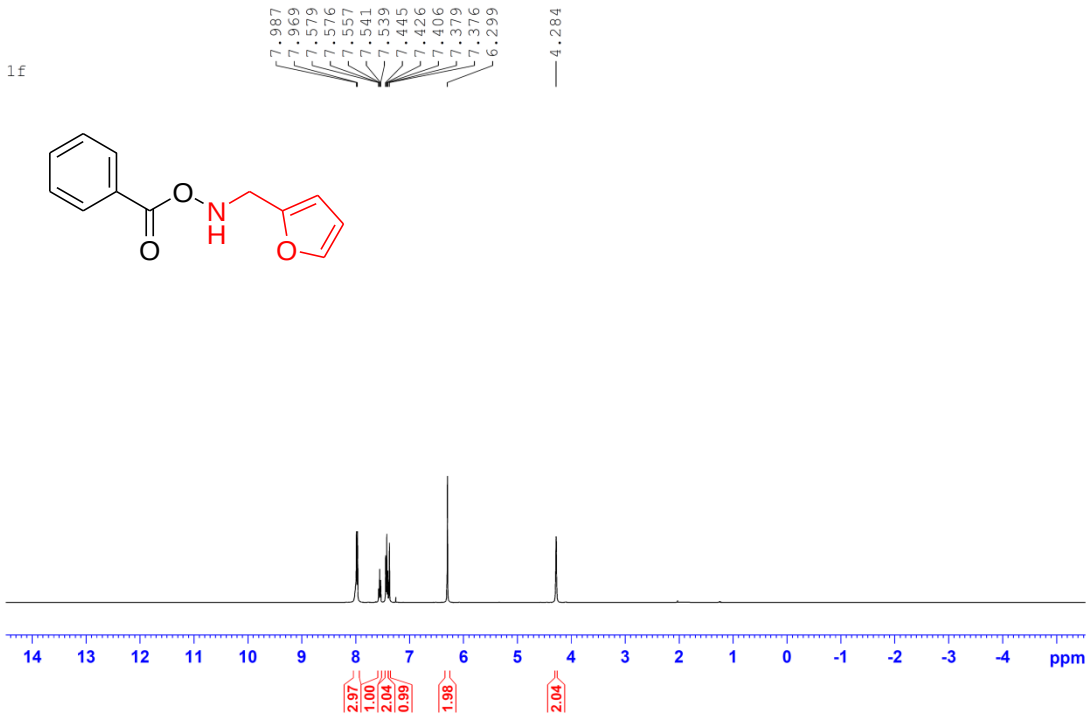

Figure A.12 ^{13}C NMR spectrum of **1f**

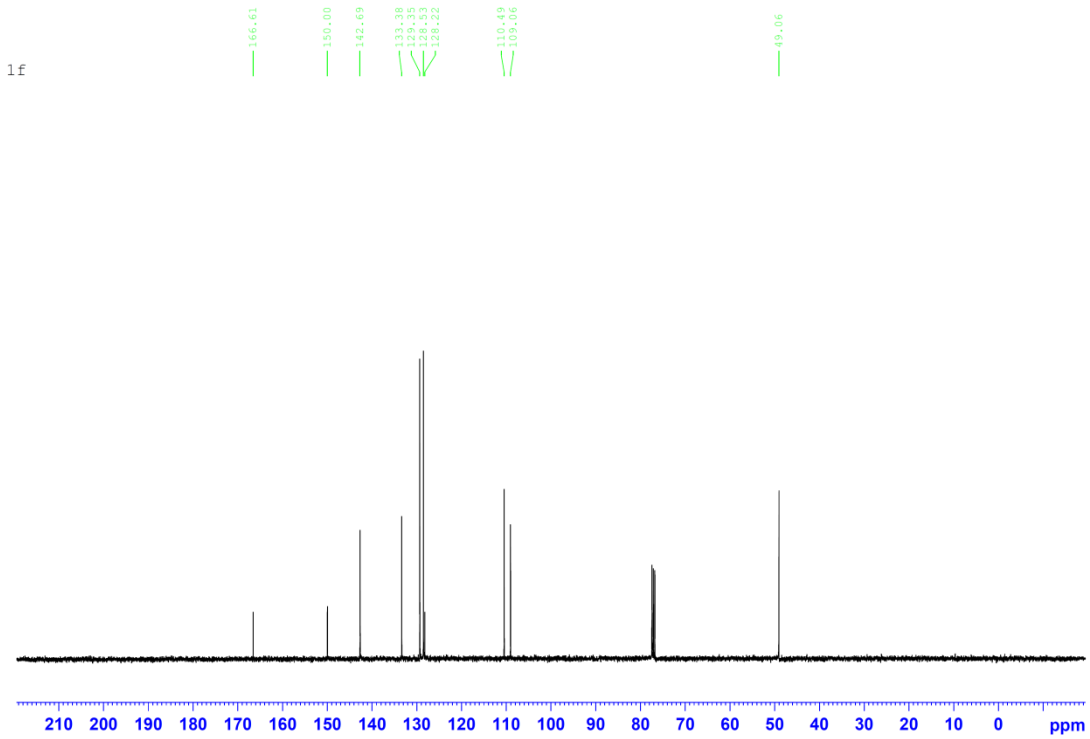

Figure A.13 ^{1}H NMR spectrum of **1g**

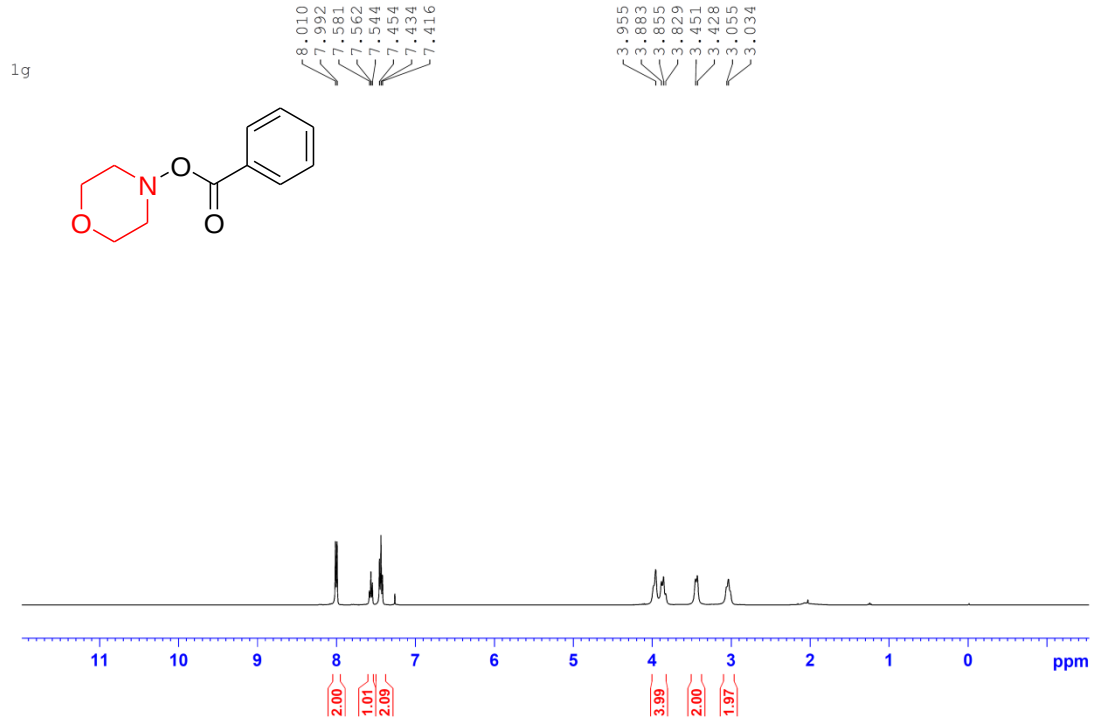

Figure A.14 ^{13}C NMR spectrum of **1g**

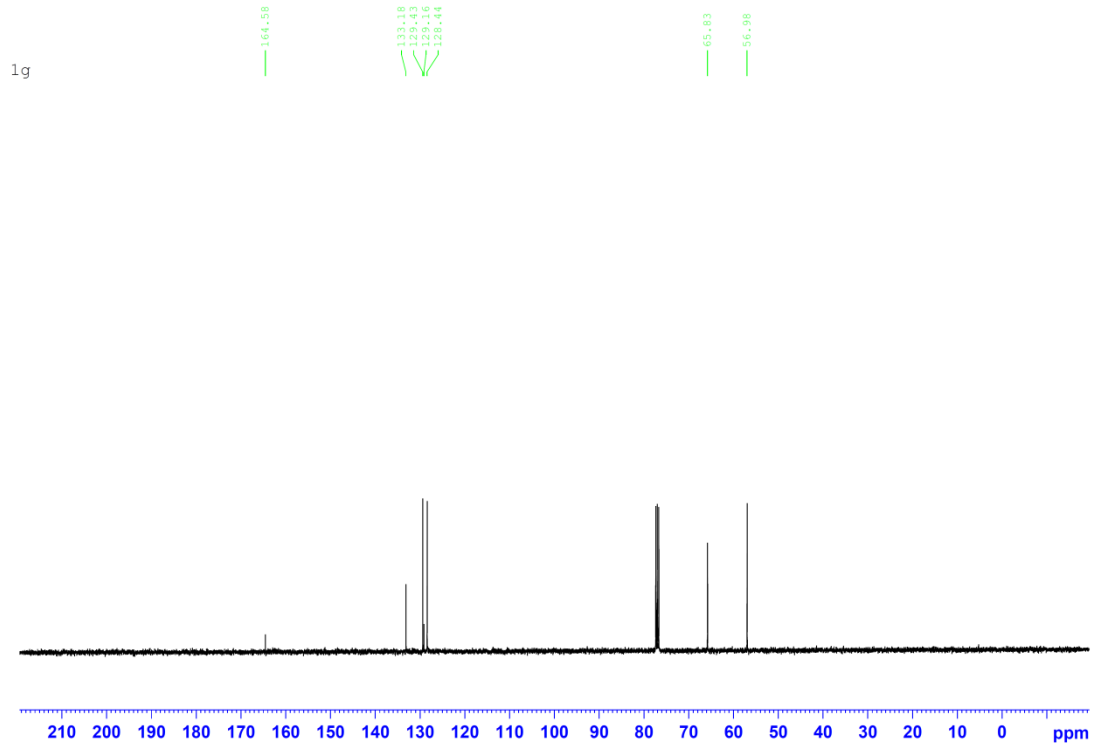

Figure A.15 ^{1}H NMR spectrum of **1h**

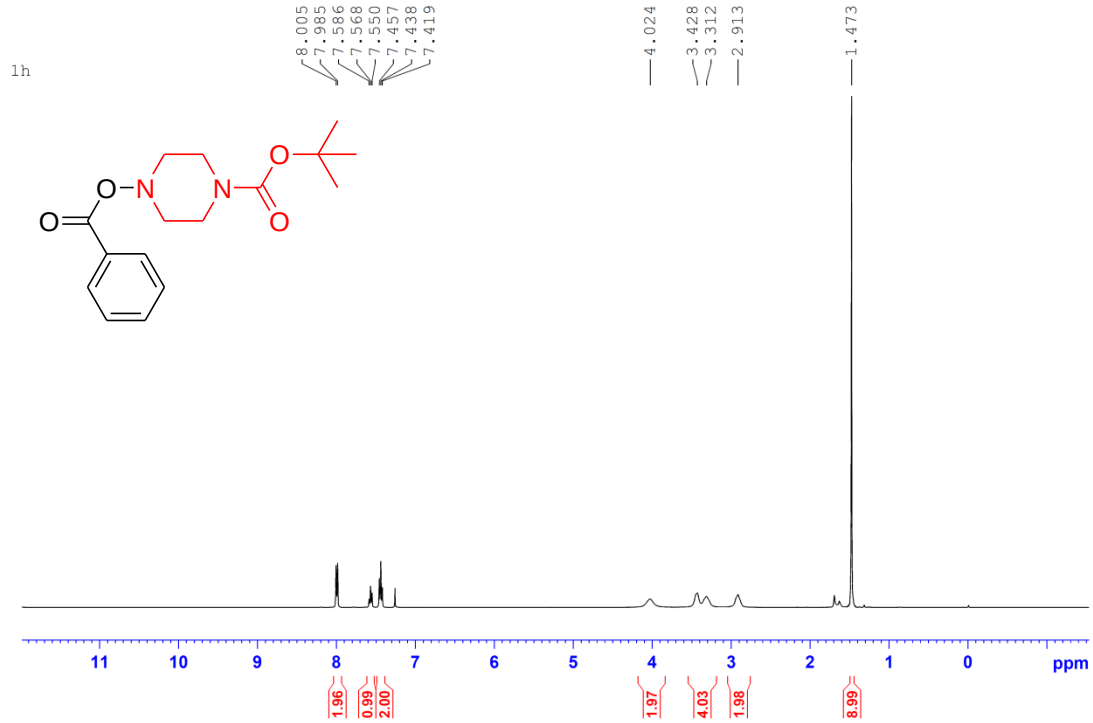

Figure A.16 ^{13}C NMR spectrum of **1h**

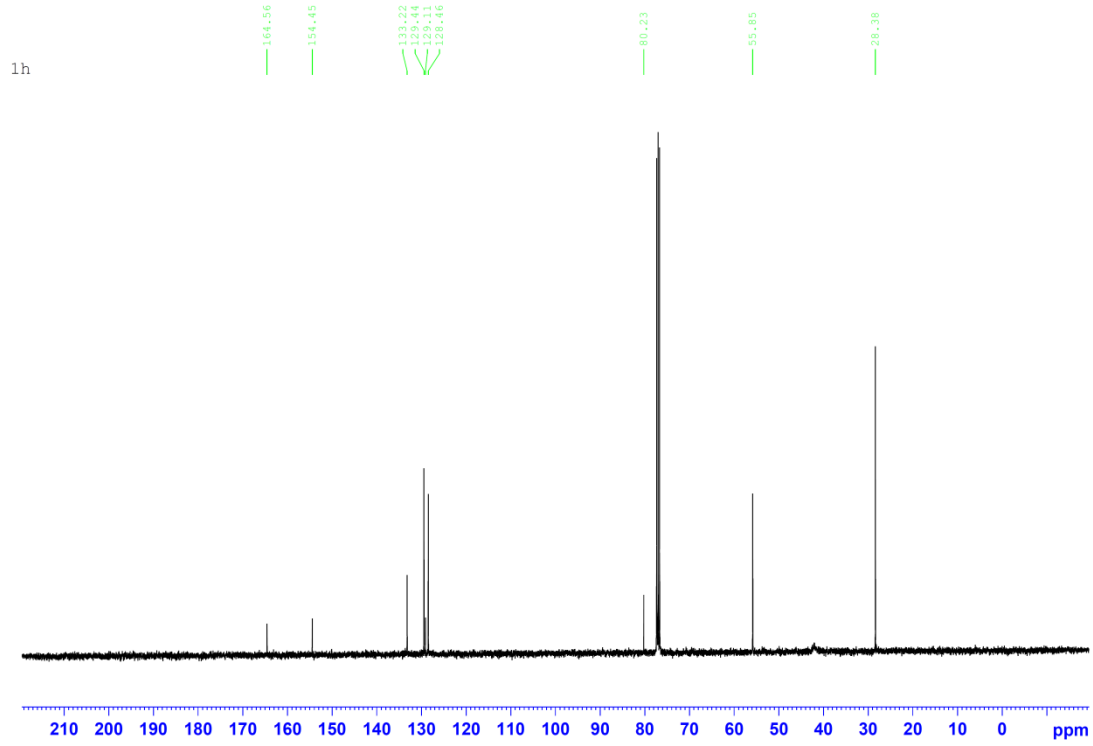

Figure A.17 ^{1}H NMR spectrum of **1i**

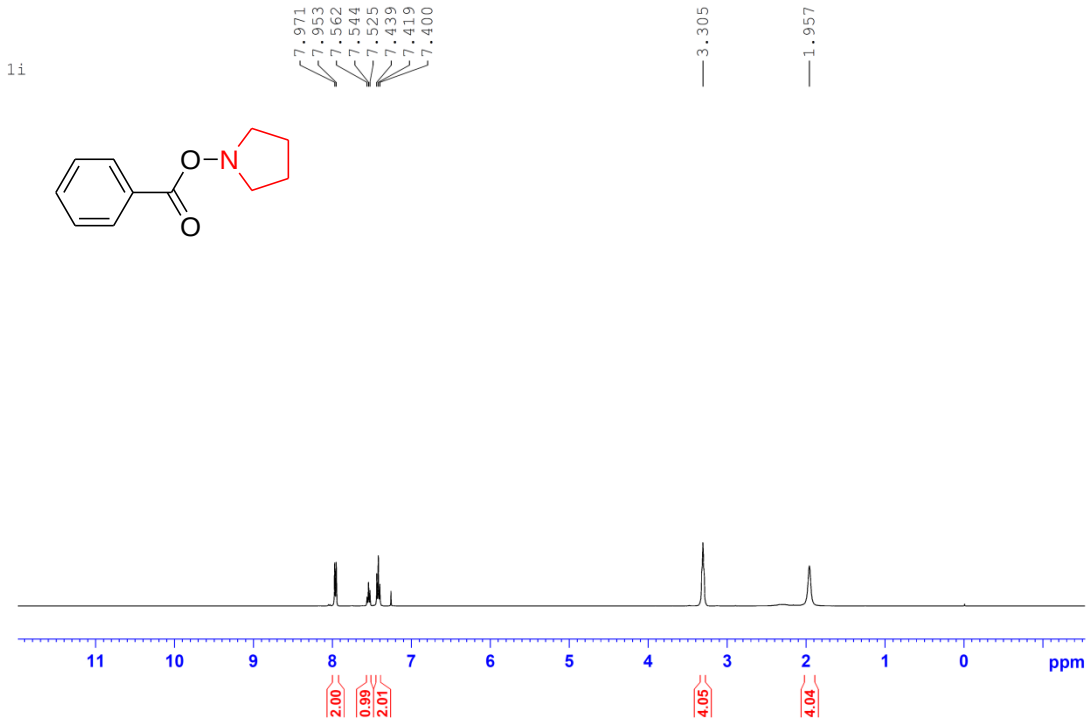

Figure A.18 ^{13}C NMR spectrum of **1i**

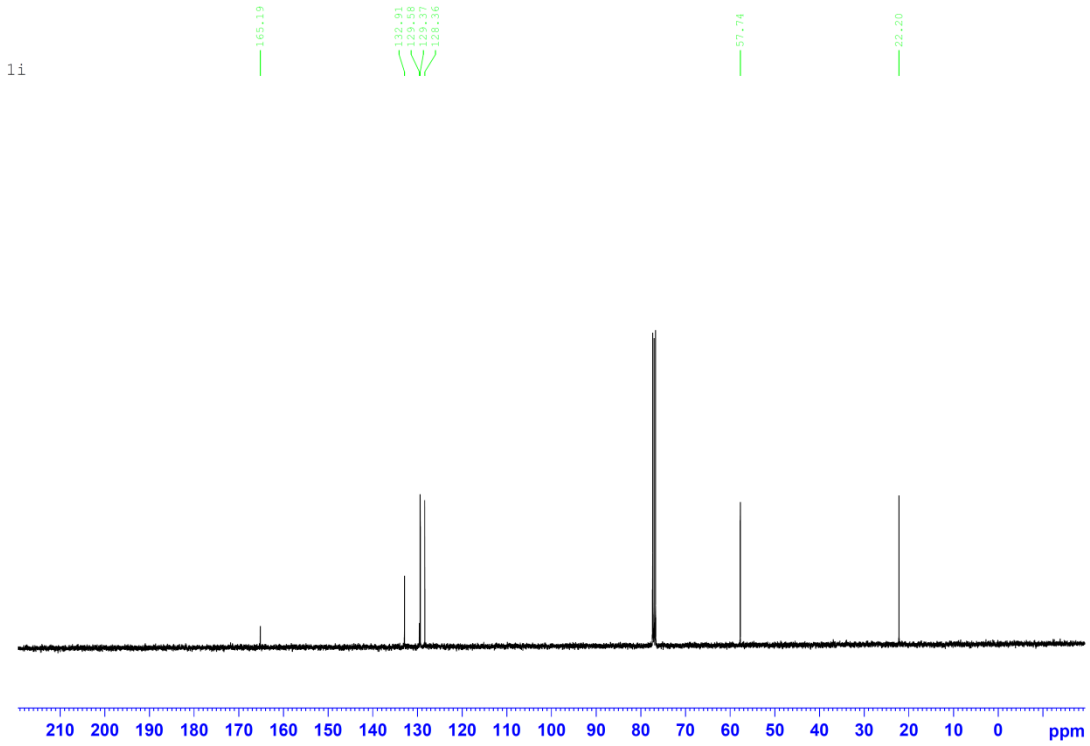

Figure A.19 ^{1}H NMR spectrum of **1j**

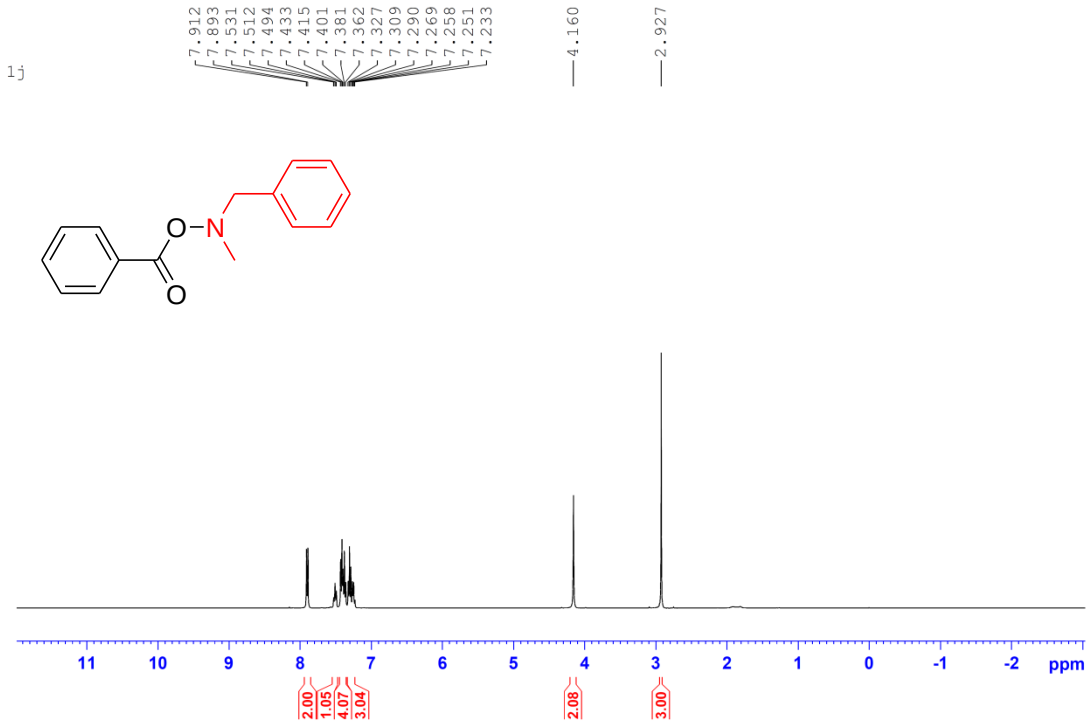

Figure A.20 ^{13}C NMR spectrum of **1j**

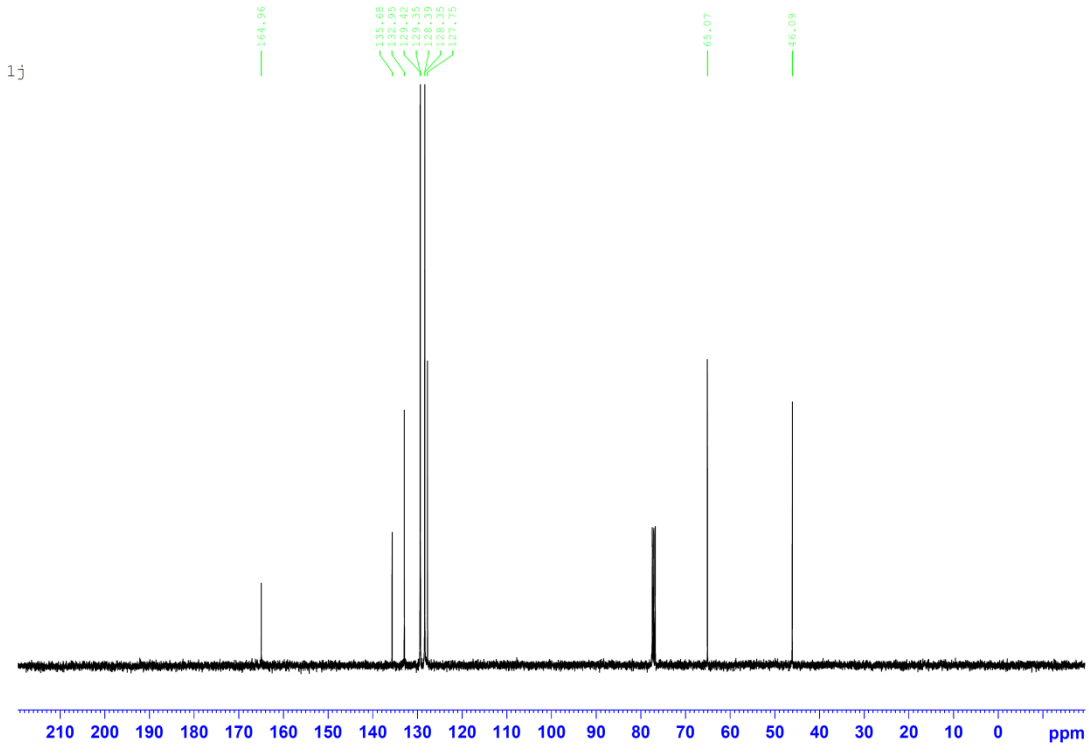

Figure A.21 ^{1}H NMR spectrum of **1k**

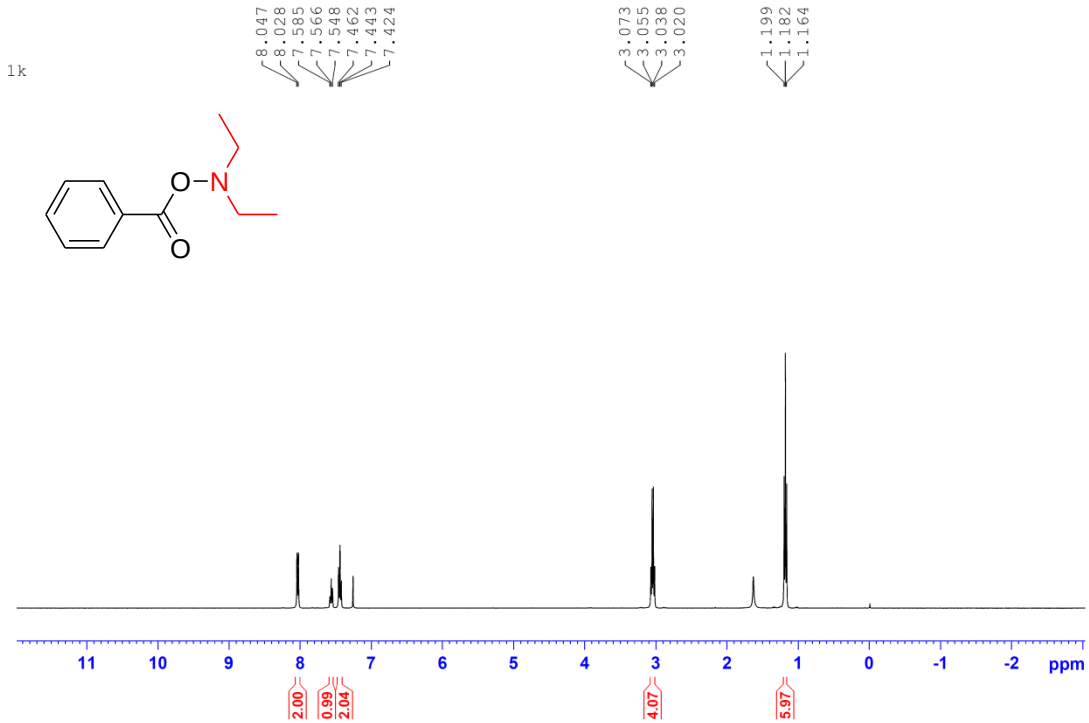

Figure A.22 ^{13}C NMR spectrum of **1k**

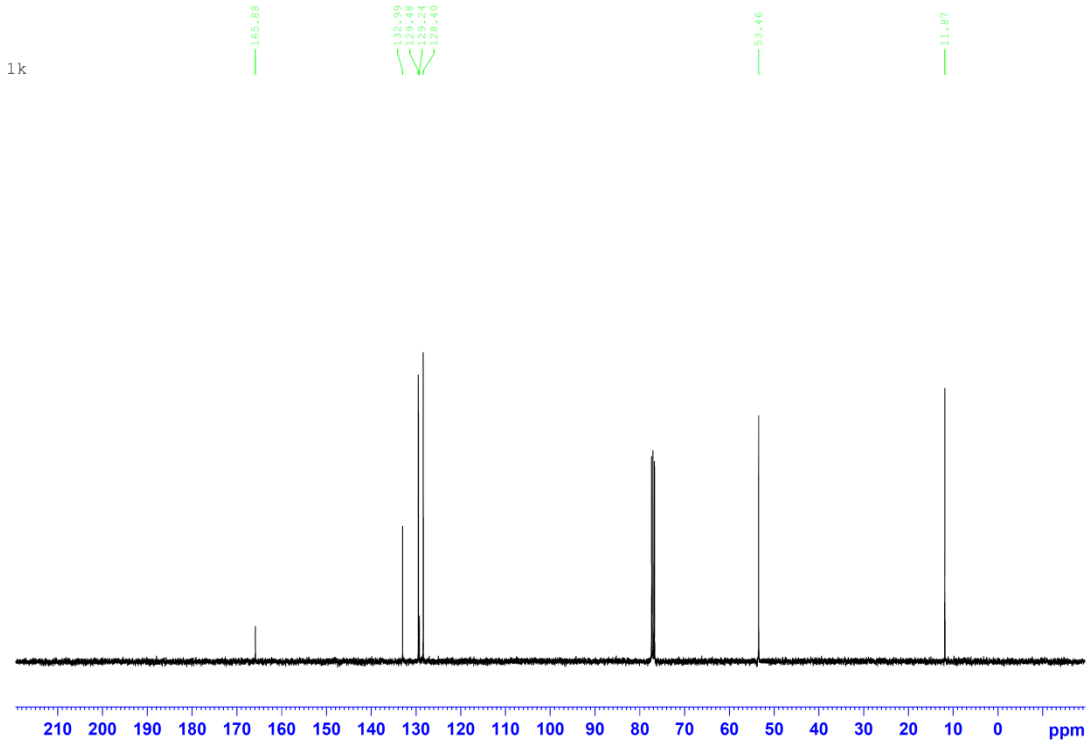

Figure A.23 ^{1}H NMR spectrum of **1l**

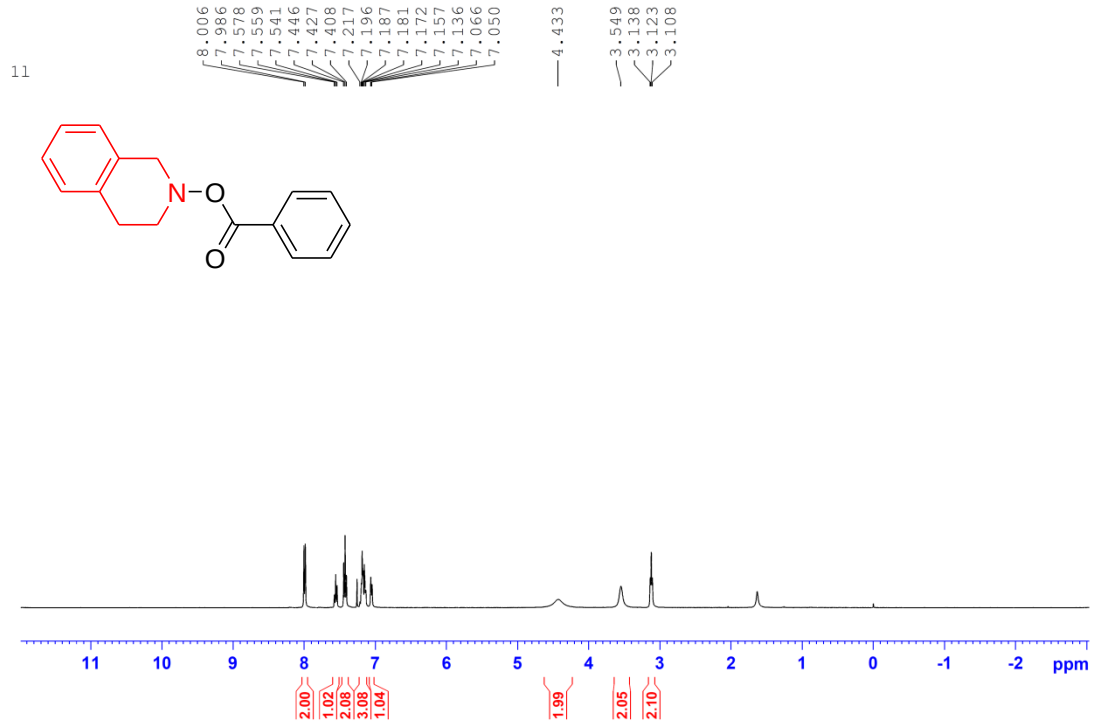

Figure A.24 ^{13}C NMR spectrum of **1l**

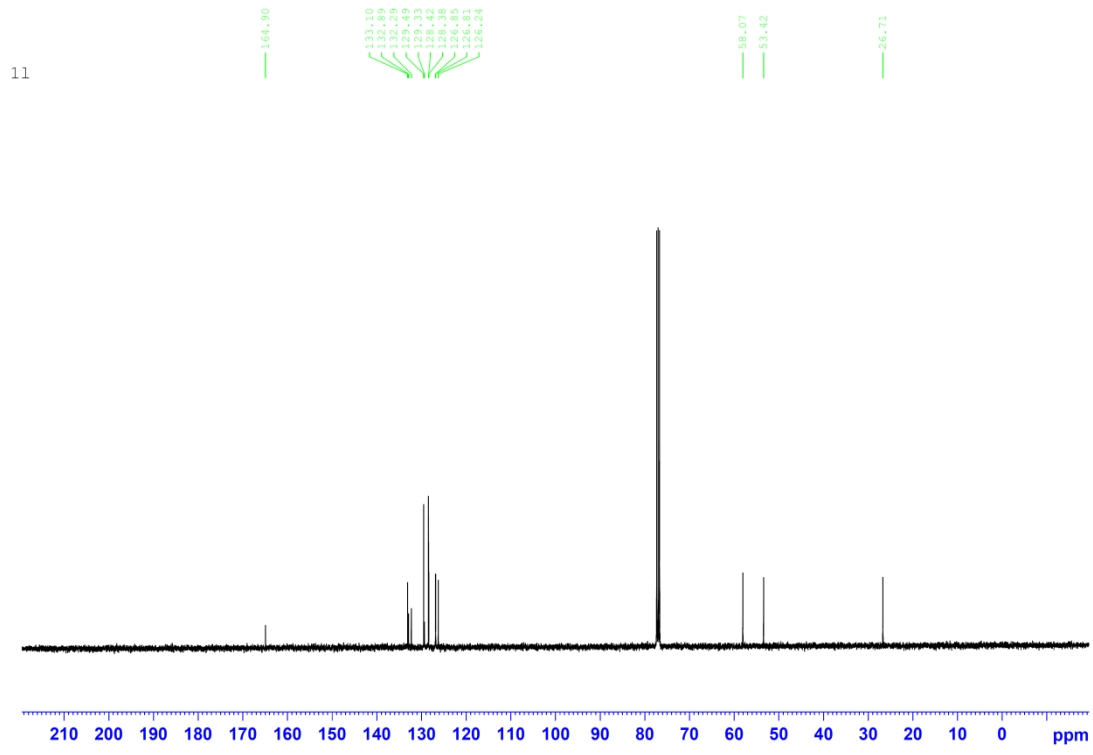

Figure A.25 ^{1}H NMR spectrum of **3a**

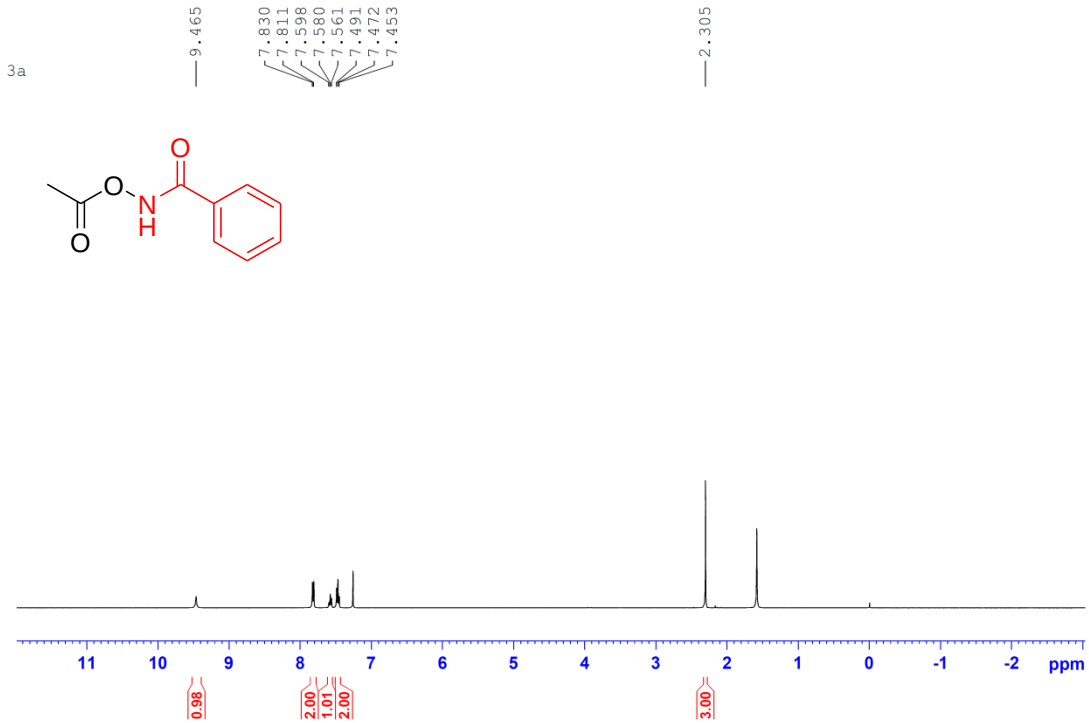

Figure A.26 ^{13}C NMR spectrum of **3a**

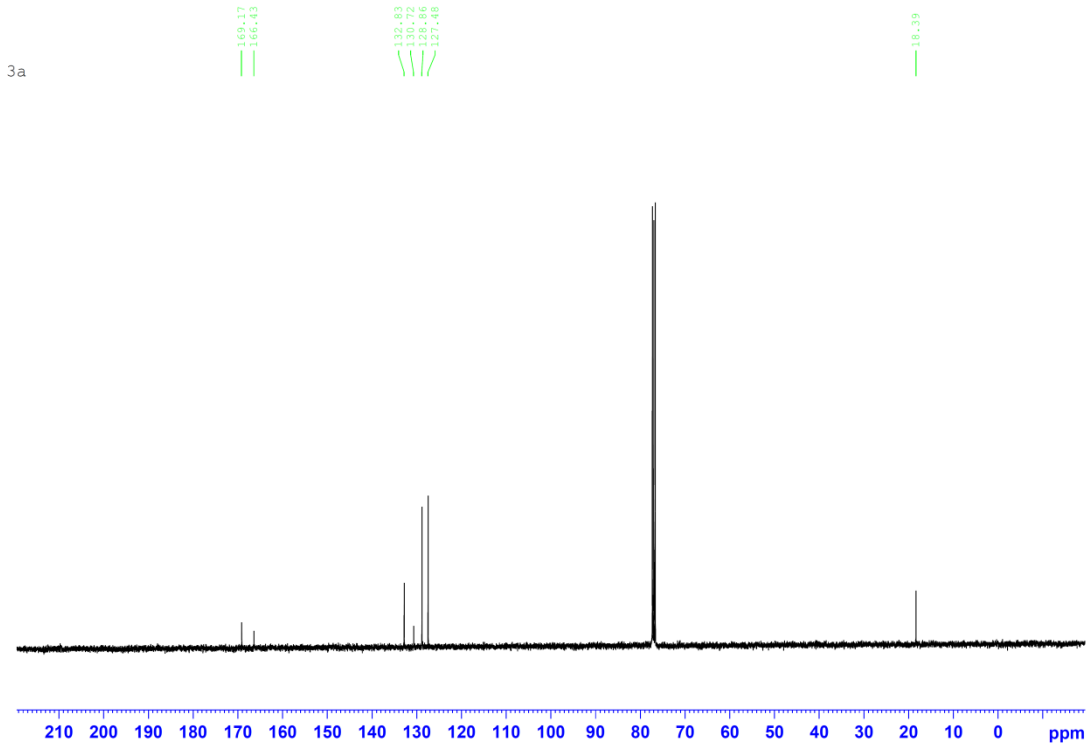

Figure A.27 ^{1}H NMR spectrum of **3b**

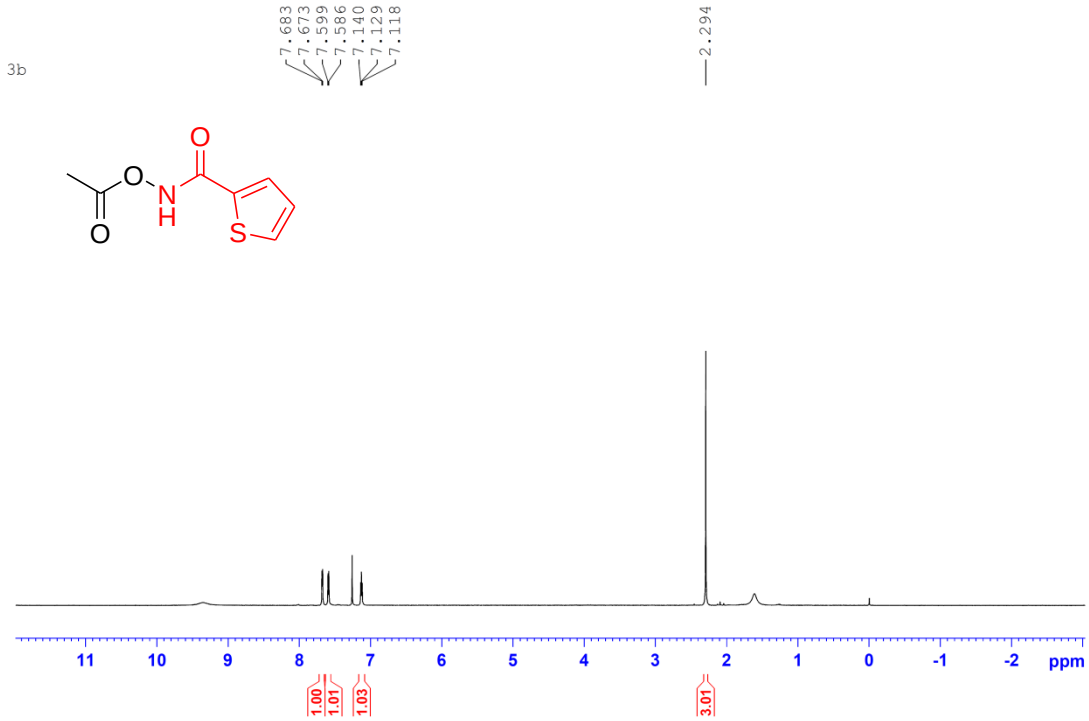

Figure A.28 ^{13}C NMR spectrum of **3b**

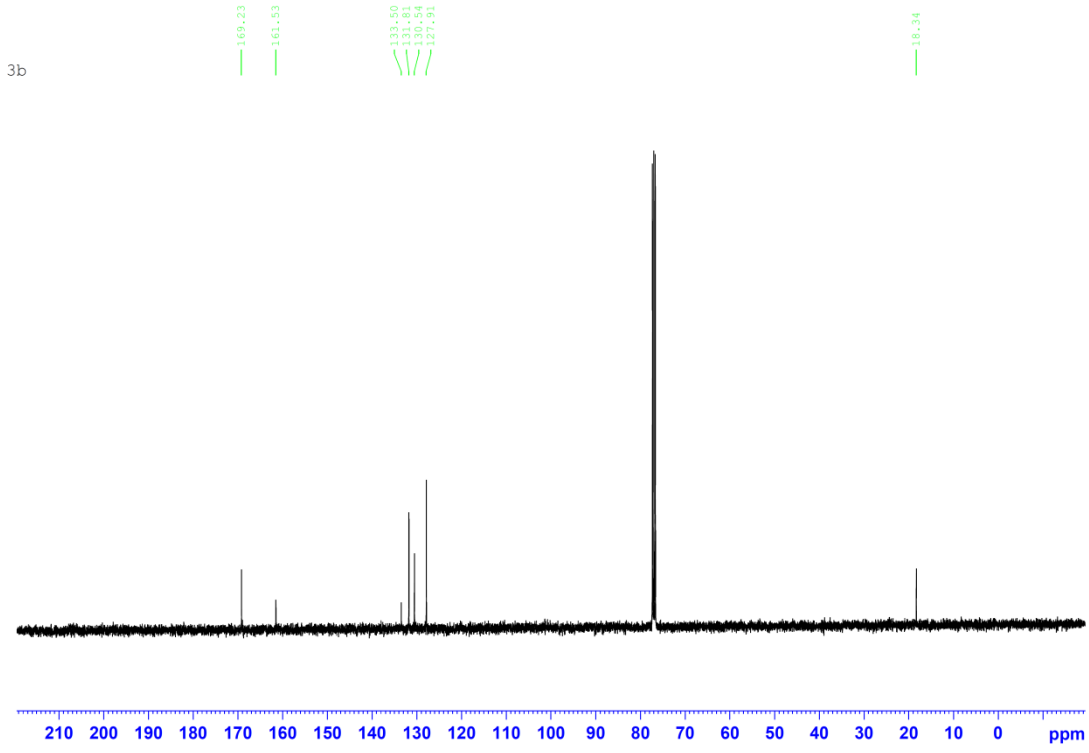

Figure A.29 ^{1}H NMR spectrum of **3c**

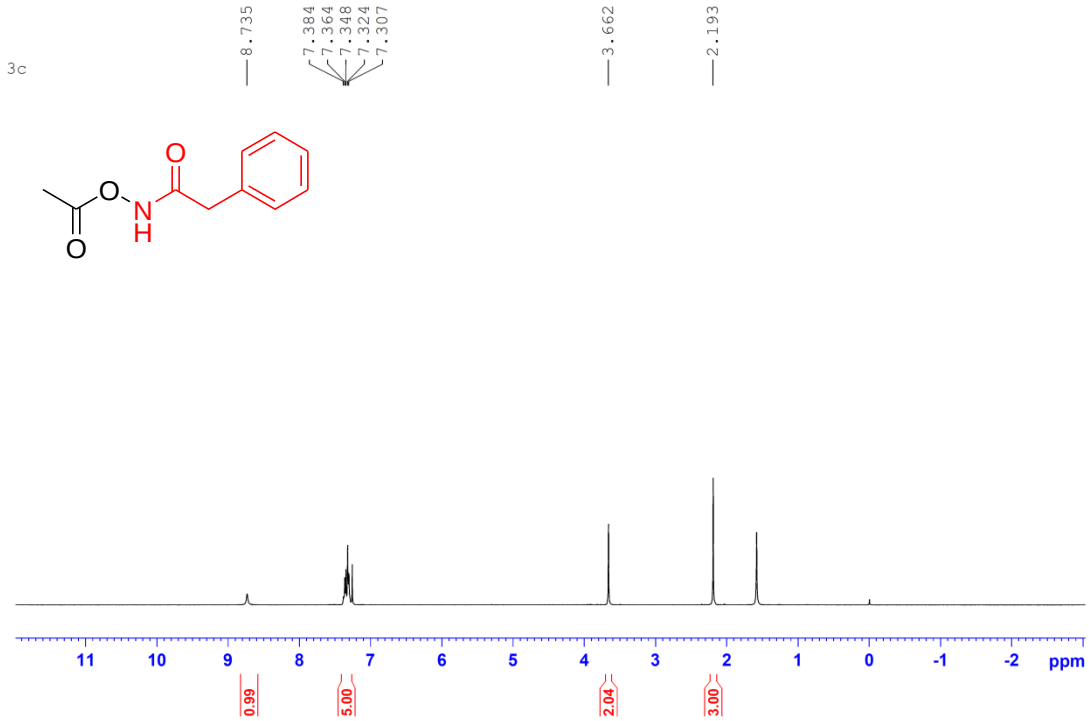

Figure A.30 ^{13}C NMR spectrum of **3c**

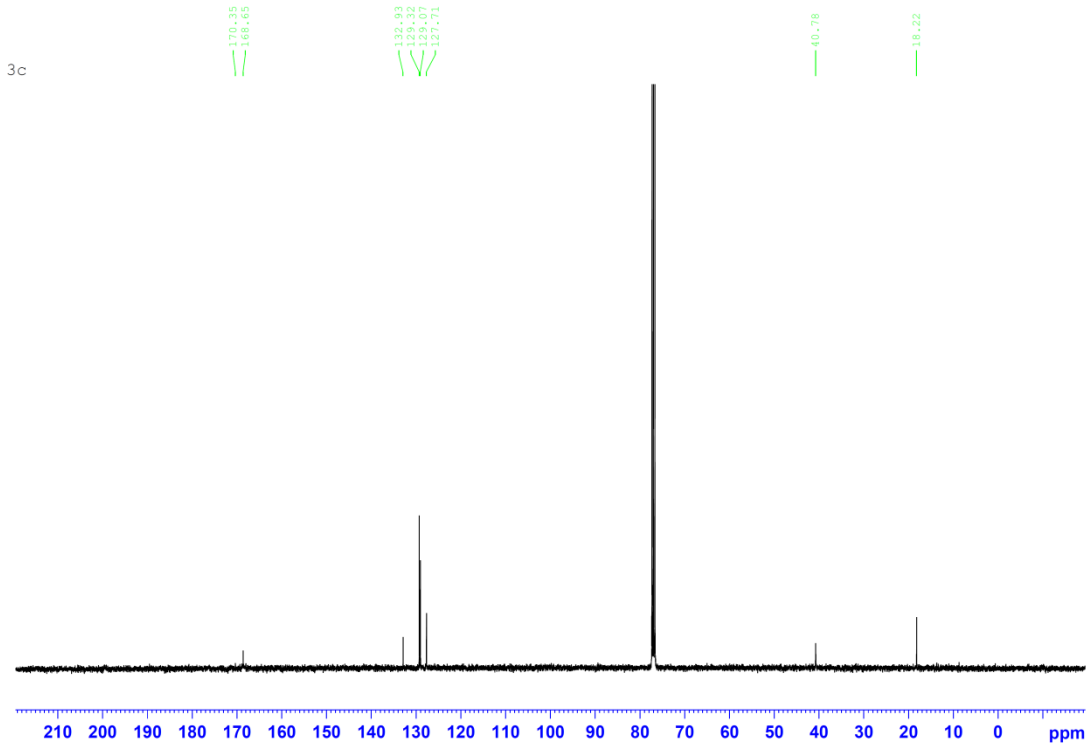

Figure A.31 ^{1}H NMR spectrum of **3d**

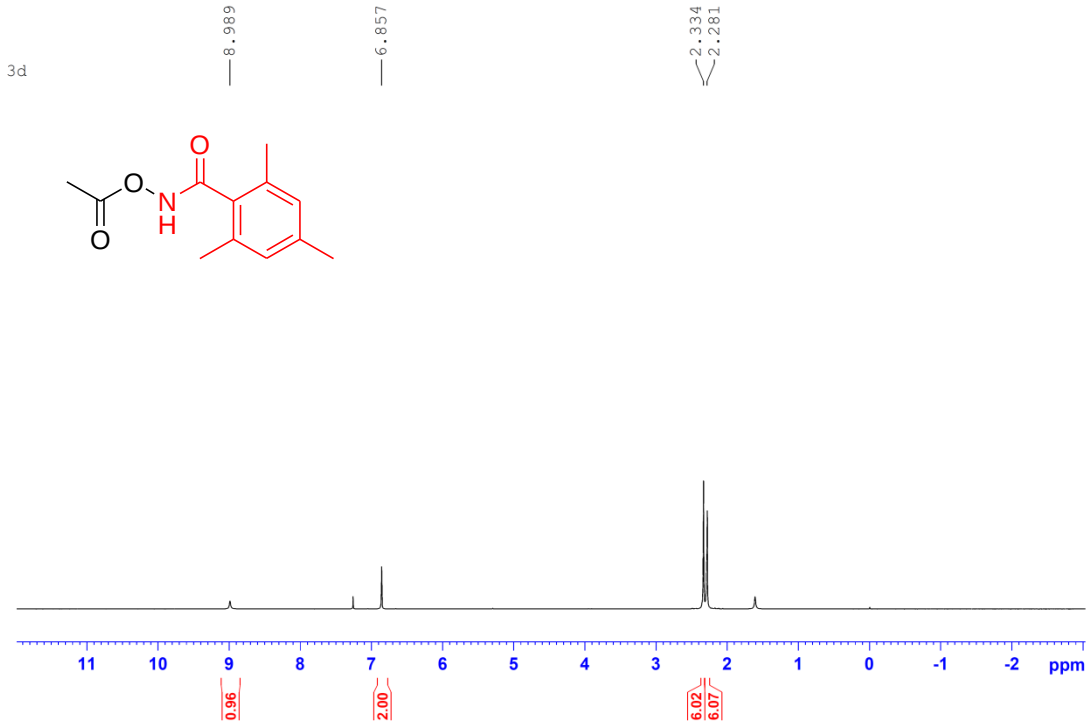

Figure A.32 ^{13}C NMR spectrum of **3d**

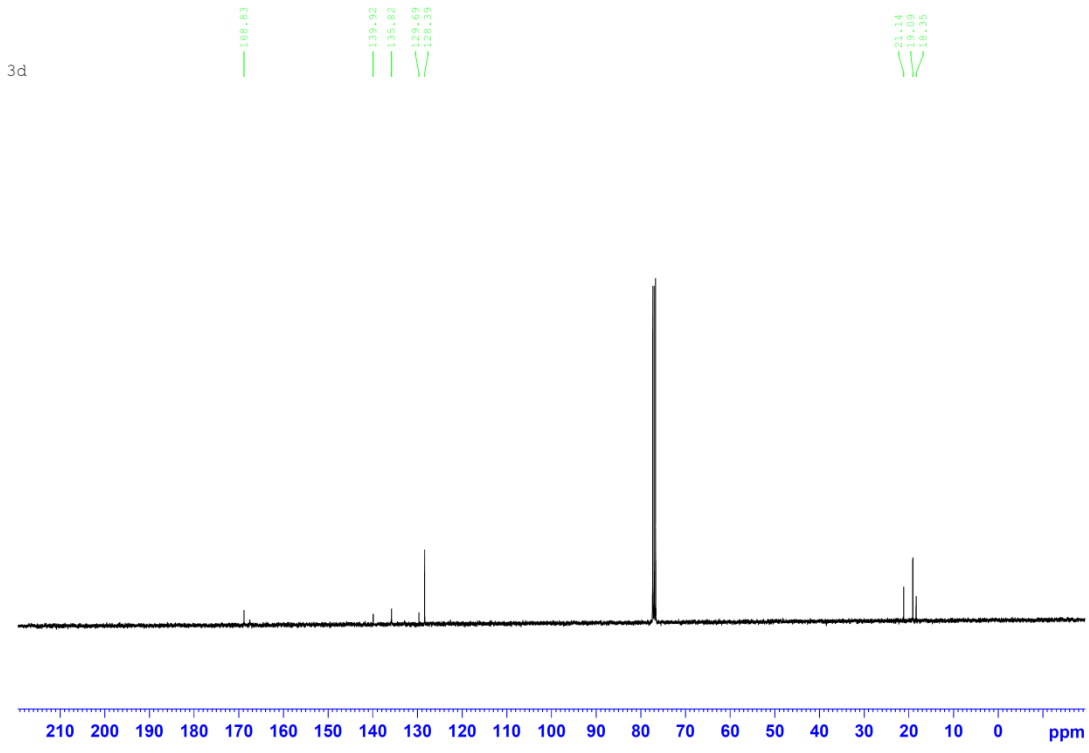

Figure A.33 ^{1}H NMR spectrum of **7a**

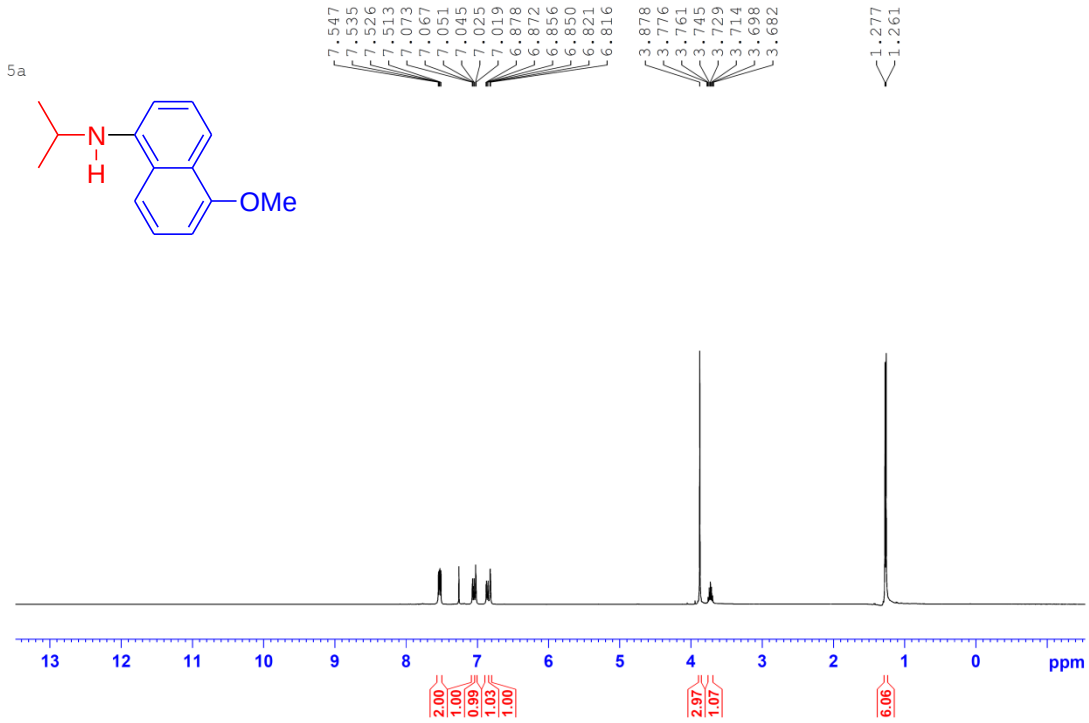

Figure A.34 ^{13}C NMR spectrum of **7a**

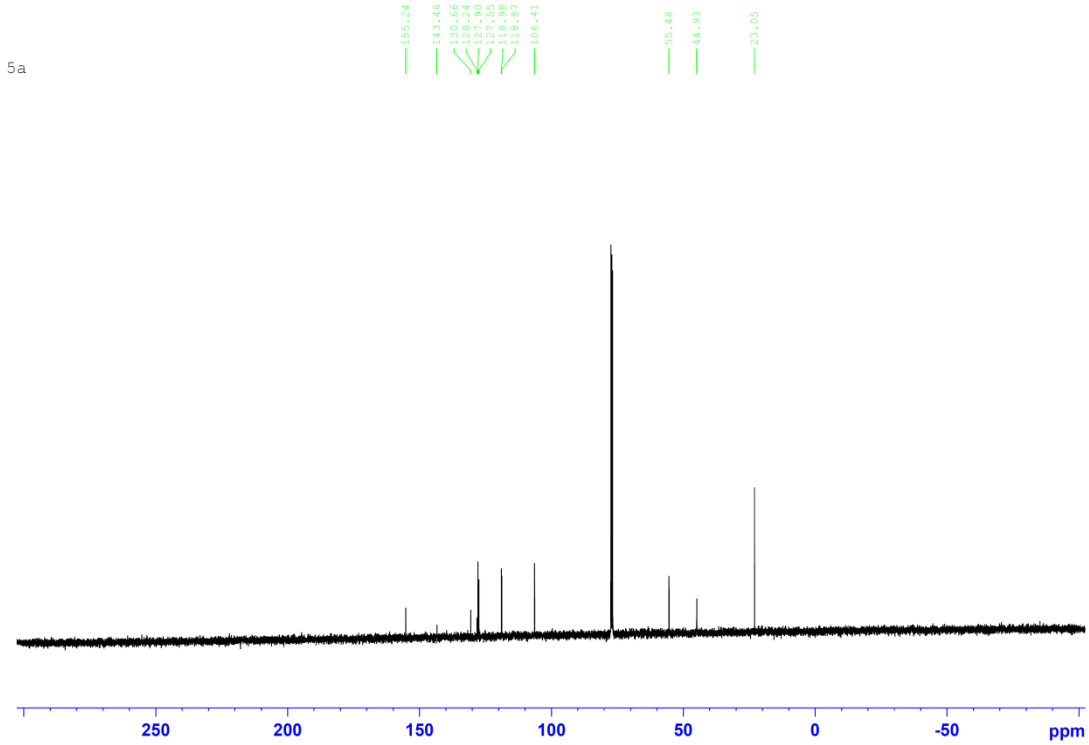

Figure A.35 ^{1}H NMR spectrum of **7b**

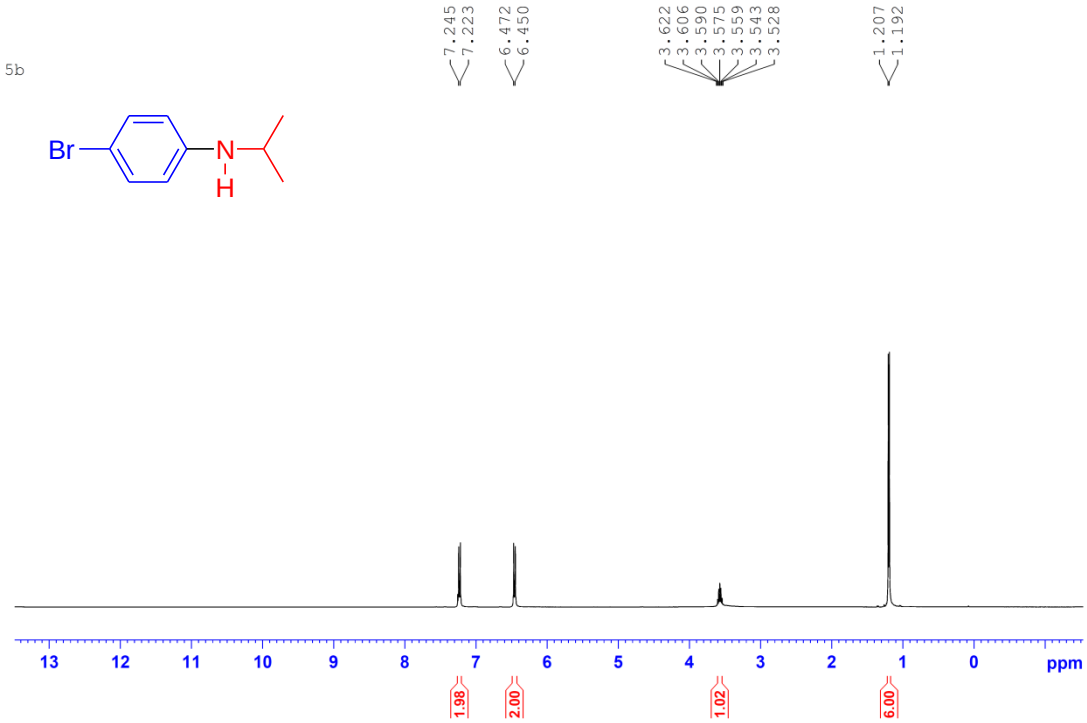

Figure A.36 ^{13}C NMR spectrum of **7b**

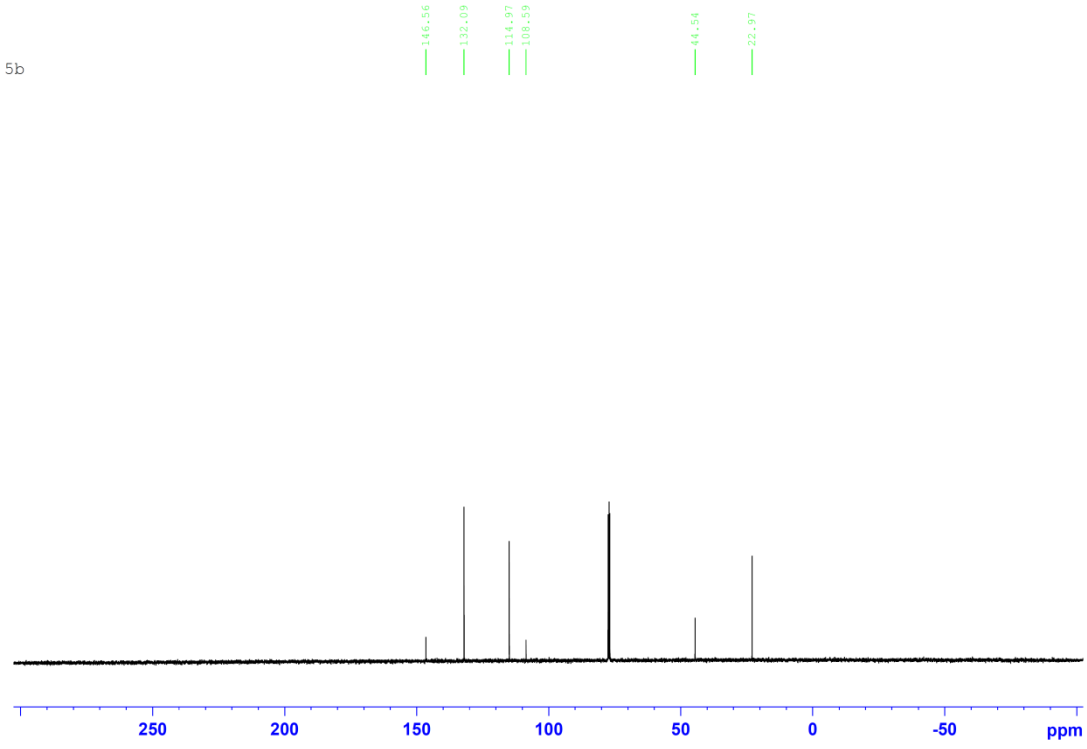

Figure A.37 ^{1}H NMR spectrum of **7c**

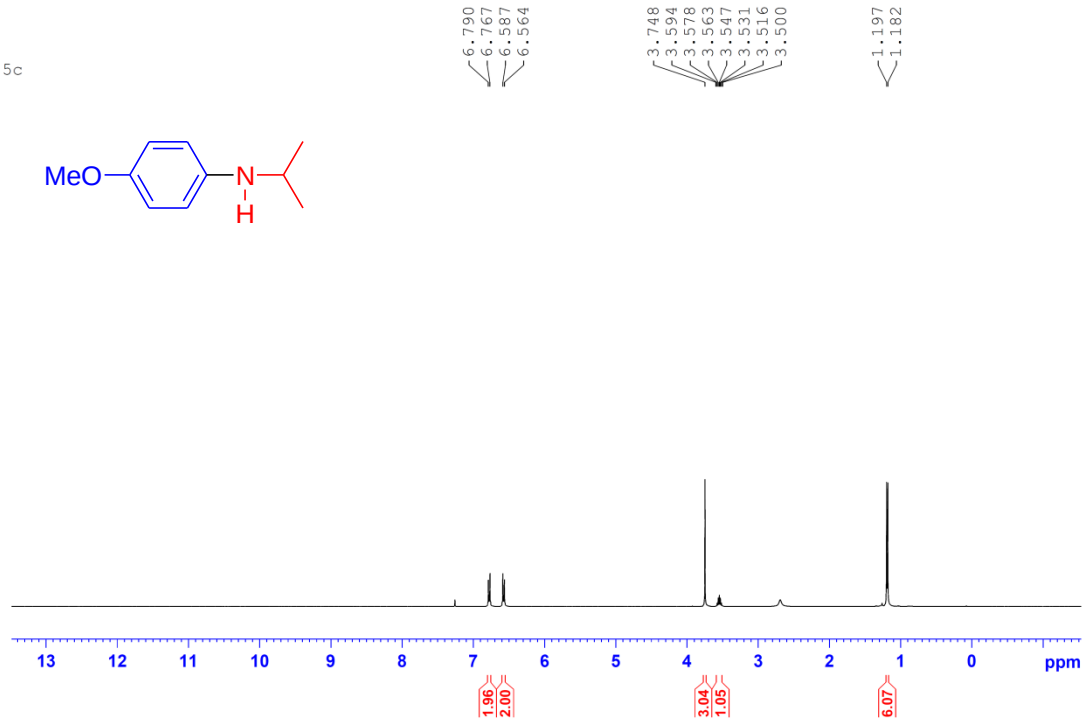

Figure A.38 ^{13}C NMR spectrum of **7c**

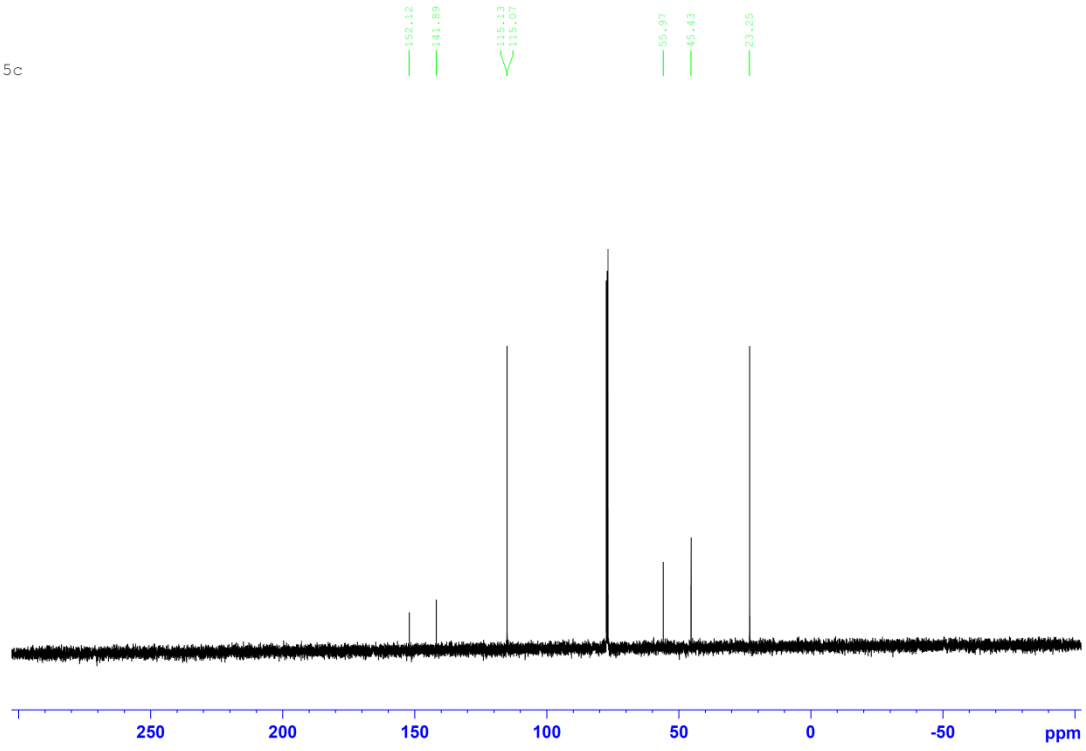

Figure A.39 ^{1}H NMR spectrum of **7d**

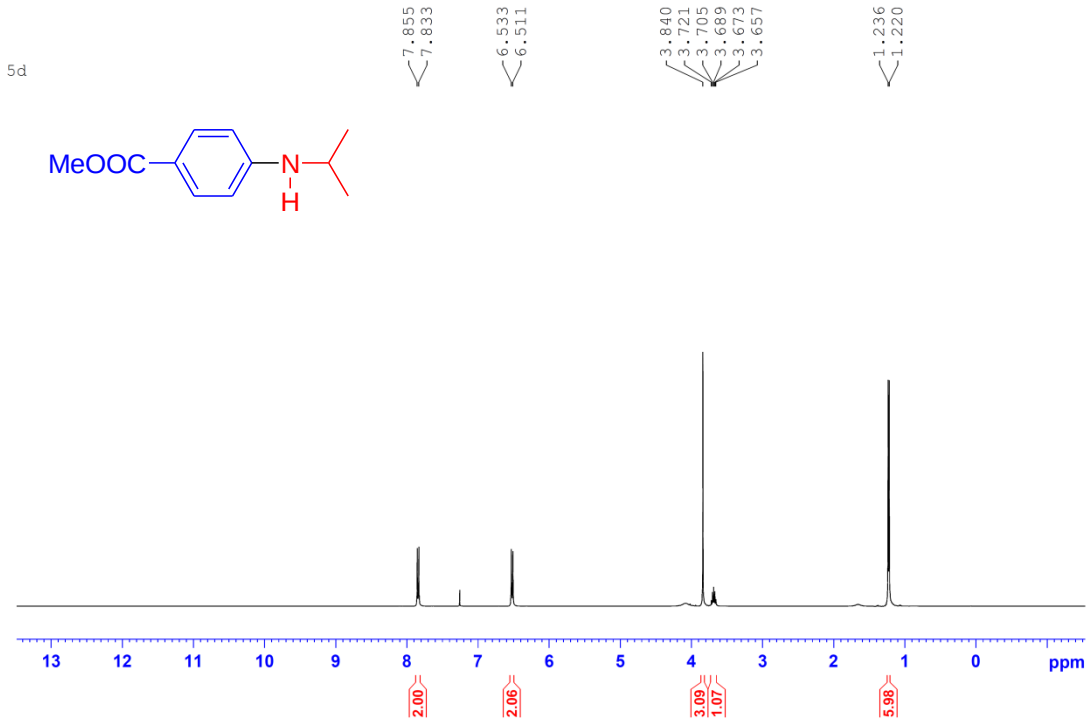

Figure A.40 ^{13}C NMR spectrum of **7d**

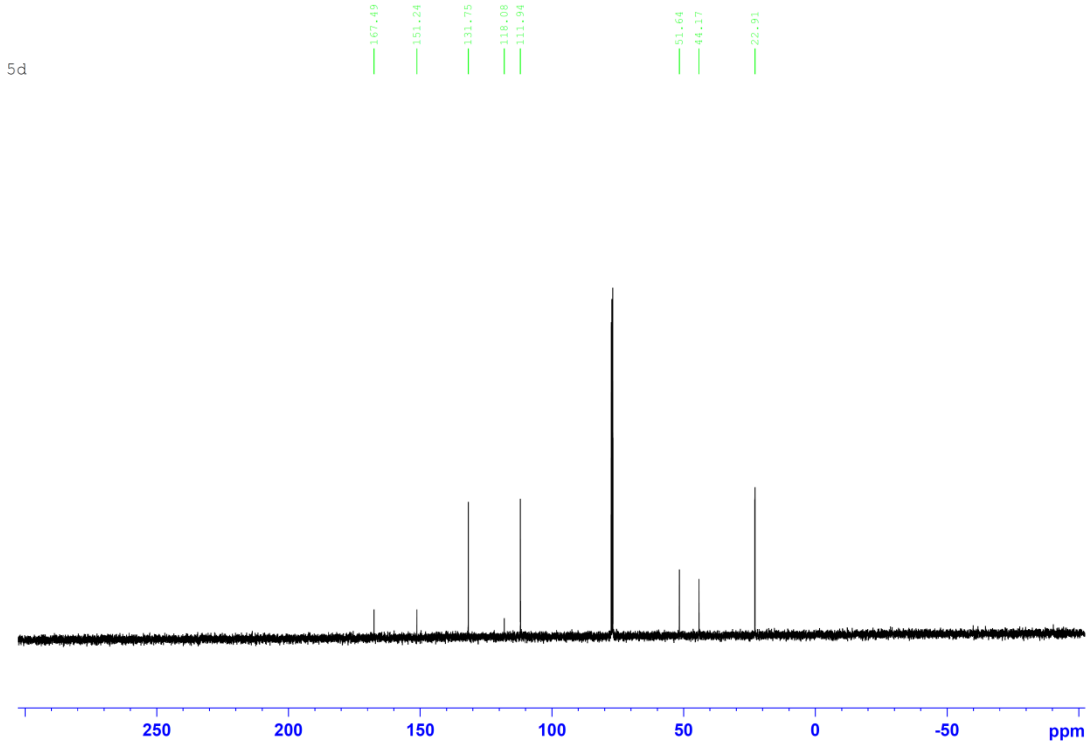

Figure A.41 ^{1}H NMR spectrum of **7e**

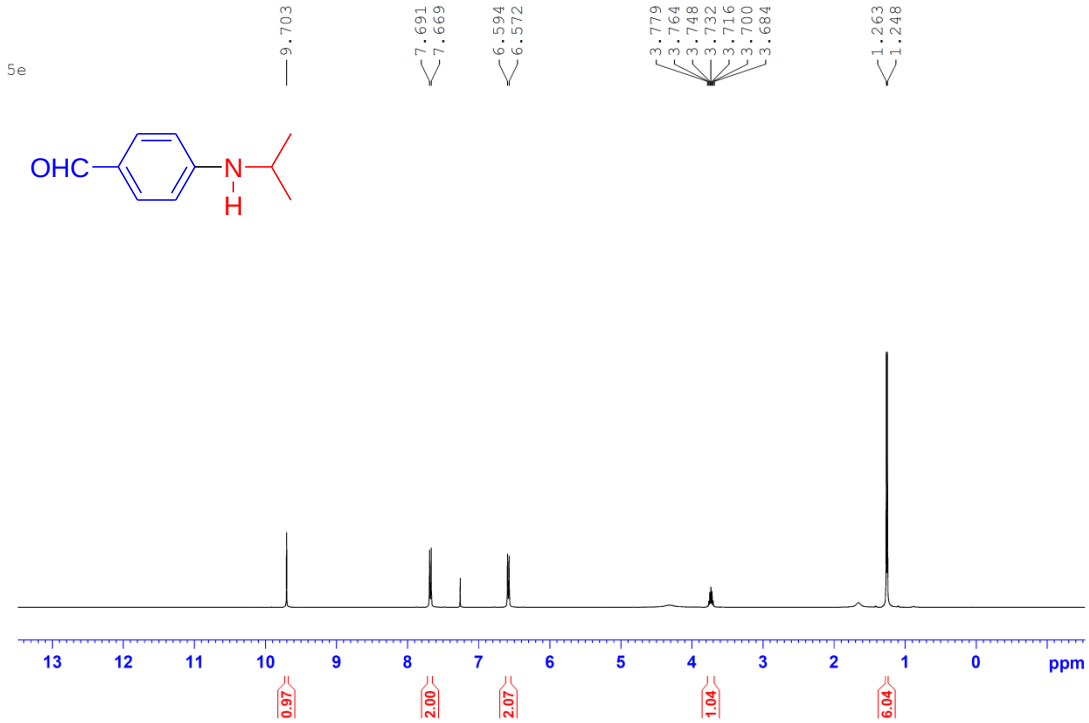

Figure A.42 ^{13}C NMR spectrum of **7e**

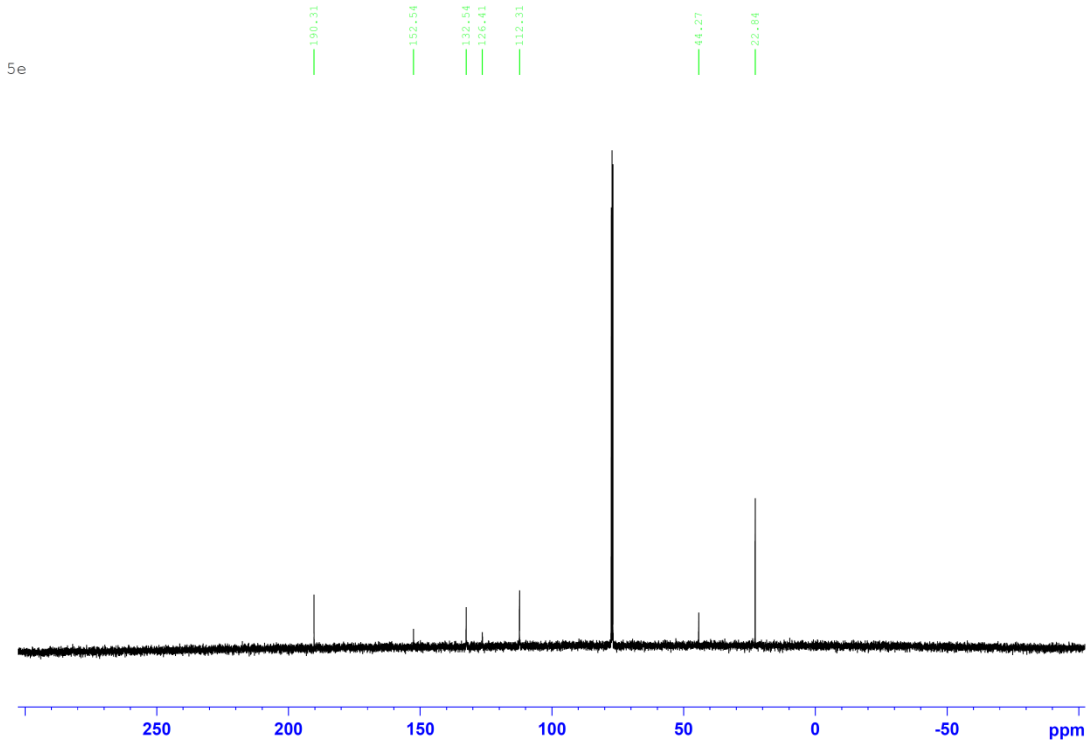

Figure A.43 ^{1}H NMR spectrum of **7f**

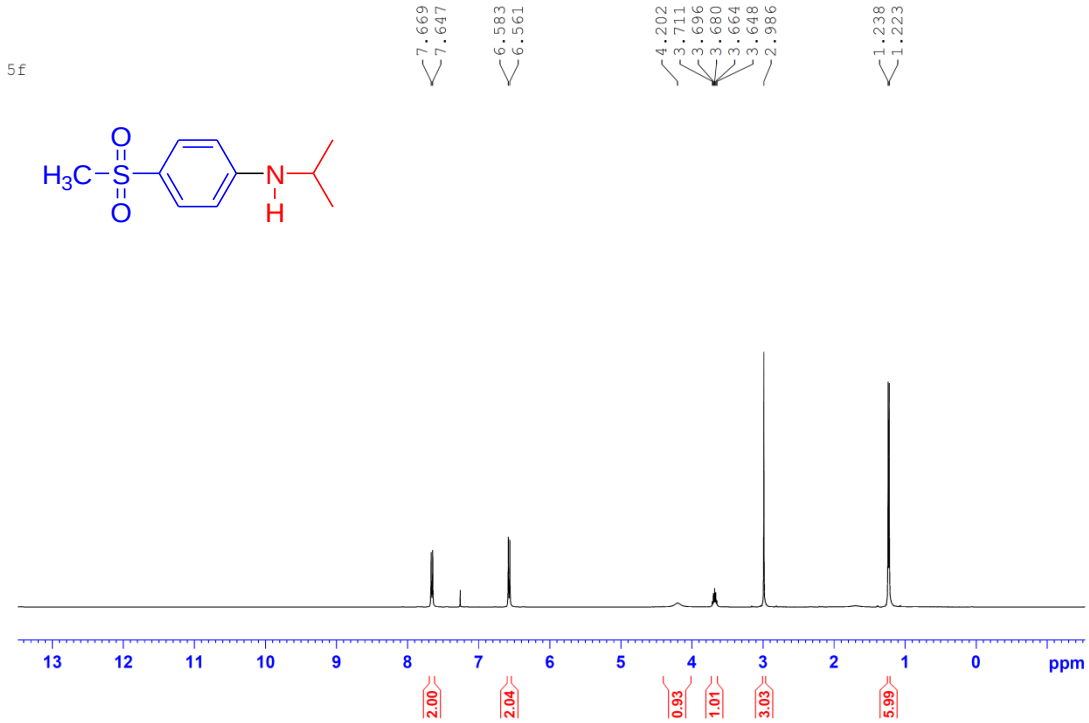

Figure A.44 ^{13}C NMR spectrum of **7f**

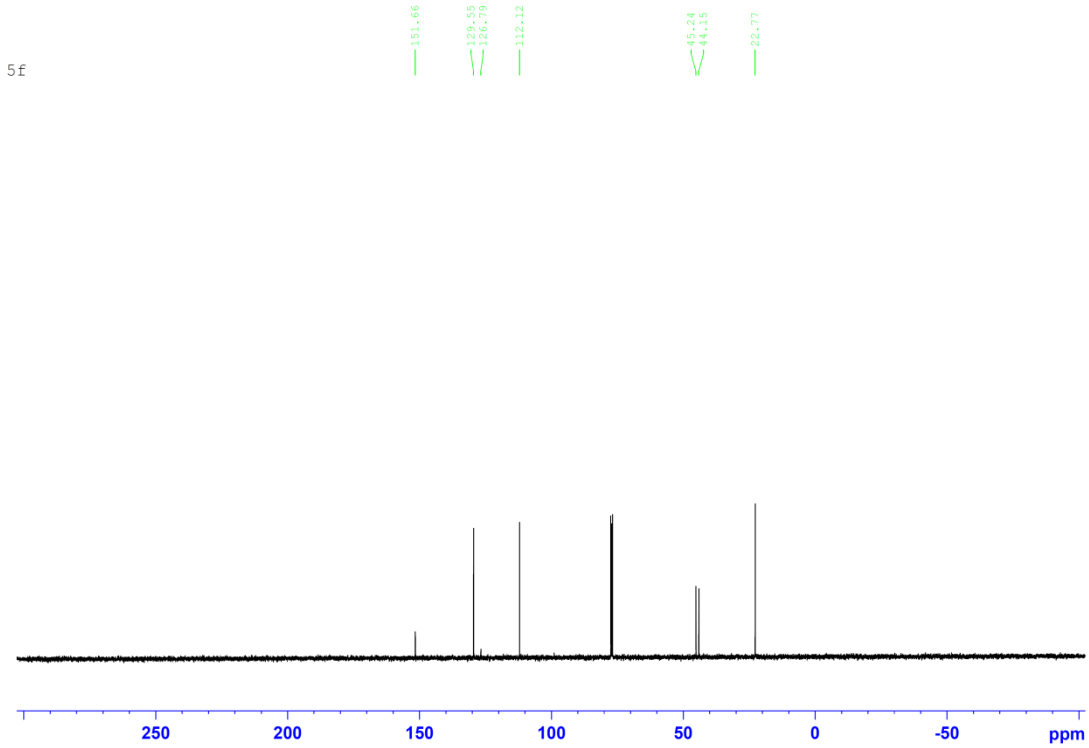

Figure A.45 ^{1}H NMR spectrum of **7g**

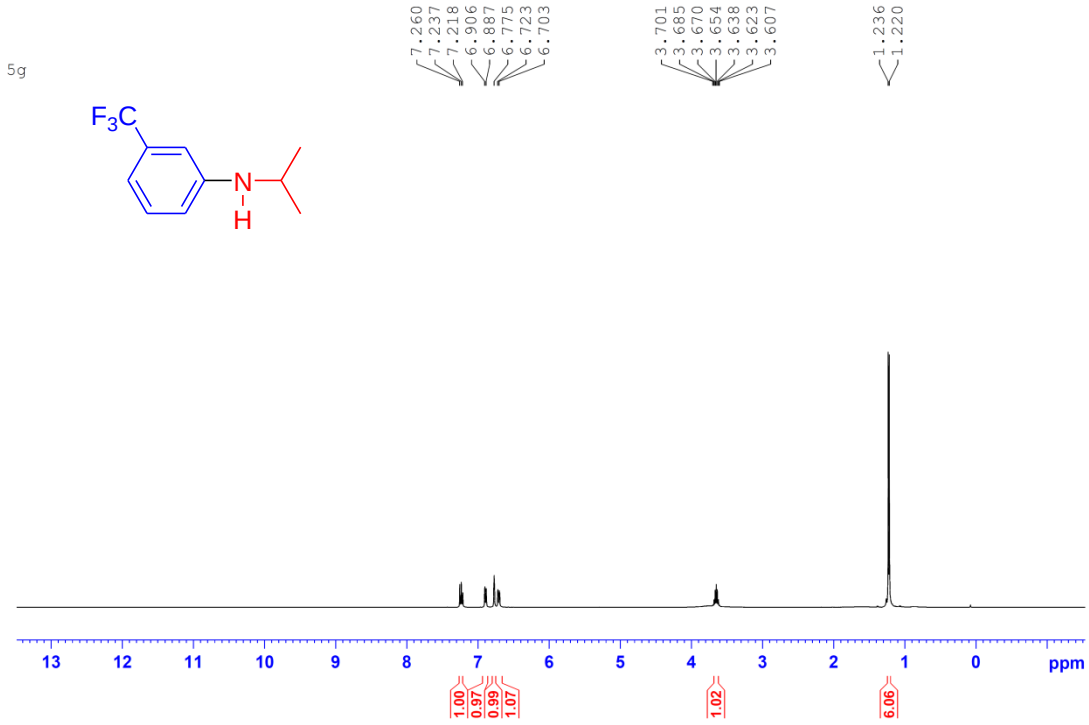

Figure A.46 ^{13}C NMR spectrum of **7g**

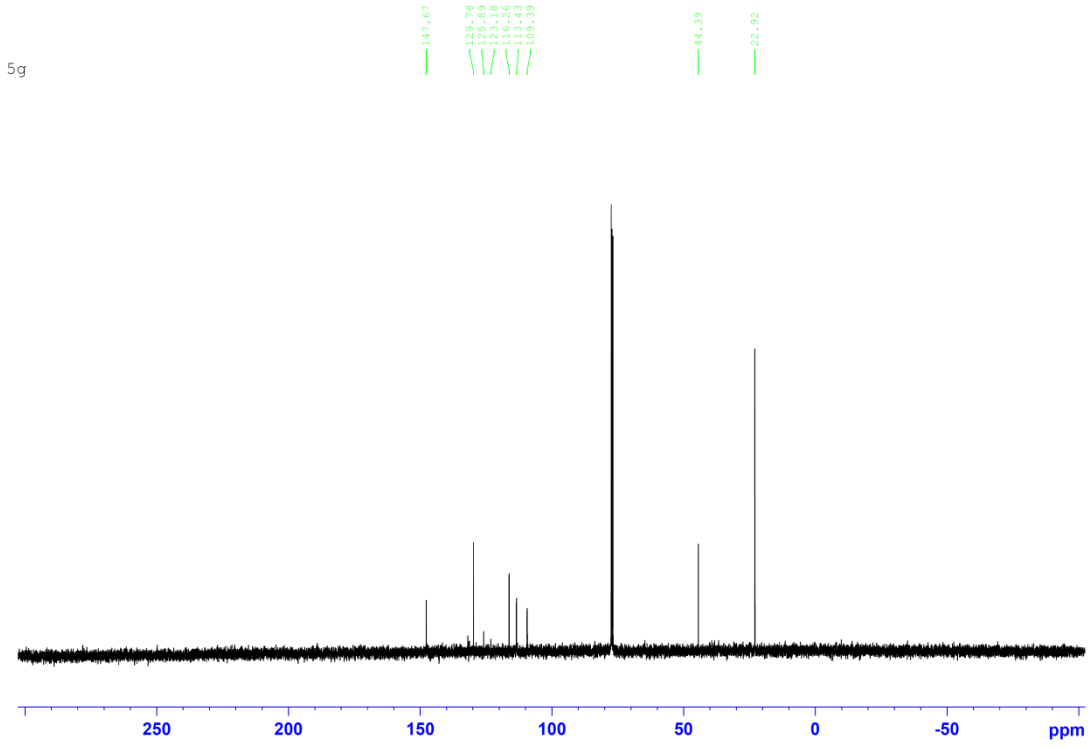

Figure A.47 ^{19}F NMR spectrum of **7g**

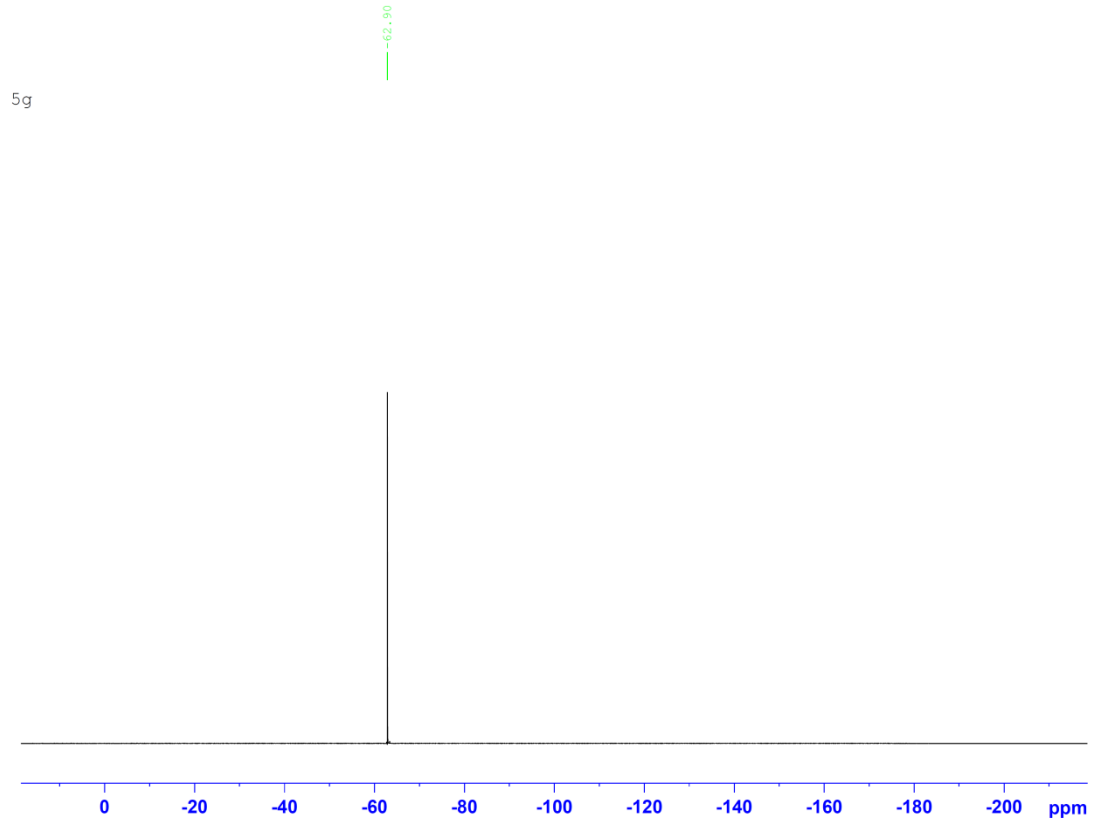

Figure A.48 ^{1}H NMR spectrum of **7h**

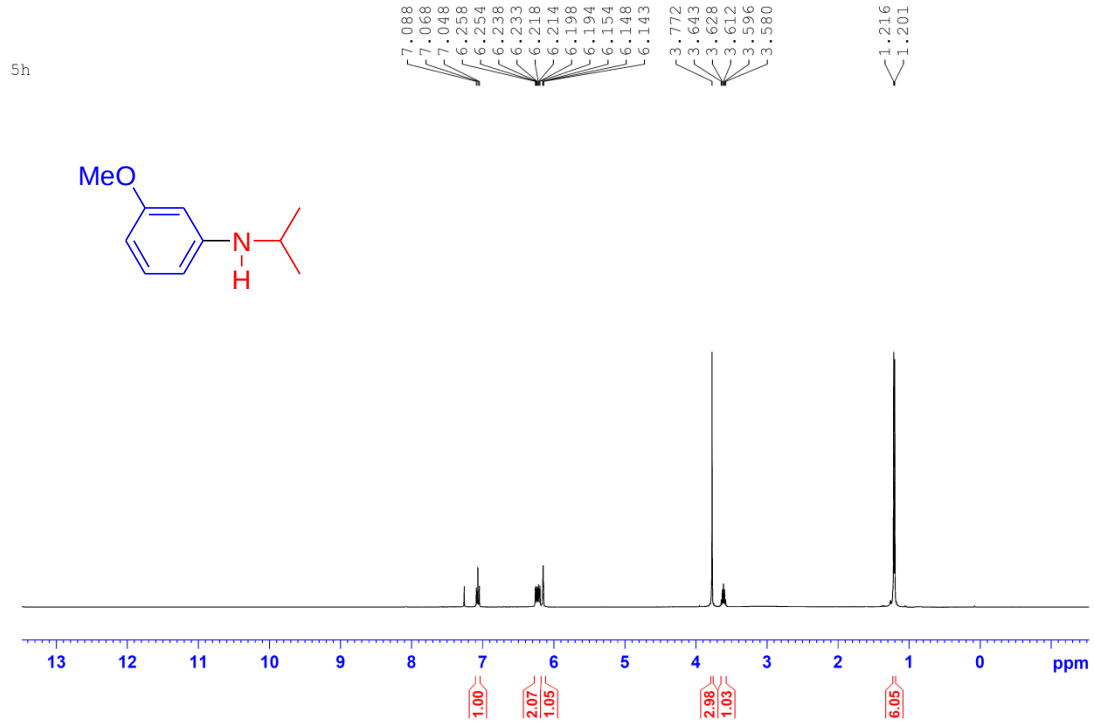

Figure A.49 ^{13}C NMR spectrum of **7h**

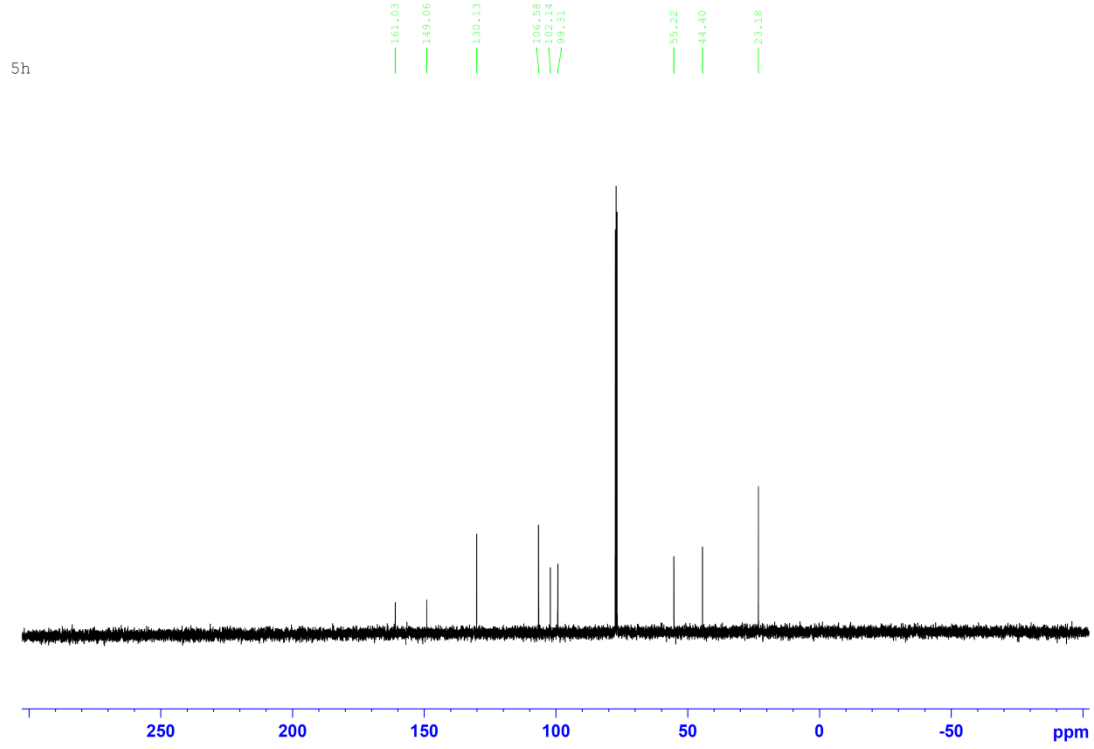

Figure A.50 ^{1}H NMR spectrum of **7i**

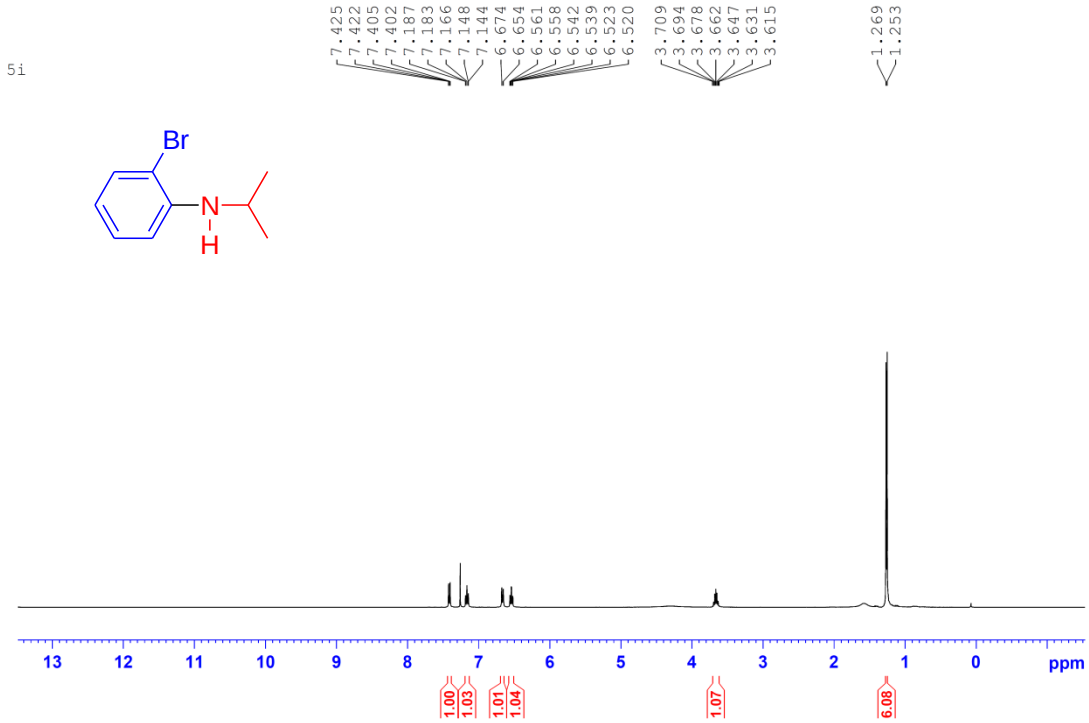

Figure A.51 ^{13}C NMR spectrum of **7i**

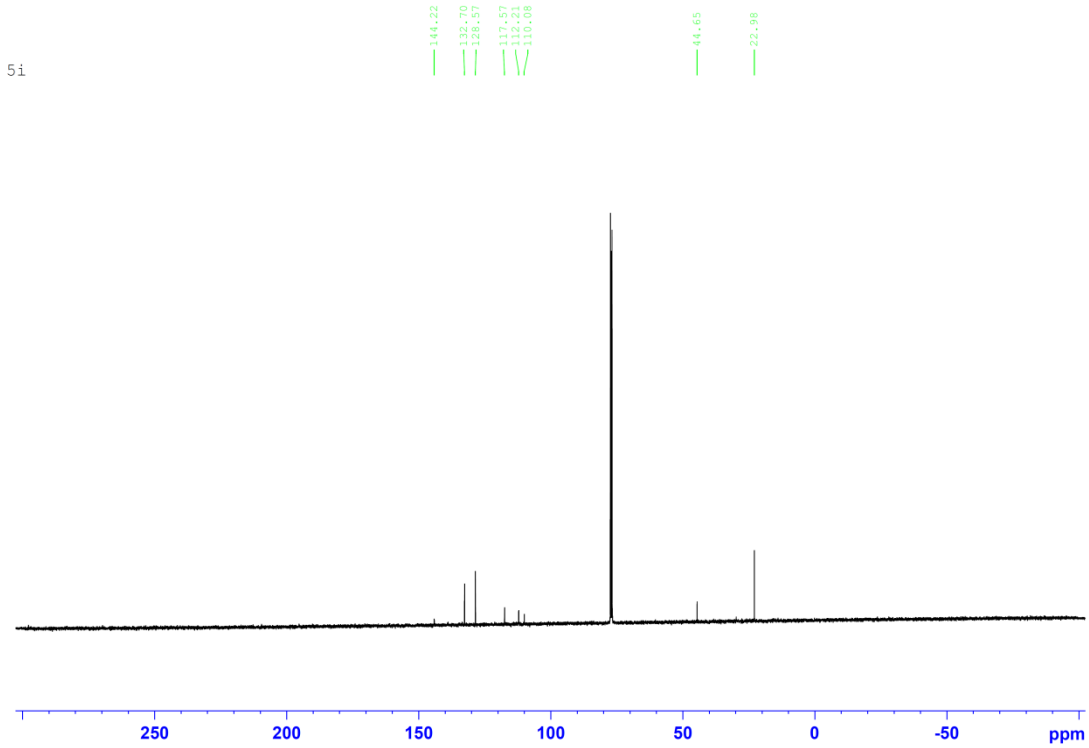

Figure A.52 ^{1}H NMR spectrum of **7j**

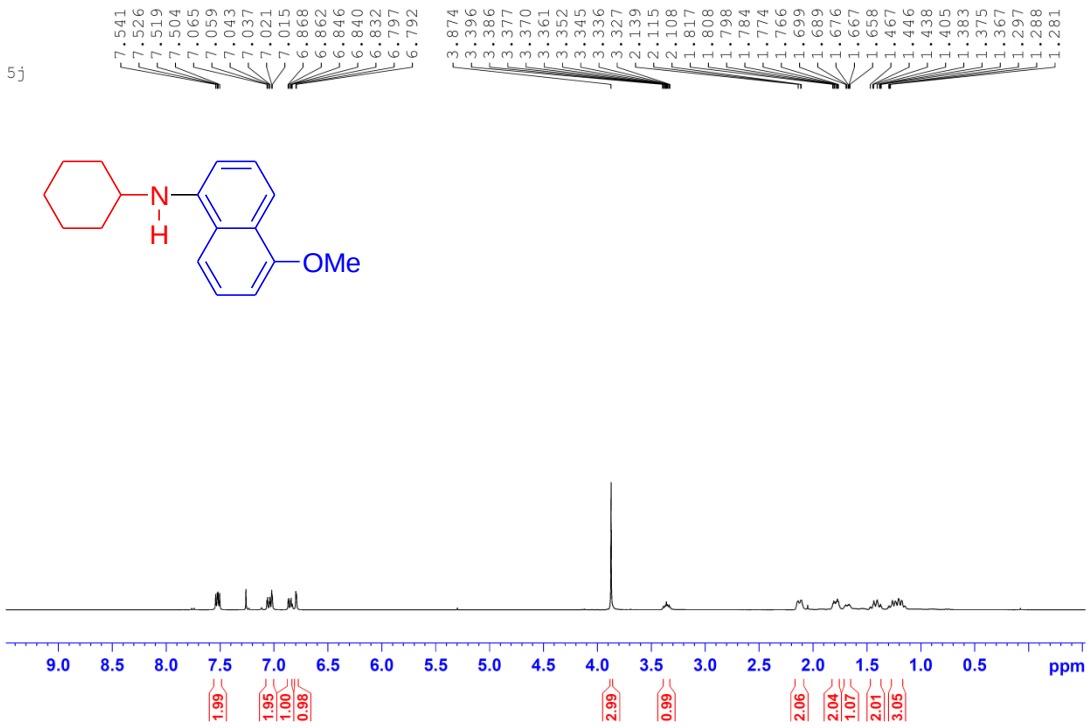

Figure A.53 ^{13}C NMR spectrum of **7j**

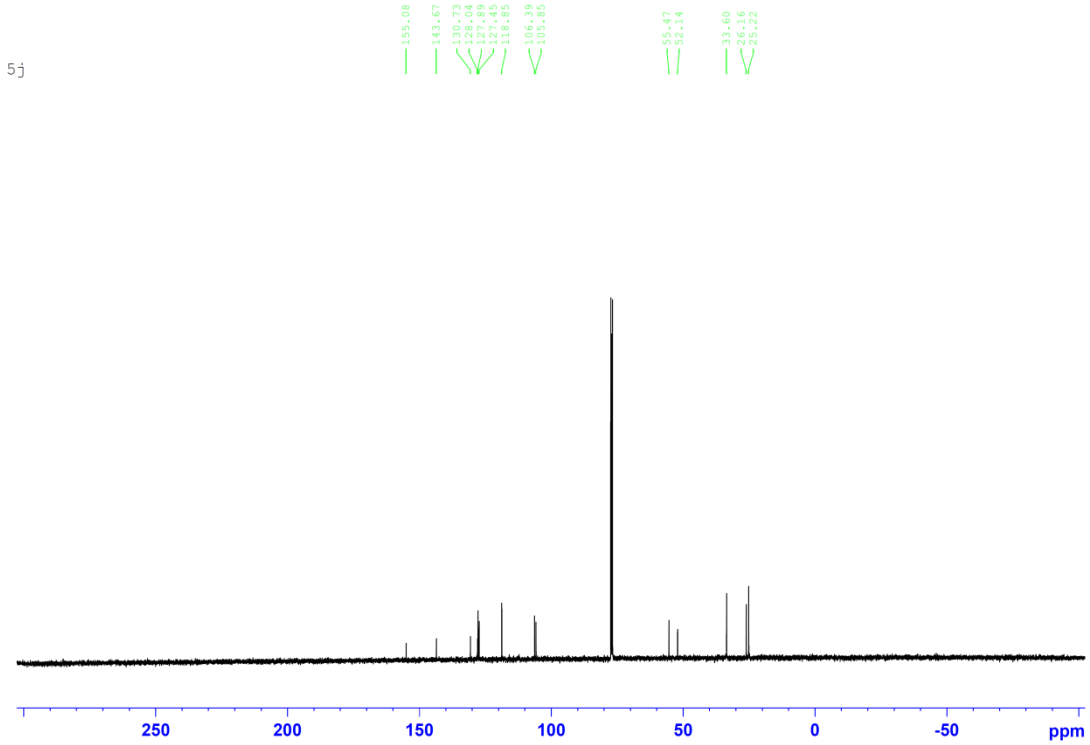

Figure A.54 ^{1}H NMR spectrum of **7k**

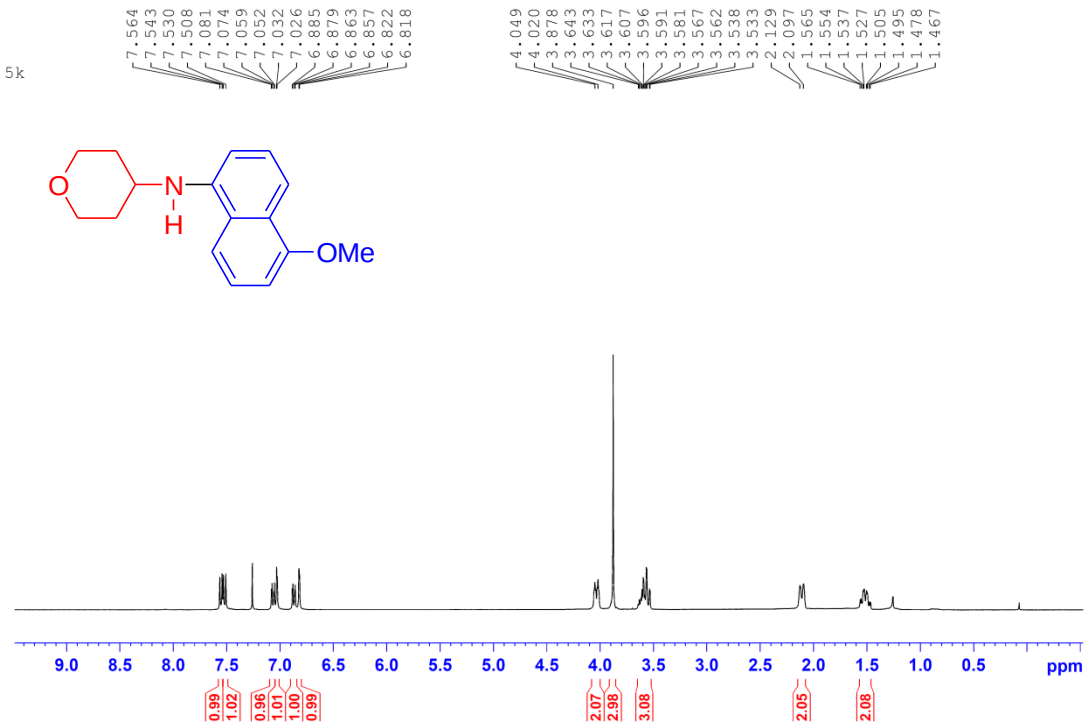

Figure A.55 ^{13}C NMR spectrum of **7k**

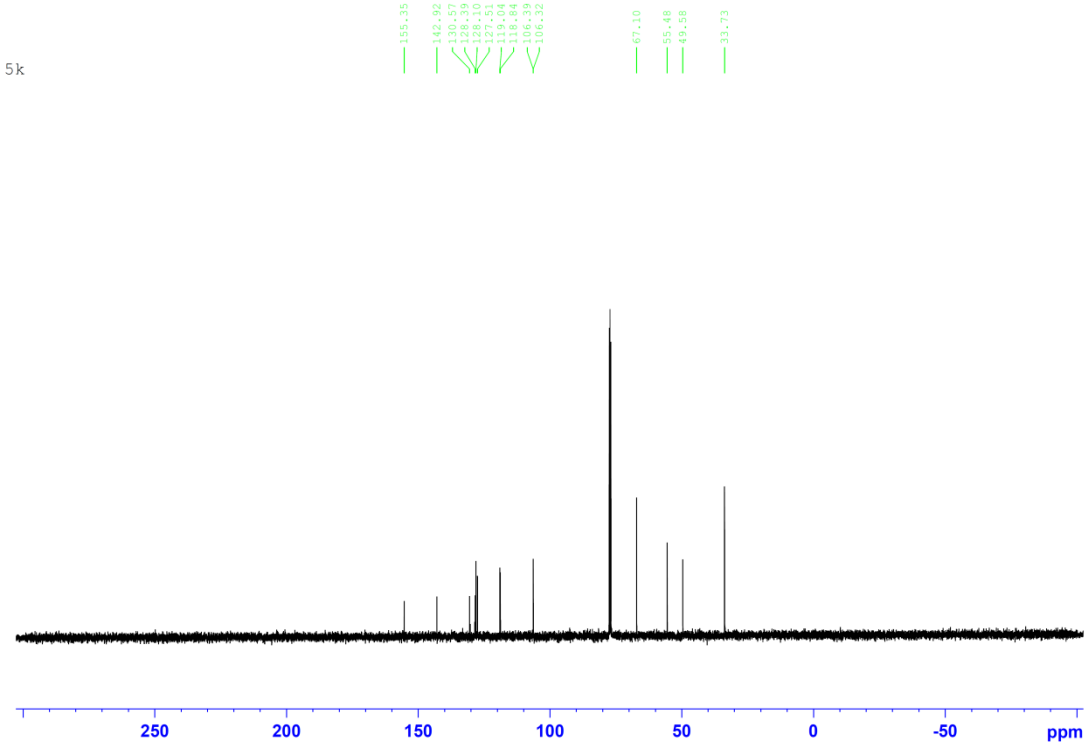

Figure A.56 ^{1}H NMR spectrum of **7l**

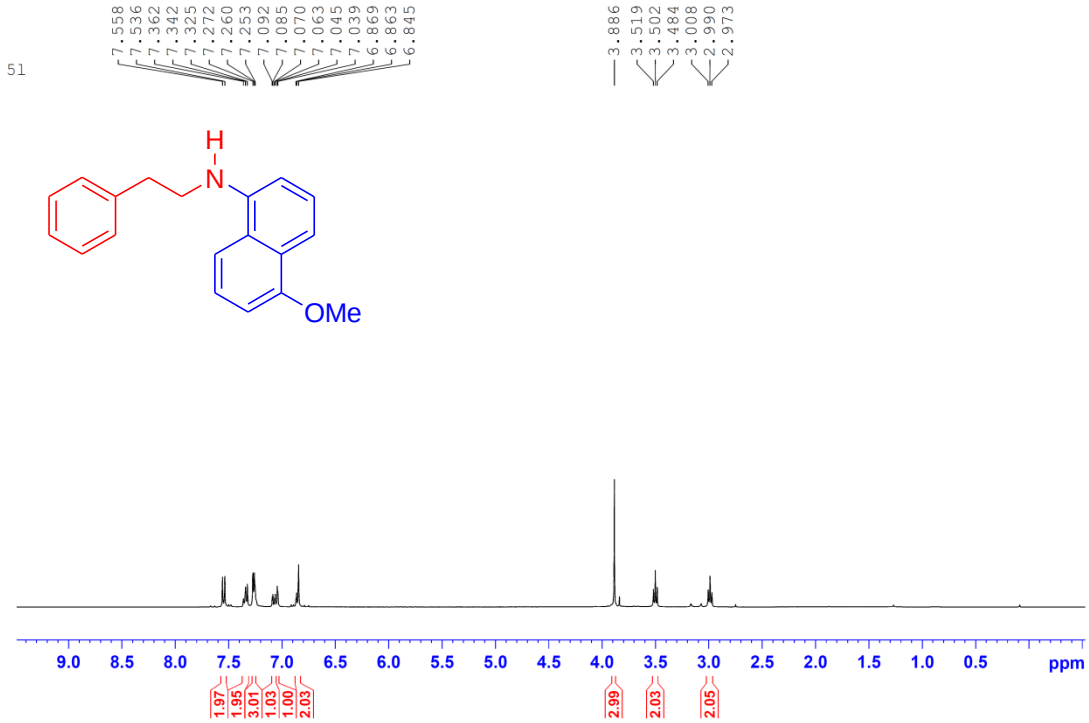

Figure A.57 ^{13}C NMR spectrum of **7l**

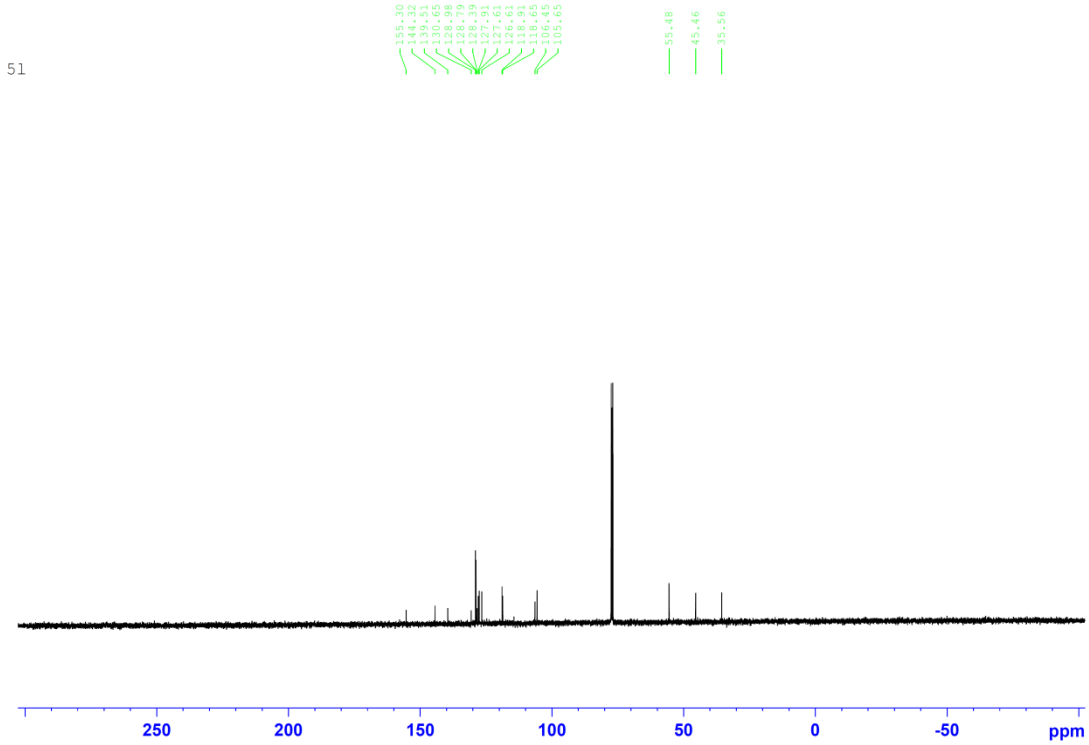

Figure A.58 ^{1}H NMR spectrum of **7m**

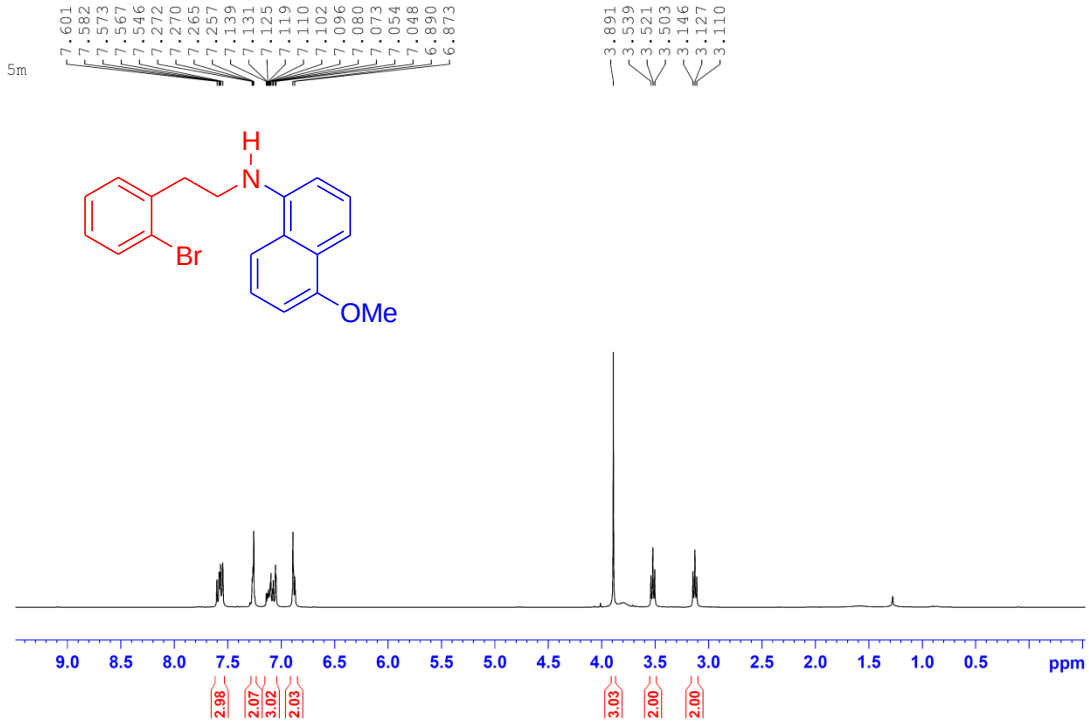

Figure A.59 ^{13}C NMR spectrum of **7m**

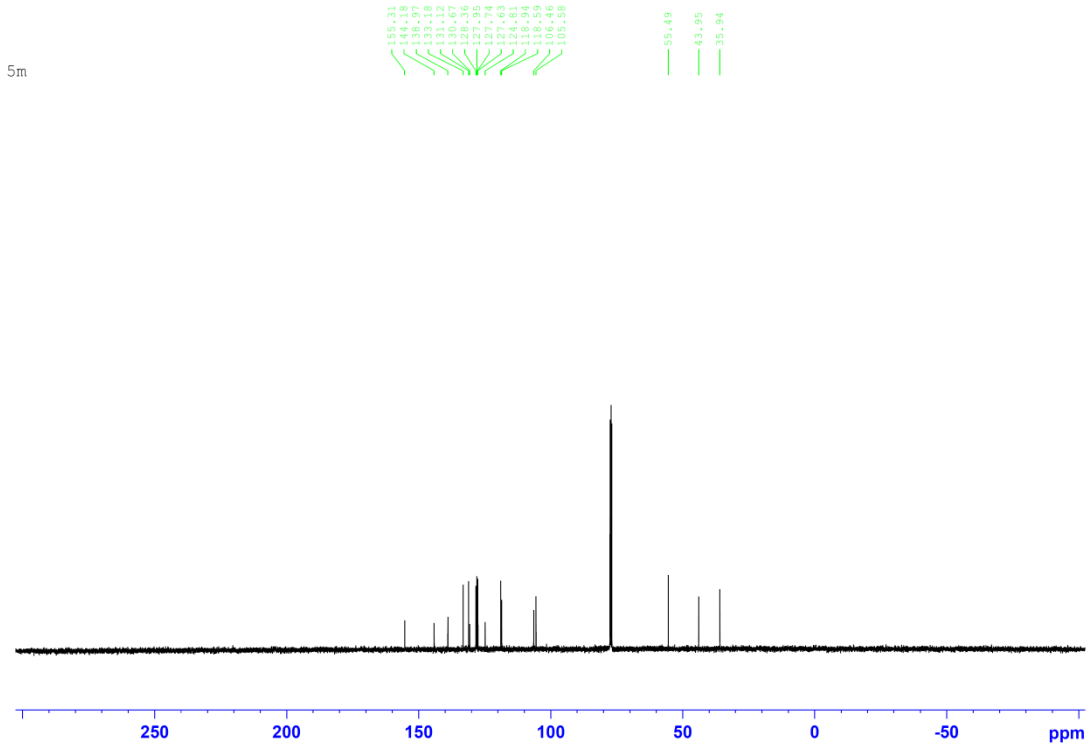

Figure A.60 ^{1}H NMR spectrum of **7n**

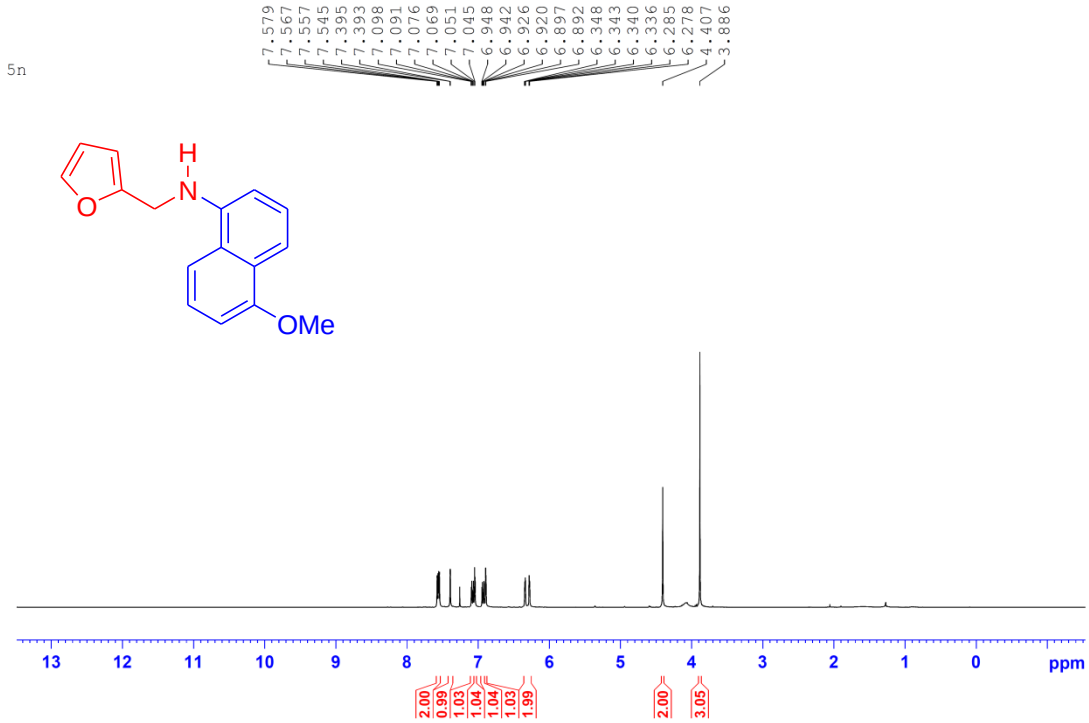

Figure A.61 ^{13}C NMR spectrum of **7n**

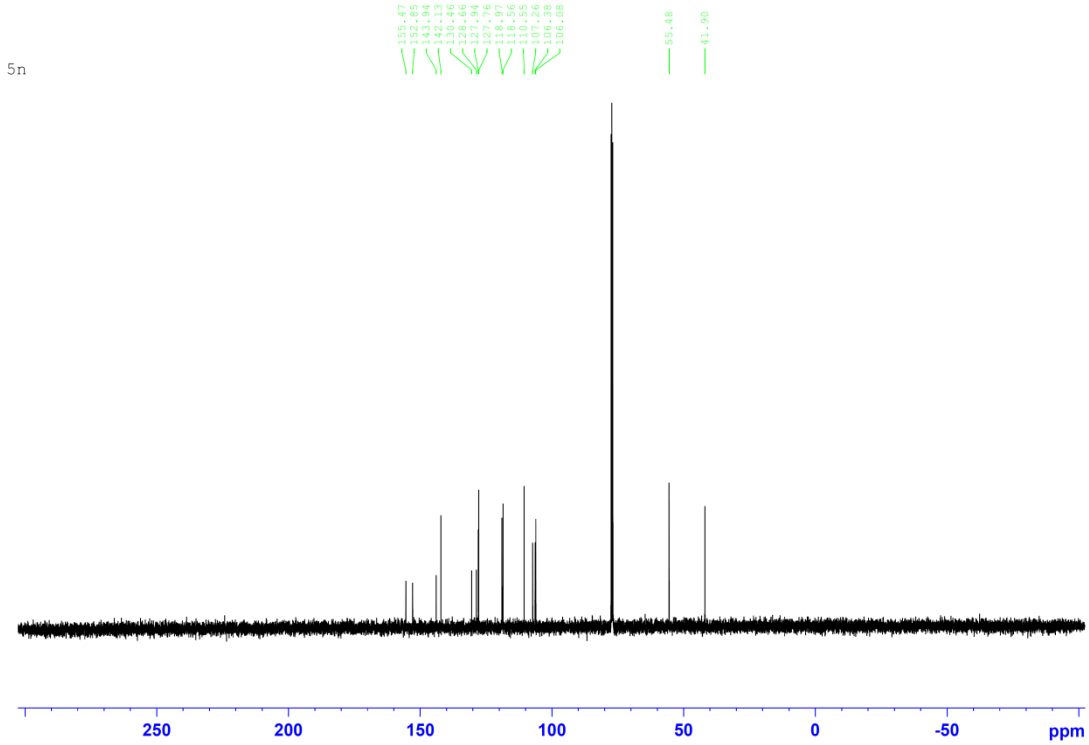

Figure A.62 ^{1}H NMR spectrum of **7o**

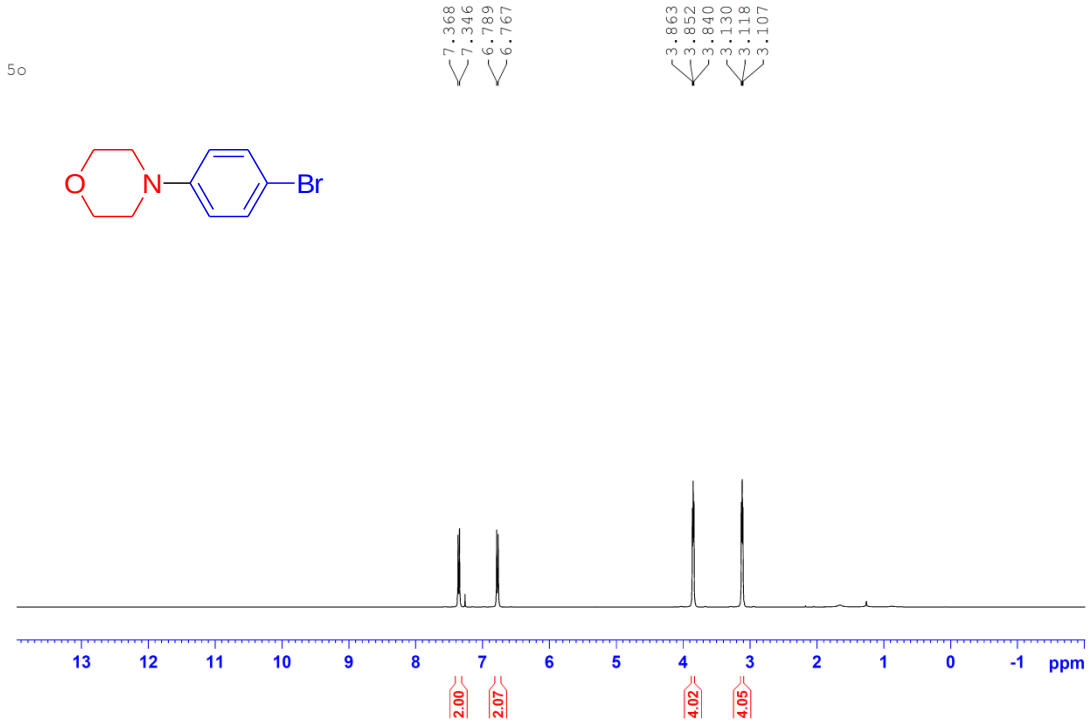

Figure A.63 ^{13}C NMR spectrum of **7o**

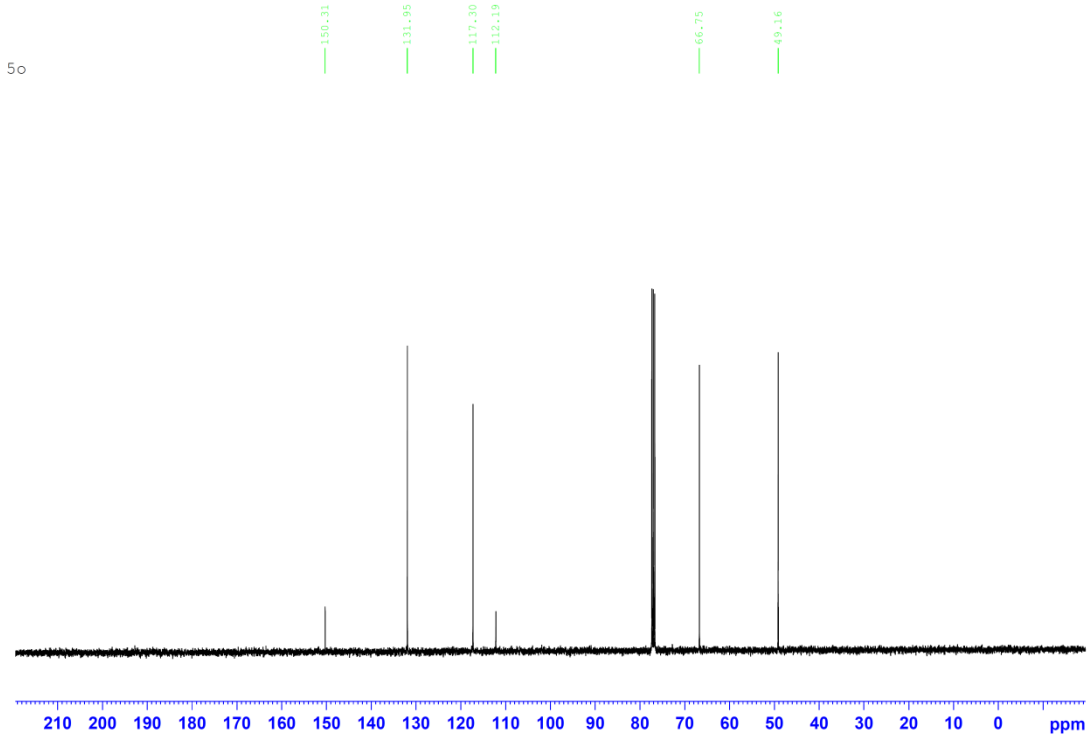

Figure A.64 ^{1}H NMR spectrum of **7p**

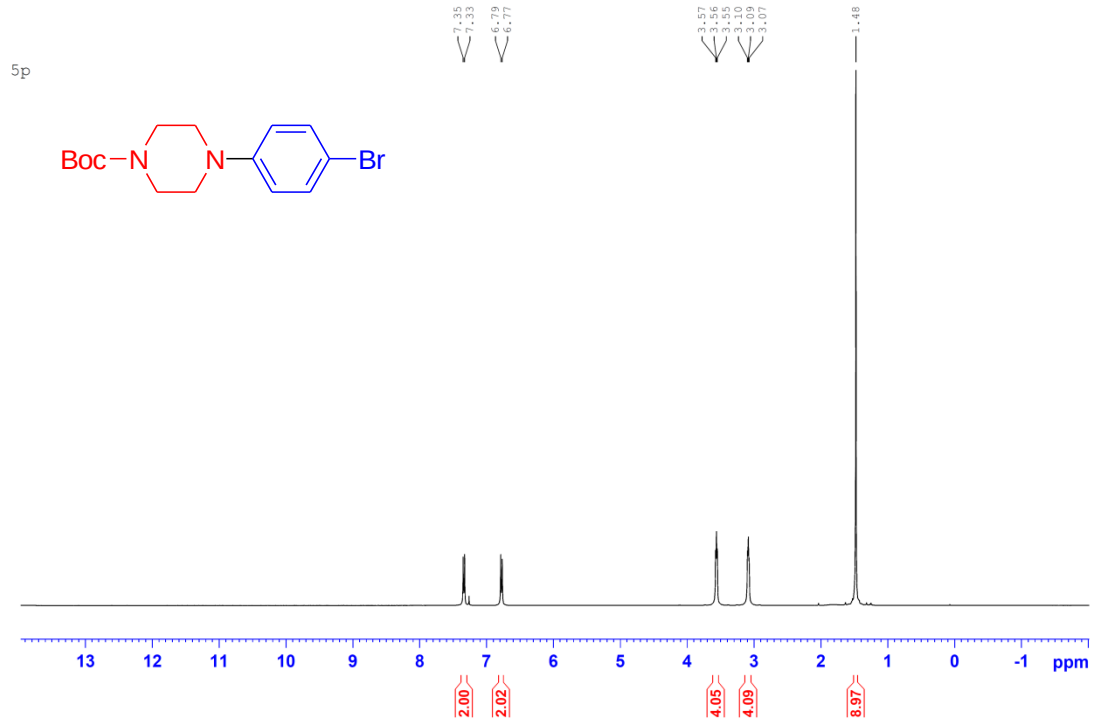

Figure A.65 ^{13}C NMR spectrum of **7p**

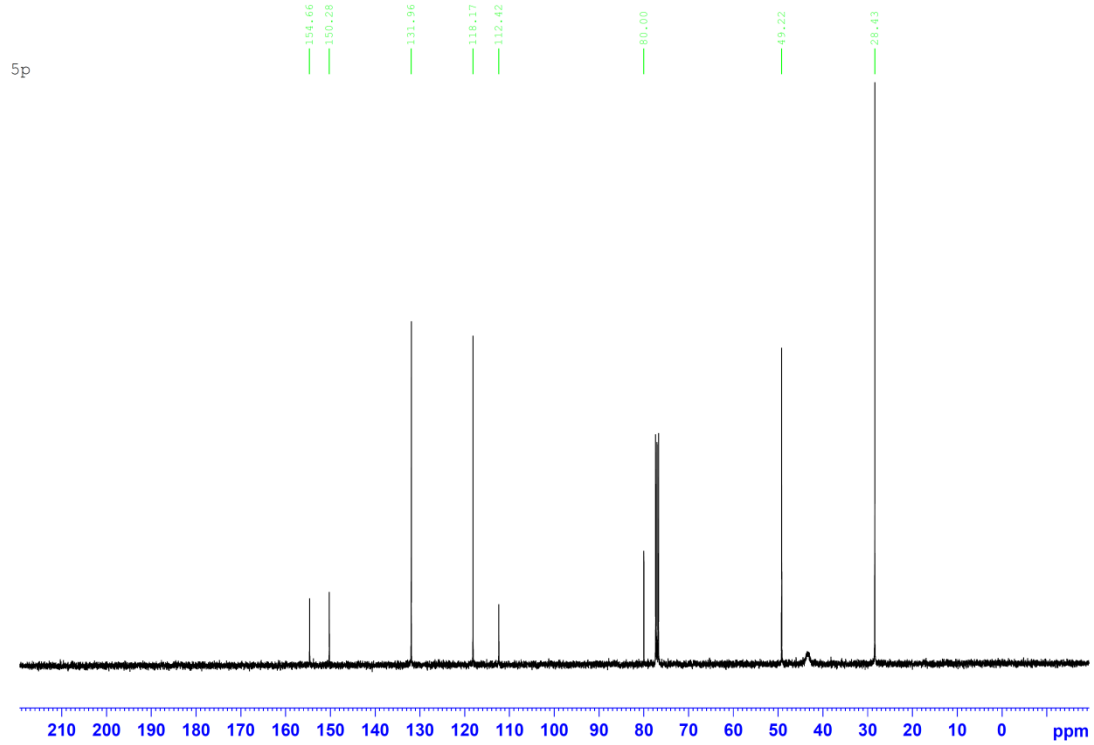

Figure A.66 ^{1}H NMR spectrum of **7q**

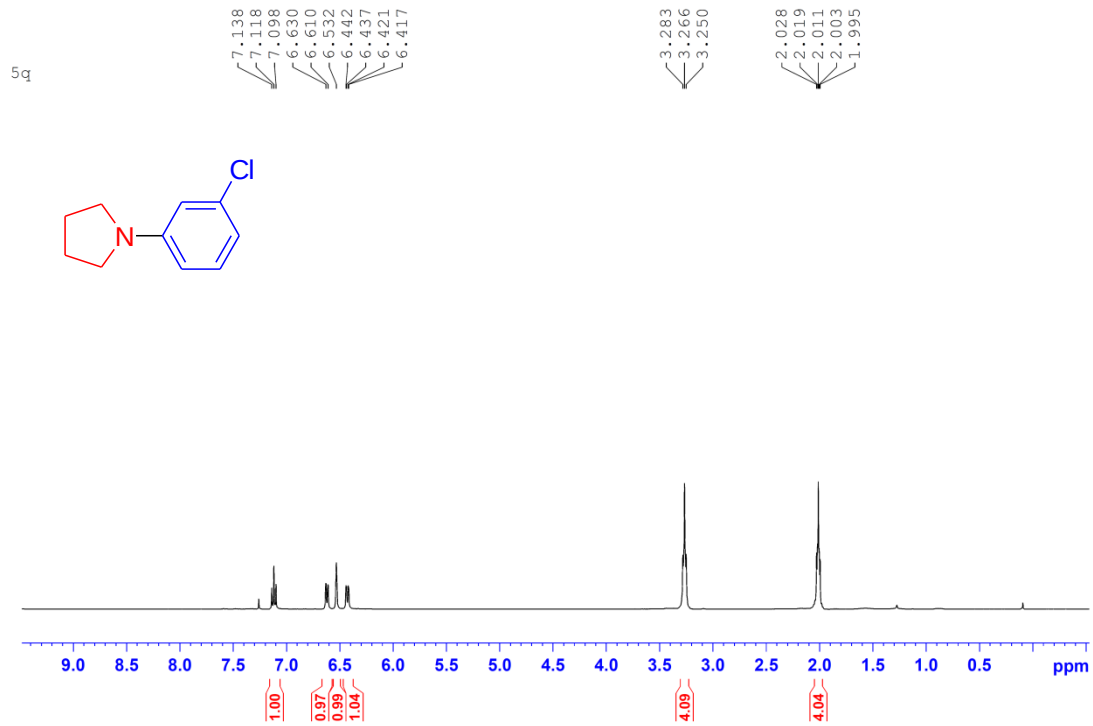

Figure A.67 ^{13}C NMR spectrum of **7q**

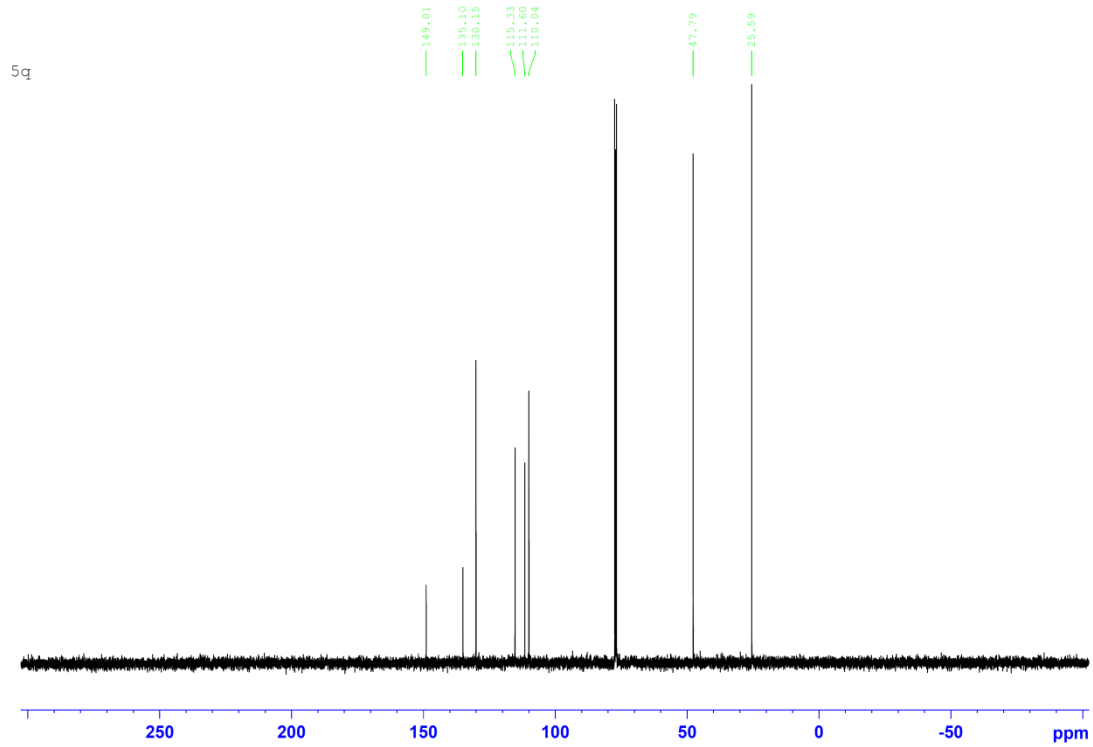

Figure A.68 ^{1}H NMR spectrum of **7r**

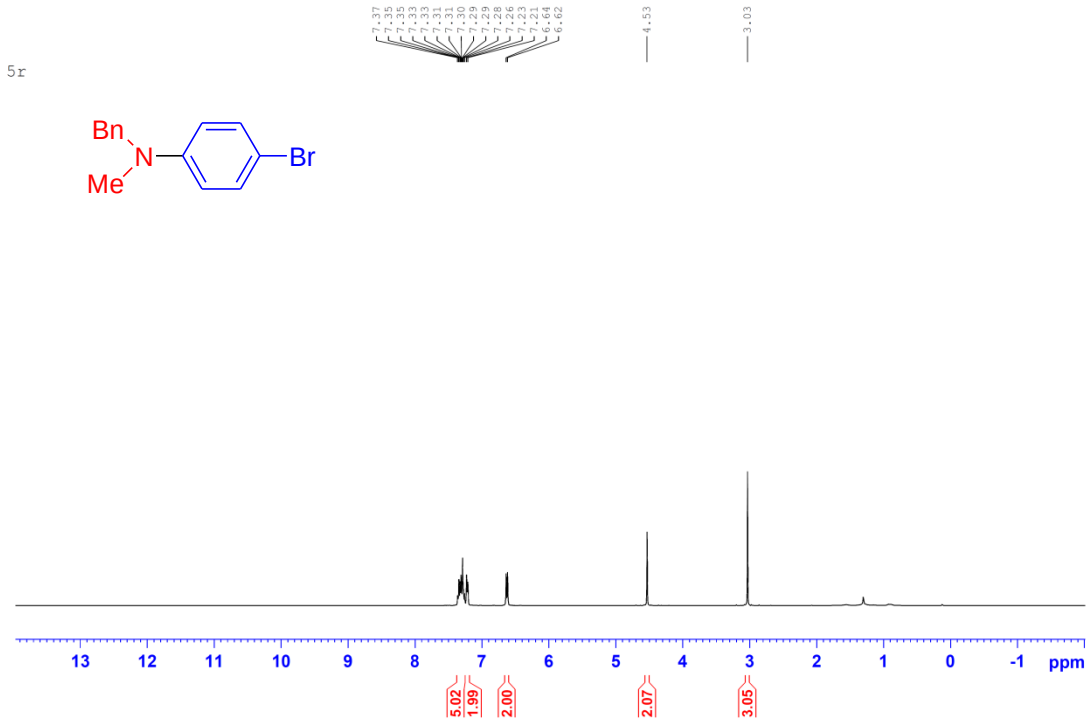

Figure A.69 ^{13}C NMR spectrum of **7r**

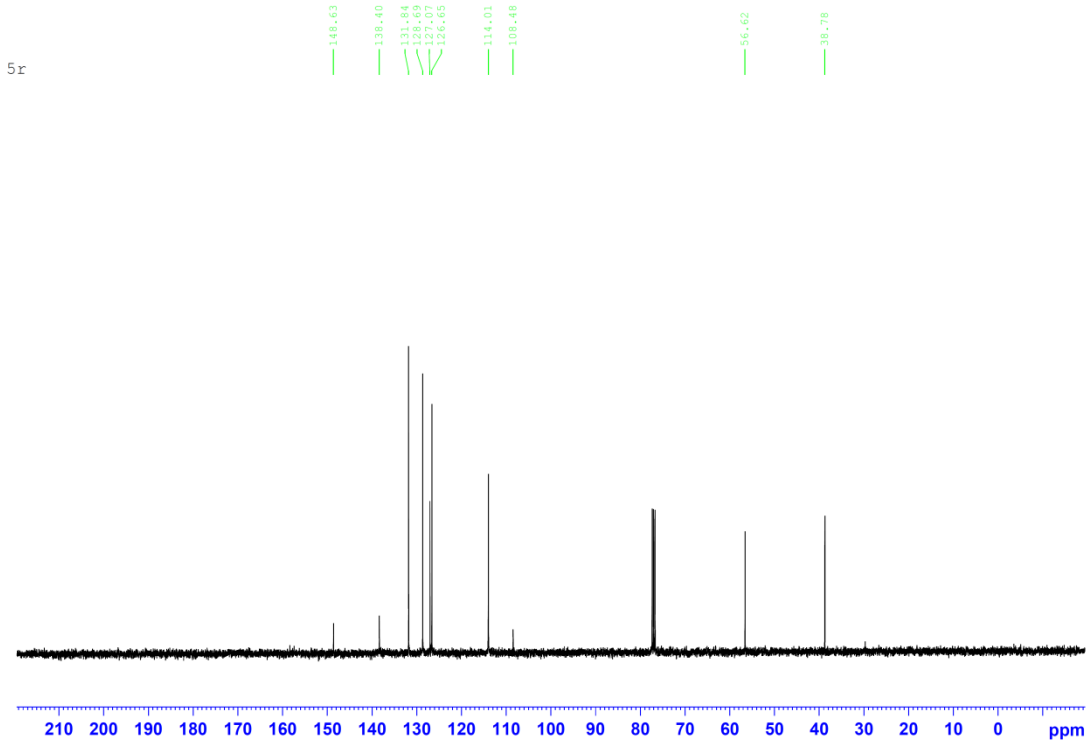

Figure A.70 ^{1}H NMR spectrum of **7s**

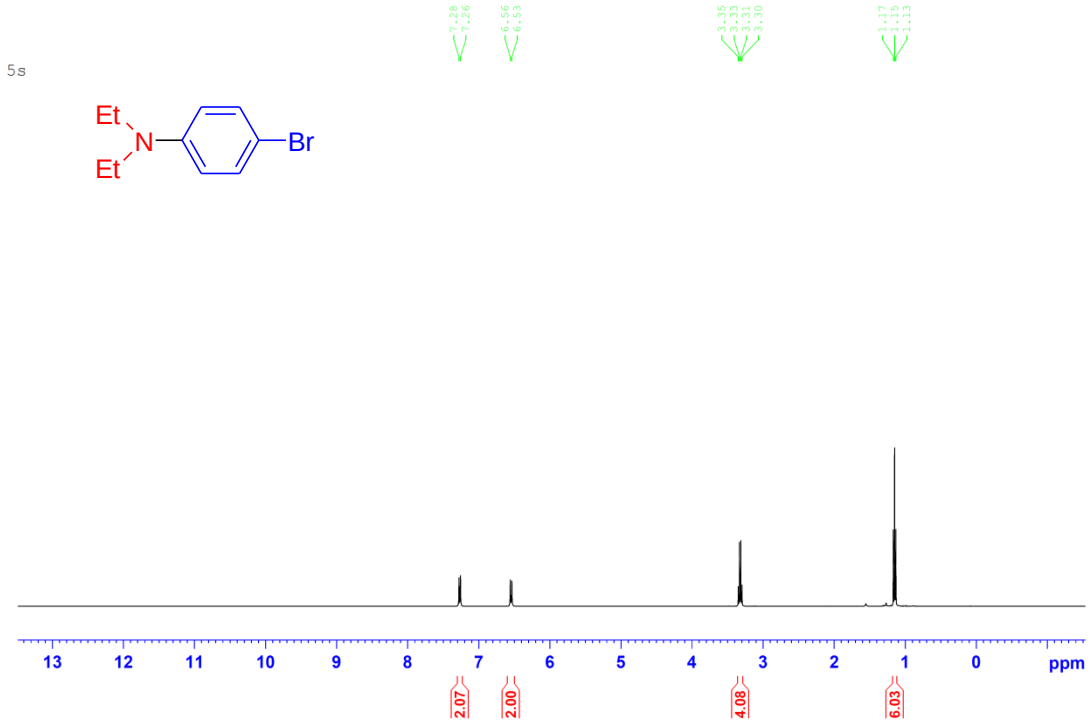

Figure A.71 ^{13}C NMR spectrum of **7s**

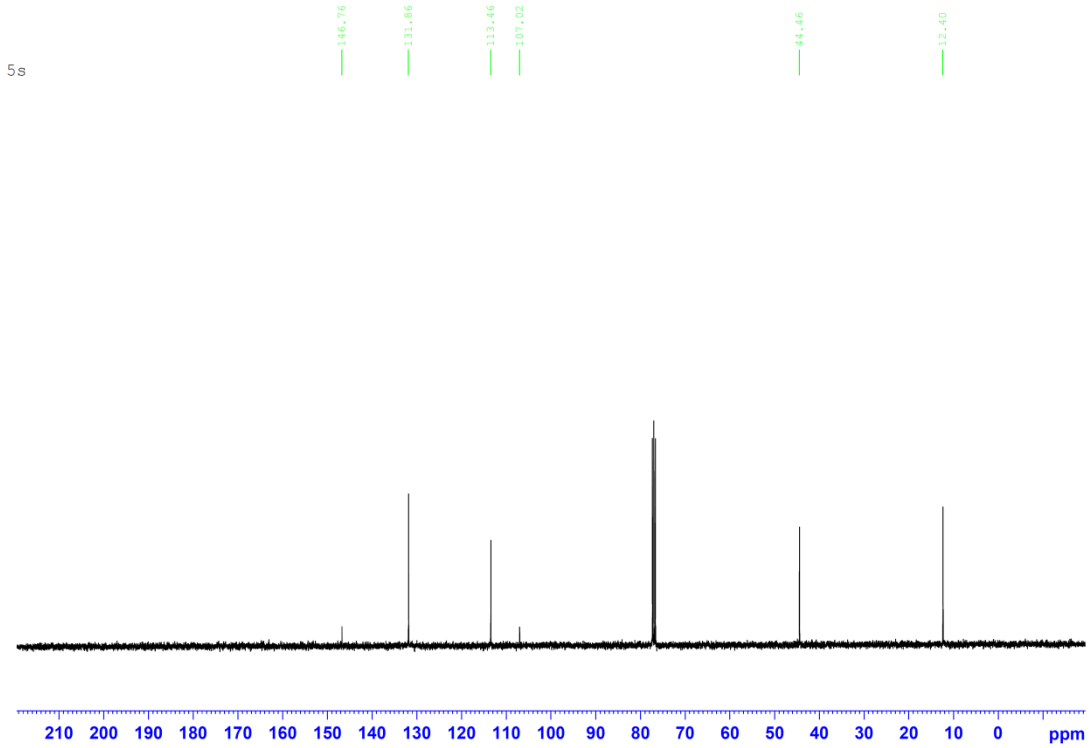

Figure A.72 ^{1}H NMR spectrum of **7t**

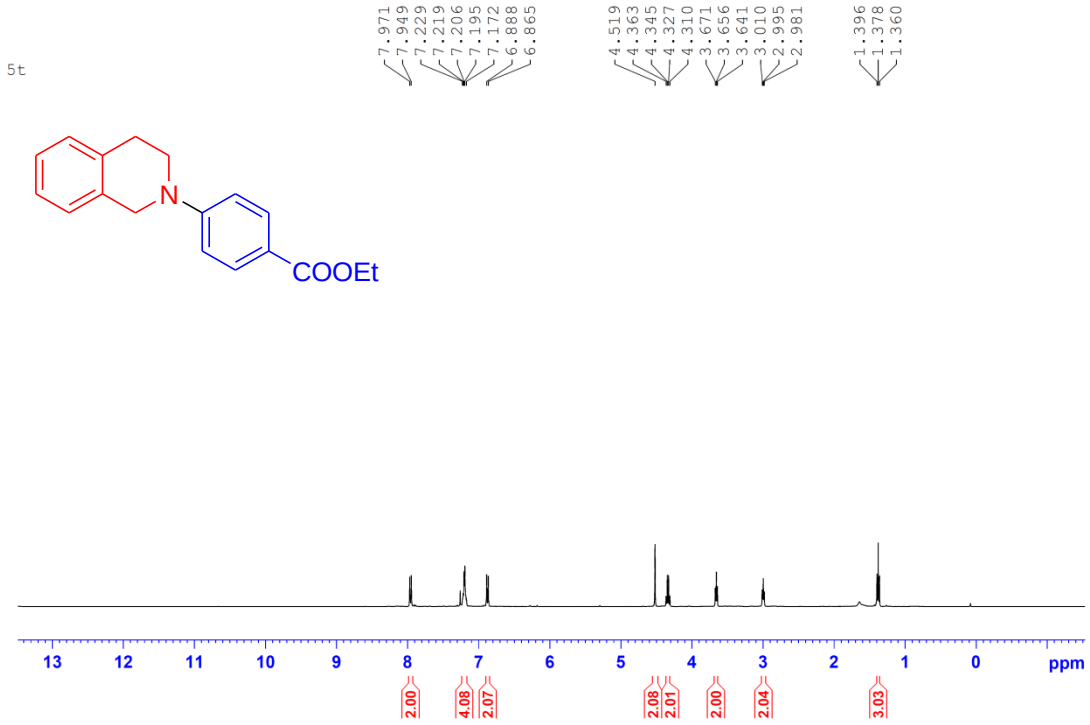

Figure A.73 ^{13}C NMR spectrum of **7t**

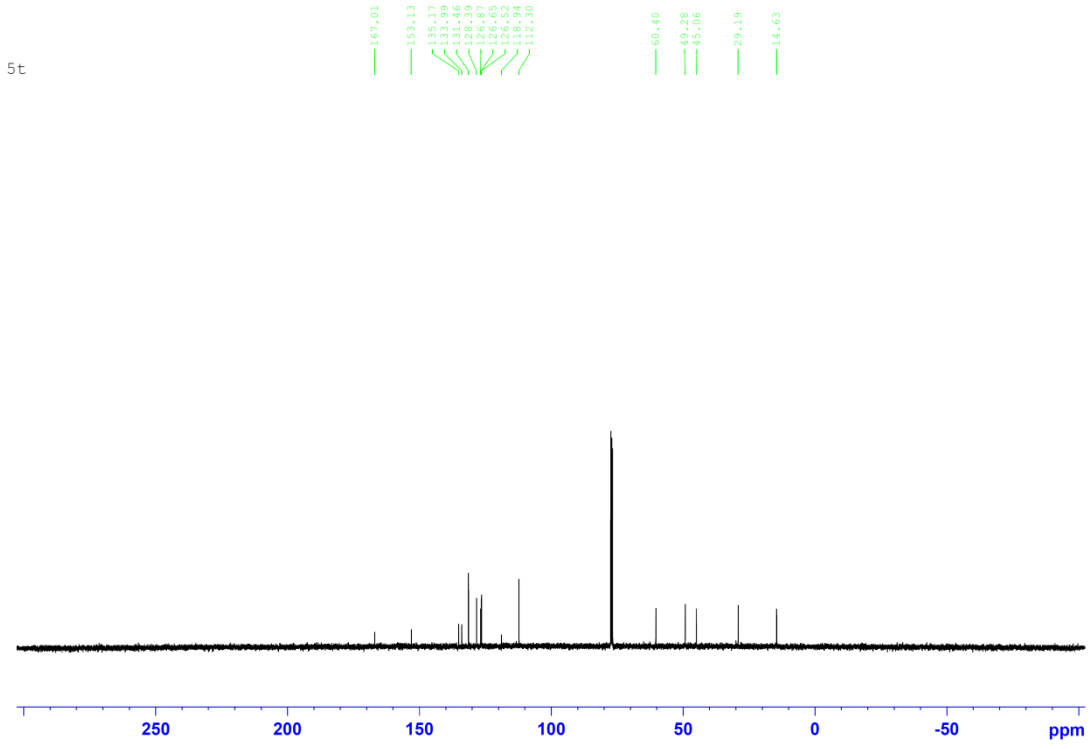

Figure A.74 ^{1}H NMR spectrum of **7u**

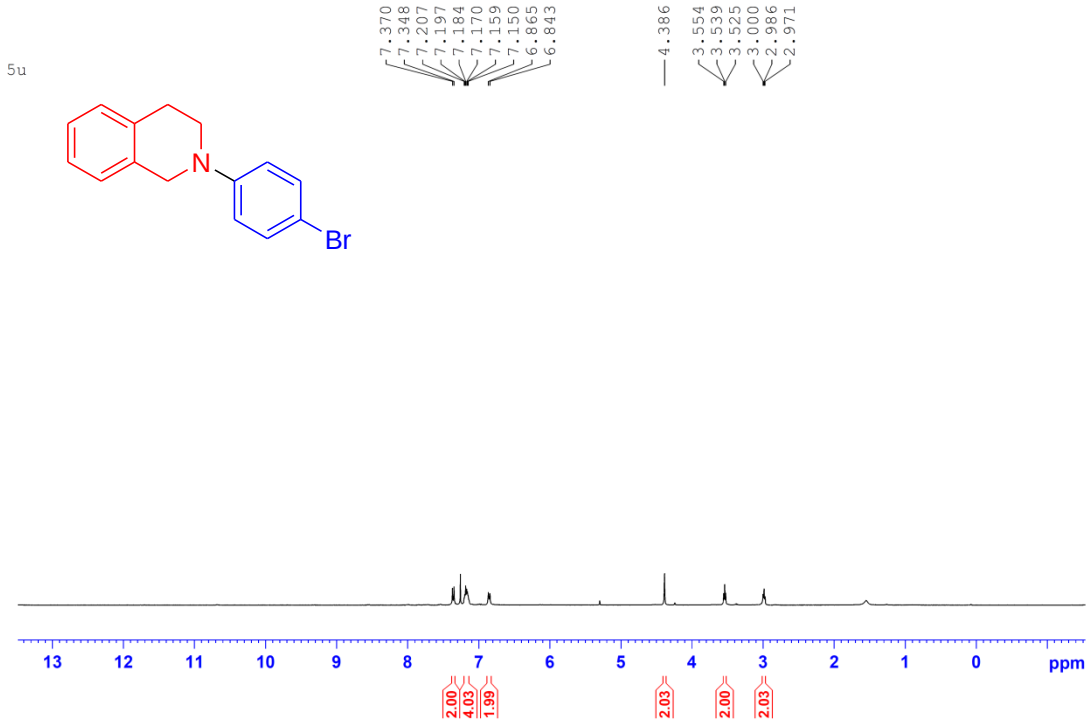

Figure A.75 ^{13}C NMR spectrum of **7u**

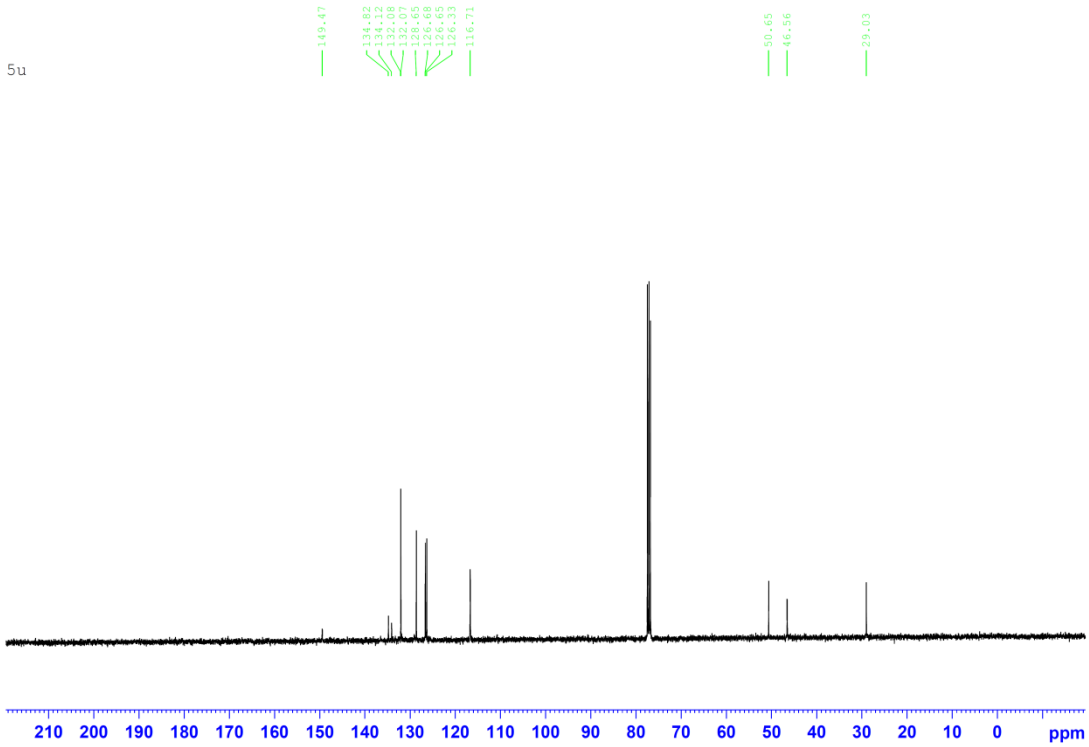

Figure A.76 ^{1}H NMR spectrum of **7v**

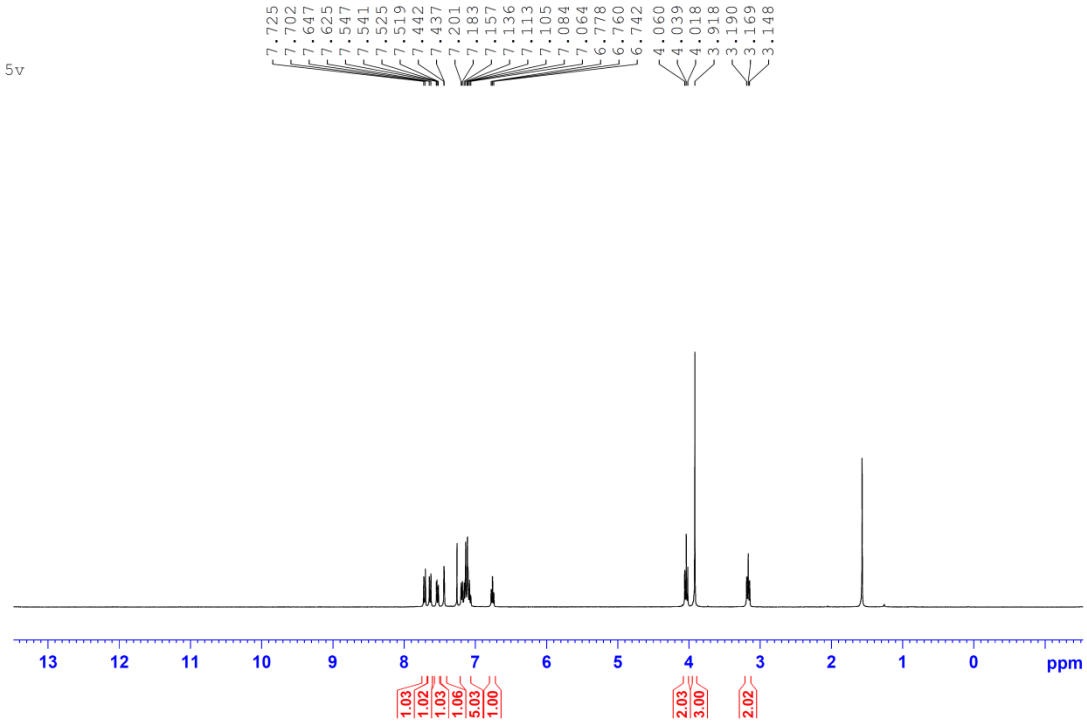

Figure A.77 ^{13}C NMR spectrum of **7v**

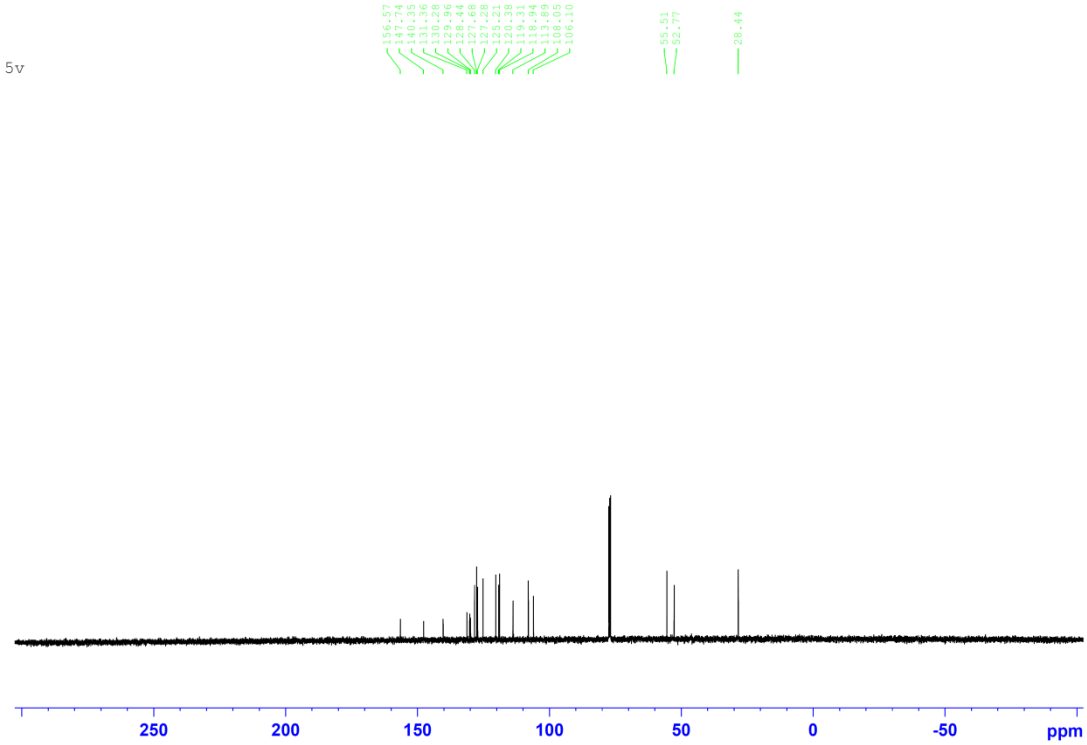

Figure A.78 ^{1}H NMR spectrum of **8a**

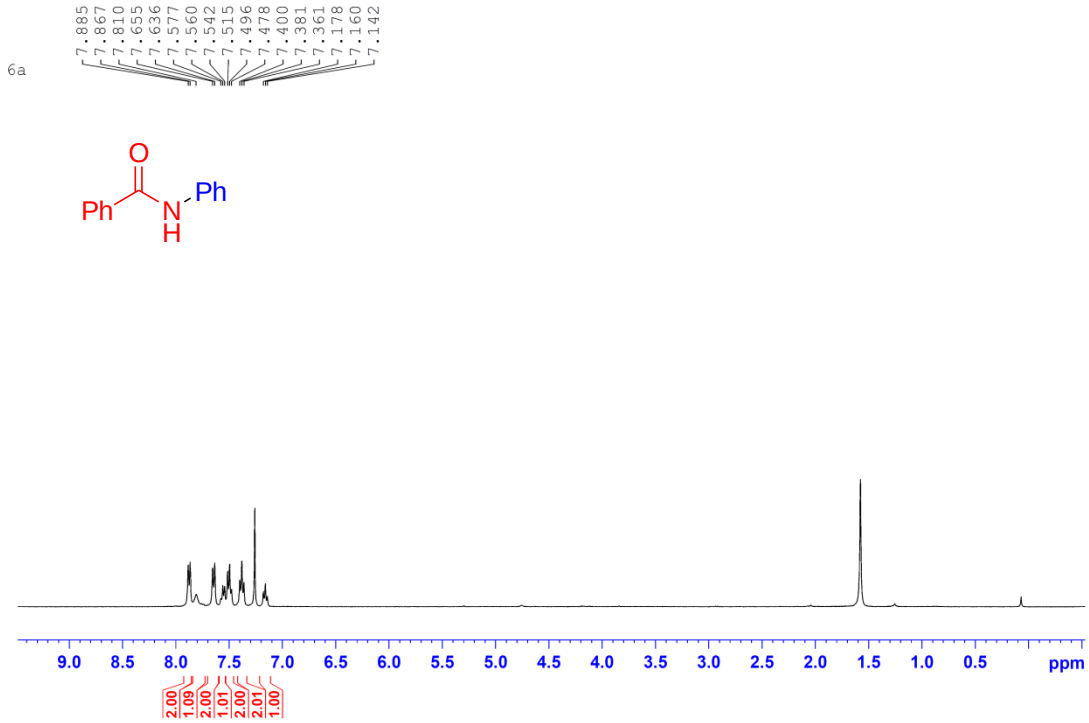

Figure A.79 ^{13}C NMR spectrum of **8a**

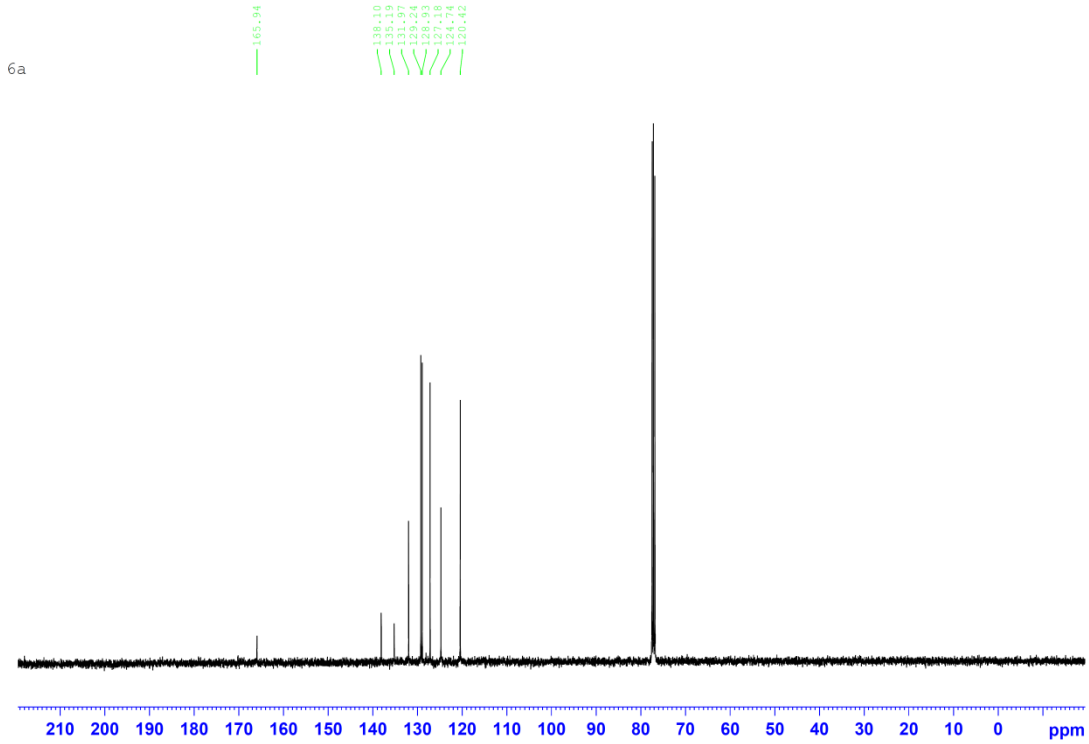

Figure A.80 ^{1}H NMR spectrum of **8b**

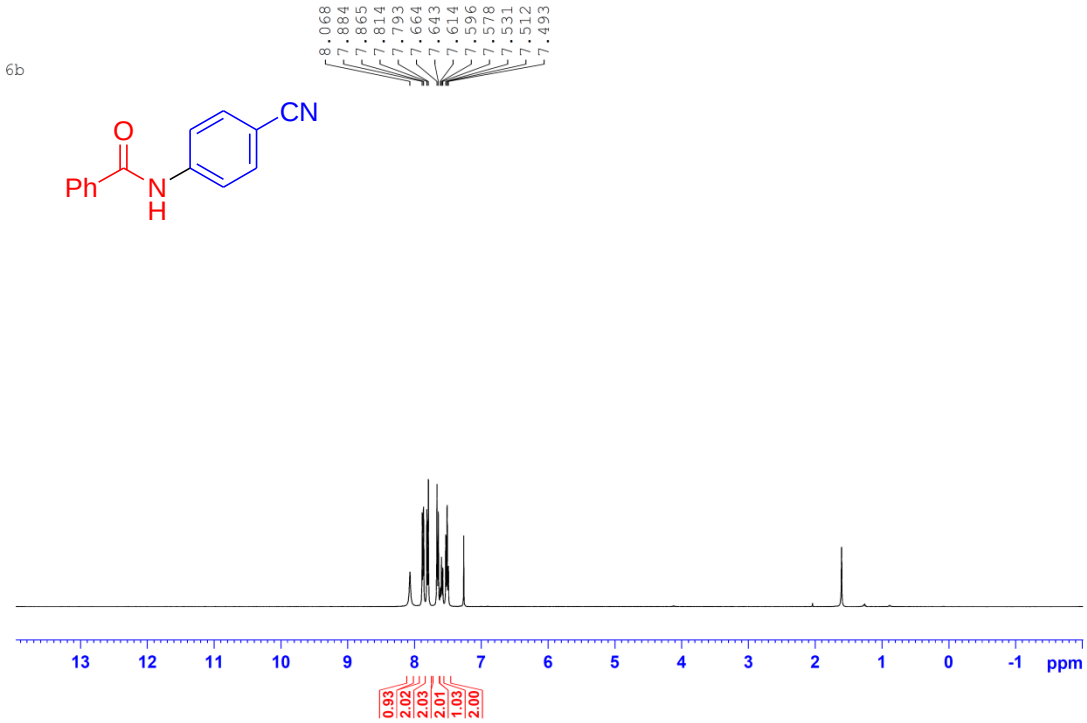

Figure A.81 ^{13}C NMR spectrum of **8b**

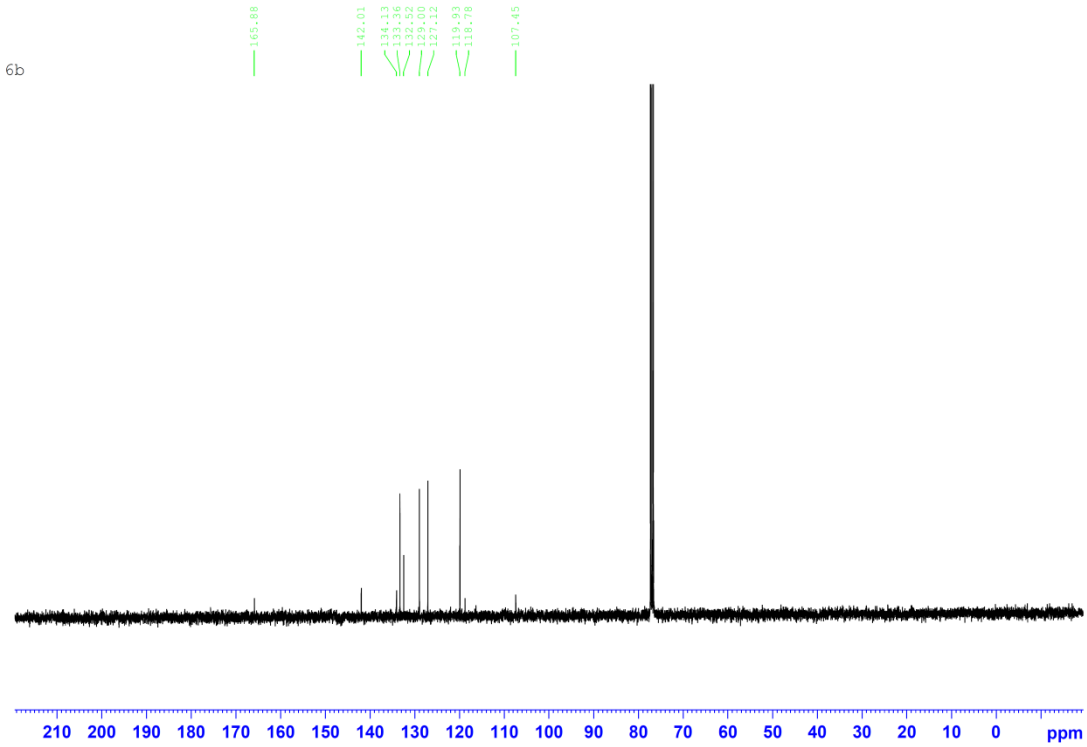

Figure A.82 ^{1}H NMR spectrum of **8c**

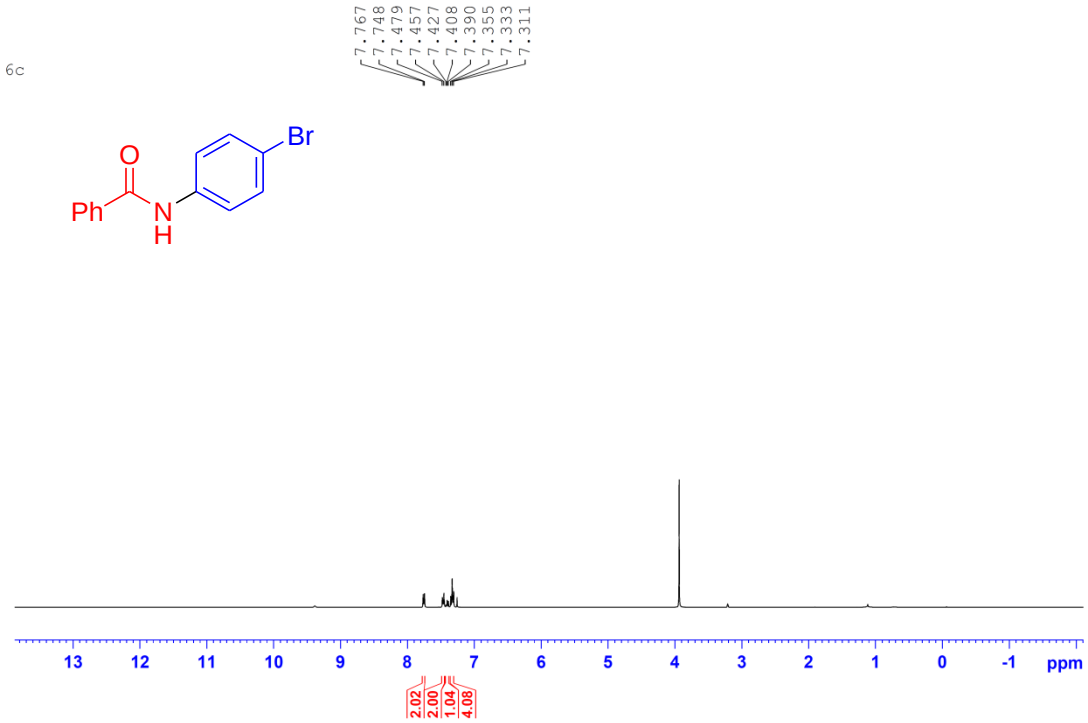

Figure A.83 ^{13}C NMR spectrum of **8c**

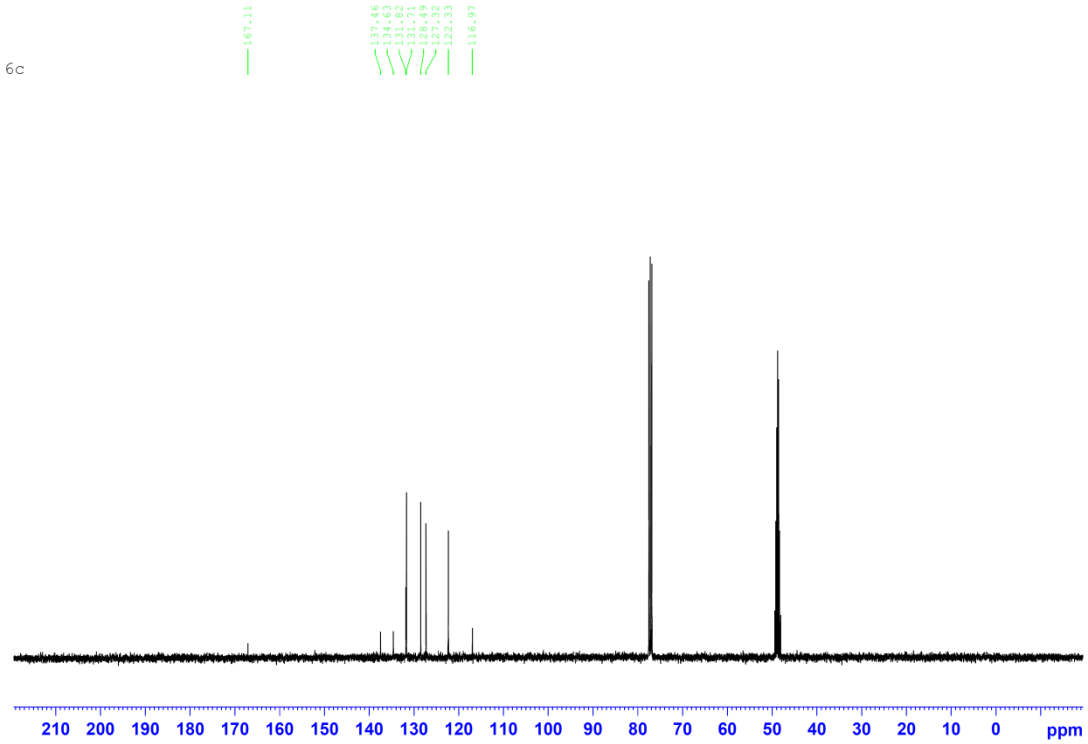

Figure A.84 ^{1}H NMR spectrum of **8d**

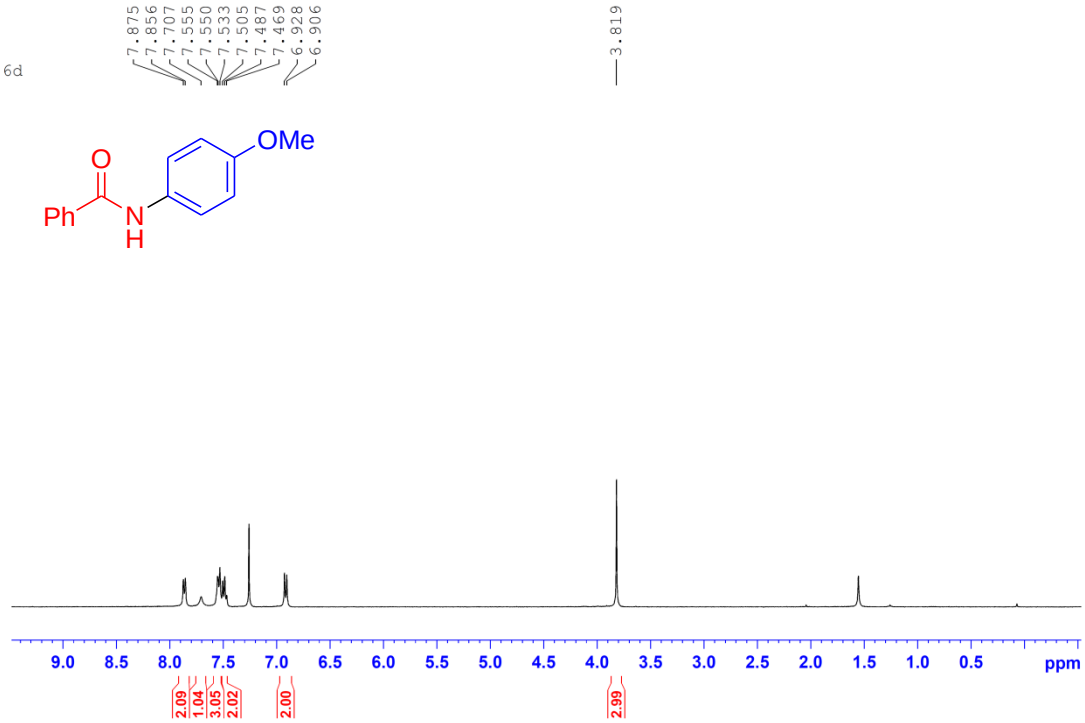

Figure A.85 ^{13}C NMR spectrum of **8d**

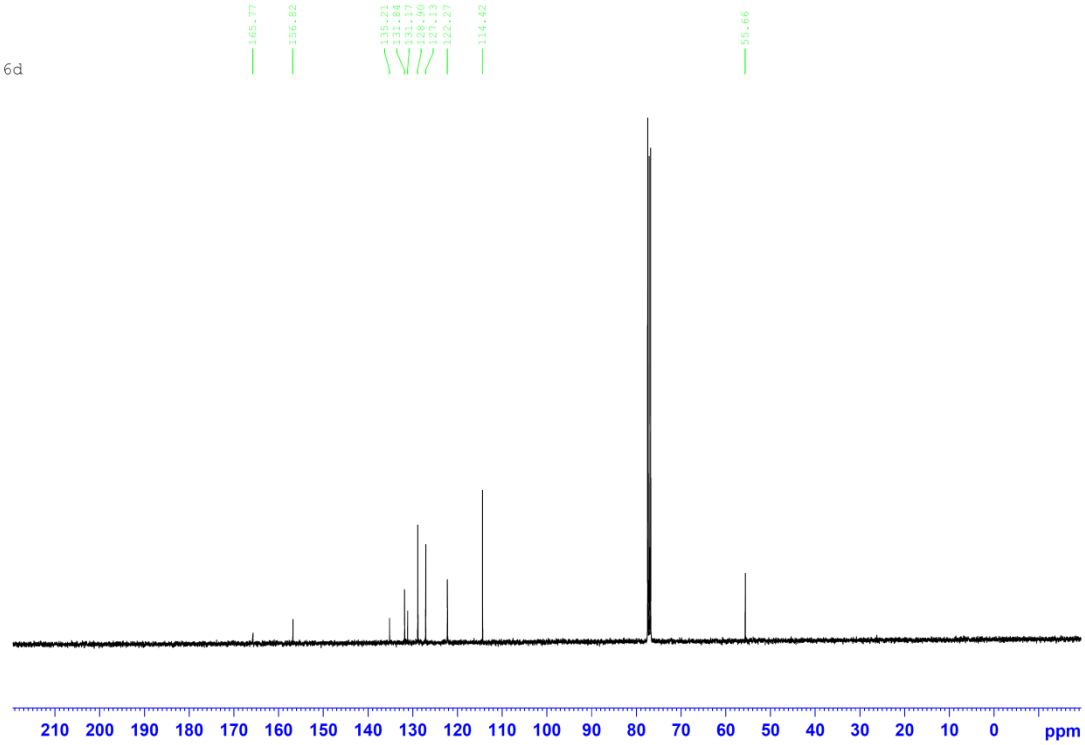

Figure A.86 ^{1}H NMR spectrum of **8e**

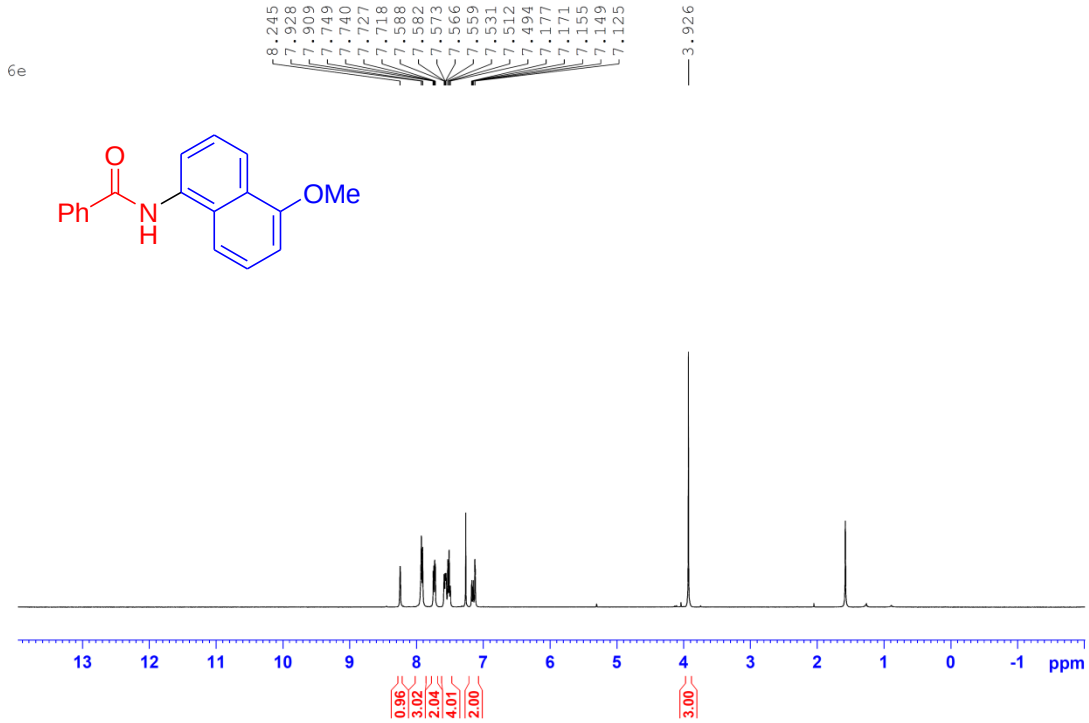

Figure A.87 ^{13}C NMR spectrum of **8e**

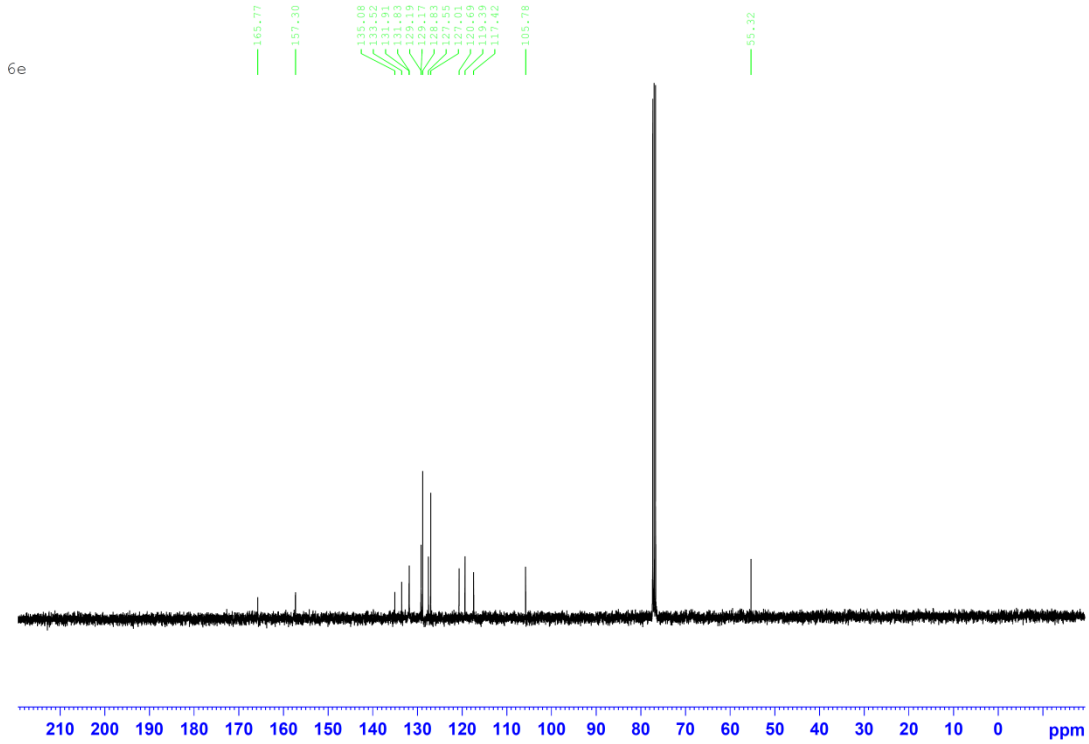

Figure A.88 ^{1}H NMR spectrum of **8f**

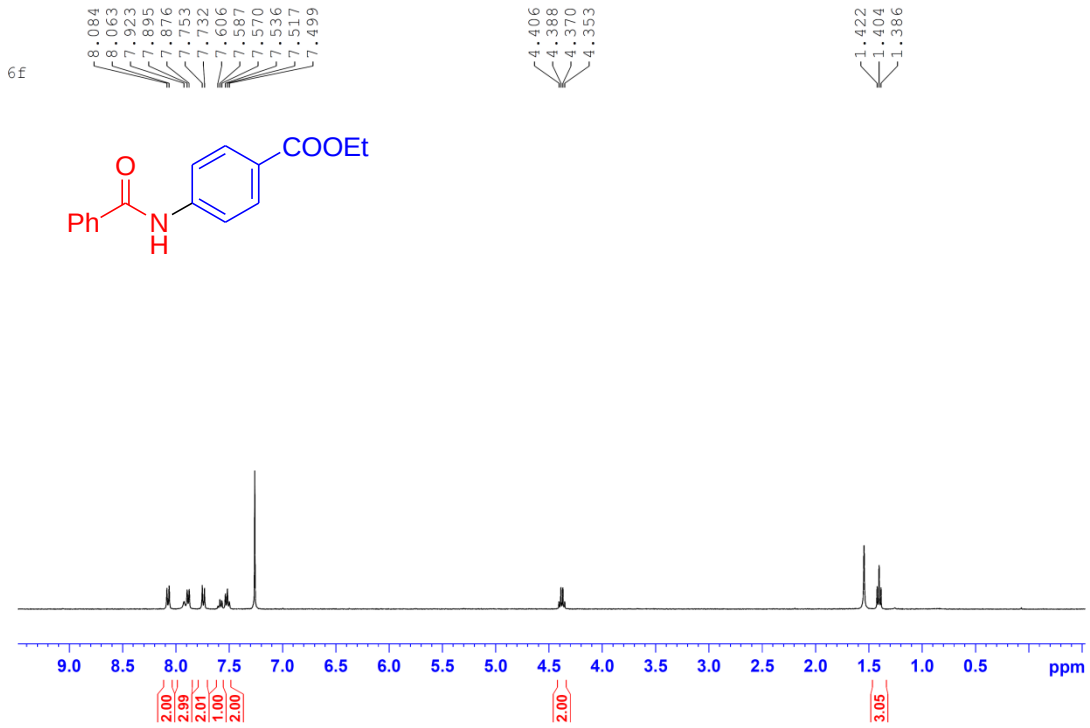

Figure A.89 ^{13}C NMR spectrum of **8f**

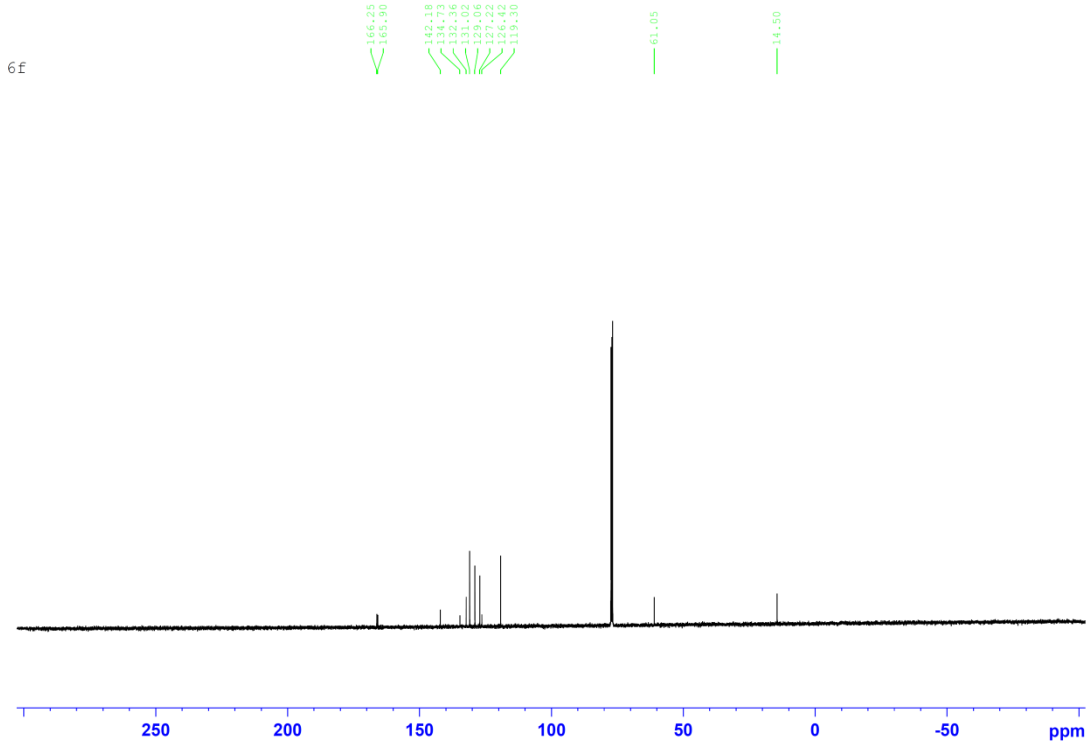

Figure A.90 ^{1}H NMR spectrum of **8g**

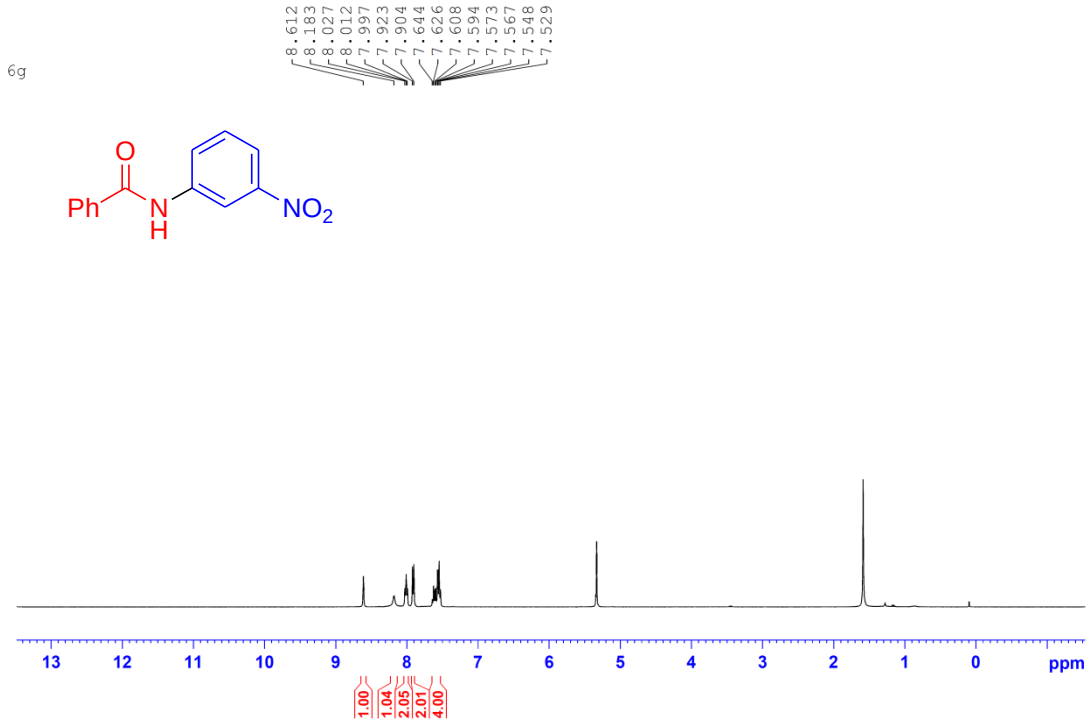

Figure A.91 ^{13}C NMR spectrum of **8g**

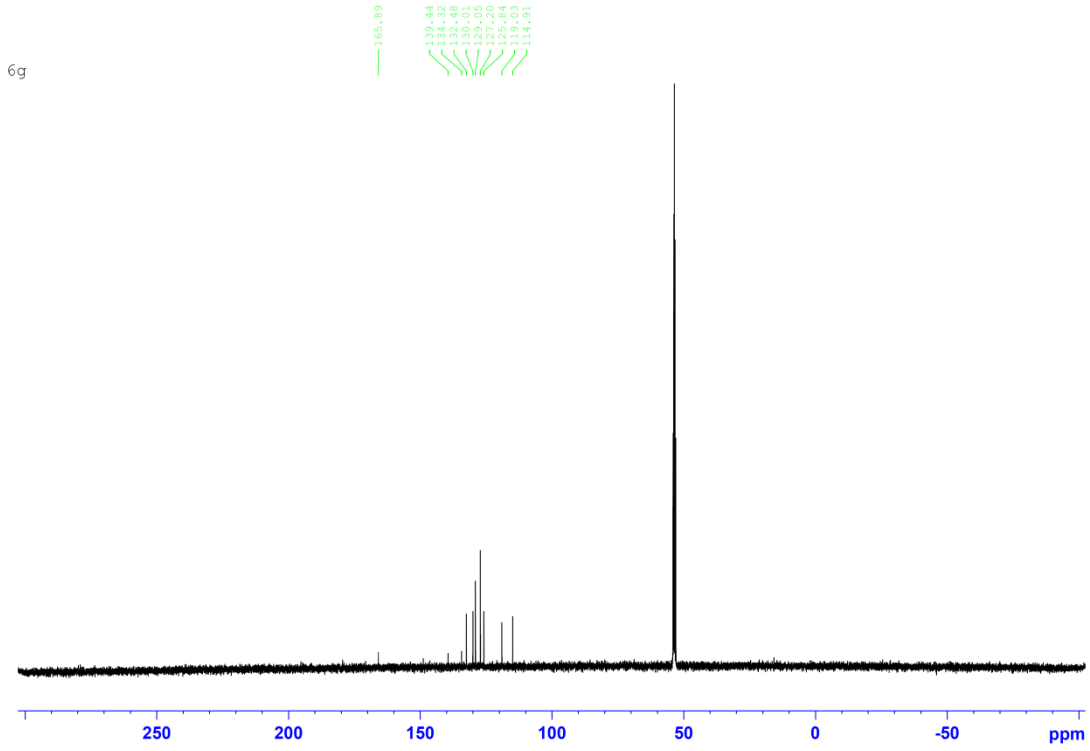

Figure A.92 ^{1}H NMR spectrum of **8h**

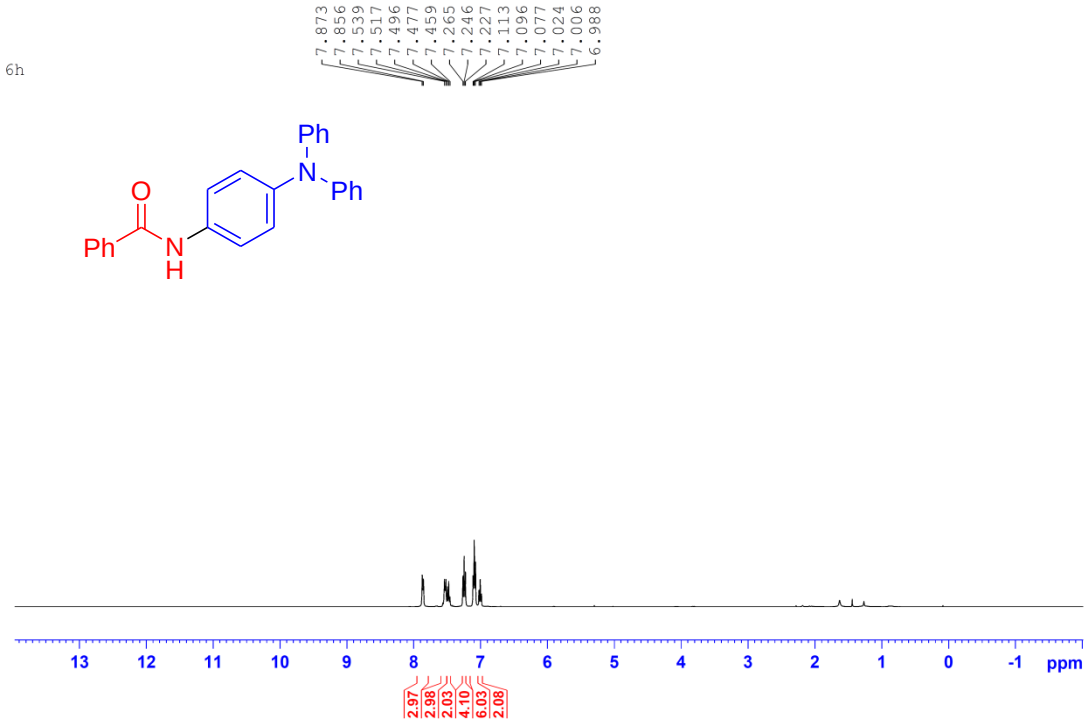

Figure A.93 ^{13}C NMR spectrum of **8h**

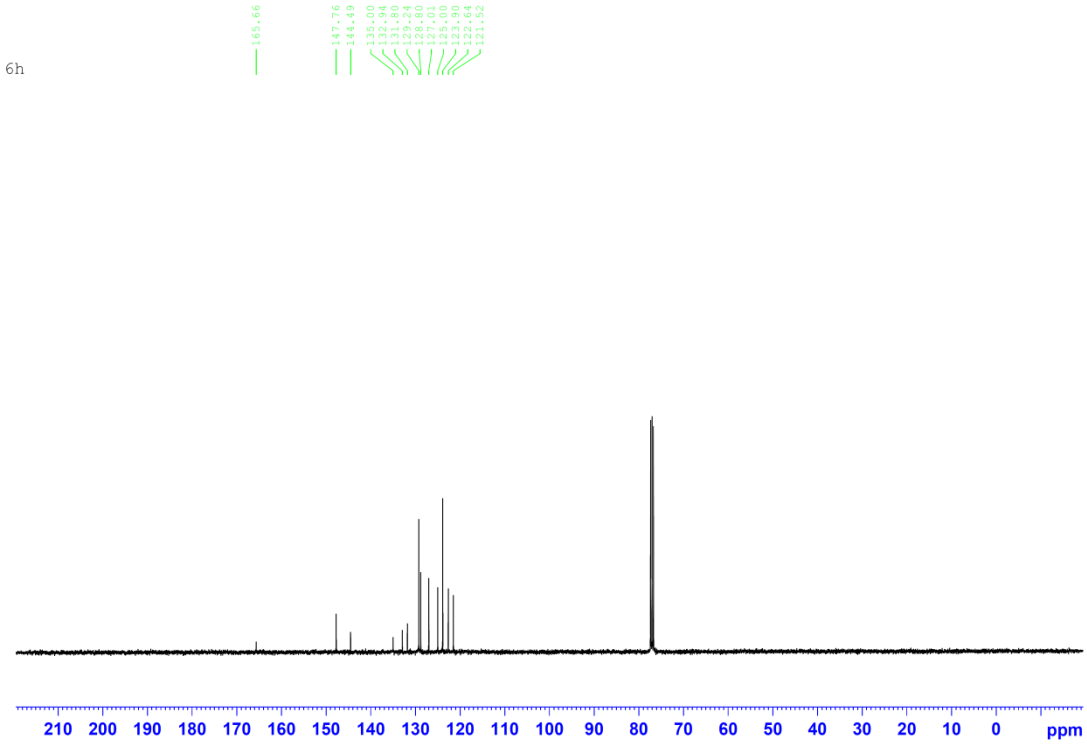

Figure A.94 ^{1}H NMR spectrum of **8i**

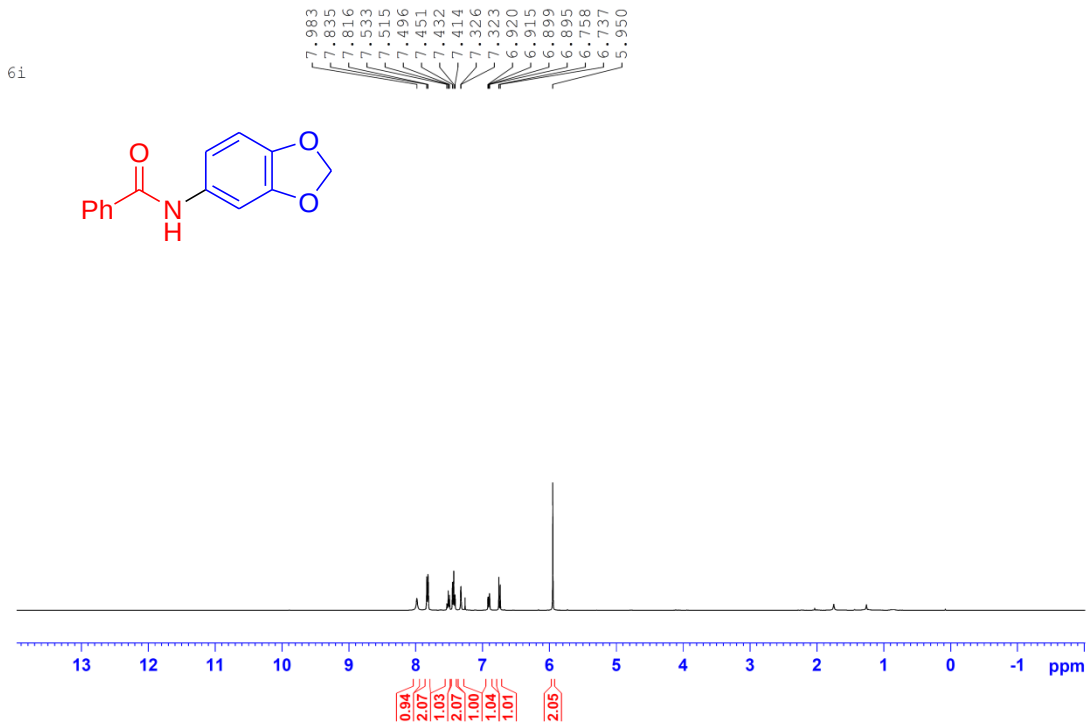

Figure A.95 ^{13}C NMR spectrum of **8i**

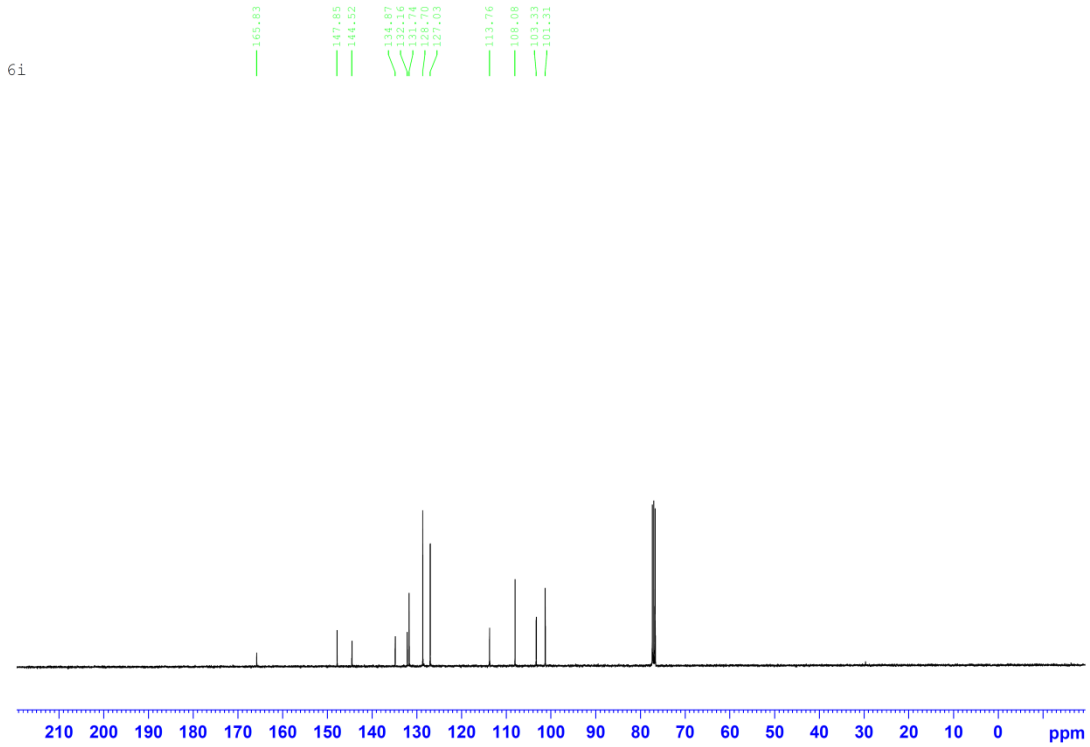

Figure A.96 ^{1}H NMR spectrum of **8j**

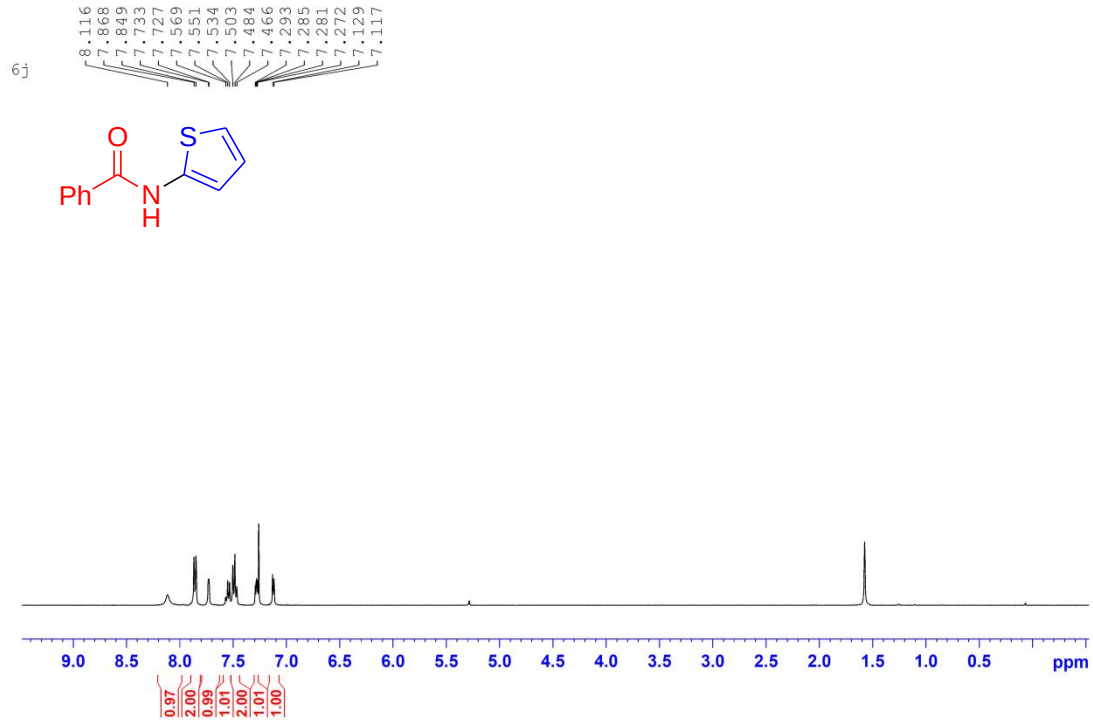

Figure A.97 ^{13}C NMR spectrum of **8j**

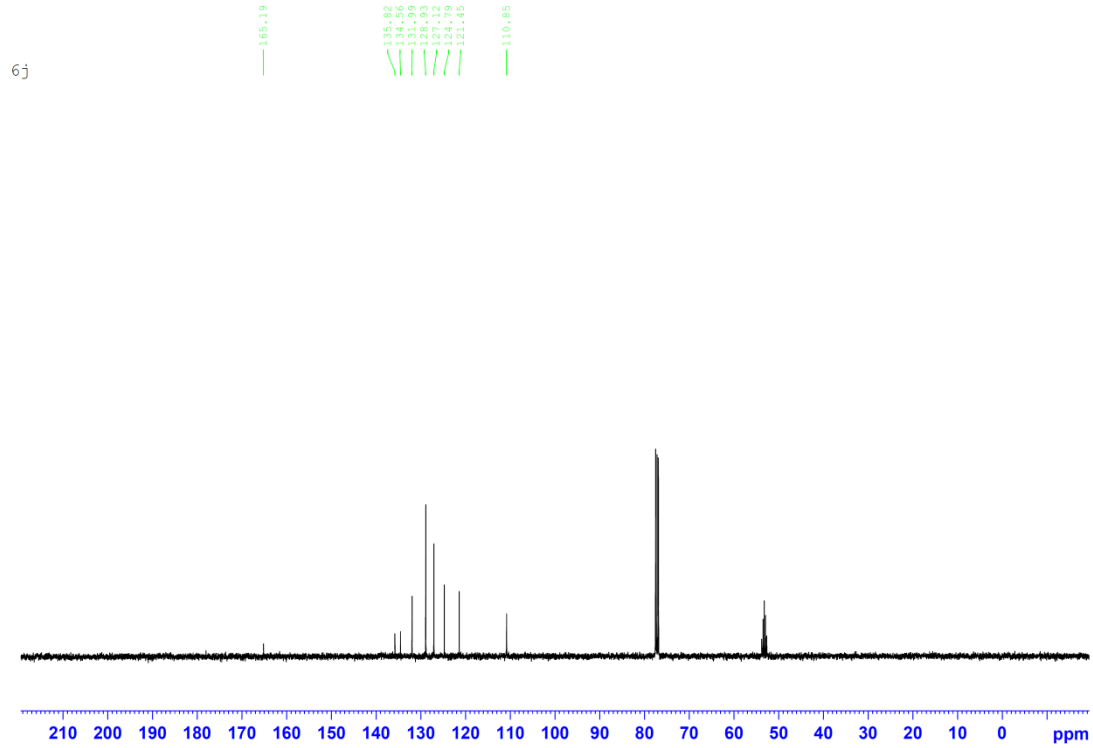

Figure A.98 ^{1}H NMR spectrum of **8k**

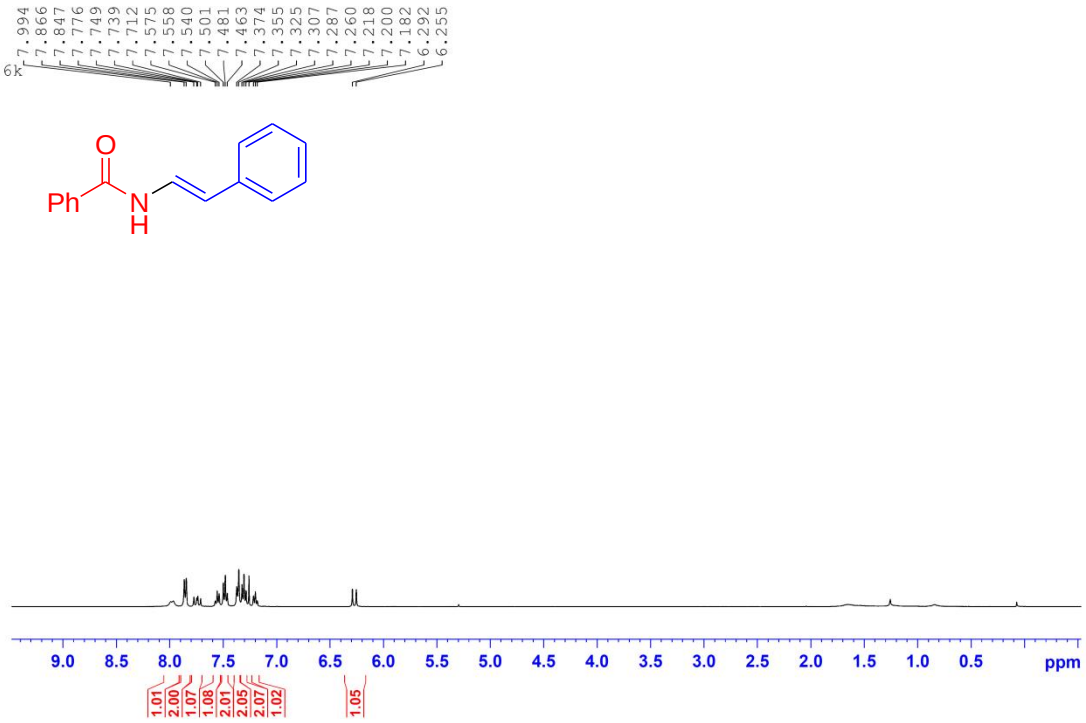

Figure A.99 ^{13}C NMR spectrum of **8k**

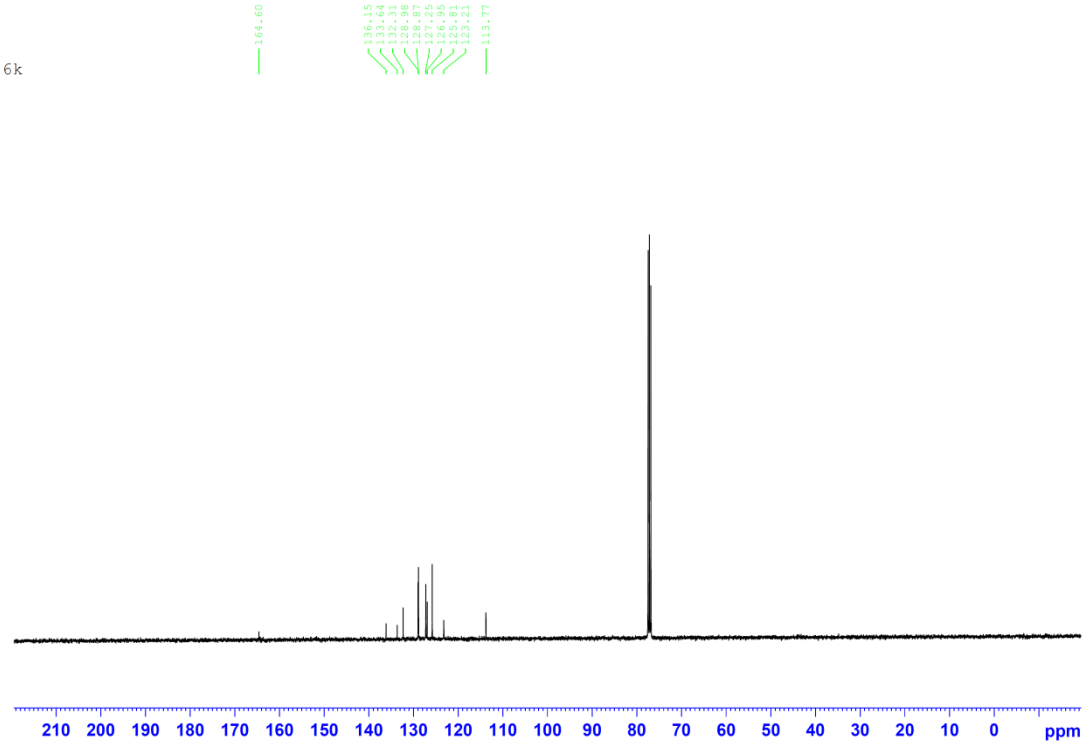

Figure A.100 ^{1}H NMR spectrum of **8l**

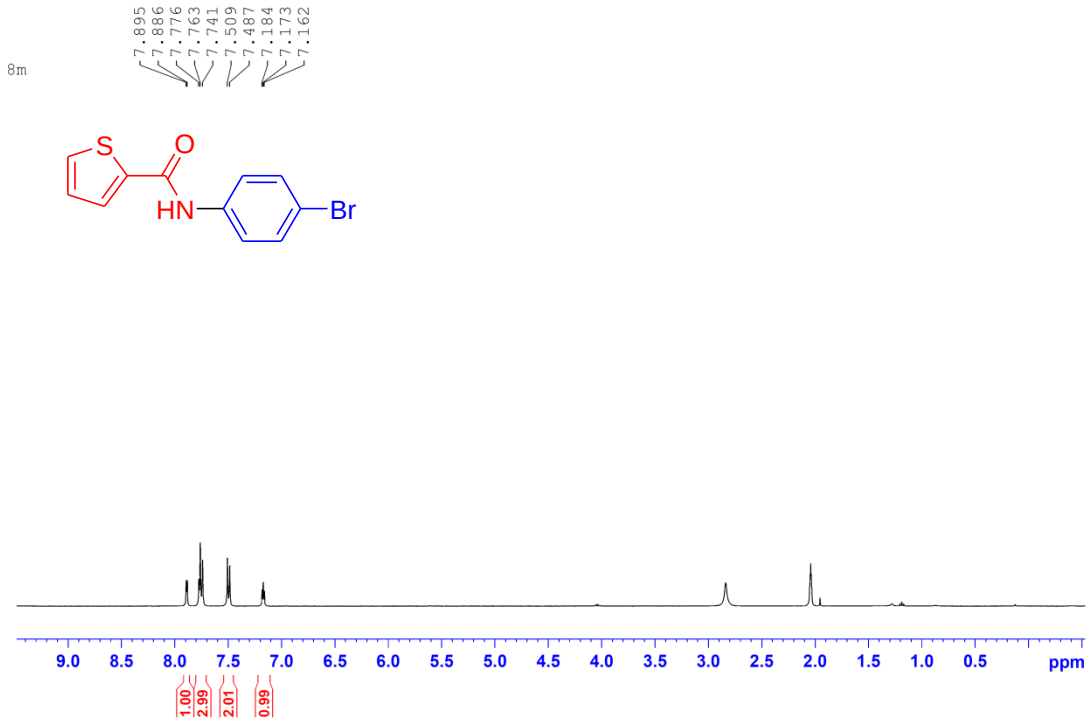

Figure A.101 ^{13}C NMR spectrum of **8l**

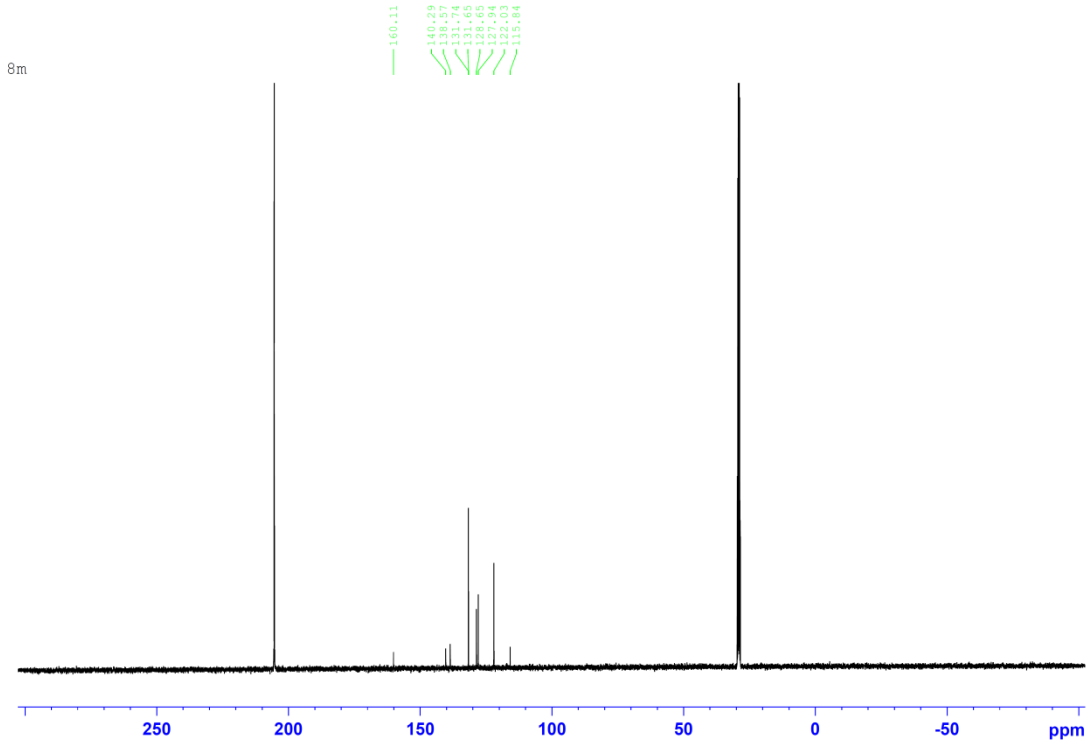

Figure A.102 ^{1}H NMR spectrum of **8m**

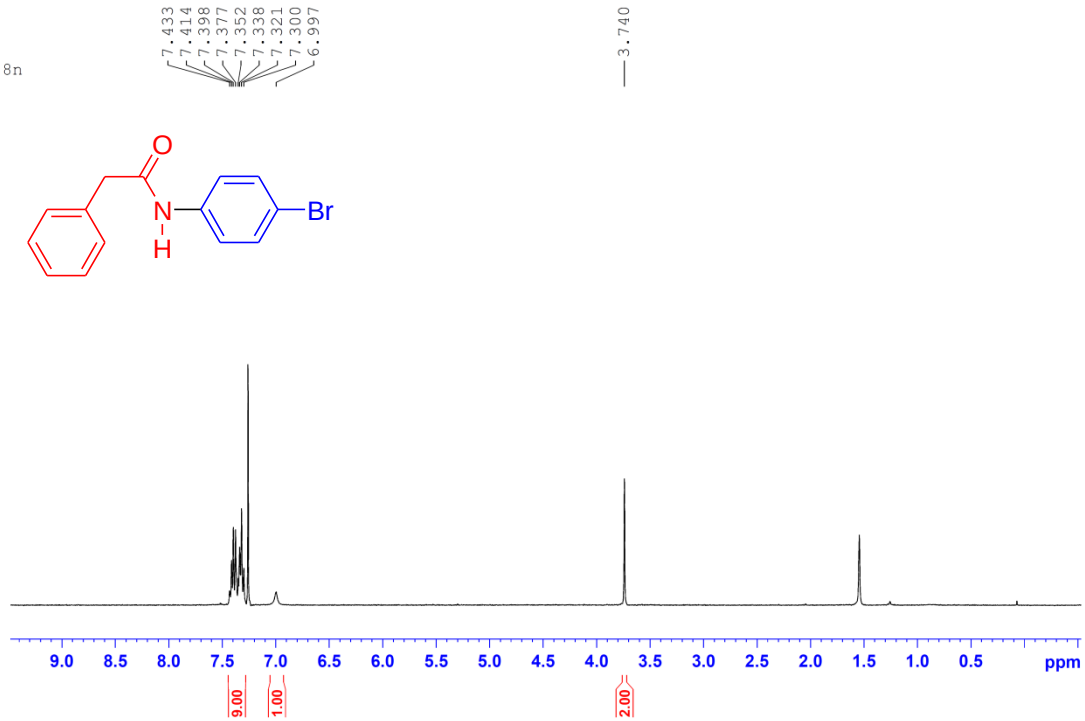

Figure A.103 ^{13}C NMR spectrum of **8m**

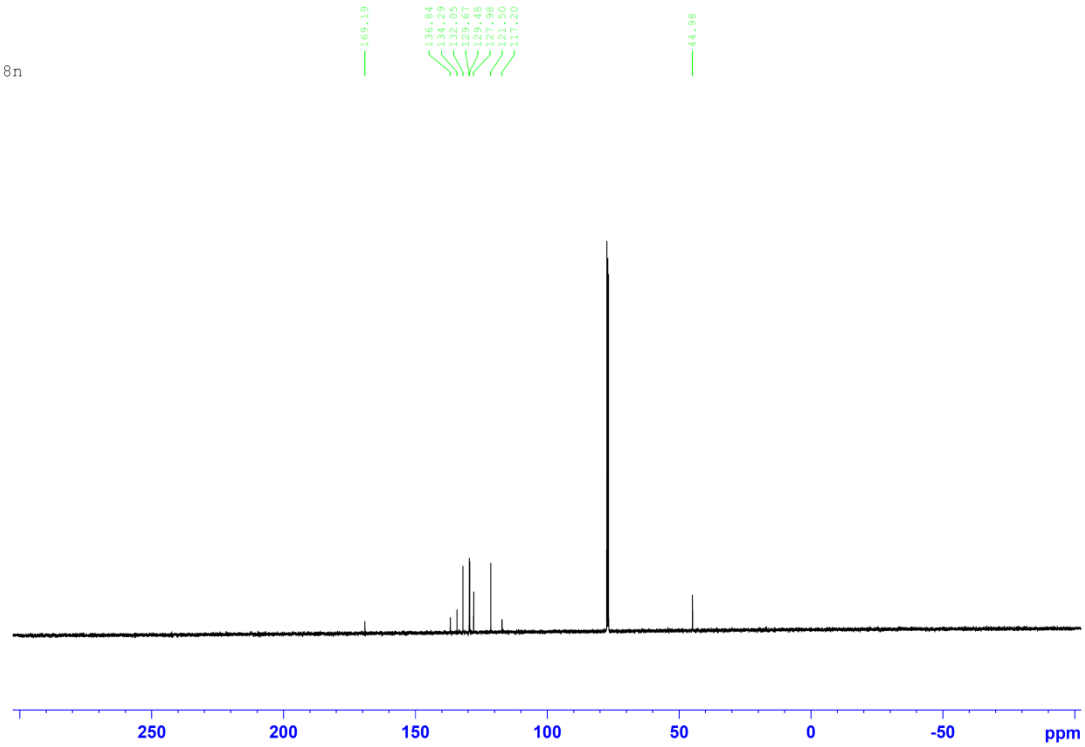

Figure A.104 ^{1}H NMR spectrum of **8n**

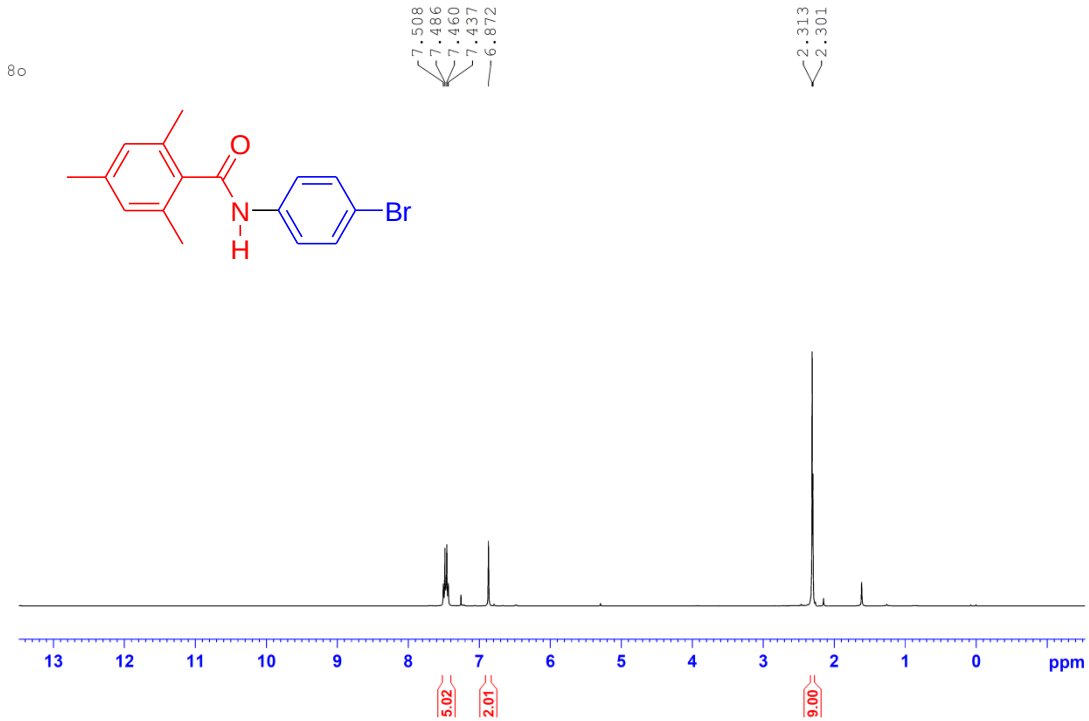

Figure A.105 ^{13}C NMR spectrum of **8n**

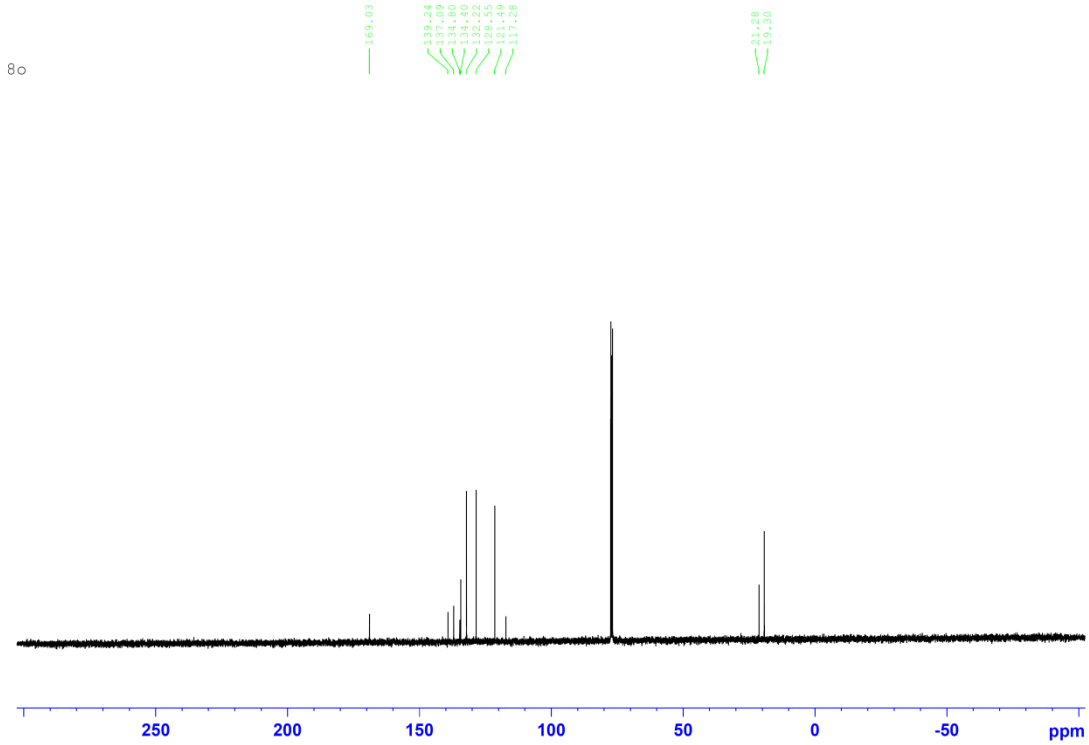

Figure A.106 ^{1}H NMR spectrum of **9a**

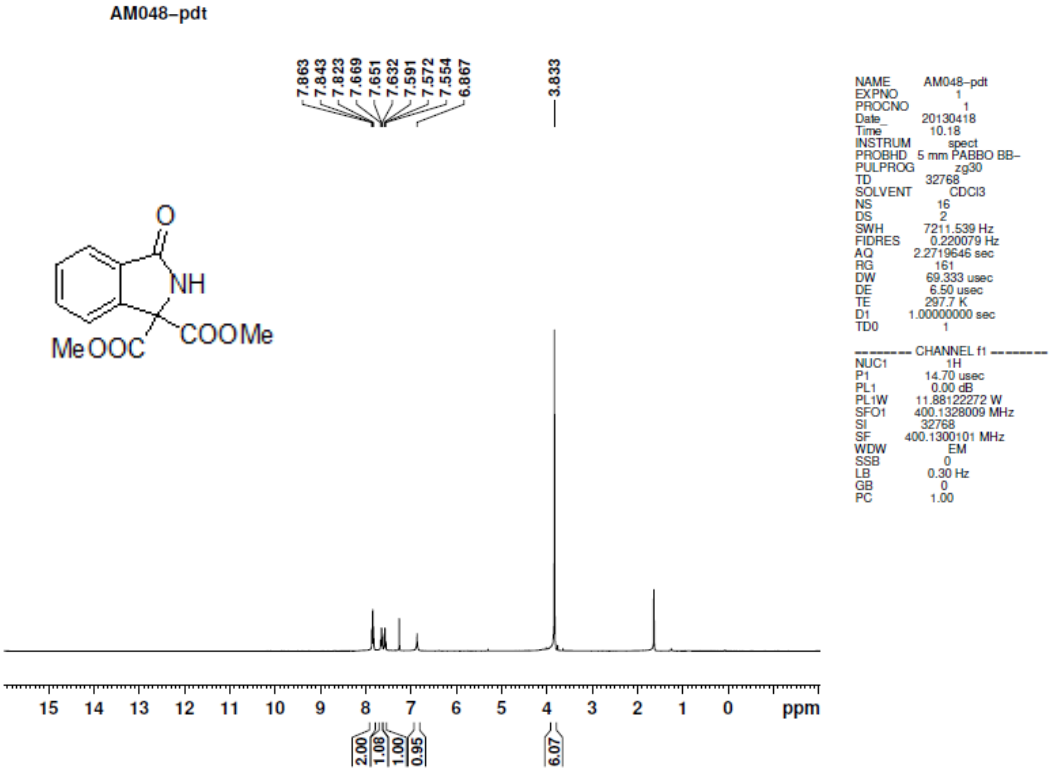

Figure A.107 ^{13}C NMR spectrum of **9a**

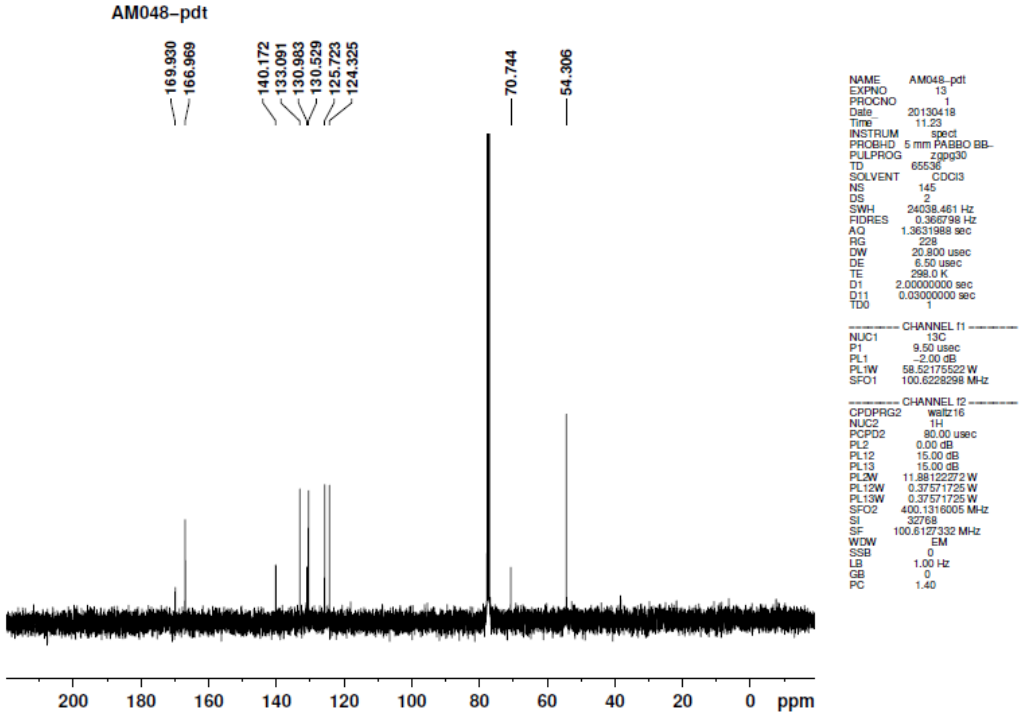

Figure A.108 ^{1}H NMR spectrum of **9b**

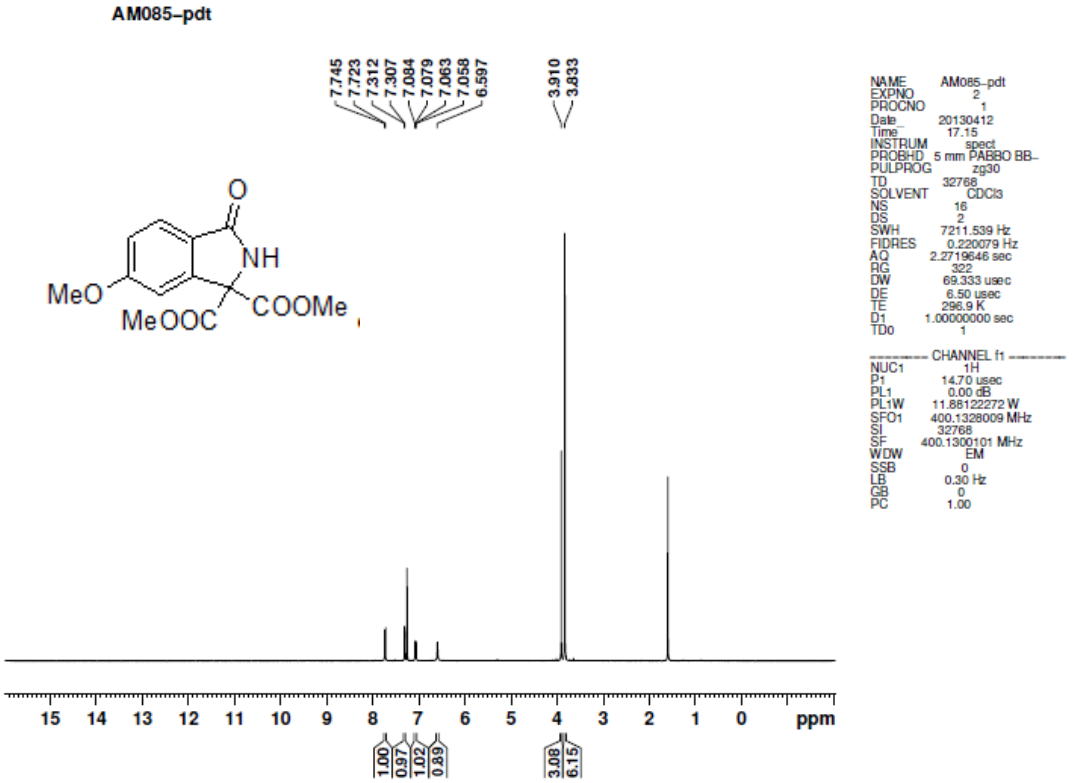

Figure A.109 ^{13}C NMR spectrum of **9b**

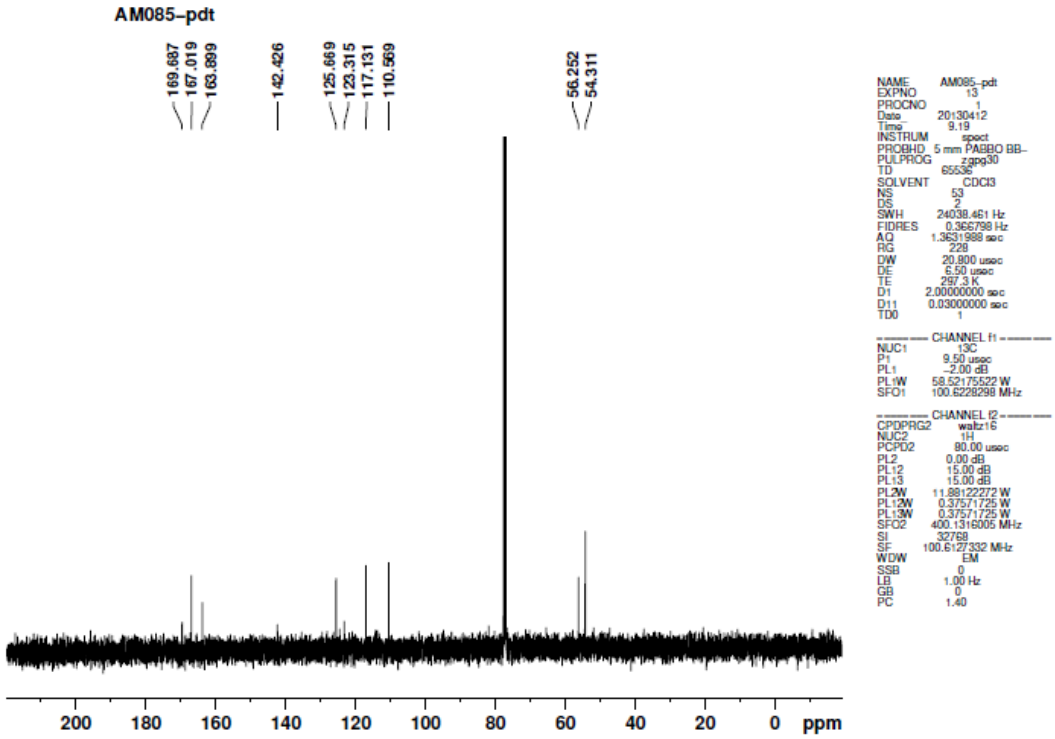

Figure A.110 ^{1}H NMR spectrum of **9c**

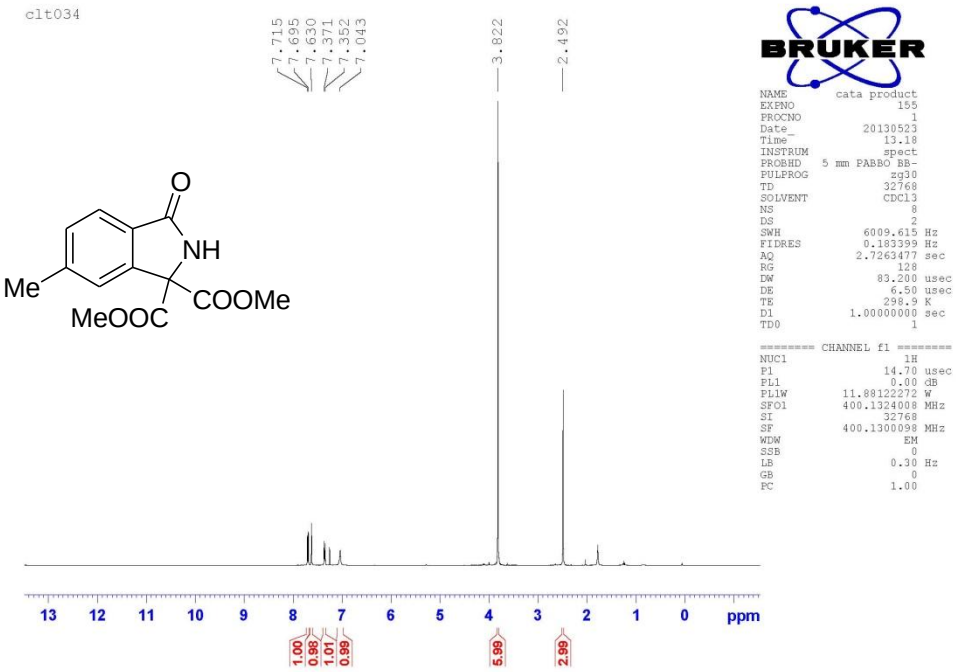

Figure A.111 ^{13}C NMR spectrum of **9c**

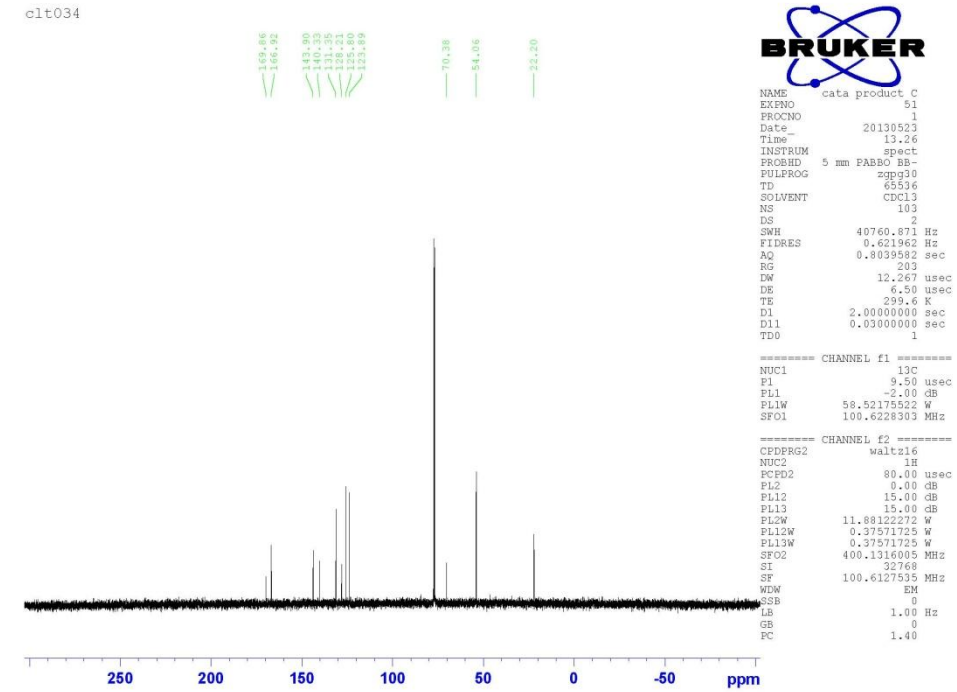

Figure A.112 ^{1}H NMR spectrum of **9d**

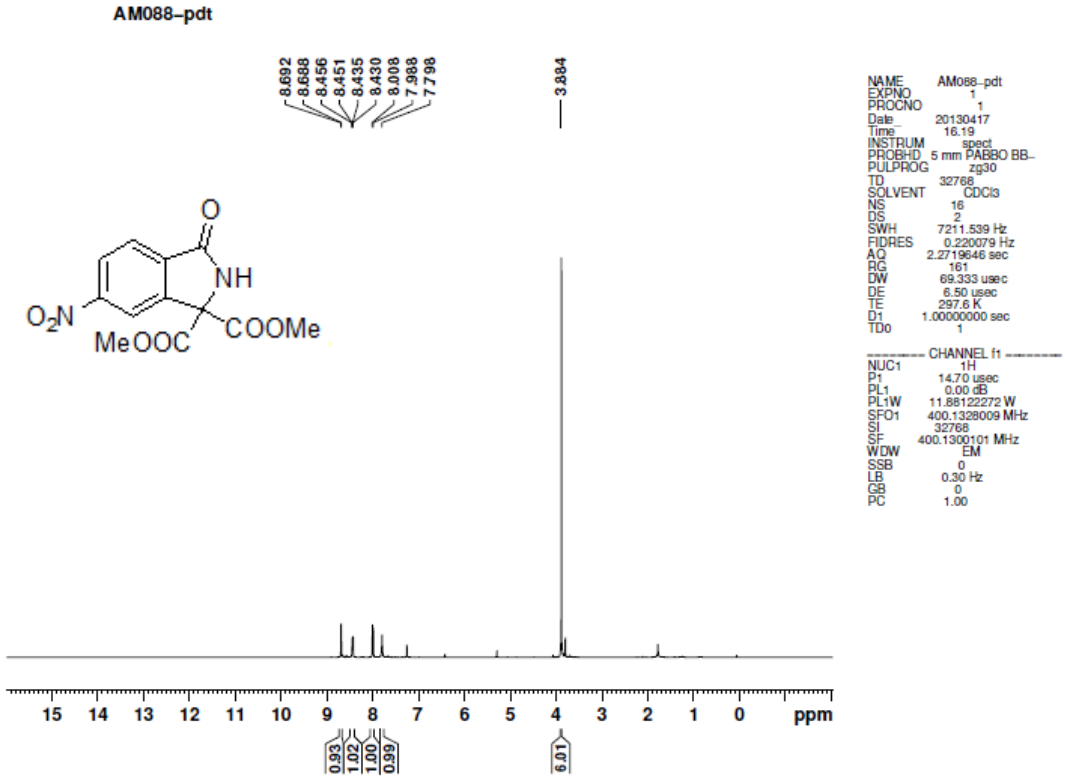

Figure A.113 ^{13}C NMR spectrum of **9d**

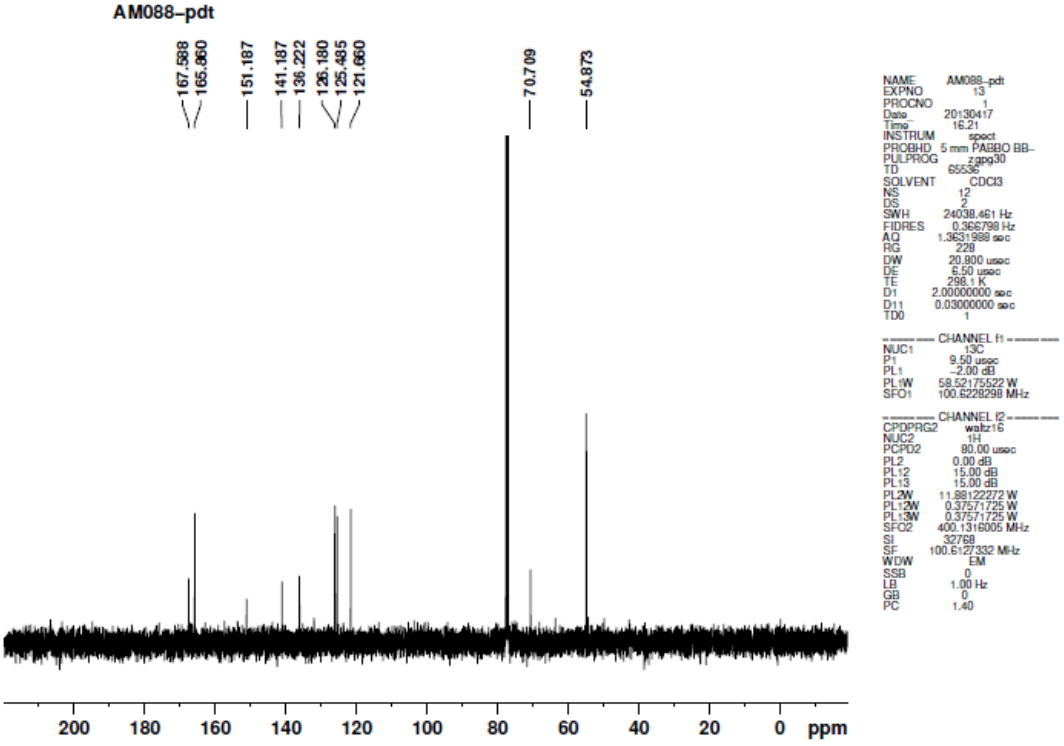

Figure A.114 ^{1}H NMR spectrum of **9e**

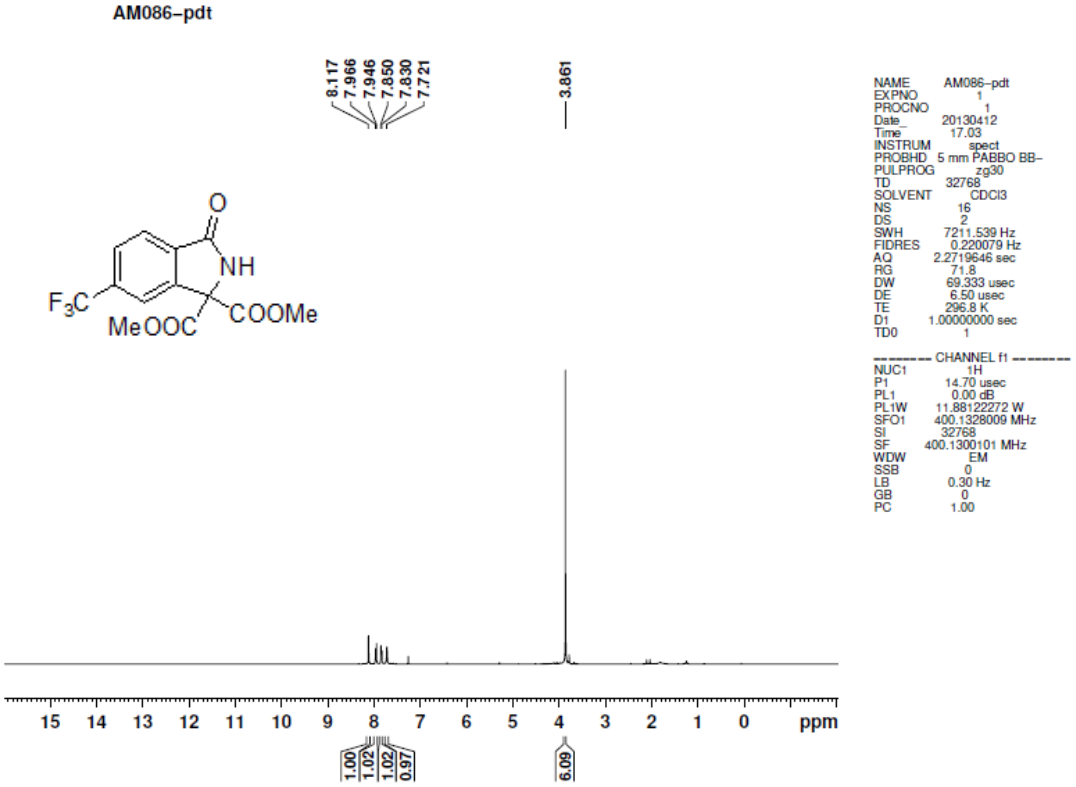

Figure A.115 ^{13}C NMR spectrum of **9e**

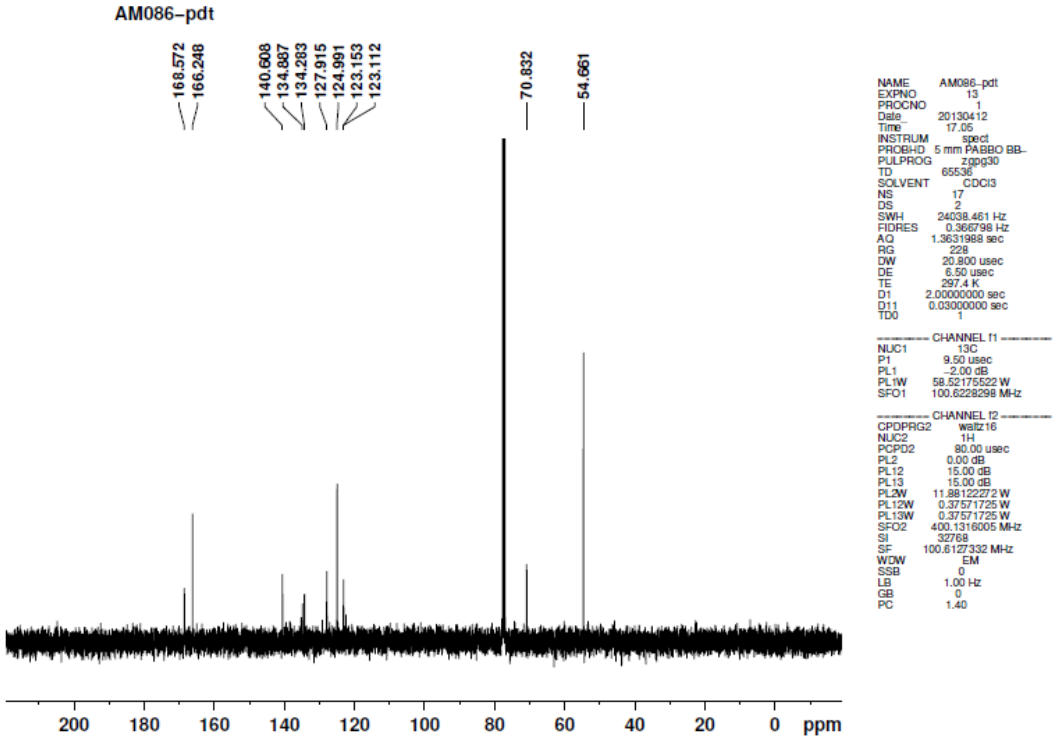

Figure A.116 ^{1}H NMR spectrum of **9f**

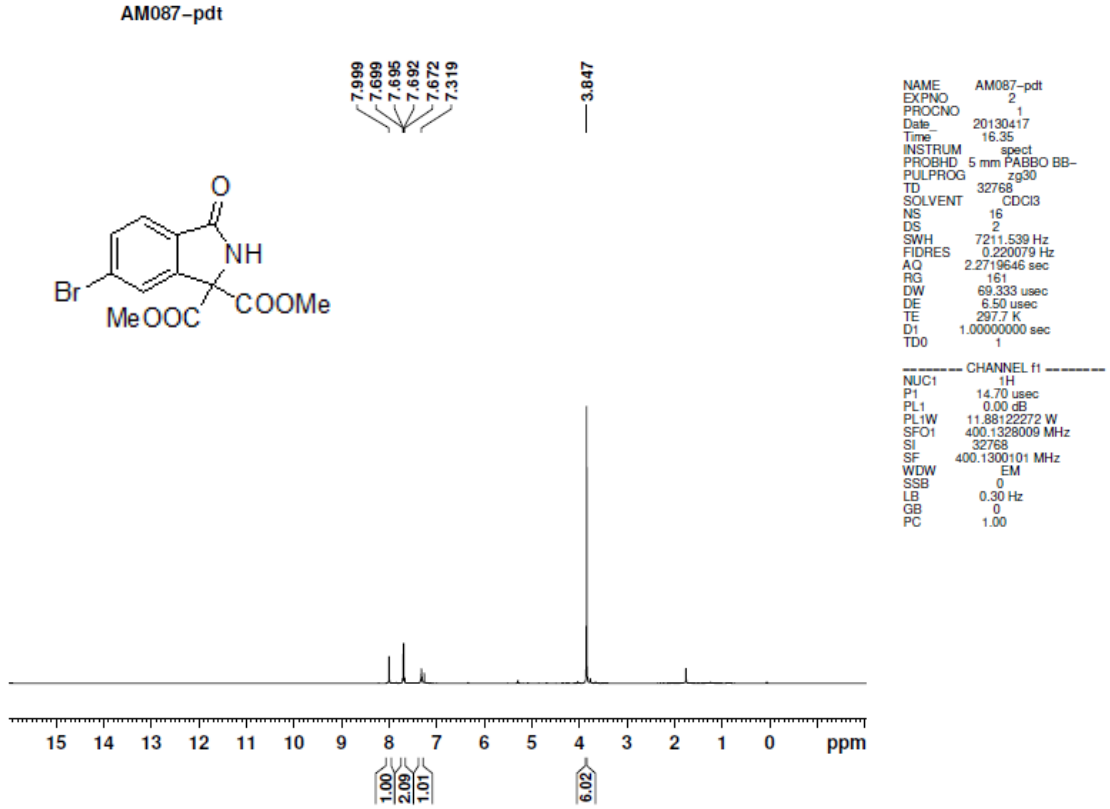

Figure A.117 ^{13}C NMR spectrum of **9f**

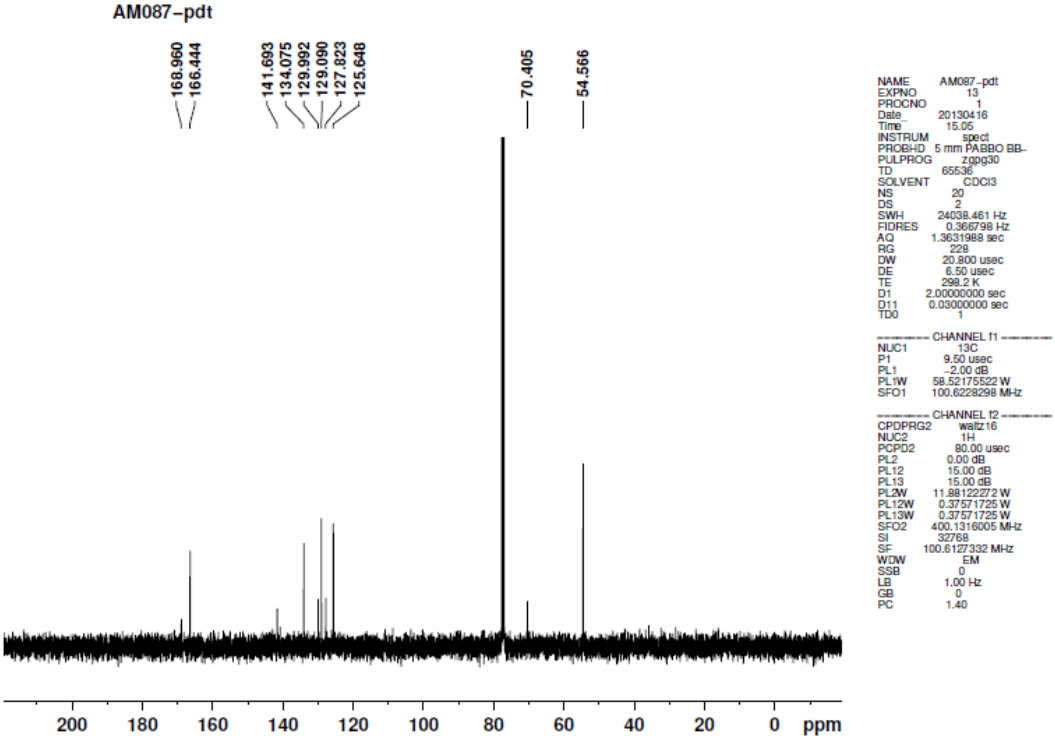

Figure A.118 ^{1}H NMR spectrum of **9g**

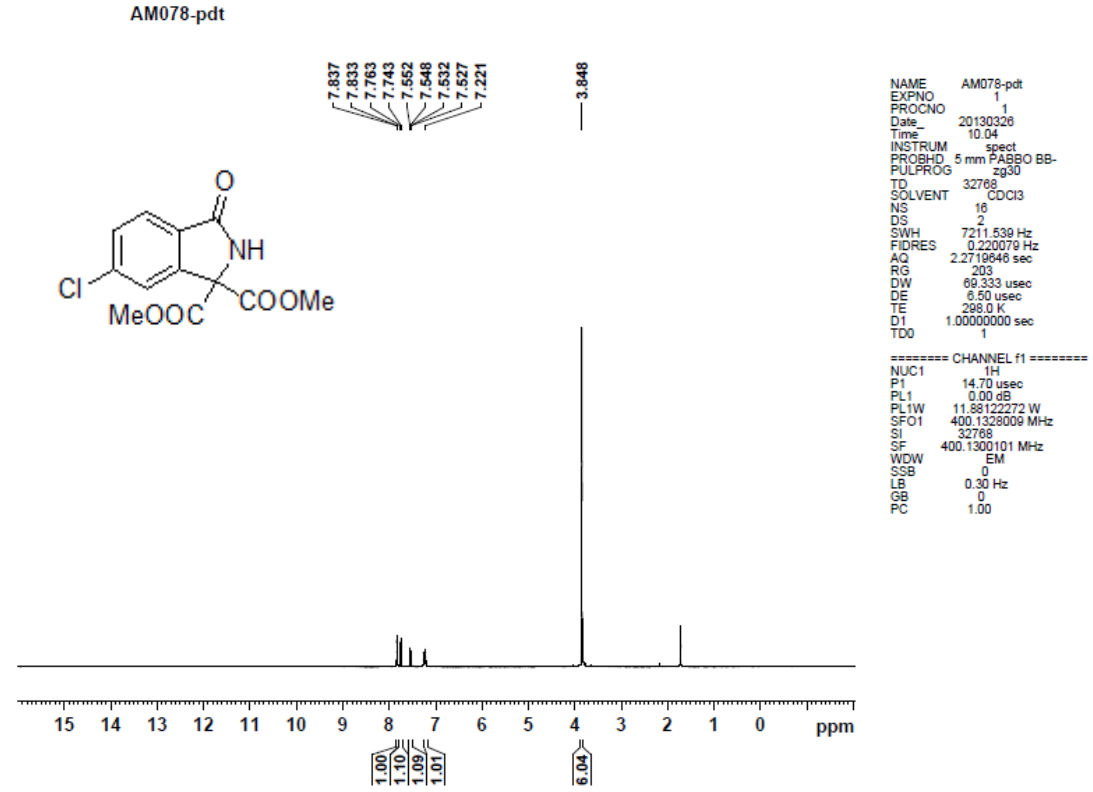

Figure A.119 ^{13}C NMR spectrum of **9g**

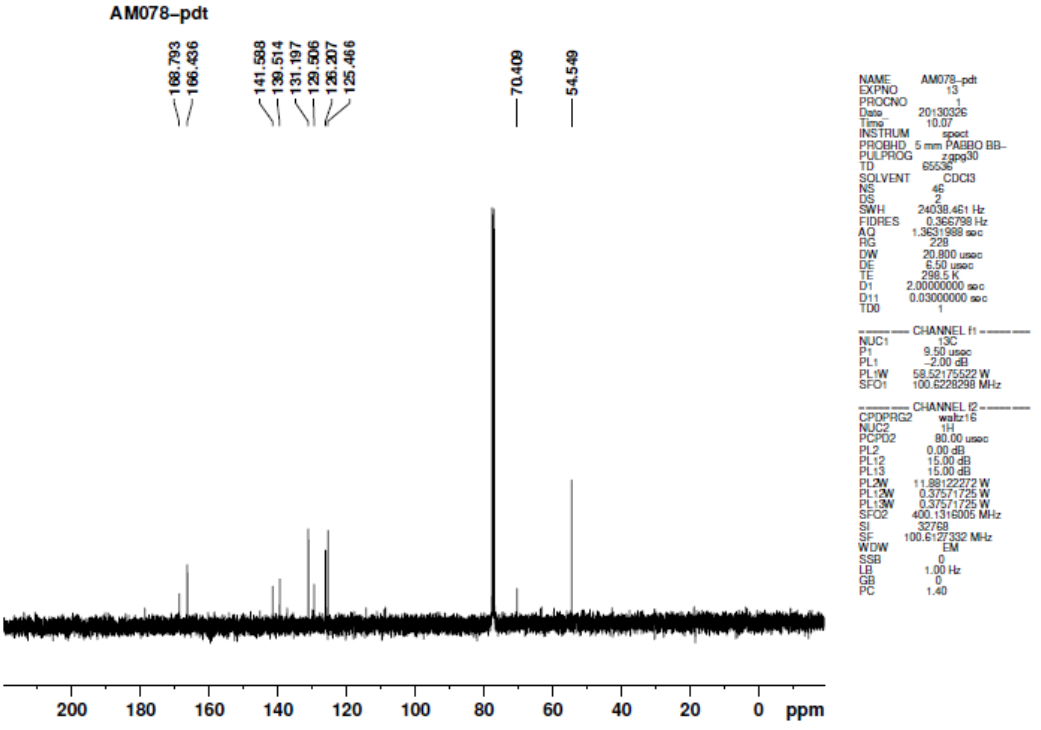

Figure A.120 ^{1}H NMR spectrum of **9h**

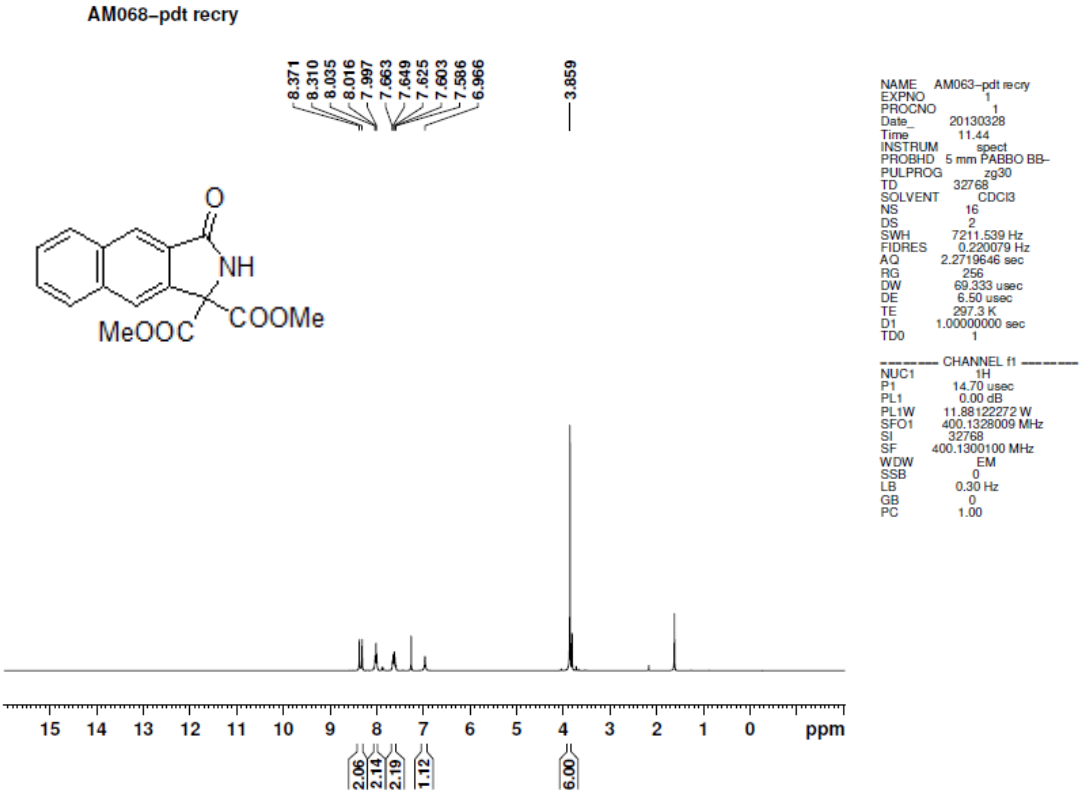

Figure A.121 ^{13}C NMR spectrum of **9h**

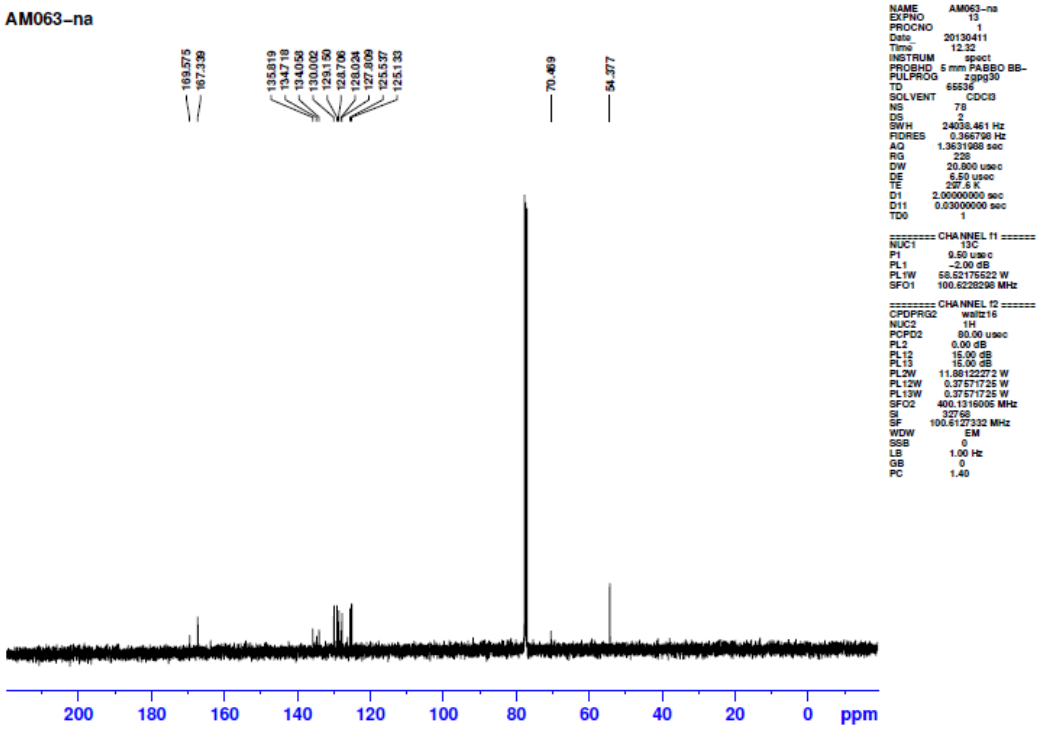

Figure A.122 ^{1}H NMR spectrum of **9i**

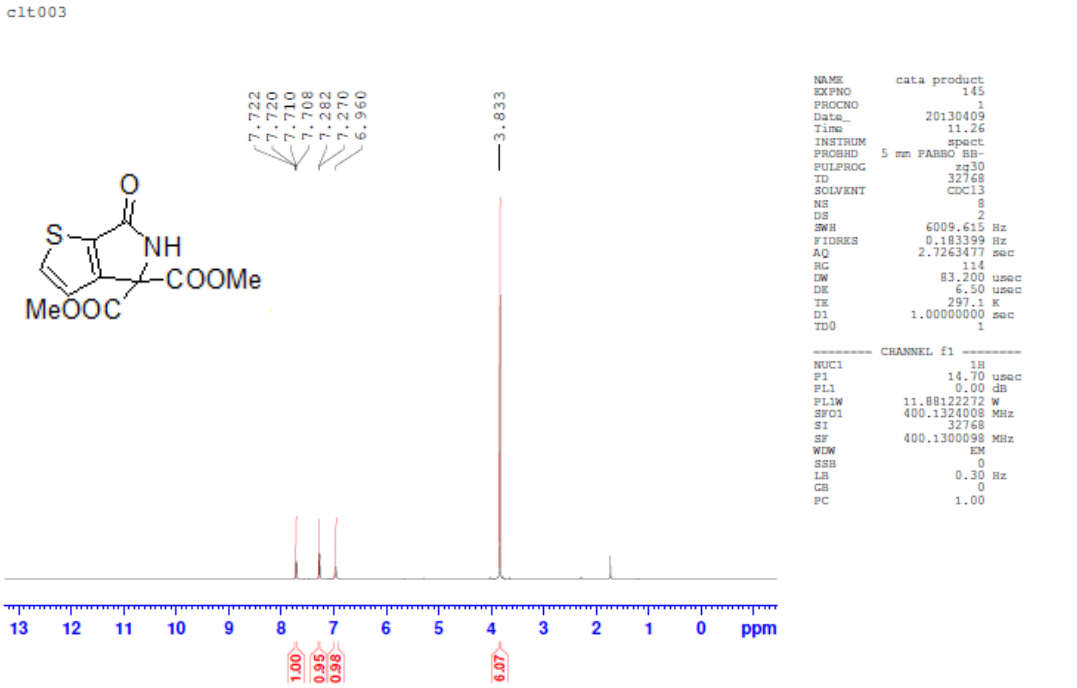

Figure A.123 ^{13}C NMR spectrum of **9i**

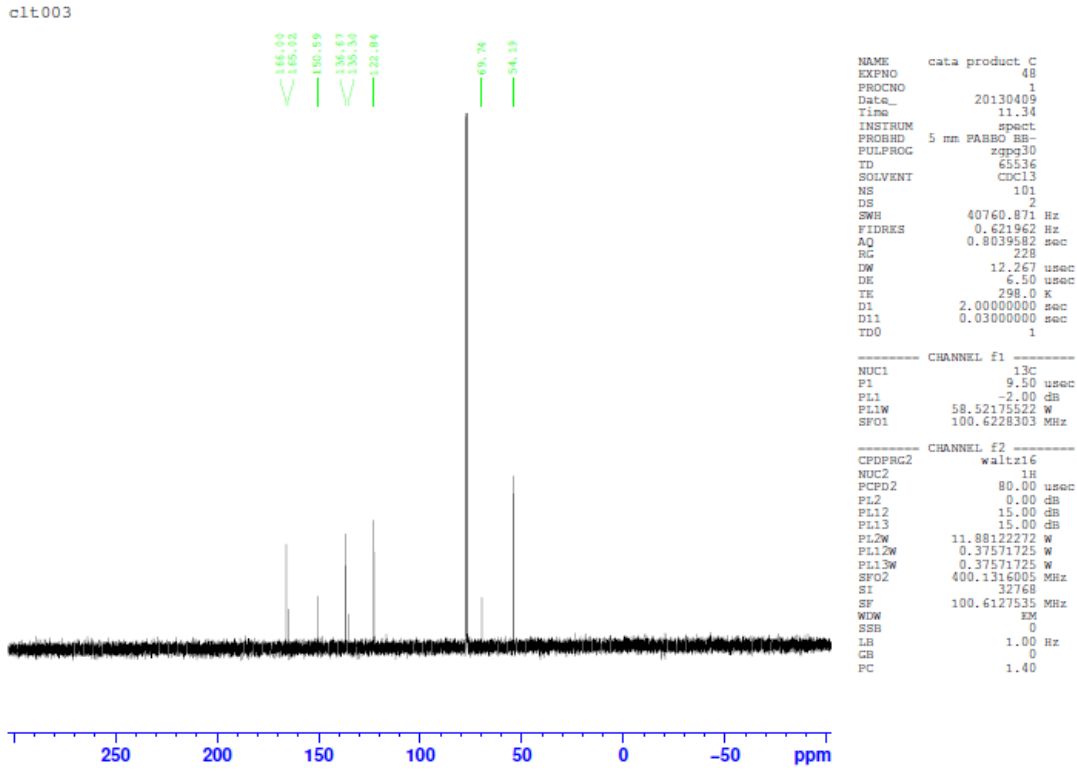

Figure A.124 ^{1}H NMR spectrum of **9j**

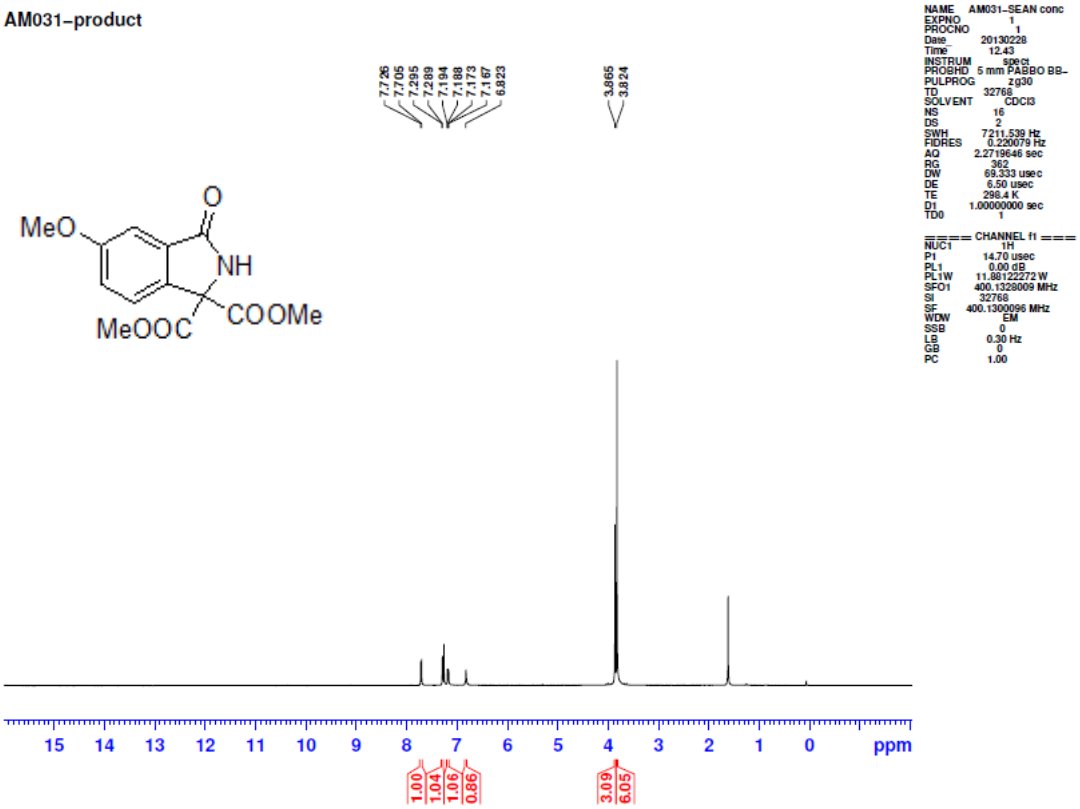

Figure A.125 ^{13}C NMR spectrum of **9j**

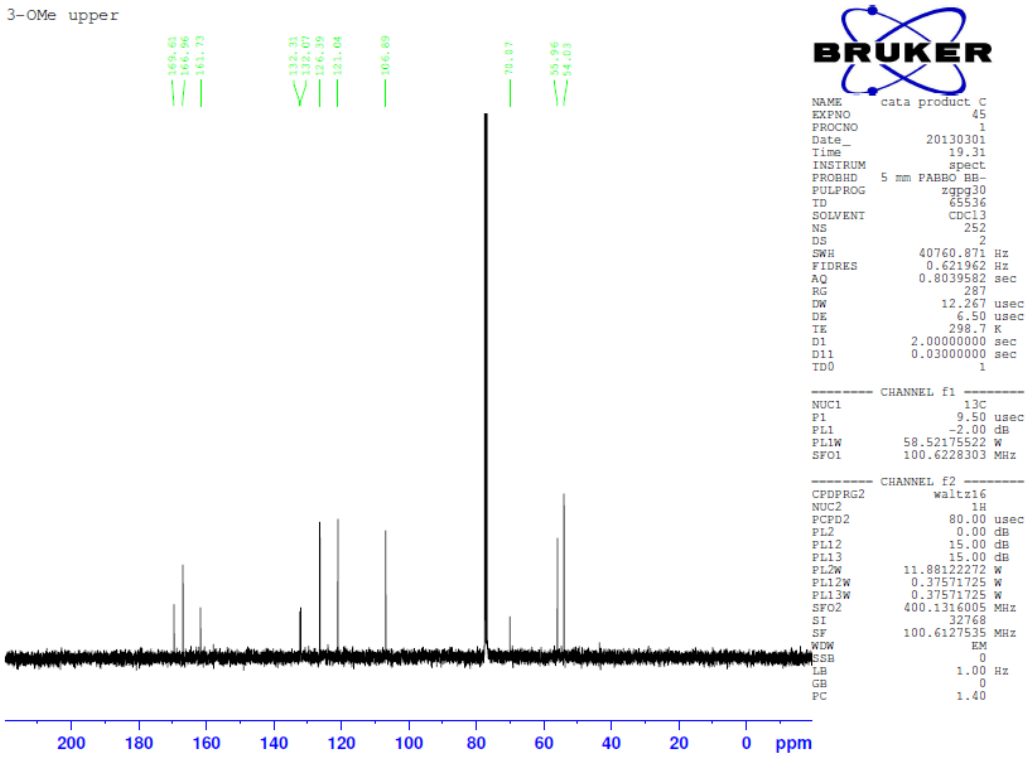

Figure A.126 ^{1}H NMR spectrum of **9j'**

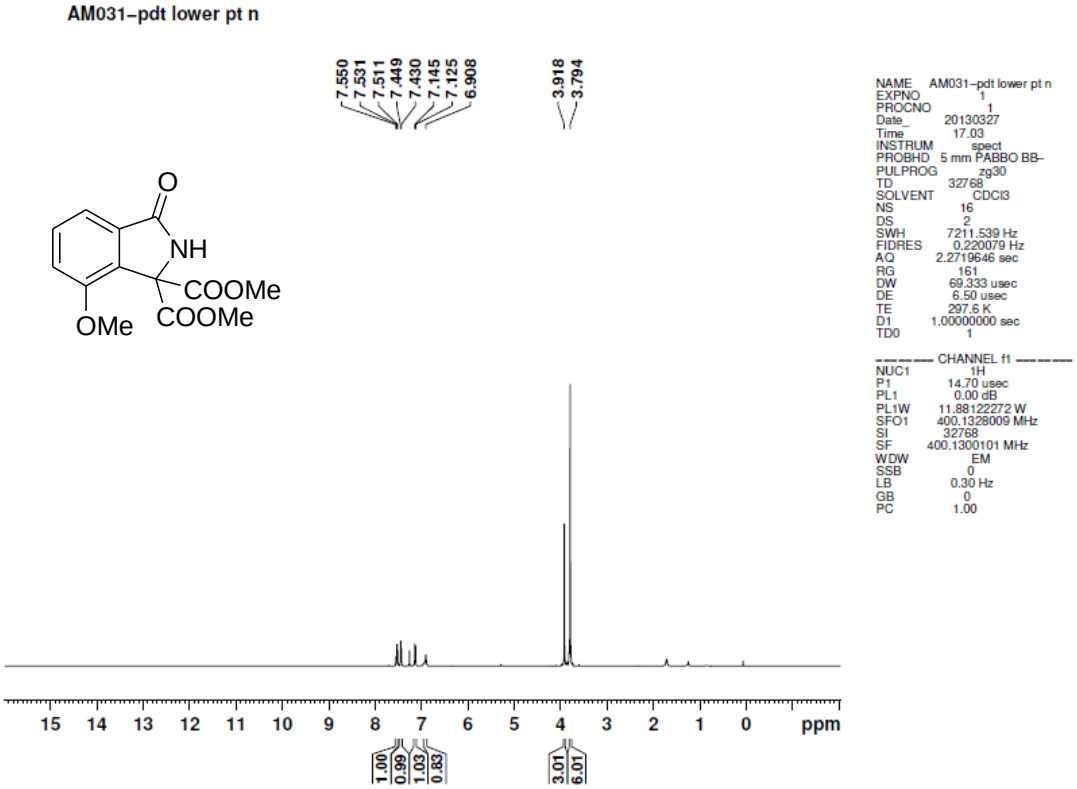

Figure A.127 ^{13}C NMR spectrum of **9j'**

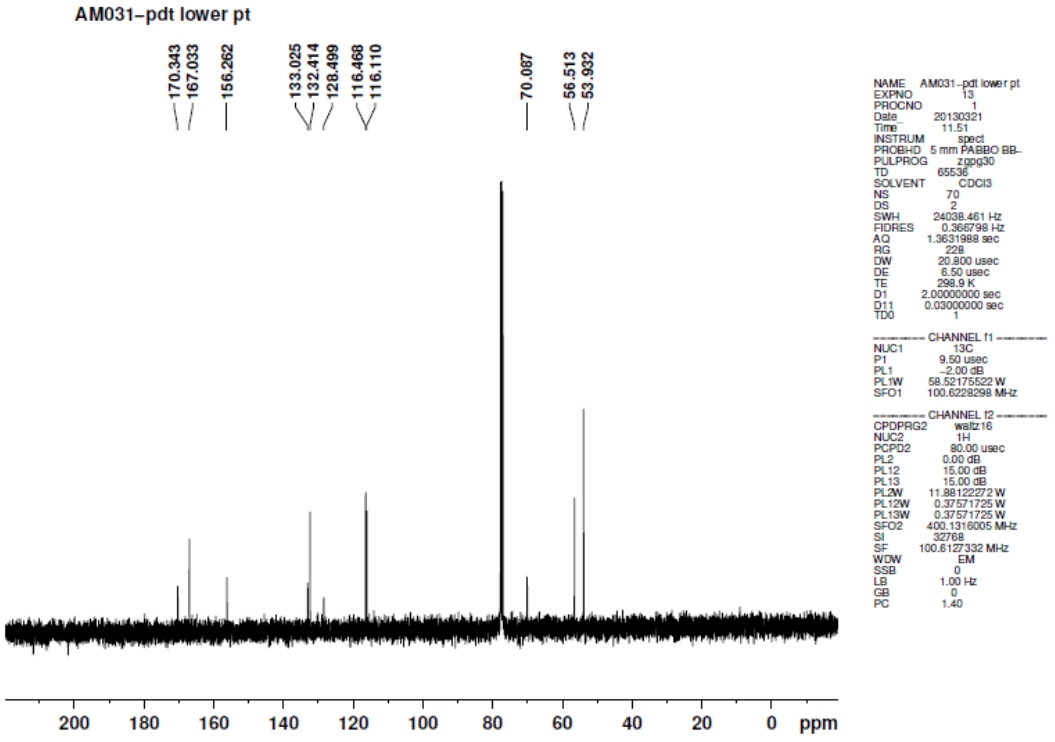

Figure A.128 ^{1}H NMR spectrum of **9k**

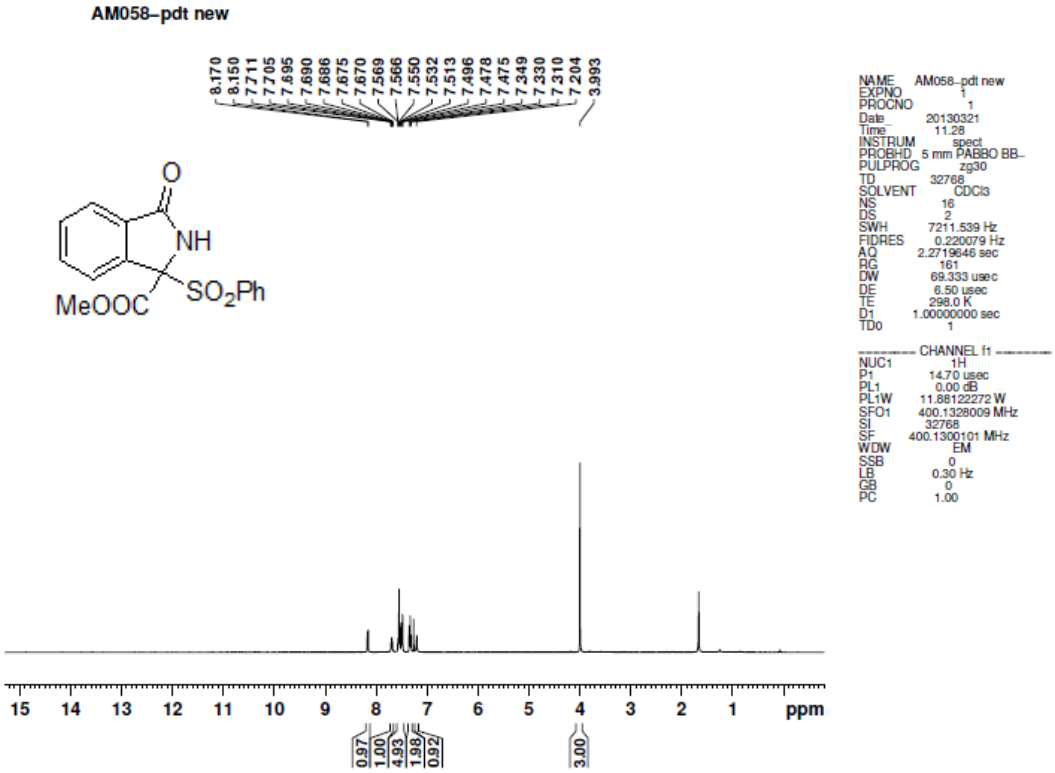

Figure A.129 ^{13}C NMR spectrum of **9k**

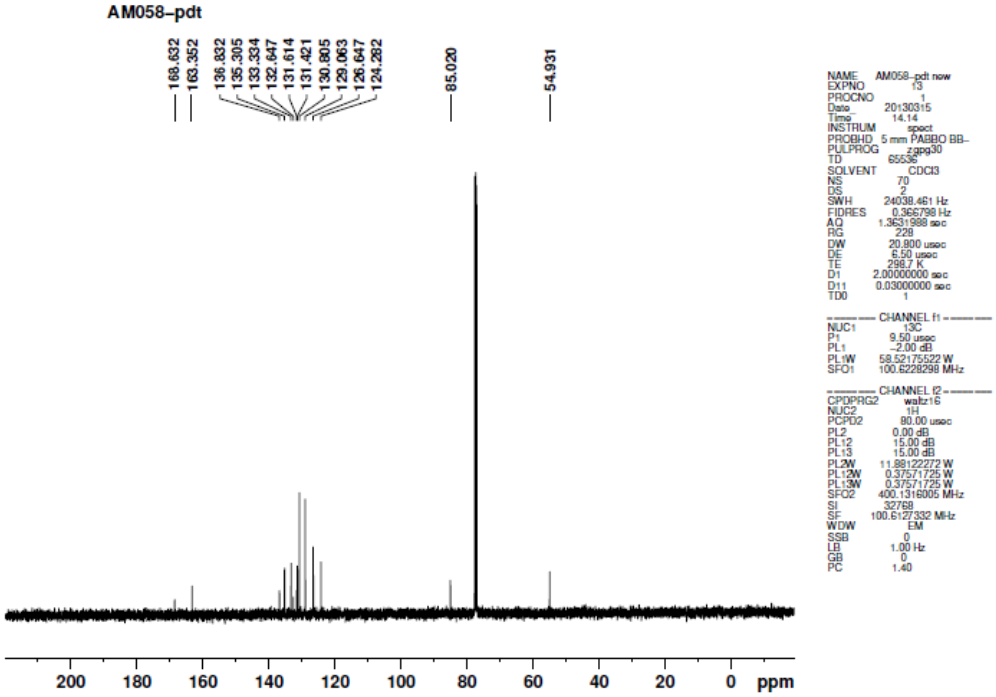

Figure A.130 ^{1}H NMR spectrum of **9l**

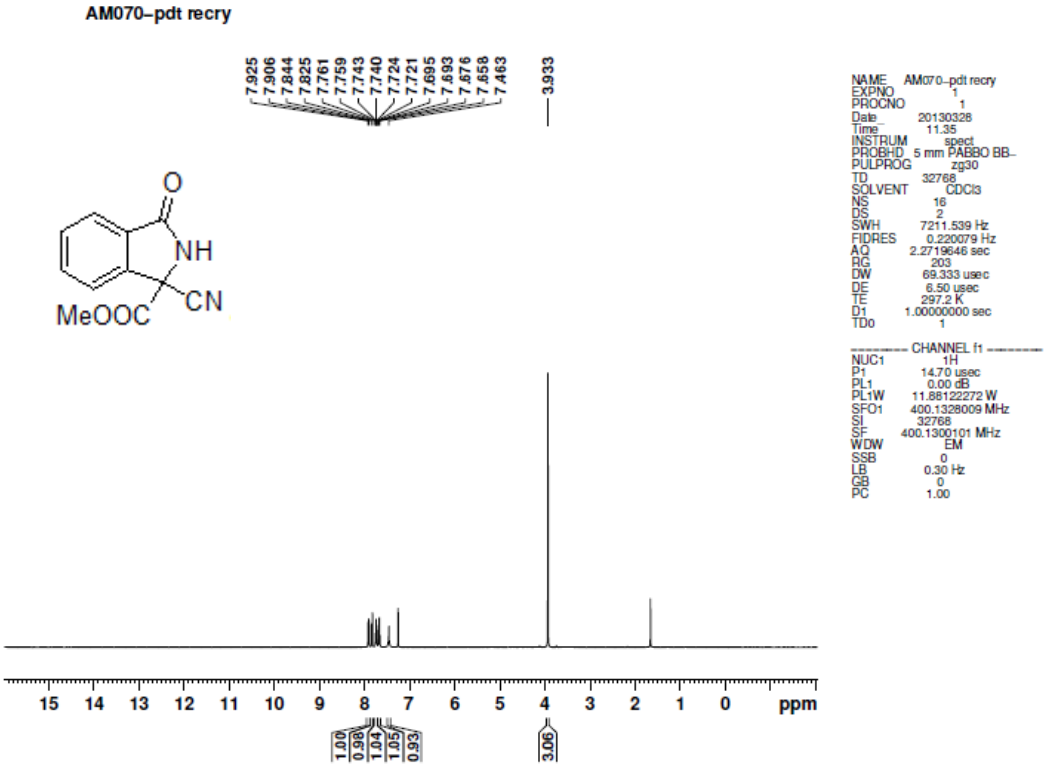

Figure A.131 ^{13}C NMR spectrum of **9l**

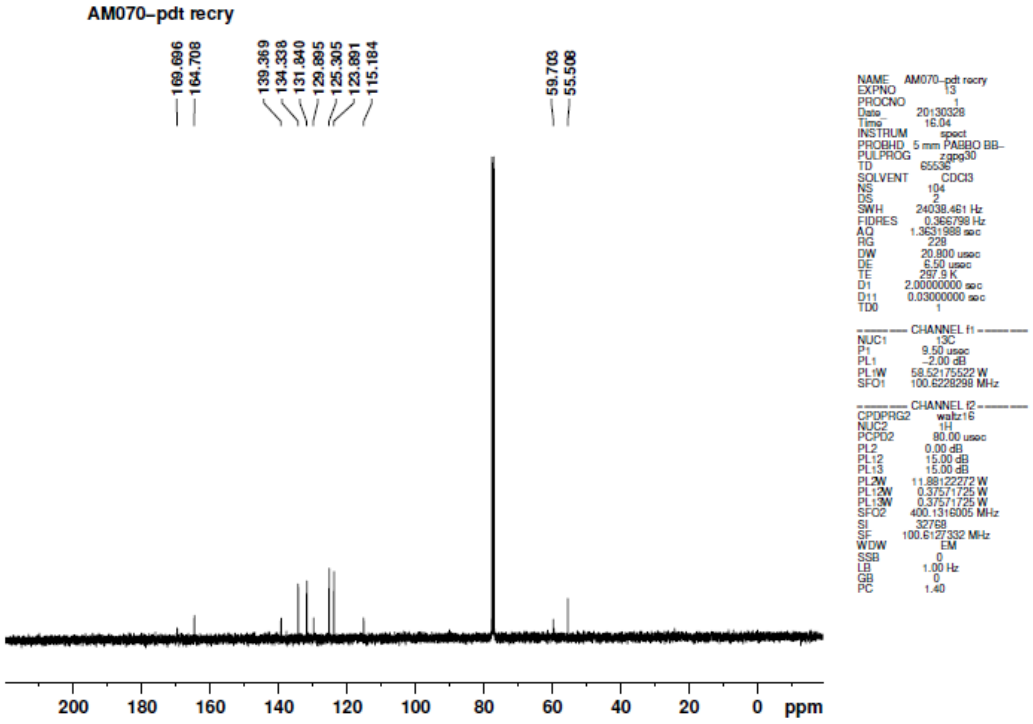

Figure A.132 ^{1}H NMR spectrum of **9m**

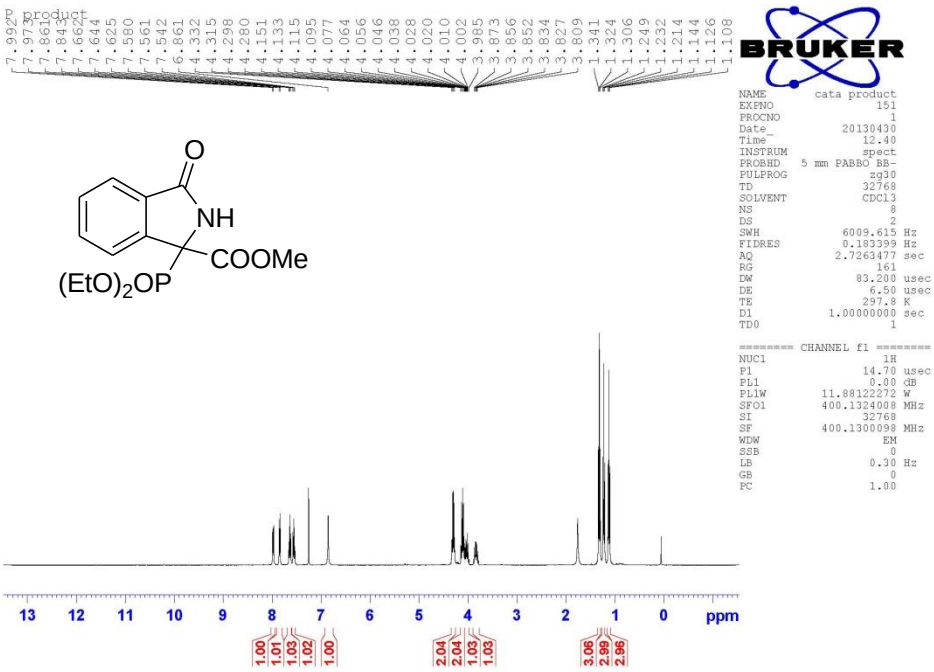

Figure A.133 ^{13}C NMR spectrum of **9m**

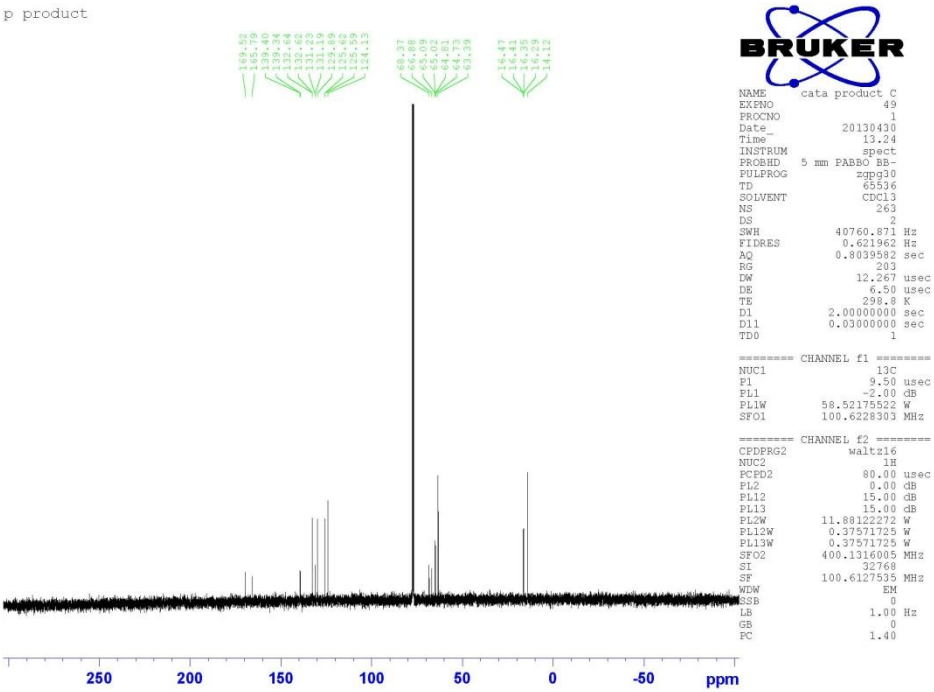

Figure A.134 ^{31}P NMR spectrum of **9m**

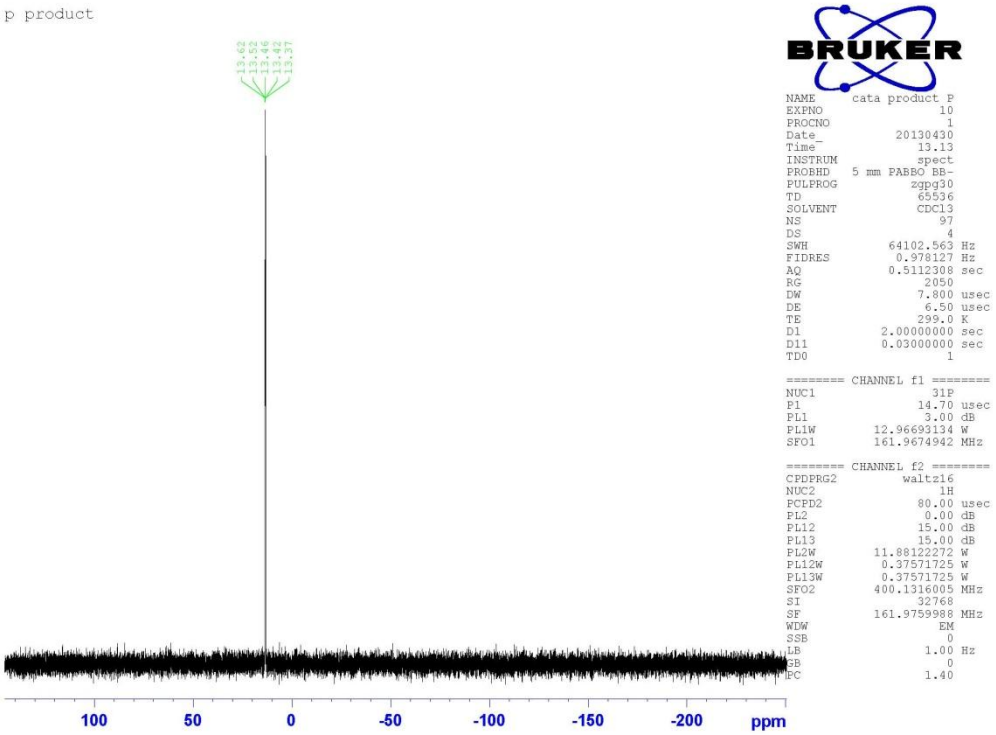

Figure A.135 ^{1}H NMR spectrum of **9n**

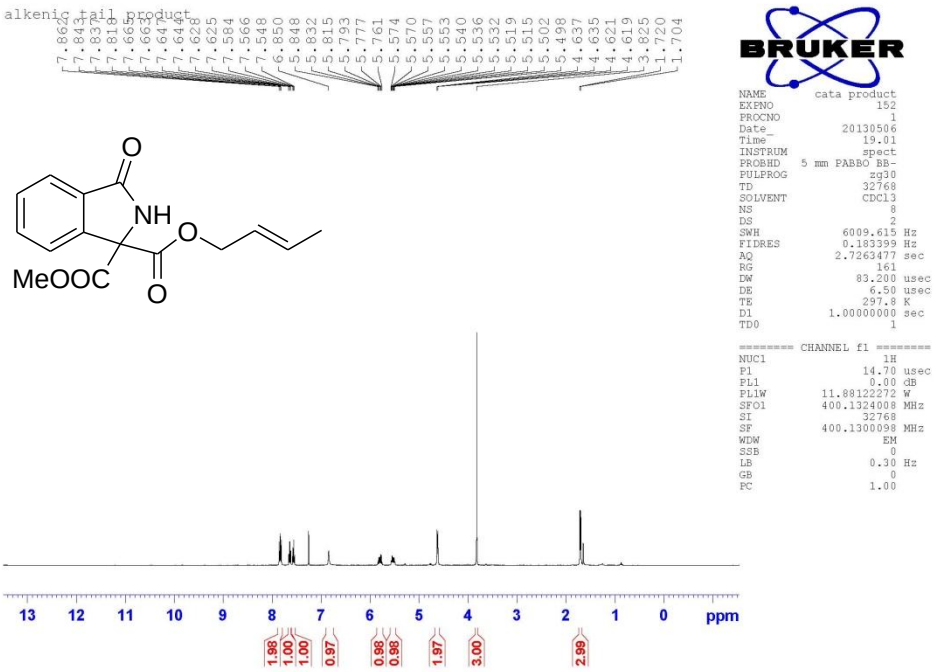

Figure A.136 ^{1}H NMR spectrum of **9n**

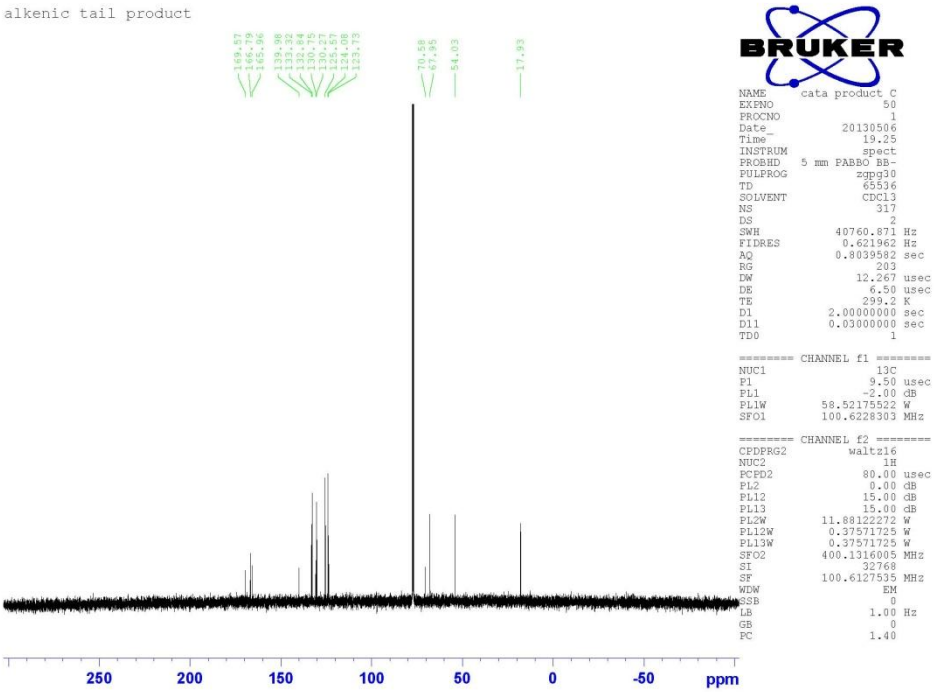

Figure A.137 ^{1}H NMR spectrum of **9o**

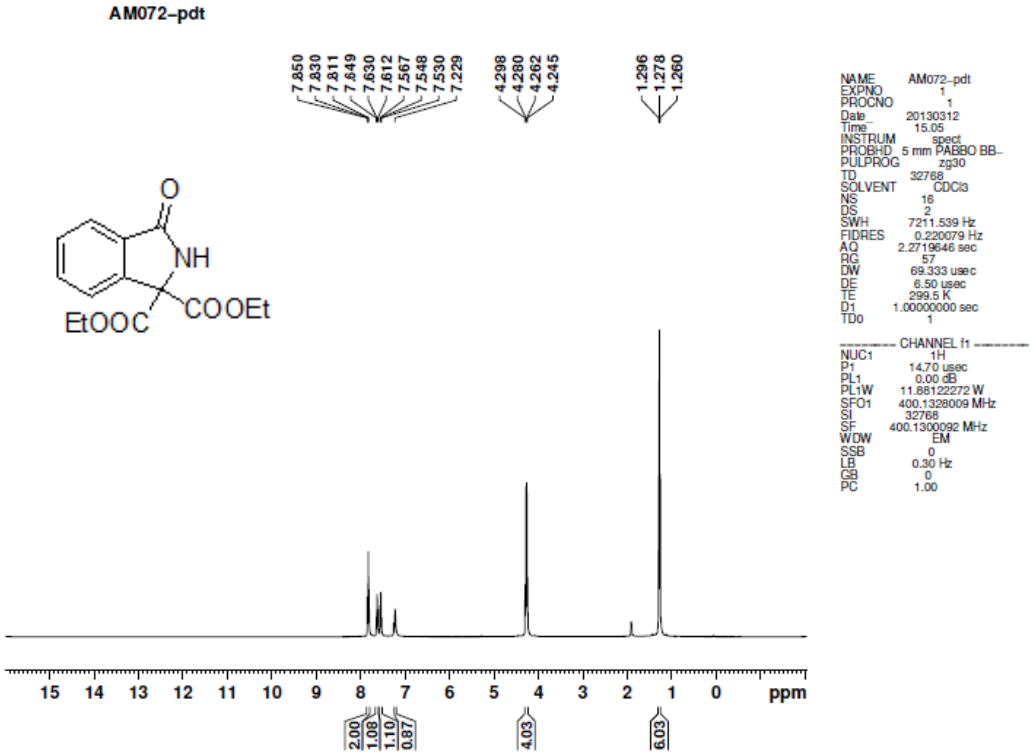

Figure A.138 ^{13}C NMR spectrum of **9o**

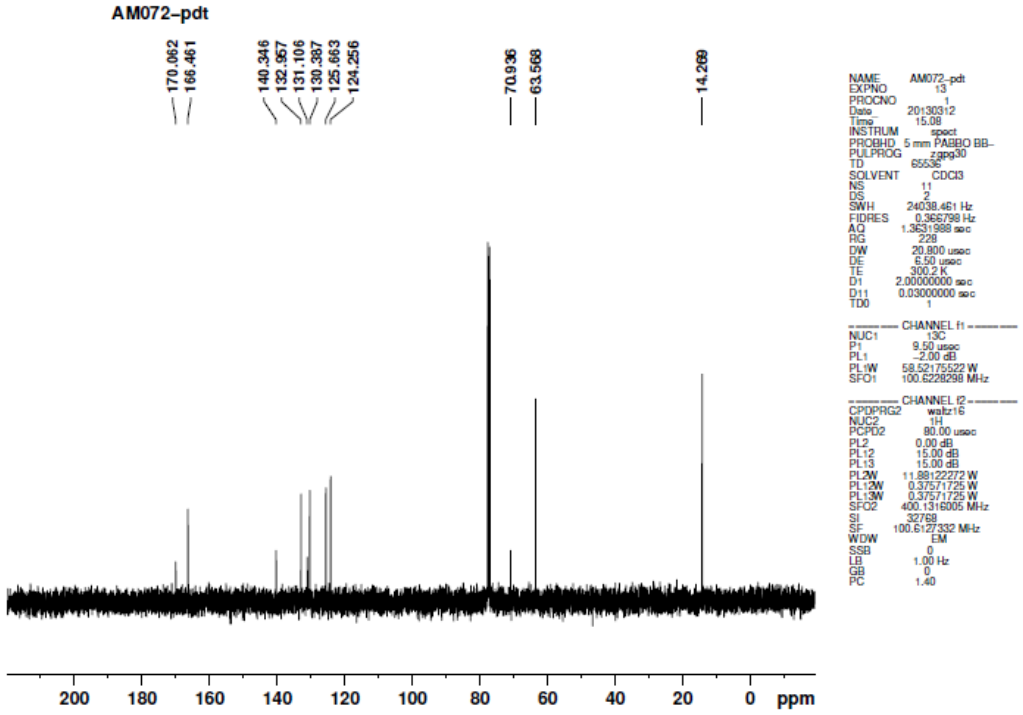

Figure A.139 ^{1}H NMR spectrum of **9p**

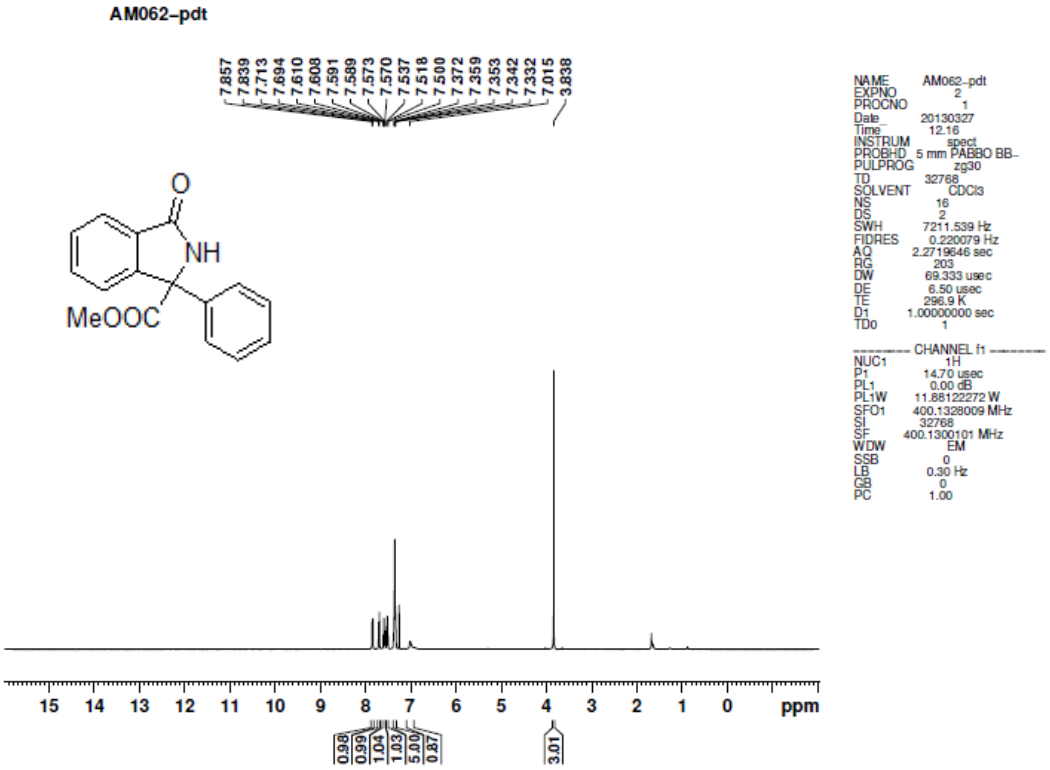

Figure A.140 ^{13}C NMR spectrum of **9p**

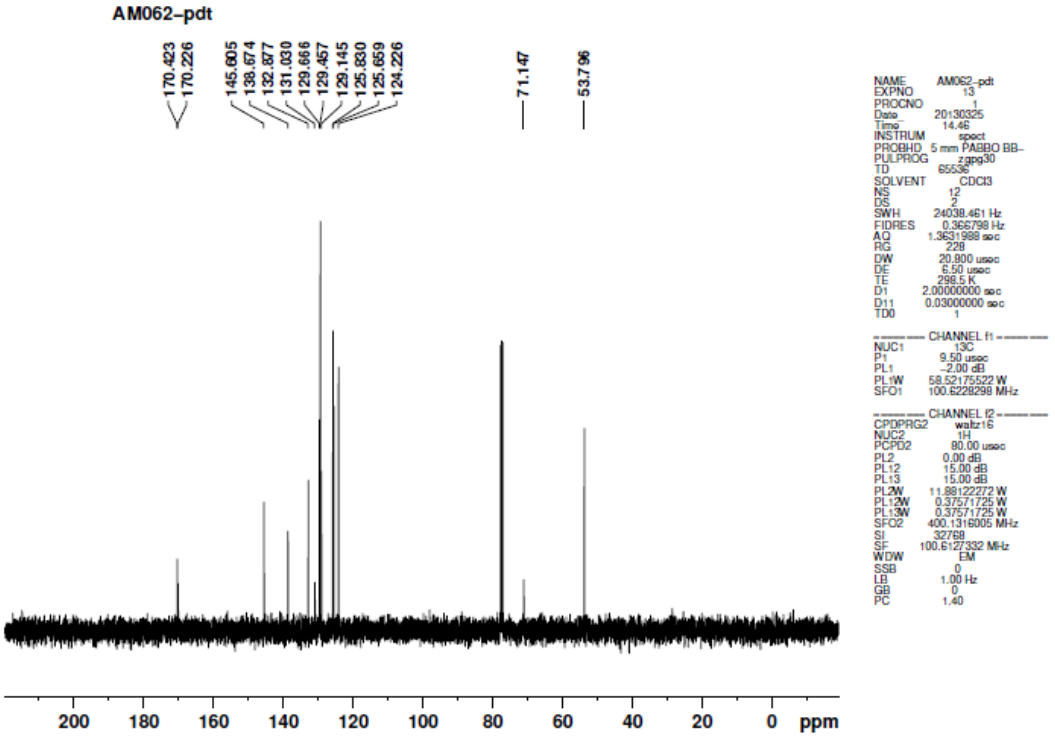

Figure A.141 ^{1}H NMR spectrum of **9q**

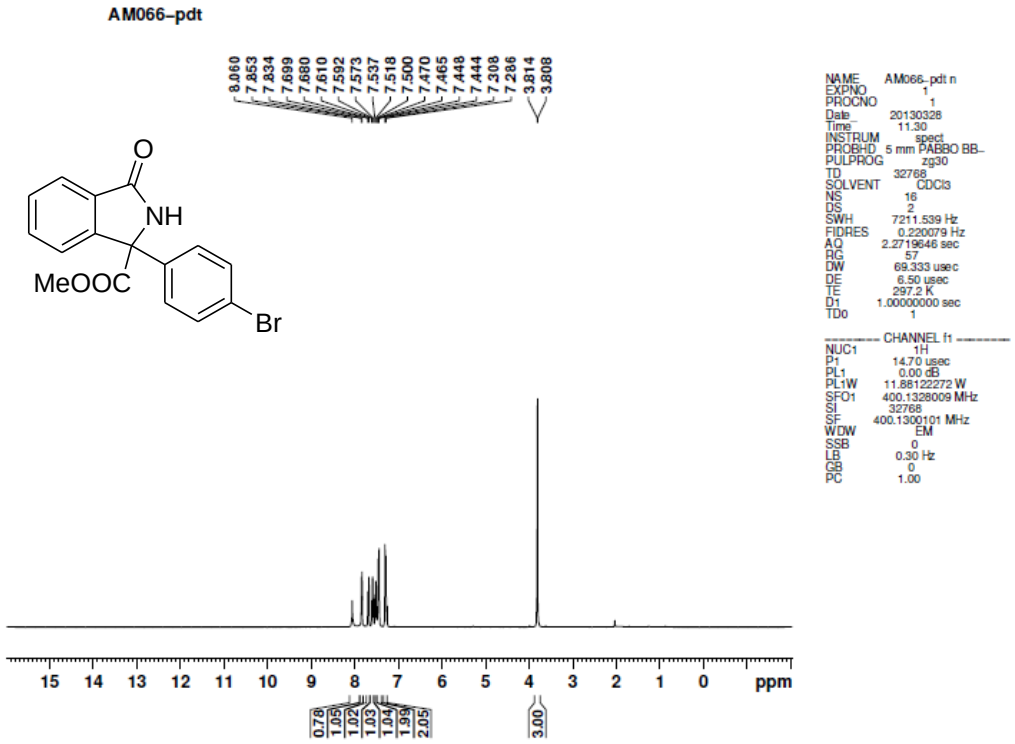

Figure A.142 ^{13}C NMR spectrum of **9q**

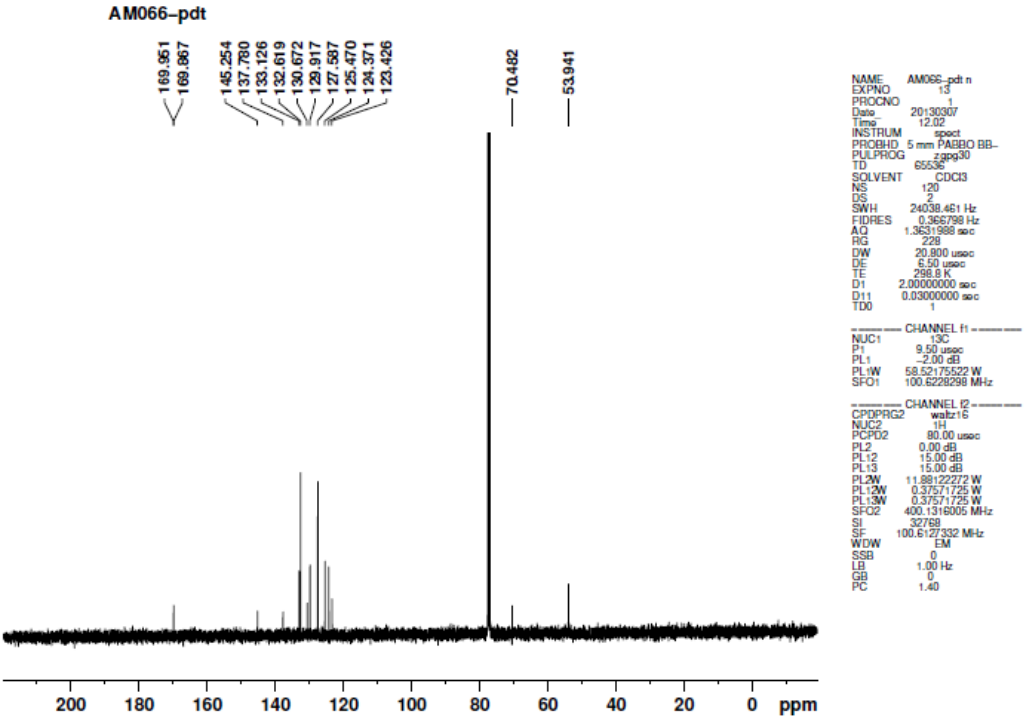

Figure A.143 ^{1}H NMR spectrum of **9r**

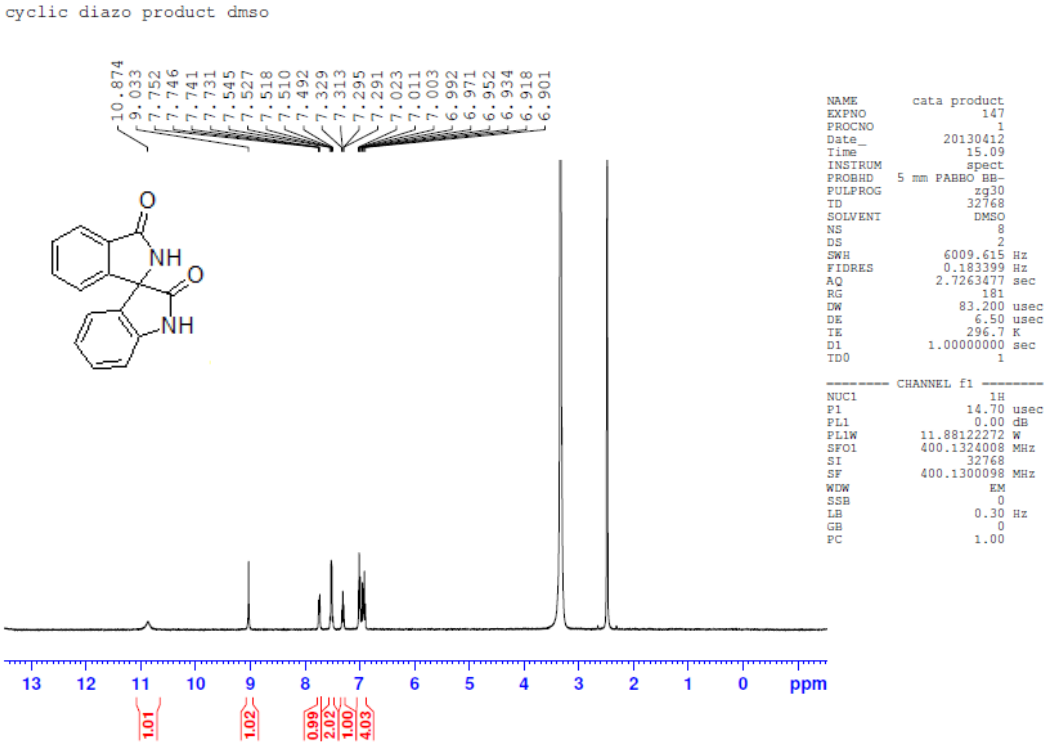

Figure A.144 ^{13}C NMR spectrum of **9r**

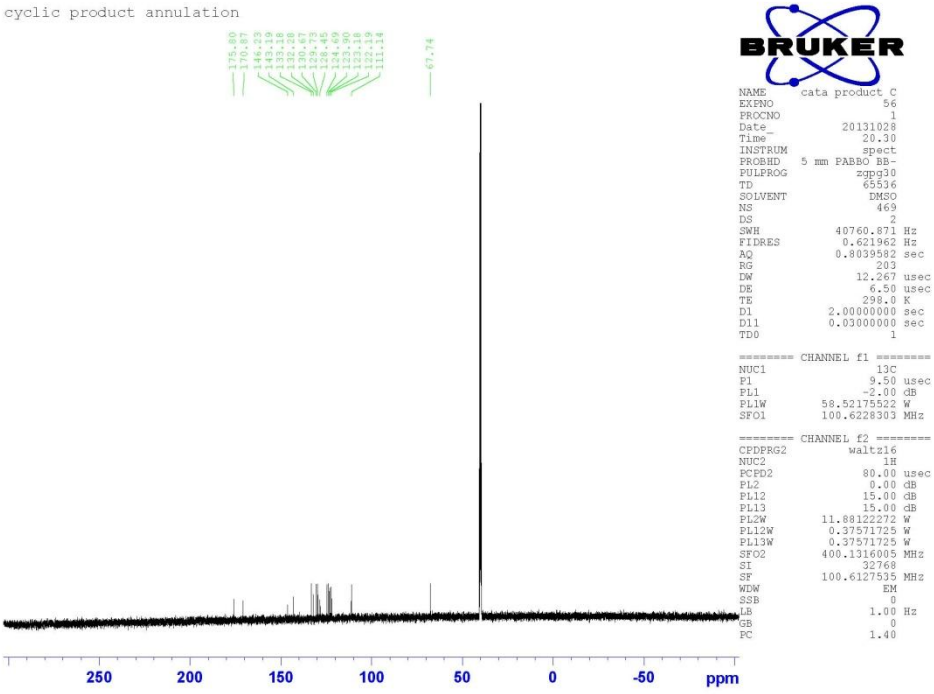

Figure A.145 ^{1}H NMR spectrum of **9s**

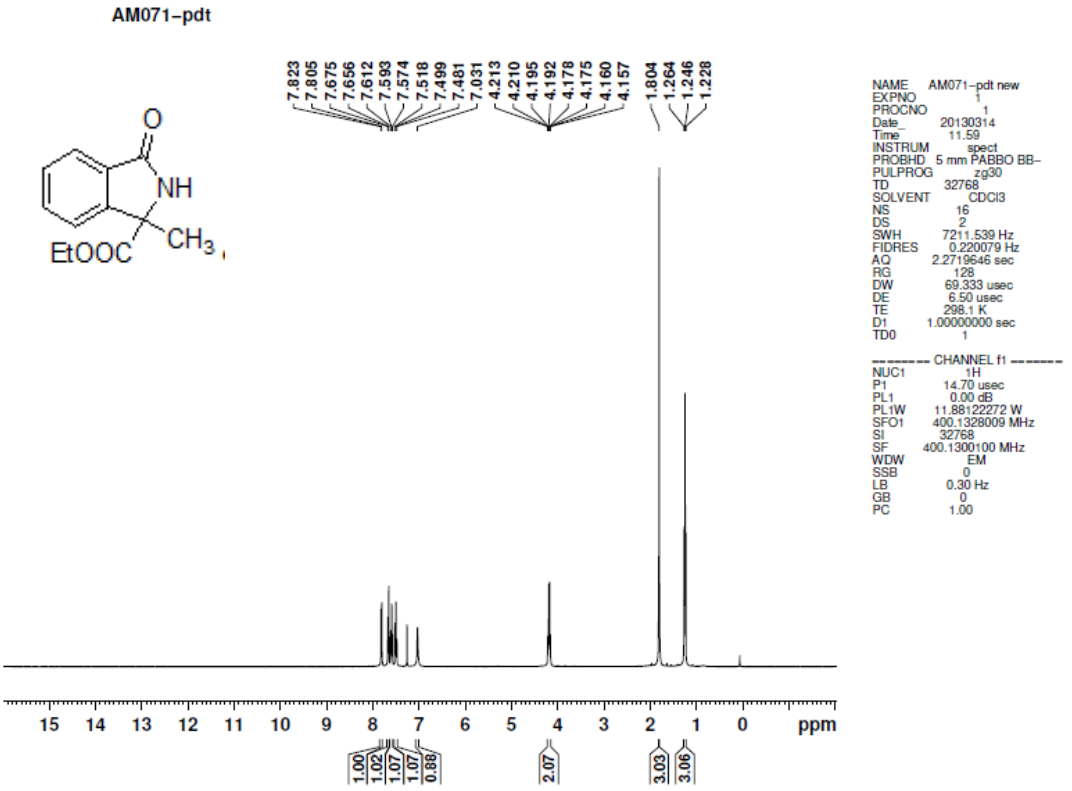

Figure A.146 ^{13}C NMR spectrum of **9s**

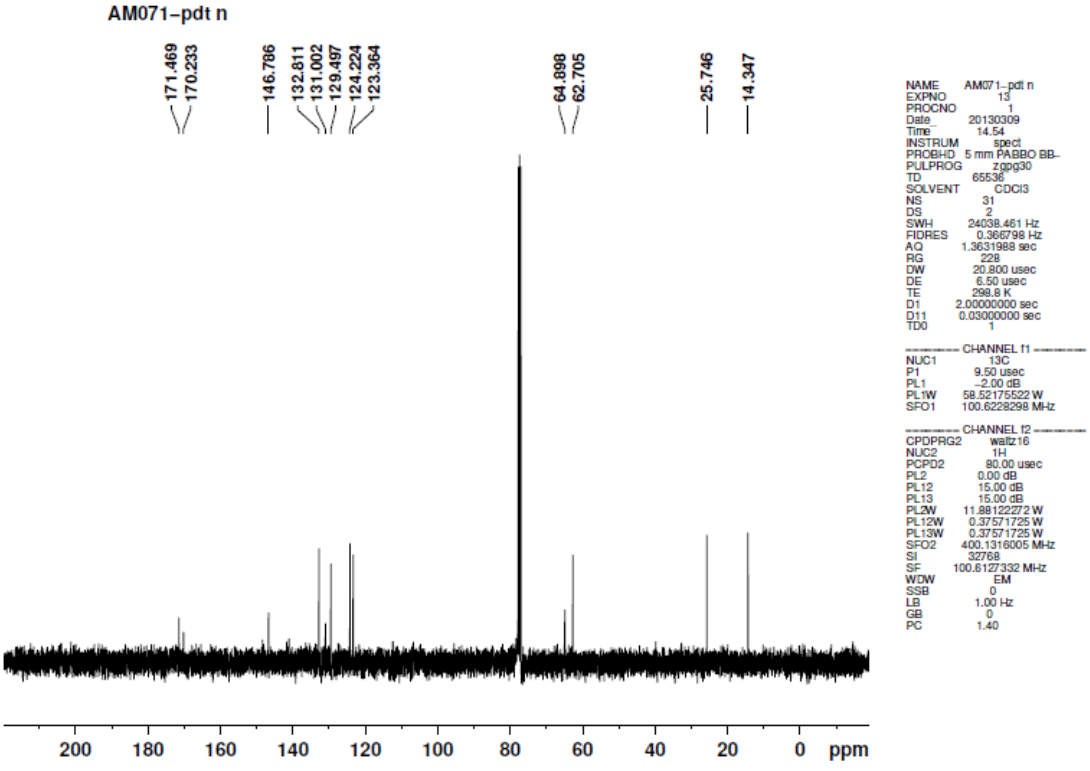

Figure A.147 ^{1}H NMR spectrum of **9t**

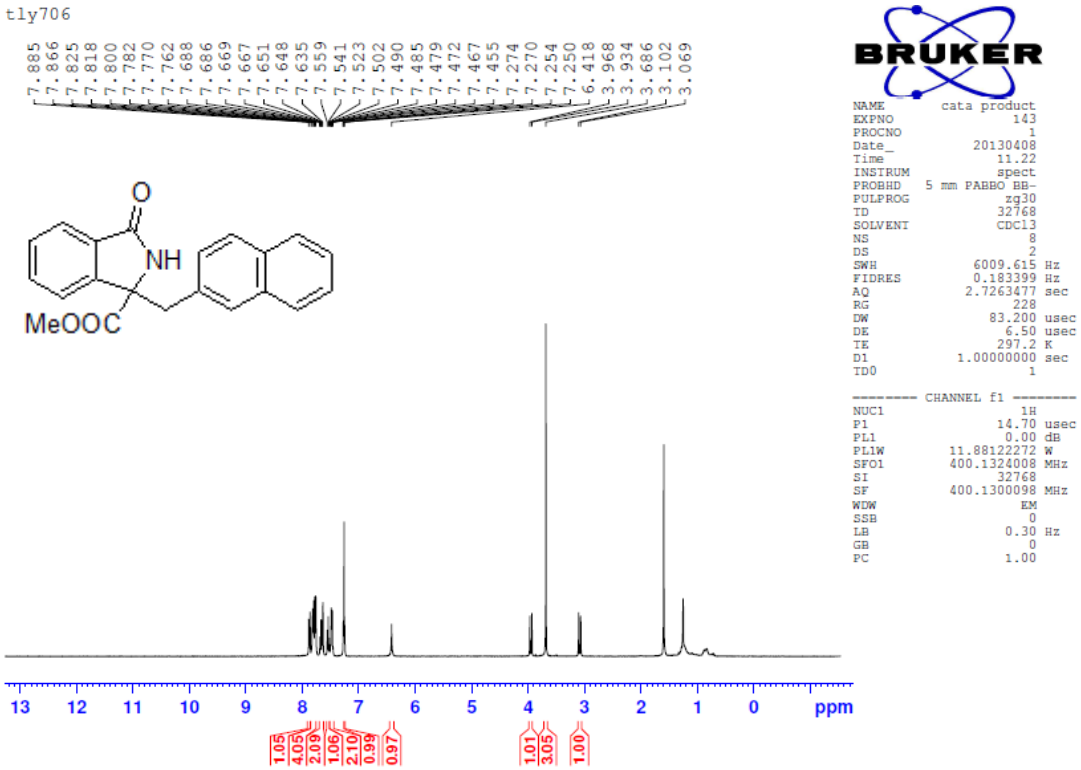

Figure A.148 ^{13}C NMR spectrum of **9t**

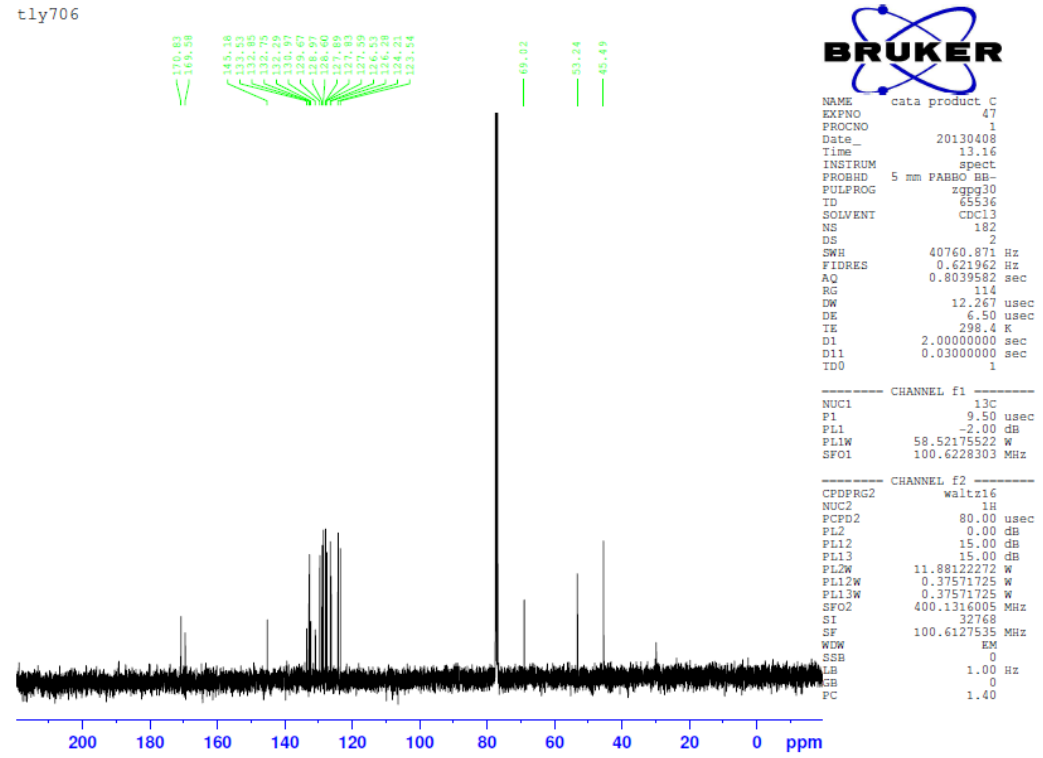

Figure A.149 ^{1}H NMR spectrum of **9u**

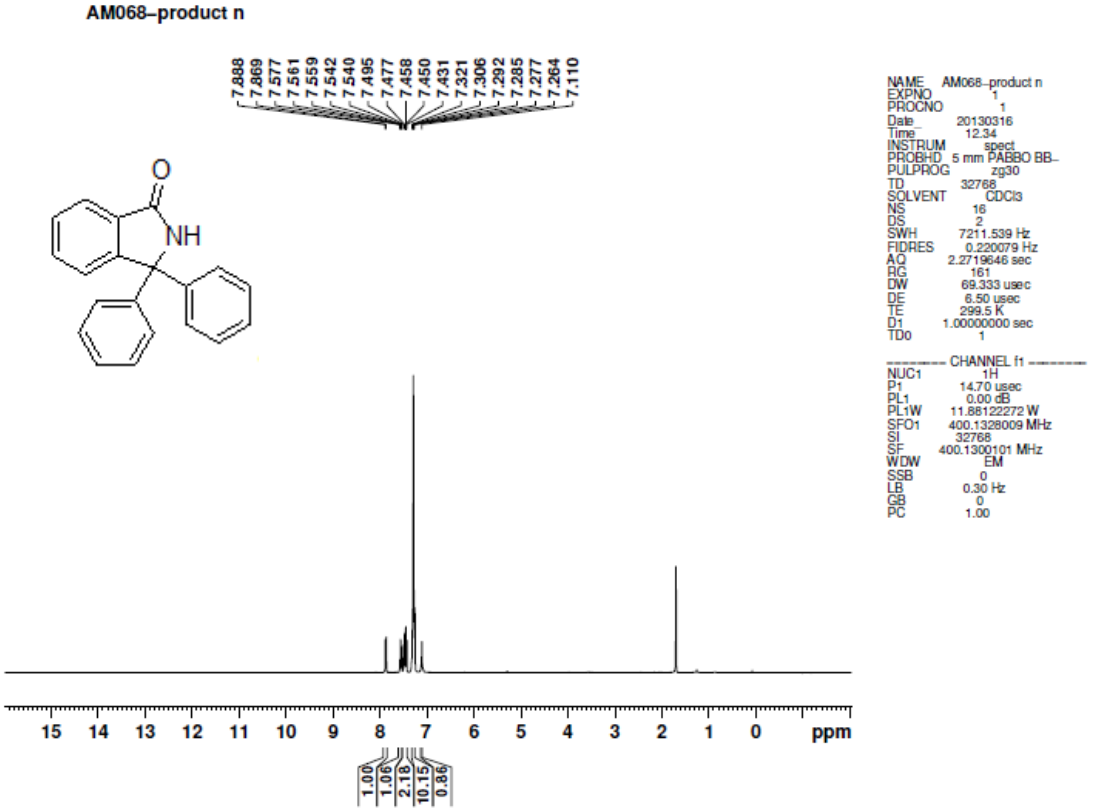

Figure A.150 ^{13}C NMR spectrum of **9u**

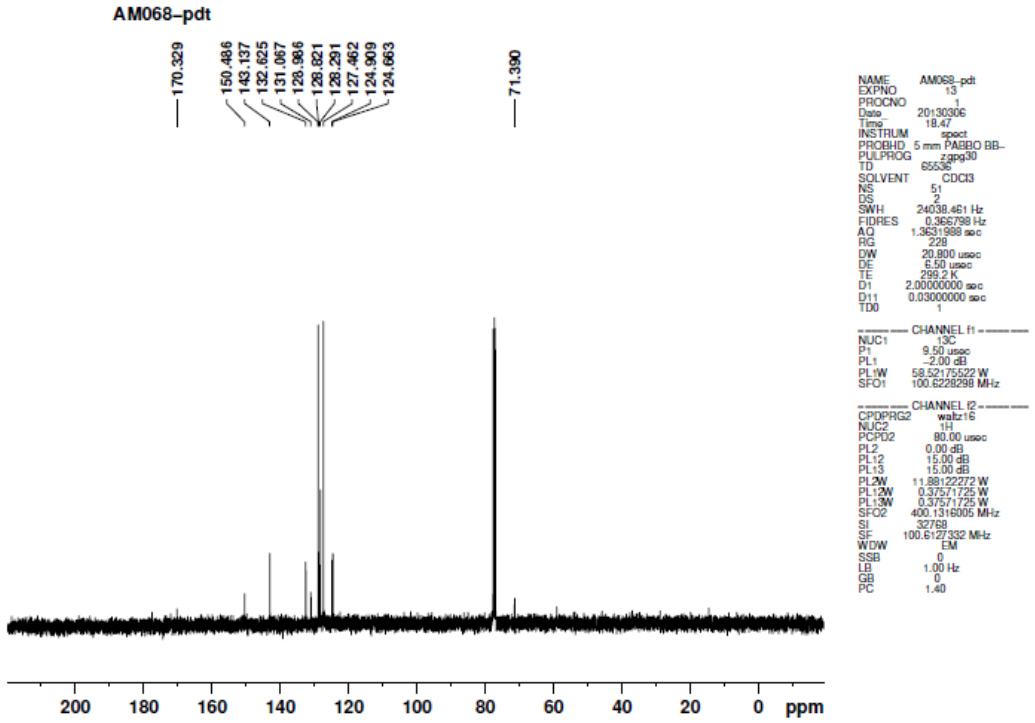

Figure A.151 ^{1}H NMR spectrum of **5a**

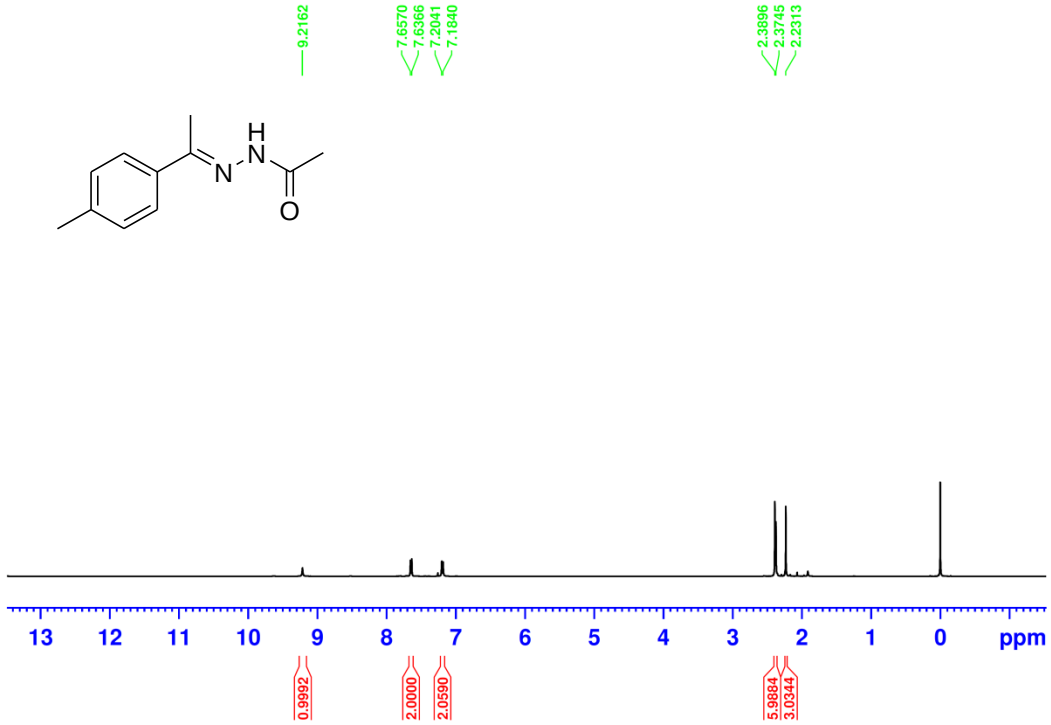

Figure A.152 ^{13}C NMR spectrum of **5a**

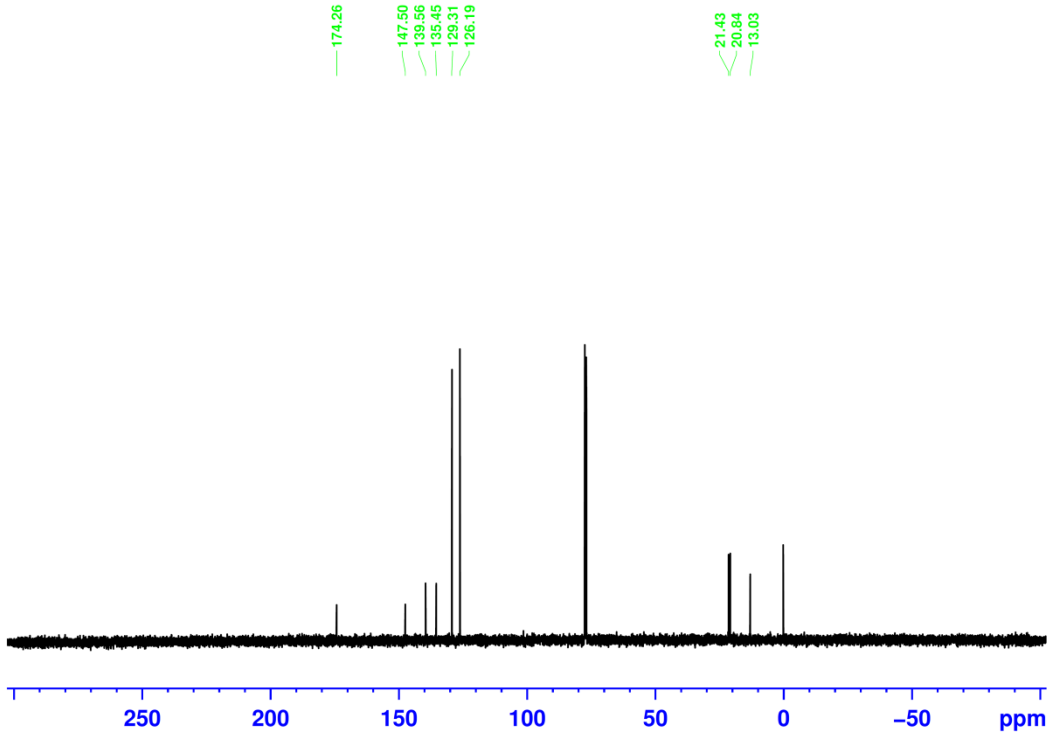

Figure A.153 ^{1}H NMR spectrum of **5b**

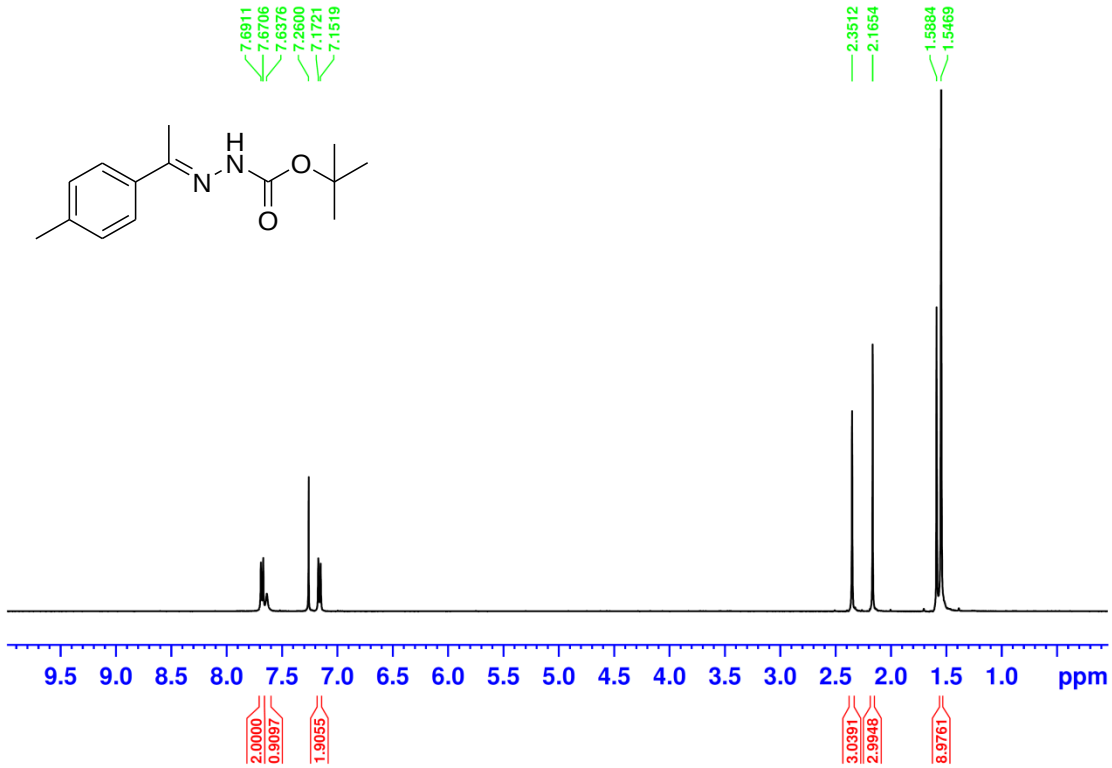

Figure A.154 ^{13}C NMR spectrum of **5b**

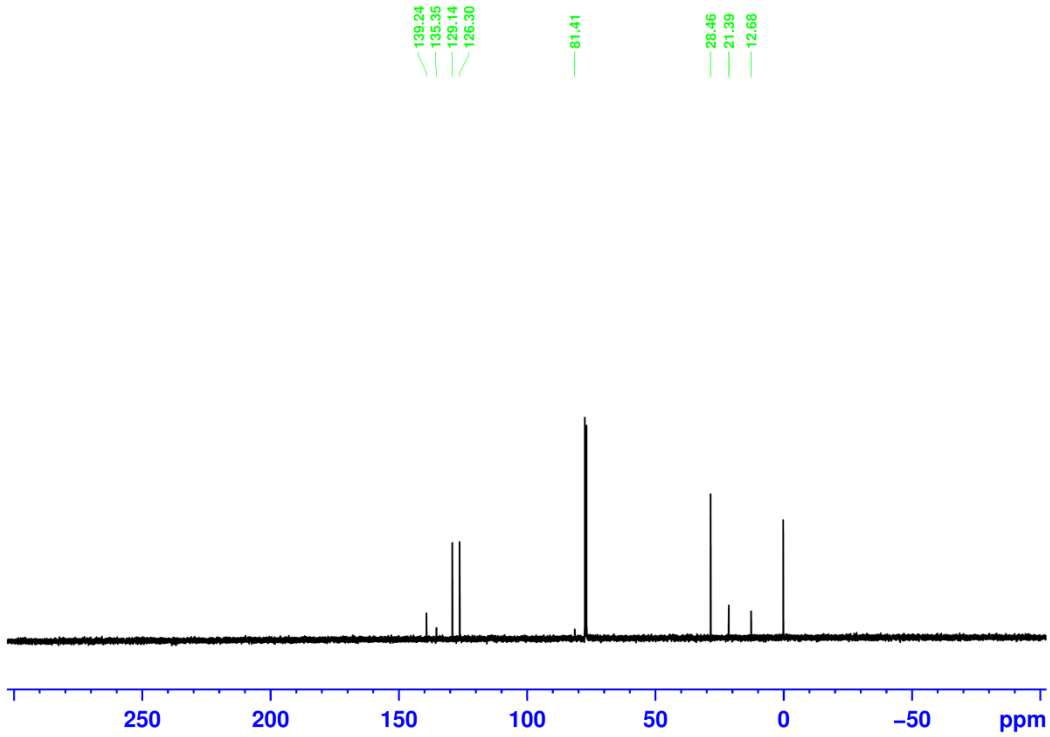

Figure A.155 ^{1}H NMR spectrum of **5c**

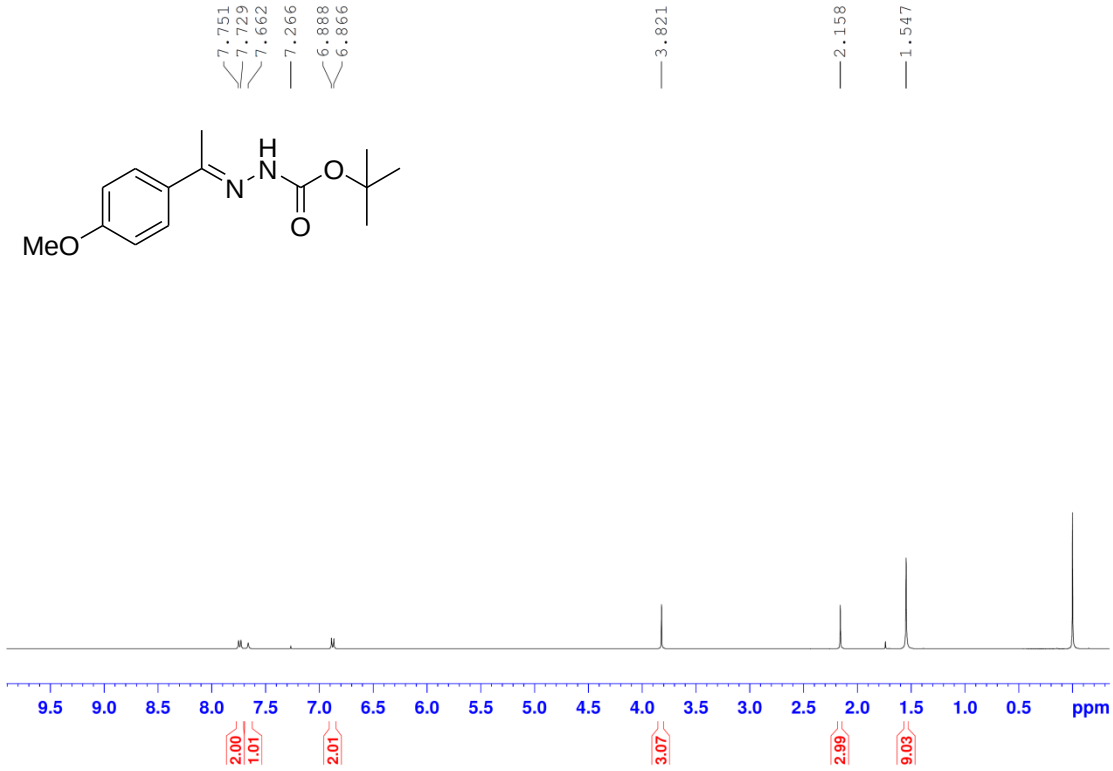

Figure A.156 ^{13}C NMR spectrum of **5c**

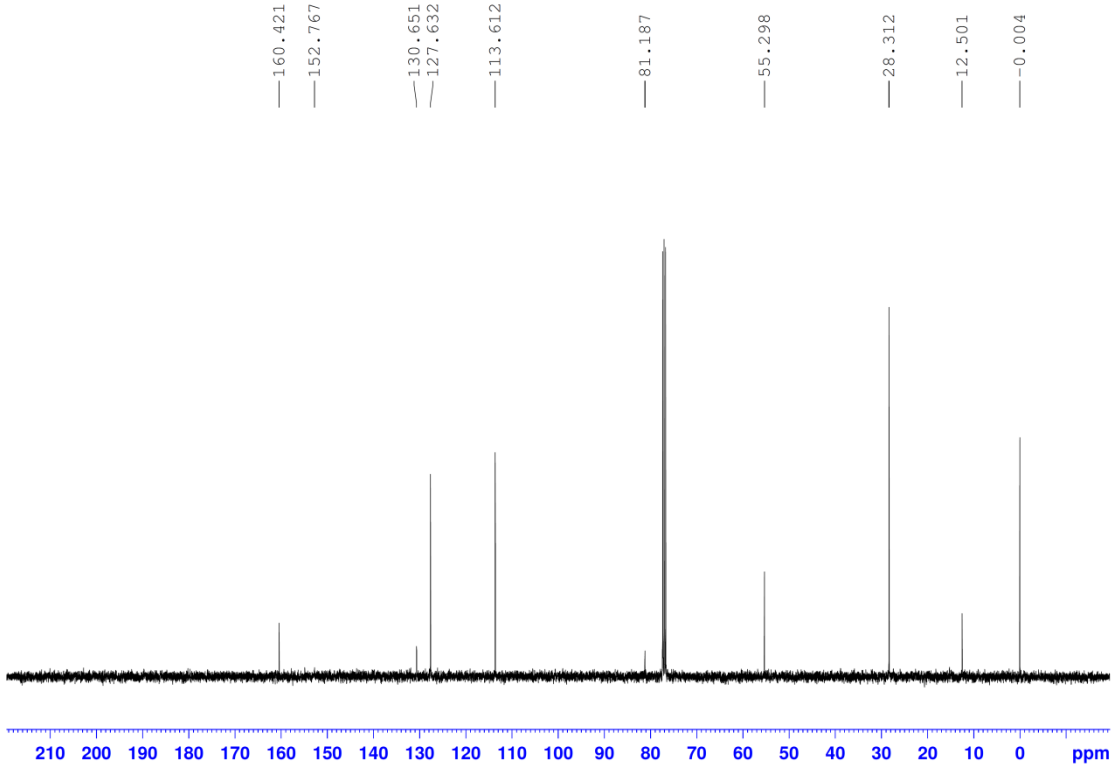

Figure A.157 ^{1}H NMR spectrum of **5d**

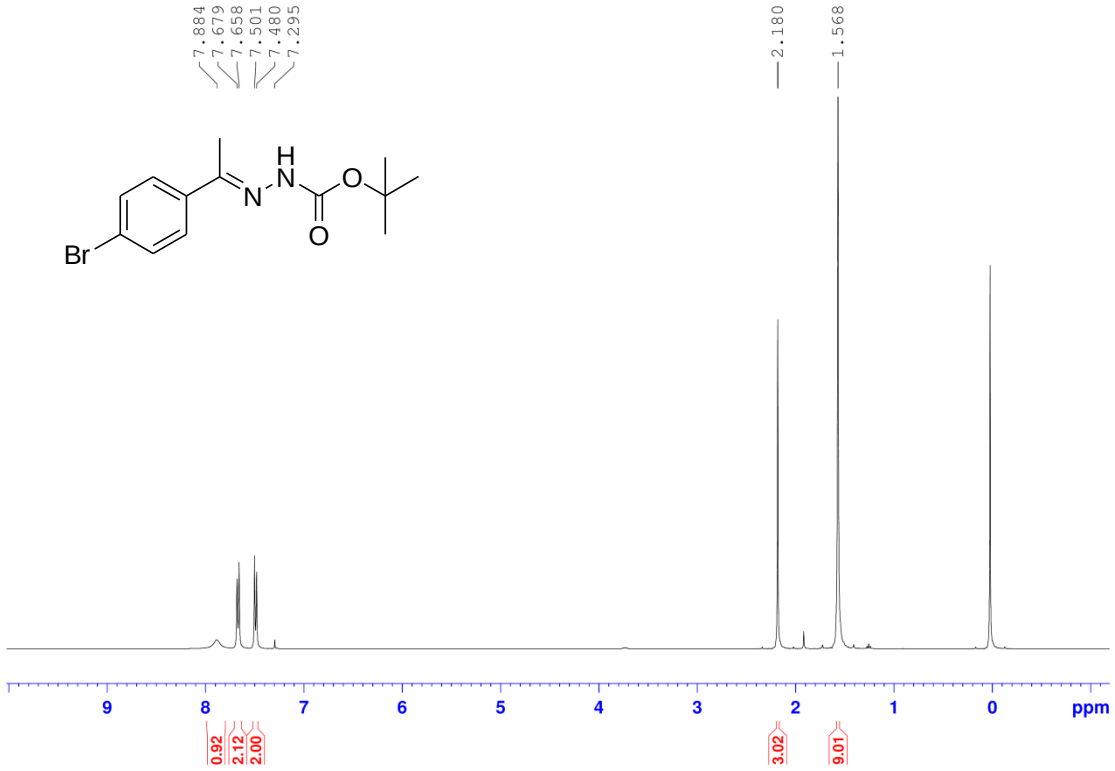

Figure A.158 ^{13}C NMR spectrum of **5d**

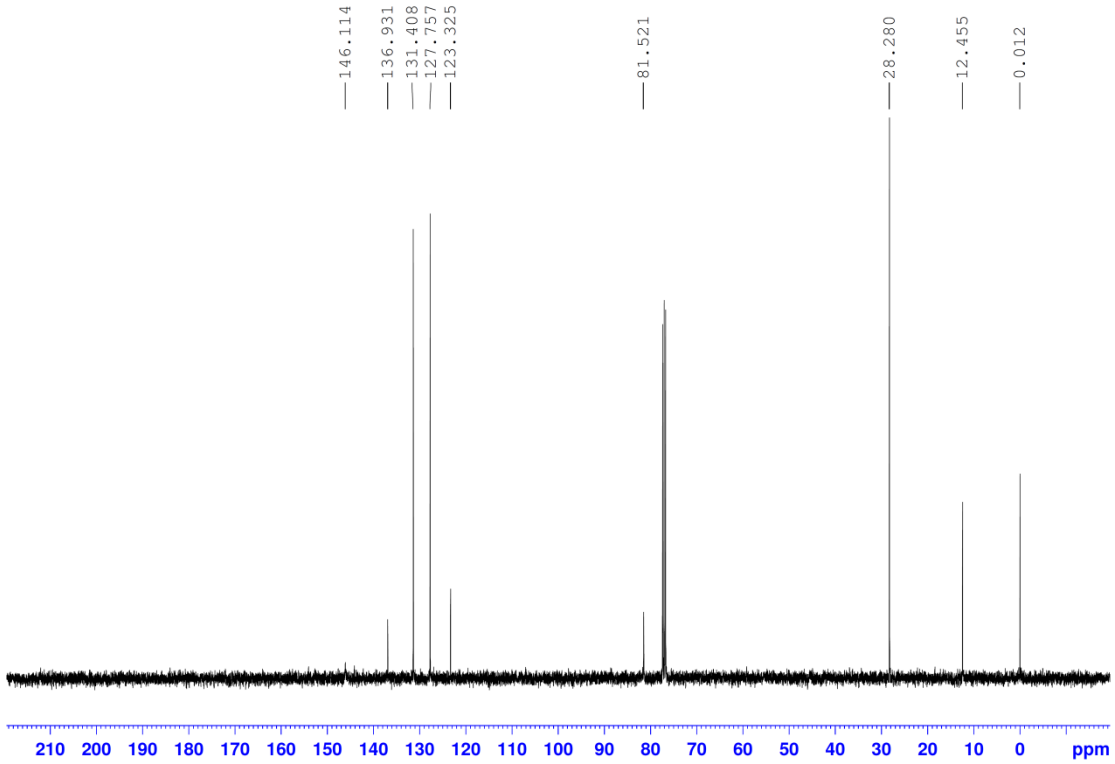

Figure A.159 ^{1}H NMR spectrum of **5e**

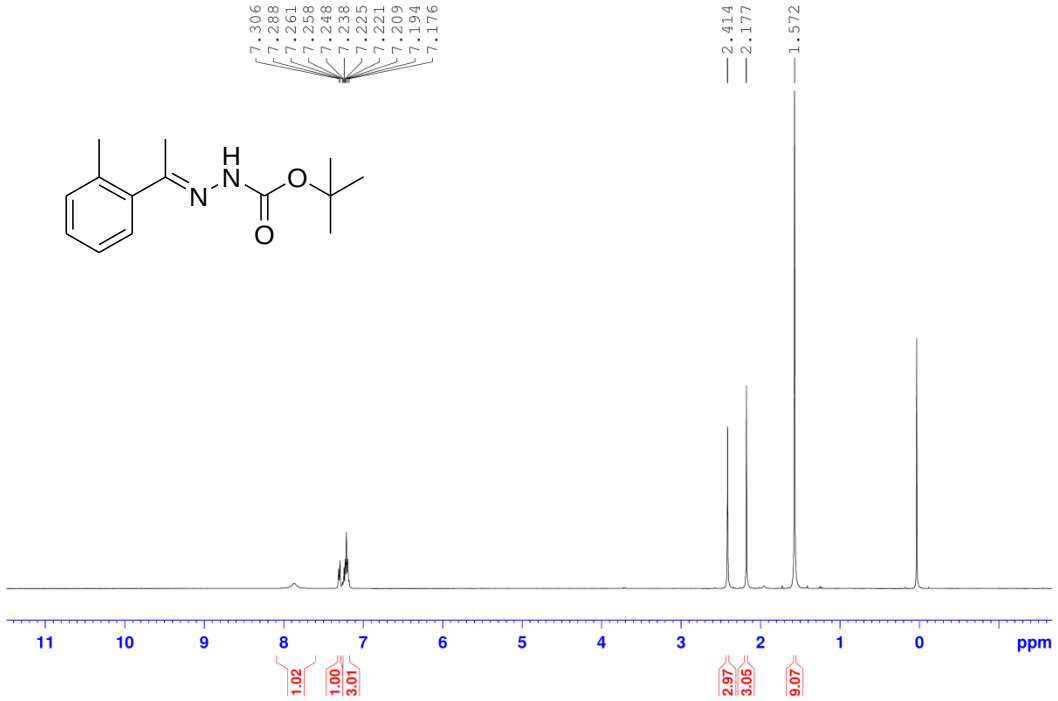

Figure A.160 ^{13}C NMR spectrum of **5e**

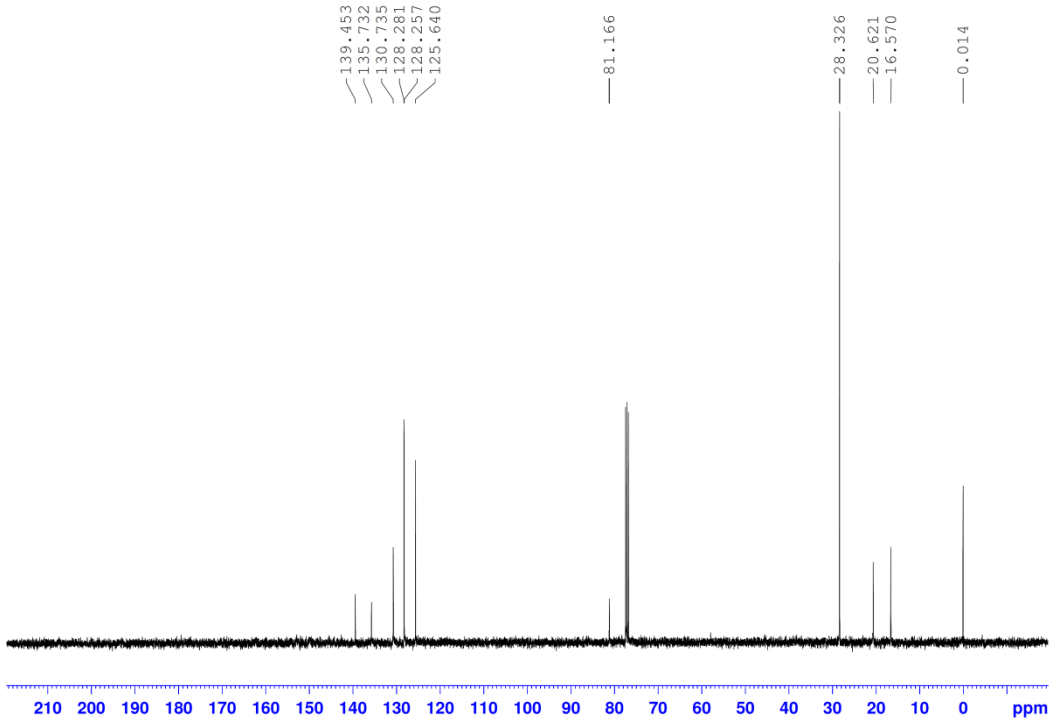

Figure A.161 ^{1}H NMR spectrum of **5f**

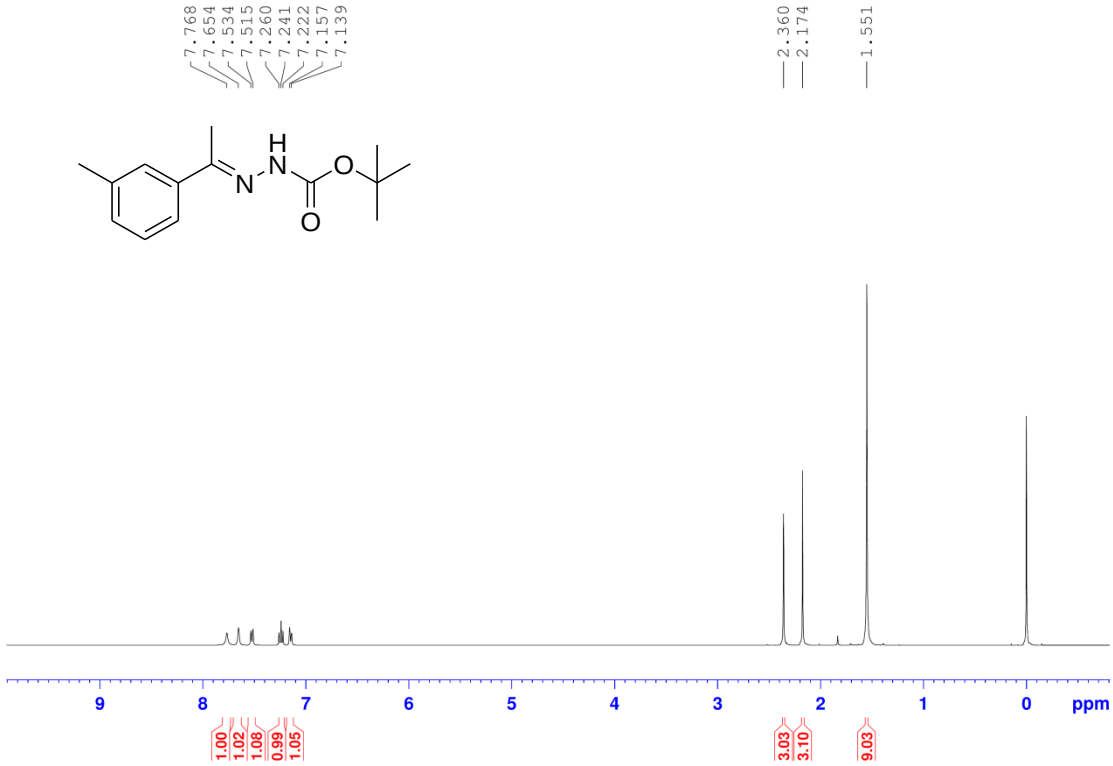

Figure A.162 ^{13}C NMR spectrum of **5f**

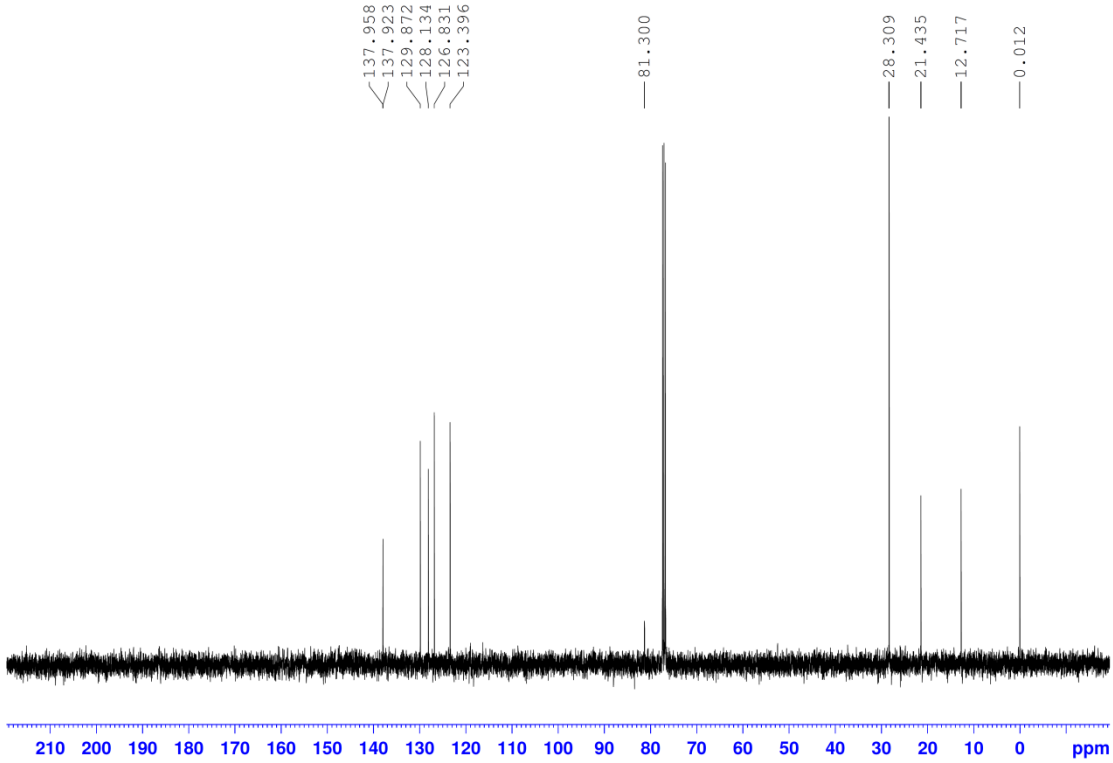

Figure A.163 ^{1}H NMR spectrum of **6**

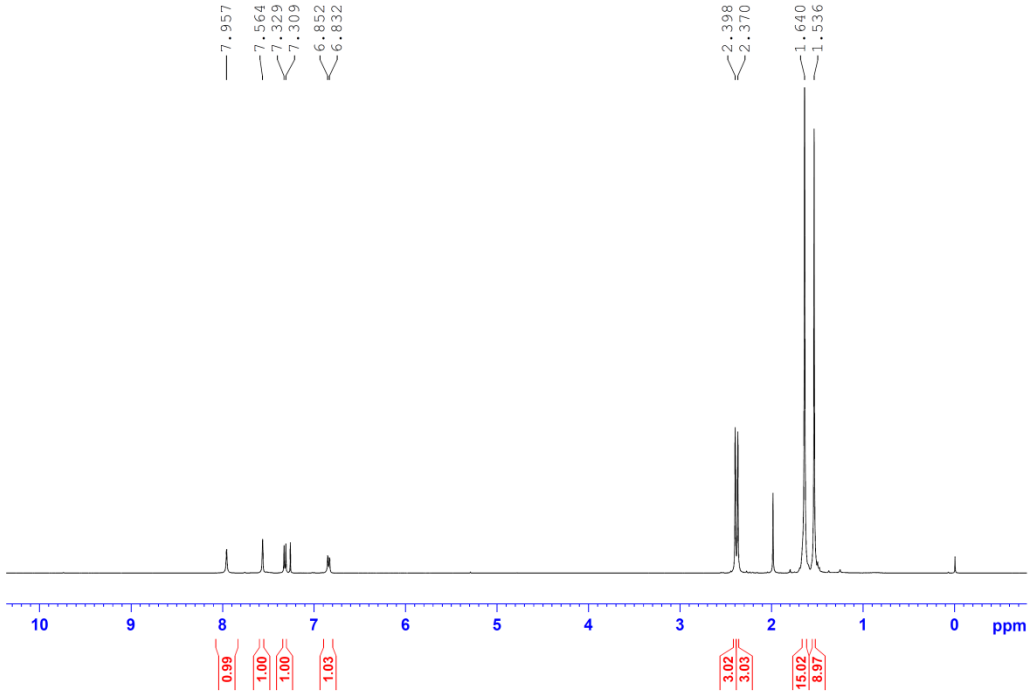

Figure A.164 ^{13}C NMR spectrum of **6**

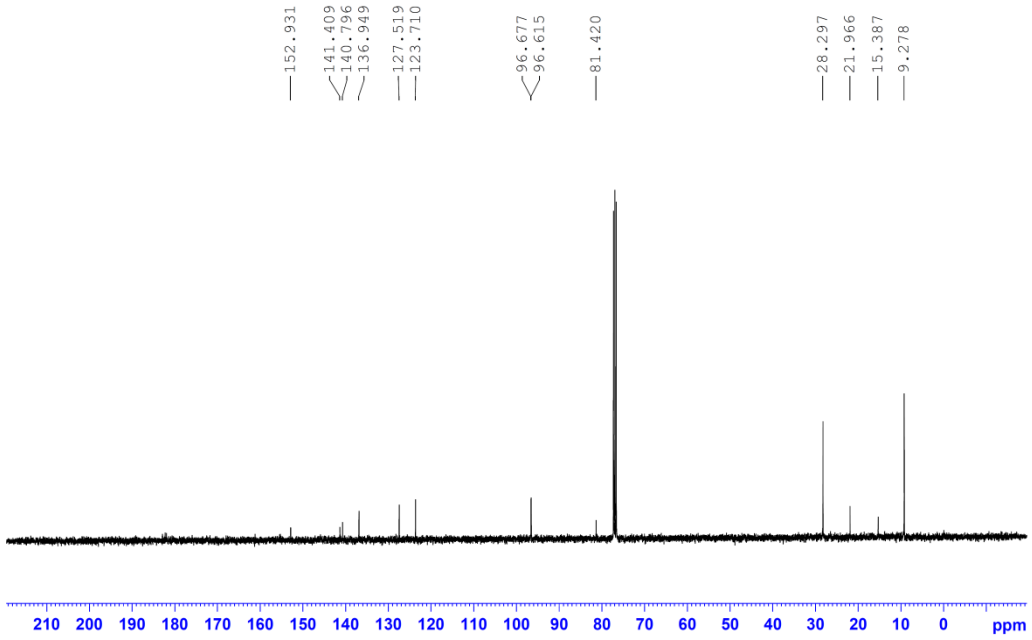

Figure A.165 Molecular structure of **9a**

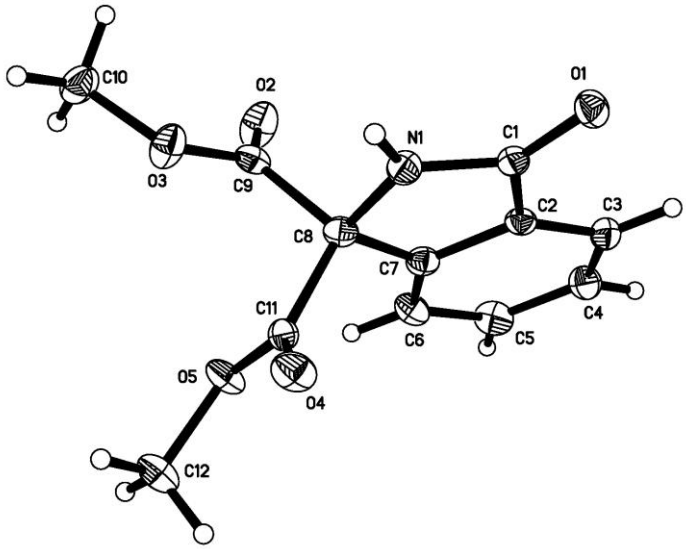

Table A01. Atomic coordinates (x 10^4) and equivalent isotropic displacement parameters (Å ^{2}x 10^3) for **9a**. U(eq) is defined as one third of the trace of the orthogonalized U^{ij} tensor.

	x	y	z	U(eq)
O(1)	-154(4)	6373(3)	3374(3)	52(1)
O(2)	1624(4)	772(4)	1259(4)	78(1)
O(3)	2328(4)	184(4)	3571(3)	64(1)
O(4)	4851(4)	2461(4)	4084(4)	63(1)
O(5)	5607(3)	765(4)	2097(3)	55(1)
N(1)	1523(4)	3734(4)	3431(4)	46(1)
C(1)	931(4)	5171(4)	2757(4)	40(1)
C(2)	1814(4)	5009(4)	1130(4)	40(1)
C(3)	1610(5)	6136(5)	-87(5)	52(1)
C(4)	2556(6)	5629(6)	-1478(5)	58(1)
C(5)	3674(6)	4079(7)	-1711(5)	63(1)
C(6)	3879(5)	2963(6)	-517(5)	55(1)
C(7)	2941(4)	3453(5)	913(4)	45(1)
C(8)	2808(4)	2550(5)	2423(4)	43(1)
C(9)	2160(4)	1076(5)	2335(4)	45(1)

C(10)	1836(6)	-1268(6)	3622(6)	66(1)
C(11)	4547(4)	1931(4)	2998(4)	39(1)
C(12)	7310(6)	-49(7)	2504(6)	65(1)

Table A02. Bond lengths [Å] and angles [°] for **9a**.

O(1)-C(1)	1.231(4)
O(2)-C(9)	1.197(5)
O(3)-C(9)	1.299(5)
O(3)-C(10)	1.446(5)
O(4)-C(11)	1.191(5)
O(5)-C(11)	1.317(4)
O(5)-C(12)	1.464(5)
N(1)-C(1)	1.336(5)
N(1)-C(8)	1.443(4)
N(1)-H(1A)	0.8600
C(1)-C(2)	1.483(5)
C(2)-C(7)	1.388(5)
C(2)-C(3)	1.403(6)
C(3)-C(4)	1.350(6)
C(3)-H(3A)	0.9300
C(4)-C(5)	1.384(7)
C(4)-H(4A)	0.9300
C(5)-C(6)	1.382(7)
C(5)-H(5A)	0.9300
C(6)-C(7)	1.374(5)
C(6)-H(6A)	0.9300
C(7)-C(8)	1.506(5)
C(8)-C(11)	1.538(5)
C(8)-C(9)	1.555(6)
C(10)-H(10A)	0.9600
C(10)-H(10B)	0.9600
C(10)-H(10C)	0.9600
C(12)-H(12A)	0.9600
C(12)-H(12B)	0.9600
C(12)-H(12C)	0.9600

C(9)-O(3)-C(10)	116.9(3)
C(11)-O(5)-C(12)	117.7(3)
C(1)-N(1)-C(8)	113.9(3)
C(1)-N(1)-H(1A)	123.1
C(8)-N(1)-H(1A)	123.1

O(1)-C(1)-N(1)	126.2(3)
O(1)-C(1)-C(2)	127.4(3)
N(1)-C(1)-C(2)	106.4(3)
C(7)-C(2)-C(3)	121.5(3)
C(7)-C(2)-C(1)	108.8(3)
C(3)-C(2)-C(1)	129.7(3)
C(4)-C(3)-C(2)	116.7(4)
C(4)-C(3)-H(3A)	121.6
C(2)-C(3)-H(3A)	121.6
C(3)-C(4)-C(5)	122.3(4)
C(3)-C(4)-H(4A)	118.8
C(5)-C(4)-H(4A)	118.8
C(6)-C(5)-C(4)	121.2(4)
C(6)-C(5)-H(5A)	119.4
C(4)-C(5)-H(5A)	119.4
C(7)-C(6)-C(5)	117.5(4)
C(7)-C(6)-H(6A)	121.2
C(5)-C(6)-H(6A)	121.2
C(6)-C(7)-C(2)	120.7(4)
C(6)-C(7)-C(8)	131.3(4)
C(2)-C(7)-C(8)	108.0(3)
N(1)-C(8)-C(7)	102.9(3)
N(1)-C(8)-C(11)	112.6(3)
C(7)-C(8)-C(11)	112.0(3)
N(1)-C(8)-C(9)	109.0(3)
C(7)-C(8)-C(9)	112.8(3)
C(11)-C(8)-C(9)	107.6(3)
O(2)-C(9)-O(3)	124.2(4)
O(2)-C(9)-C(8)	124.9(4)
O(3)-C(9)-C(8)	110.9(3)
O(3)-C(10)-H(10A)	109.5
O(3)-C(10)-H(10B)	109.5
H(10A)-C(10)-H(10B)	109.5
O(3)-C(10)-H(10C)	109.5
H(10A)-C(10)-H(10C)	109.5
H(10B)-C(10)-H(10C)	109.5
O(4)-C(11)-O(5)	126.9(3)
O(4)-C(11)-C(8)	123.9(3)

O(5)-C(11)-C(8)	109.2(3)
O(5)-C(12)-H(12A)	109.5
O(5)-C(12)-H(12B)	109.5
H(12A)-C(12)-H(12B)	109.5
O(5)-C(12)-H(12C)	109.5
H(12A)-C(12)-H(12C)	109.5
H(12B)-C(12)-H(12C)	109.5

Symmetry transformations used to generate equivalent atoms:

Table A03. Anisotropic displacement parameters ($Å^2 x\ 10^3$)for **9a**. The anisotropic displacement factor exponent takes the form: $-2\ ^2[\ h^2 a^{*2} U^{11} + ... + 2\ h\ k\ a^*\ b^*\ U^{12}\ ]$

	U^{11}	U^{22}	U^{33}	U^{23}	U^{13}	U^{12}
O(1)	51(1)	43(1)	54(2)	-7(1)	-3(1)	-8(1)
O(2)	119(2)	78(2)	65(2)	16(1)	-53(2)	-56(2)
O(3)	93(2)	61(2)	59(2)	11(1)	-35(1)	-42(1)
O(4)	58(1)	69(2)	67(2)	-17(1)	-25(1)	-17(1)
O(5)	39(1)	57(2)	62(2)	-19(1)	-17(1)	4(1)
N(1)	47(1)	45(2)	43(2)	-6(1)	2(1)	-14(1)
C(1)	37(1)	40(2)	46(2)	-2(1)	-9(1)	-15(1)
C(2)	33(1)	44(2)	46(2)	-3(1)	-10(1)	-14(1)
C(3)	50(2)	46(2)	61(2)	7(2)	-14(2)	-16(2)
C(4)	58(2)	62(2)	54(2)	19(2)	-21(2)	-17(2)
C(5)	61(2)	85(3)	41(2)	-3(2)	-6(2)	-21(2)
C(6)	45(2)	60(2)	52(2)	-9(2)	-7(2)	-5(2)
C(7)	41(1)	51(2)	47(2)	-5(1)	-12(1)	-18(1)
C(8)	39(1)	52(2)	38(2)	-3(1)	-8(1)	-15(1)
C(9)	33(1)	51(2)	51(2)	-12(2)	-10(1)	-8(1)
C(10)	73(2)	64(2)	74(3)	4(2)	-18(2)	-39(2)
C(11)	41(1)	40(2)	35(2)	4(1)	-9(1)	-12(1)
C(12)	50(2)	72(3)	65(3)	-9(2)	-23(2)	1(2)

Table A04. Hydrogen coordinates (x 10^4) and isotropic displacement parameters (Å ^{2}x 10^3) for **9a**.

	x	y	z	U(eq)
H(1A)	1172	3534	4379	55
H(3A)	860	7180	57	62
H(4A)	2452	6348	-2309	69
H(5A)	4301	3782	-2689	76
H(6A)	4623	1918	-676	66
H(10A)	1978	-1807	4597	98
H(10B)	2553	-1969	2807	98
H(10C)	651	-993	3497	98
H(12A)	7956	-861	1757	98
H(12B)	7177	-543	3505	98
H(12C)	7913	724	2516	98

Table A05. Torsion angles [°] for **9a**.

C(8)-N(1)-C(1)-O(1)	-179.5(4)
C(8)-N(1)-C(1)-C(2)	1.5(4)
O(1)-C(1)-C(2)-C(7)	180.0(4)
N(1)-C(1)-C(2)-C(7)	-1.0(4)
O(1)-C(1)-C(2)-C(3)	-1.8(6)
N(1)-C(1)-C(2)-C(3)	177.2(4)
C(7)-C(2)-C(3)-C(4)	0.3(6)
C(1)-C(2)-C(3)-C(4)	-177.7(4)
C(2)-C(3)-C(4)-C(5)	0.1(7)
C(3)-C(4)-C(5)-C(6)	0.0(8)
C(4)-C(5)-C(6)-C(7)	-0.5(7)
C(5)-C(6)-C(7)-C(2)	1.0(6)
C(5)-C(6)-C(7)-C(8)	177.6(4)
C(3)-C(2)-C(7)-C(6)	-0.9(6)
C(1)-C(2)-C(7)-C(6)	177.5(4)
C(3)-C(2)-C(7)-C(8)	-178.2(3)
C(1)-C(2)-C(7)-C(8)	0.2(4)
C(1)-N(1)-C(8)-C(7)	-1.4(4)
C(1)-N(1)-C(8)-C(11)	119.3(4)
C(1)-N(1)-C(8)-C(9)	-121.4(3)
C(6)-C(7)-C(8)-N(1)	-176.3(4)
C(2)-C(7)-C(8)-N(1)	0.7(4)
C(6)-C(7)-C(8)-C(11)	62.6(5)
C(2)-C(7)-C(8)-C(11)	-120.5(3)
C(6)-C(7)-C(8)-C(9)	-59.0(5)
C(2)-C(7)-C(8)-C(9)	118.0(3)
C(10)-O(3)-C(9)-O(2)	0.4(6)
C(10)-O(3)-C(9)-C(8)	-177.7(3)
N(1)-C(8)-C(9)-O(2)	105.3(4)
C(7)-C(8)-C(9)-O(2)	-8.4(5)
C(11)-C(8)-C(9)-O(2)	-132.4(4)
N(1)-C(8)-C(9)-O(3)	-76.7(4)
C(7)-C(8)-C(9)-O(3)	169.7(3)
C(11)-C(8)-C(9)-O(3)	45.7(4)
C(12)-O(5)-C(11)-O(4)	4.0(6)
C(12)-O(5)-C(11)-C(8)	-176.7(4)

N(1)-C(8)-C(11)-O(4)	-5.8(5)
C(7)-C(8)-C(11)-O(4)	109.6(4)
C(9)-C(8)-C(11)-O(4)	-125.9(4)
N(1)-C(8)-C(11)-O(5)	174.9(3)
C(7)-C(8)-C(11)-O(5)	-69.7(4)
C(9)-C(8)-C(11)-O(5)	54.8(4)

Symmetry transformations used to generate equivalent atoms:

Table A06. Hydrogen bonds for **9a** [Å and °].

D-H...A	d(D-H)	d(H...A)	d(D...A)	<(DHA)
N(1)-H(1A)...O(1)#1	0.86	2.00	2.849(4)	166.6

Symmetry transformations used to generate equivalent atoms:
#1 -x,-y+1,-z+1

Figure A.166 Molecular structure of **[Rh($C_{19}H_{21}NO_3$)]$_2$**

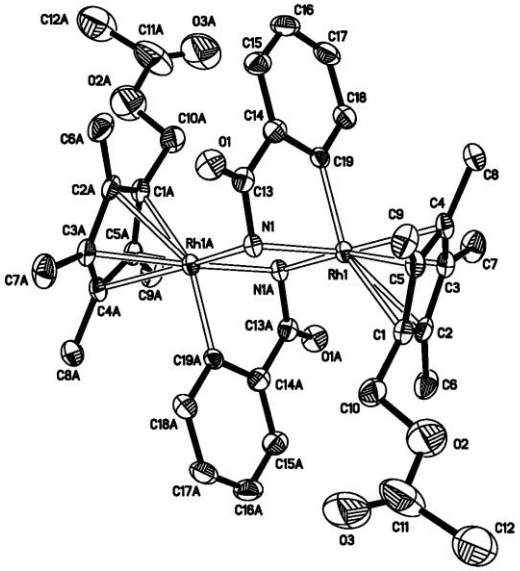

Table A07. Atomic coordinates (x 10^4) and equivalent isotropic displacement parameters (Å^{2}x 10^3) for **[Rh($C_{19}H_{21}NO_3$)]$_2$**. U(eq) is defined as one third of the trace of the orthogonalized U^{ij} tensor.

	x	y	z	U(eq)
Rh(1)	3582(1)	1450(1)	7676(1)	38(1)
O(1)	2868(1)	801(1)	3737(4)	71(1)
O(2)	4999(2)	1983(2)	5939(7)	148(3)
N(1)	3313(1)	1407(1)	5344(4)	42(1)
C(1)	4295(1)	1636(1)	7198(5)	49(1)
C(2)	4288(1)	1800(1)	8761(6)	53(1)
C(3)	3969(1)	1427(1)	9736(5)	51(1)
C(4)	3816(1)	1035(1)	8796(5)	52(1)
C(5)	3991(1)	1158(1)	7220(5)	50(1)
C(6)	4577(2)	2267(2)	9351(8)	83(2)
C(7)	3890(2)	1459(2)	11495(6)	84(2)
C(8)	3540(2)	568(2)	9416(8)	77(2)
C(9)	3922(2)	842(2)	5833(7)	72(1)
C(10)	4564(2)	1905(2)	5768(7)	77(2)
C(13)	2960(1)	981(1)	5067(5)	48(1)

C(14)	2711(1)	773(1)	6589(6)	54(1)
C(15)	2279(2)	406(1)	6600(7)	66(1)
C(16)	2058(2)	255(2)	8058(8)	78(2)
C(17)	2267(2)	463(2)	9485(7)	74(2)
C(18)	2703(2)	816(1)	9468(6)	60(1)
C(19)	2935(1)	978(1)	8003(5)	43(1)
O(3)	5157(2)	2319(3)	3533(8)	218(3)
C(11)	5245(2)	2198(3)	4644(8)	197(6)
C(12)	5741(2)	2308(4)	5227(18)	265(10)

Table A08. Bond lengths [Å] and angles [°] for **[Rh($C_{19}H_{21}NO_3$)]$_2$**.

Rh(1)-C(19)	2.024(3)
Rh(1)-N(1)	2.111(3)
Rh(1)-C(5)	2.142(4)
Rh(1)-N(1)#1	2.169(3)
Rh(1)-C(4)	2.176(4)
Rh(1)-C(3)	2.190(4)
Rh(1)-C(1)	2.251(4)
Rh(1)-C(2)	2.297(4)
O(1)-C(13)	1.224(5)
O(2)-C(11)	1.337(6)
O(2)-C(10)	1.397(8)
N(1)-C(13)	1.383(4)
N(1)-Rh(1)#1	2.169(3)
C(1)-C(2)	1.416(6)
C(1)-C(5)	1.447(5)
C(1)-C(10)	1.503(7)
C(2)-C(3)	1.451(5)
C(2)-C(6)	1.493(6)
C(3)-C(4)	1.416(6)
C(3)-C(7)	1.491(6)
C(4)-C(5)	1.408(6)
C(4)-C(8)	1.496(6)
C(5)-C(9)	1.519(6)
C(6)-H(6A)	0.9600
C(6)-H(6B)	0.9600
C(6)-H(6C)	0.9600
C(7)-H(7A)	0.9600
C(7)-H(7B)	0.9600
C(7)-H(7C)	0.9600
C(8)-H(8A)	0.9600
C(8)-H(8B)	0.9600
C(8)-H(8C)	0.9600
C(9)-H(9A)	0.9600
C(9)-H(9B)	0.9600
C(9)-H(9C)	0.9600
C(10)-H(10A)	0.9700

C(10)-H(10B)	0.9700
C(13)-C(14)	1.490(6)
C(14)-C(19)	1.385(6)
C(14)-C(15)	1.395(5)
C(15)-C(16)	1.381(8)
C(15)-H(15A)	0.9300
C(16)-C(17)	1.381(9)
C(16)-H(16A)	0.9300
C(17)-C(18)	1.386(6)
C(17)-H(17A)	0.9300
C(18)-C(19)	1.405(6)
C(18)-H(18A)	0.9300
O(3)-C(11)	1.113(7)
C(11)-C(12)	1.632(8)
C(12)-H(12A)	0.9600
C(12)-H(12B)	0.9600
C(12)-H(12C)	0.9600

C(19)-Rh(1)-N(1)	78.11(13)
C(19)-Rh(1)-C(5)	111.52(15)
N(1)-Rh(1)-C(5)	100.26(15)
C(19)-Rh(1)-N(1)#1	85.48(13)
N(1)-Rh(1)-N(1)#1	81.24(13)
C(5)-Rh(1)-N(1)#1	162.93(11)
C(19)-Rh(1)-C(4)	92.05(14)
N(1)-Rh(1)-C(4)	129.57(15)
C(5)-Rh(1)-C(4)	38.06(16)
N(1)#1-Rh(1)-C(4)	147.90(14)
C(19)-Rh(1)-C(3)	108.40(15)
N(1)-Rh(1)-C(3)	164.07(15)
C(5)-Rh(1)-C(3)	63.90(16)
N(1)#1-Rh(1)-C(3)	113.32(14)
C(4)-Rh(1)-C(3)	37.85(16)
C(19)-Rh(1)-C(1)	149.88(16)
N(1)-Rh(1)-C(1)	104.00(14)
C(5)-Rh(1)-C(1)	38.37(14)
N(1)#1-Rh(1)-C(1)	124.63(12)
C(4)-Rh(1)-C(1)	63.04(14)

C(3)-Rh(1)-C(1)	62.90(15)
C(19)-Rh(1)-C(2)	145.94(16)
N(1)-Rh(1)-C(2)	135.11(13)
C(5)-Rh(1)-C(2)	62.49(15)
N(1)#1-Rh(1)-C(2)	104.41(14)
C(4)-Rh(1)-C(2)	62.20(14)
C(3)-Rh(1)-C(2)	37.65(14)
C(1)-Rh(1)-C(2)	36.26(16)
C(11)-O(2)-C(10)	110.7(6)
C(13)-N(1)-Rh(1)	110.4(2)
C(13)-N(1)-Rh(1)#1	111.4(3)
Rh(1)-N(1)-Rh(1)#1	98.76(13)
C(2)-C(1)-C(5)	107.3(3)
C(2)-C(1)-C(10)	126.6(4)
C(5)-C(1)-C(10)	126.0(4)
C(2)-C(1)-Rh(1)	73.6(2)
C(5)-C(1)-Rh(1)	66.7(2)
C(10)-C(1)-Rh(1)	124.3(3)
C(1)-C(2)-C(3)	107.9(3)
C(1)-C(2)-C(6)	126.6(4)
C(3)-C(2)-C(6)	125.5(4)
C(1)-C(2)-Rh(1)	70.1(2)
C(3)-C(2)-Rh(1)	67.2(2)
C(6)-C(2)-Rh(1)	131.0(4)
C(4)-C(3)-C(2)	107.5(4)
C(4)-C(3)-C(7)	127.5(4)
C(2)-C(3)-C(7)	124.1(4)
C(4)-C(3)-Rh(1)	70.5(2)
C(2)-C(3)-Rh(1)	75.2(2)
C(7)-C(3)-Rh(1)	128.1(4)
C(5)-C(4)-C(3)	108.5(3)
C(5)-C(4)-C(8)	126.1(4)
C(3)-C(4)-C(8)	125.3(4)
C(5)-C(4)-Rh(1)	69.7(3)
C(3)-C(4)-Rh(1)	71.6(2)
C(8)-C(4)-Rh(1)	127.7(3)
C(4)-C(5)-C(1)	108.3(3)
C(4)-C(5)-C(9)	126.1(4)

C(1)-C(5)-C(9)	125.1(4)
C(4)-C(5)-Rh(1)	72.3(3)
C(1)-C(5)-Rh(1)	74.9(3)
C(9)-C(5)-Rh(1)	124.7(3)
C(2)-C(6)-H(6A)	109.5
C(2)-C(6)-H(6B)	109.5
H(6A)-C(6)-H(6B)	109.5
C(2)-C(6)-H(6C)	109.5
H(6A)-C(6)-H(6C)	109.5
H(6B)-C(6)-H(6C)	109.5
C(3)-C(7)-H(7A)	109.5
C(3)-C(7)-H(7B)	109.5
H(7A)-C(7)-H(7B)	109.5
C(3)-C(7)-H(7C)	109.5
H(7A)-C(7)-H(7C)	109.5
H(7B)-C(7)-H(7C)	109.5
C(4)-C(8)-H(8A)	109.5
C(4)-C(8)-H(8B)	109.5
H(8A)-C(8)-H(8B)	109.5
C(4)-C(8)-H(8C)	109.5
H(8A)-C(8)-H(8C)	109.5
H(8B)-C(8)-H(8C)	109.5
C(5)-C(9)-H(9A)	109.5
C(5)-C(9)-H(9B)	109.5
H(9A)-C(9)-H(9B)	109.5
C(5)-C(9)-H(9C)	109.5
H(9A)-C(9)-H(9C)	109.5
H(9B)-C(9)-H(9C)	109.5
O(2)-C(10)-C(1)	108.3(5)
O(2)-C(10)-H(10A)	110.0
C(1)-C(10)-H(10A)	110.0
O(2)-C(10)-H(10B)	110.0
C(1)-C(10)-H(10B)	110.0
H(10A)-C(10)-H(10B)	108.4
O(1)-C(13)-N(1)	123.9(4)
O(1)-C(13)-C(14)	124.8(3)
N(1)-C(13)-C(14)	111.4(3)
C(19)-C(14)-C(15)	122.1(4)

C(19)-C(14)-C(13)	115.0(3)
C(15)-C(14)-C(13)	122.9(4)
C(16)-C(15)-C(14)	119.2(5)
C(16)-C(15)-H(15A)	120.4
C(14)-C(15)-H(15A)	120.4
C(15)-C(16)-C(17)	120.0(4)
C(15)-C(16)-H(16A)	120.0
C(17)-C(16)-H(16A)	120.0
C(16)-C(17)-C(18)	120.4(5)
C(16)-C(17)-H(17A)	119.8
C(18)-C(17)-H(17A)	119.8
C(17)-C(18)-C(19)	120.9(4)
C(17)-C(18)-H(18A)	119.6
C(19)-C(18)-H(18A)	119.6
C(14)-C(19)-C(18)	117.3(3)
C(14)-C(19)-Rh(1)	114.3(3)
C(18)-C(19)-Rh(1)	128.2(3)
O(3)-C(11)-O(2)	130.5(7)
O(3)-C(11)-C(12)	127.5(7)
O(2)-C(11)-C(12)	101.4(6)
C(11)-C(12)-H(12A)	109.5
C(11)-C(12)-H(12B)	109.5
H(12A)-C(12)-H(12B)	109.5
C(11)-C(12)-H(12C)	109.5
H(12A)-C(12)-H(12C)	109.5
H(12B)-C(12)-H(12C)	109.5

Symmetry transformations used to generate equivalent atoms:

#1 -x+2/3,-y+1/3,-z+4/3

Table A09. Anisotropic displacement parameters ($Å^2 x\ 10^3$) for **$[Rh(C_{19}H_{21}NO_3)]_2$**. The anisotropic displacement factor exponent takes the form: $-2\ ^2[\ h^2 a^{*2} U^{11} + ... + 2\ h\ k\ a^*\ b^*\ U^{12}\ ]$

	U^{11}	U^{22}	U^{33}	U^{23}	U^{13}	U^{12}
Rh(1)	45(1)	40(1)	36(1)	-1(1)	-2(1)	26(1)
O(1)	89(2)	66(2)	55(2)	-24(1)	-11(2)	37(1)
O(2)	123(3)	165(4)	168(6)	52(4)	45(4)	80(3)
N(1)	50(1)	46(1)	38(2)	4(1)	-2(1)	30(1)
C(1)	51(1)	57(2)	49(2)	0(1)	-6(1)	35(1)
C(2)	47(1)	58(2)	63(2)	-10(2)	-22(2)	31(1)
C(3)	56(1)	76(2)	38(2)	-1(1)	-4(1)	46(1)
C(4)	60(1)	57(1)	55(2)	9(1)	-3(2)	42(1)
C(5)	53(1)	60(2)	50(2)	-3(1)	-6(2)	38(1)
C(6)	77(2)	60(2)	113(4)	-25(2)	-41(3)	35(2)
C(7)	93(3)	129(4)	41(2)	-3(2)	-6(2)	65(2)
C(8)	76(2)	64(2)	97(4)	21(2)	-9(2)	41(2)
C(9)	83(2)	81(2)	76(3)	-30(2)	-20(2)	60(1)
C(10)	58(2)	102(3)	76(3)	16(3)	13(2)	44(2)
C(13)	58(1)	43(1)	53(2)	-11(1)	-8(2)	33(1)
C(14)	56(2)	43(1)	70(3)	-8(2)	-8(2)	29(1)
C(15)	60(2)	41(2)	95(4)	-5(2)	-8(2)	24(1)
C(16)	56(2)	44(2)	121(5)	13(2)	7(3)	15(2)
C(17)	66(2)	62(2)	93(3)	31(2)	25(2)	31(2)
C(18)	67(2)	57(2)	56(2)	8(2)	2(2)	32(2)
C(19)	44(1)	41(1)	50(2)	9(1)	4(1)	25(1)
O(3)	131(8)	221(8)	268(9)	109(6)	55(6)	63(5)
C(11)	266(14)	145(11)	162(11)	43(7)	19(10)	89(8)
C(12)	274(19)	159(14)	225(15)	36(11)	-6(15)	6(13)

Table A10. Hydrogen coordinates (x 10^4) and isotropic displacement parameters (Å ^{2}x 10^3) for **[Rh($C_{19}H_{21}NO_3$)]$_2$**.

	x	y	z	U(eq)
H(6A)	4855	2304	9728	124
H(6B)	4429	2325	10222	124
H(6C)	4630	2472	8481	124
H(7A)	4115	1441	12117	125
H(7B)	3601	1217	11791	125
H(7C)	3903	1738	11708	125
H(8A)	3732	469	9855	115
H(8B)	3368	375	8543	115
H(8C)	3342	562	10246	115
H(9A)	4145	755	5882	108
H(9B)	3946	989	4821	108
H(9C)	3631	582	5919	108
H(10A)	4433	1743	4772	92
H(10B)	4565	2186	5725	92
H(15A)	2141	265	5637	79
H(16A)	1769	13	8080	94
H(17A)	2114	366	10462	89
H(18A)	2843	946	10440	72
H(12A)	5960	2510	4471	398
H(12B)	5752	2036	5272	398
H(12C)	5803	2443	6281	398

Table A11. Torsion angles [°] for **[Rh($C_{19}H_{21}NO_3$)]$_2$**.

C(19)-Rh(1)-N(1)-C(13)	-29.7(3)
C(5)-Rh(1)-N(1)-C(13)	80.4(3)
N(1)#1-Rh(1)-N(1)-C(13)	-116.9(3)
C(4)-Rh(1)-N(1)-C(13)	53.0(3)
C(3)-Rh(1)-N(1)-C(13)	86.3(5)
C(1)-Rh(1)-N(1)-C(13)	119.5(3)
C(2)-Rh(1)-N(1)-C(13)	141.5(3)
C(19)-Rh(1)-N(1)-Rh(1)#1	87.19(15)
C(5)-Rh(1)-N(1)-Rh(1)#1	-162.76(12)
N(1)#1-Rh(1)-N(1)-Rh(1)#1	0.0
C(4)-Rh(1)-N(1)-Rh(1)#1	169.92(12)
C(3)-Rh(1)-N(1)-Rh(1)#1	-156.9(4)
C(1)-Rh(1)-N(1)-Rh(1)#1	-123.66(13)
C(2)-Rh(1)-N(1)-Rh(1)#1	-101.7(2)
C(19)-Rh(1)-C(1)-C(2)	-116.2(3)
N(1)-Rh(1)-C(1)-C(2)	153.5(2)
C(5)-Rh(1)-C(1)-C(2)	-117.6(4)
N(1)#1-Rh(1)-C(1)-C(2)	64.5(3)
C(4)-Rh(1)-C(1)-C(2)	-79.0(3)
C(3)-Rh(1)-C(1)-C(2)	-36.3(2)
C(19)-Rh(1)-C(1)-C(5)	1.5(4)
N(1)-Rh(1)-C(1)-C(5)	-88.9(2)
N(1)#1-Rh(1)-C(1)-C(5)	-177.8(2)
C(4)-Rh(1)-C(1)-C(5)	38.7(2)
C(3)-Rh(1)-C(1)-C(5)	81.4(3)
C(2)-Rh(1)-C(1)-C(5)	117.6(4)
C(19)-Rh(1)-C(1)-C(10)	120.3(4)
N(1)-Rh(1)-C(1)-C(10)	29.9(4)
C(5)-Rh(1)-C(1)-C(10)	118.8(5)
N(1)#1-Rh(1)-C(1)-C(10)	-59.0(4)
C(4)-Rh(1)-C(1)-C(10)	157.5(4)
C(3)-Rh(1)-C(1)-C(10)	-159.8(4)
C(2)-Rh(1)-C(1)-C(10)	-123.5(5)
C(5)-C(1)-C(2)-C(3)	-1.9(5)
C(10)-C(1)-C(2)-C(3)	177.5(4)
Rh(1)-C(1)-C(2)-C(3)	56.6(3)

C(5)-C(1)-C(2)-C(6)	174.6(5)
C(10)-C(1)-C(2)-C(6)	-5.9(8)
Rh(1)-C(1)-C(2)-C(6)	-126.9(5)
C(5)-C(1)-C(2)-Rh(1)	-58.5(3)
C(10)-C(1)-C(2)-Rh(1)	120.9(5)
C(19)-Rh(1)-C(2)-C(1)	126.5(3)
N(1)-Rh(1)-C(2)-C(1)	-37.9(3)
C(5)-Rh(1)-C(2)-C(1)	38.3(2)
N(1)#1-Rh(1)-C(2)-C(1)	-129.9(2)
C(4)-Rh(1)-C(2)-C(1)	81.5(3)
C(3)-Rh(1)-C(2)-C(1)	120.4(4)
C(19)-Rh(1)-C(2)-C(3)	6.1(4)
N(1)-Rh(1)-C(2)-C(3)	-158.3(2)
C(5)-Rh(1)-C(2)-C(3)	-82.1(3)
N(1)#1-Rh(1)-C(2)-C(3)	109.6(3)
C(4)-Rh(1)-C(2)-C(3)	-38.9(3)
C(1)-Rh(1)-C(2)-C(3)	-120.4(4)
C(19)-Rh(1)-C(2)-C(6)	-111.9(5)
N(1)-Rh(1)-C(2)-C(6)	83.7(5)
C(5)-Rh(1)-C(2)-C(6)	160.0(5)
N(1)#1-Rh(1)-C(2)-C(6)	-8.3(5)
C(4)-Rh(1)-C(2)-C(6)	-156.8(5)
C(3)-Rh(1)-C(2)-C(6)	-117.9(6)
C(1)-Rh(1)-C(2)-C(6)	121.7(6)
C(1)-C(2)-C(3)-C(4)	5.2(5)
C(6)-C(2)-C(3)-C(4)	-171.4(5)
Rh(1)-C(2)-C(3)-C(4)	63.6(3)
C(1)-C(2)-C(3)-C(7)	175.3(5)
C(6)-C(2)-C(3)-C(7)	-1.2(8)
Rh(1)-C(2)-C(3)-C(7)	-126.3(5)
C(1)-C(2)-C(3)-Rh(1)	-58.4(3)
C(6)-C(2)-C(3)-Rh(1)	125.0(5)
C(19)-Rh(1)-C(3)-C(4)	68.5(3)
N(1)-Rh(1)-C(3)-C(4)	-43.5(5)
C(5)-Rh(1)-C(3)-C(4)	-37.0(2)
N(1)#1-Rh(1)-C(3)-C(4)	161.5(2)
C(1)-Rh(1)-C(3)-C(4)	-80.1(2)
C(2)-Rh(1)-C(3)-C(4)	-115.1(4)

C(19)-Rh(1)-C(3)-C(2)	-176.4(3)
N(1)-Rh(1)-C(3)-C(2)	71.6(5)
C(5)-Rh(1)-C(3)-C(2)	78.1(3)
N(1)#1-Rh(1)-C(3)-C(2)	-83.4(3)
C(4)-Rh(1)-C(3)-C(2)	115.1(4)
C(1)-Rh(1)-C(3)-C(2)	34.9(3)
C(19)-Rh(1)-C(3)-C(7)	-54.4(4)
N(1)-Rh(1)-C(3)-C(7)	-166.4(4)
C(5)-Rh(1)-C(3)-C(7)	-160.0(4)
N(1)#1-Rh(1)-C(3)-C(7)	38.6(4)
C(4)-Rh(1)-C(3)-C(7)	-122.9(5)
C(1)-Rh(1)-C(3)-C(7)	156.9(5)
C(2)-Rh(1)-C(3)-C(7)	122.0(5)
C(2)-C(3)-C(4)-C(5)	-6.5(5)
C(7)-C(3)-C(4)-C(5)	-176.2(5)
Rh(1)-C(3)-C(4)-C(5)	60.2(3)
C(2)-C(3)-C(4)-C(8)	169.7(4)
C(7)-C(3)-C(4)-C(8)	0.0(8)
Rh(1)-C(3)-C(4)-C(8)	-123.6(5)
C(2)-C(3)-C(4)-Rh(1)	-66.7(3)
C(7)-C(3)-C(4)-Rh(1)	123.6(5)
C(19)-Rh(1)-C(4)-C(5)	123.3(2)
N(1)-Rh(1)-C(4)-C(5)	47.1(2)
N(1)#1-Rh(1)-C(4)-C(5)	-151.9(2)
C(3)-Rh(1)-C(4)-C(5)	-118.7(3)
C(1)-Rh(1)-C(4)-C(5)	-39.0(2)
C(2)-Rh(1)-C(4)-C(5)	-80.0(2)
C(19)-Rh(1)-C(4)-C(3)	-117.9(2)
N(1)-Rh(1)-C(4)-C(3)	165.82(19)
C(5)-Rh(1)-C(4)-C(3)	118.7(3)
N(1)#1-Rh(1)-C(4)-C(3)	-33.2(3)
C(1)-Rh(1)-C(4)-C(3)	79.7(2)
C(2)-Rh(1)-C(4)-C(3)	38.7(2)
C(19)-Rh(1)-C(4)-C(8)	2.9(5)
N(1)-Rh(1)-C(4)-C(8)	-73.4(5)
C(5)-Rh(1)-C(4)-C(8)	-120.5(5)
N(1)#1-Rh(1)-C(4)-C(8)	87.6(5)
C(3)-Rh(1)-C(4)-C(8)	120.8(5)

C(1)-Rh(1)-C(4)-C(8)	-159.5(5)
C(2)-Rh(1)-C(4)-C(8)	159.5(5)
C(3)-C(4)-C(5)-C(1)	5.4(5)
C(8)-C(4)-C(5)-C(1)	-170.8(4)
Rh(1)-C(4)-C(5)-C(1)	66.8(3)
C(3)-C(4)-C(5)-C(9)	178.2(4)
C(8)-C(4)-C(5)-C(9)	2.0(7)
Rh(1)-C(4)-C(5)-C(9)	-120.4(4)
C(3)-C(4)-C(5)-Rh(1)	-61.4(3)
C(8)-C(4)-C(5)-Rh(1)	122.4(4)
C(2)-C(1)-C(5)-C(4)	-2.1(5)
C(10)-C(1)-C(5)-C(4)	178.5(4)
Rh(1)-C(1)-C(5)-C(4)	-65.0(3)
C(2)-C(1)-C(5)-C(9)	-175.0(4)
C(10)-C(1)-C(5)-C(9)	5.6(7)
Rh(1)-C(1)-C(5)-C(9)	122.1(4)
C(2)-C(1)-C(5)-Rh(1)	62.9(3)
C(10)-C(1)-C(5)-Rh(1)	-116.5(5)
C(19)-Rh(1)-C(5)-C(4)	-63.8(2)
N(1)-Rh(1)-C(5)-C(4)	-144.98(19)
N(1)#1-Rh(1)-C(5)-C(4)	121.4(4)
C(3)-Rh(1)-C(5)-C(4)	36.8(2)
C(1)-Rh(1)-C(5)-C(4)	115.4(3)
C(2)-Rh(1)-C(5)-C(4)	79.2(2)
C(19)-Rh(1)-C(5)-C(1)	-179.2(2)
N(1)-Rh(1)-C(5)-C(1)	99.6(2)
N(1)#1-Rh(1)-C(5)-C(1)	6.1(6)
C(4)-Rh(1)-C(5)-C(1)	-115.4(3)
C(3)-Rh(1)-C(5)-C(1)	-78.6(2)
C(2)-Rh(1)-C(5)-C(1)	-36.2(2)
C(19)-Rh(1)-C(5)-C(9)	58.3(4)
N(1)-Rh(1)-C(5)-C(9)	-22.9(3)
N(1)#1-Rh(1)-C(5)-C(9)	-116.5(5)
C(4)-Rh(1)-C(5)-C(9)	122.1(4)
C(3)-Rh(1)-C(5)-C(9)	158.9(4)
C(1)-Rh(1)-C(5)-C(9)	-122.5(4)
C(2)-Rh(1)-C(5)-C(9)	-158.7(4)
C(11)-O(2)-C(10)-C(1)	176.1(6)

C(2)-C(1)-C(10)-O(2)	80.6(7)
C(5)-C(1)-C(10)-O(2)	-100.0(6)
Rh(1)-C(1)-C(10)-O(2)	175.4(4)
Rh(1)-N(1)-C(13)-O(1)	-147.0(4)
Rh(1)#1-N(1)-C(13)-O(1)	104.2(5)
Rh(1)-N(1)-C(13)-C(14)	32.8(4)
Rh(1)#1-N(1)-C(13)-C(14)	-75.9(4)
O(1)-C(13)-C(14)-C(19)	163.1(5)
N(1)-C(13)-C(14)-C(19)	-16.8(6)
O(1)-C(13)-C(14)-C(15)	-18.2(8)
N(1)-C(13)-C(14)-C(15)	161.9(4)
C(19)-C(14)-C(15)-C(16)	3.5(8)
C(13)-C(14)-C(15)-C(16)	-175.1(5)
C(14)-C(15)-C(16)-C(17)	-0.9(9)
C(15)-C(16)-C(17)-C(18)	-1.9(9)
C(16)-C(17)-C(18)-C(19)	2.2(9)
C(15)-C(14)-C(19)-C(18)	-3.1(7)
C(13)-C(14)-C(19)-C(18)	175.5(4)
C(15)-C(14)-C(19)-Rh(1)	172.5(4)
C(13)-C(14)-C(19)-Rh(1)	-8.8(5)
C(17)-C(18)-C(19)-C(14)	0.3(7)
C(17)-C(18)-C(19)-Rh(1)	-174.7(4)
N(1)-Rh(1)-C(19)-C(14)	20.5(3)
C(5)-Rh(1)-C(19)-C(14)	-76.0(4)
N(1)#1-Rh(1)-C(19)-C(14)	102.5(3)
C(4)-Rh(1)-C(19)-C(14)	-109.6(3)
C(3)-Rh(1)-C(19)-C(14)	-144.4(3)
C(1)-Rh(1)-C(19)-C(14)	-76.9(5)
C(2)-Rh(1)-C(19)-C(14)	-148.3(3)
N(1)-Rh(1)-C(19)-C(18)	-164.4(4)
C(5)-Rh(1)-C(19)-C(18)	99.2(4)
N(1)#1-Rh(1)-C(19)-C(18)	-82.4(4)
C(4)-Rh(1)-C(19)-C(18)	65.5(4)
C(3)-Rh(1)-C(19)-C(18)	30.7(5)
C(1)-Rh(1)-C(19)-C(18)	98.2(5)
C(2)-Rh(1)-C(19)-C(18)	26.8(6)
C(10)-O(2)-C(11)-O(3)	1.1(15)
C(10)-O(2)-C(11)-C(12)	172.7(8)

Symmetry transformations used to generate equivalent atoms:
#1 -x+2/3,-y+1/3,-z+4/3

REFERENCES

Chapter 1

1. (a) Wolfe, J. P.; Wagaw, S.; Marcoux, J.-F.; Buchward, S. L. *Acc. Chem. Res.* **1998**, *31*, 805. (b) Muci, A. R.; Buchward, S. L. *Top. Curr. Chem*. **2002**, *219*, 131.
2. (a) Smith, M. B.; March, J. *March's Advanced Organic Chemistry Reactions, Mechanisms, and Structure*; *6th Ed.*; John Wiley & Sons, Inc.: New Jersey, 2007. (b) Salvatore, R. N.; Yoon, C. H.; Jung, K. W. *Tetrahedron*, **2001**, *57*, 7785.
3. Hartwig, J. F. *Angew. Chem. Int. Ed.* **1998**, *37*, 2046.
4. (a) Ackermann, L.; Vicente, R.; Kapdi, A. R. *Angew. Chem. Int. Ed*. **2009**, *48*, 9792. (b) Godula, K.; Sames, D. *Science*, **2006**, *312*, 67. (c) Dick, A. R.; Sanford, M. S. *Tetrahedron* **2006**, *62*, 2439. (d) Ritleng, V.; Sirlin, C.; Pfeffer, M. *Chem. Rev*. **2002**, *102*, 1731
5. Bergman, R. G. Nature, **2007**, *446*, 391.
6. (a) Anslyn, E. V.; Dougherty, D. A., *Modern Physical Organic Chemistry*; Murdzek, J., Ed.; University Science Book: USA, 2006. (b) Blanksby, S. J.; Ellison, G. B. *Acc. Chem. Res*. **2003**, *36*, 255
7. Ding, K.; Dai, L.-X. *Organic Chemistry-Breakthroughs and Perspectives*; Wiley-VCH: Weinheim, 2012.
8. Labinger, J. A.; Bercaw, J. E. *Nature*, **2002**, *417*, 507
9. Erdik, E.; Mehmet, AY. *Chem. Rev.* **1989**, *89*, 1947.
10. (a) Tsutsui, H.; Hayashi Y.; Narasaka, K. *Chem. Lett*. **1997**, 317. (b) Narasaka, K. *Pure Appl. Chem.* **2002**, *74*, 143. (c) Kitamura, M.; Suga, T.; Chiba, S.; Narasaka, K. *Org. Lett.* **2004**, *6*, 4619–4621.
11. Ricci, A. *Amino Group Chemistry: From Synthesis to the Life Sciences, 1st Ed.*; John Wiley & Sons, Inc.: New Jersey, 2008.
12. Kovacic, P.; Lowery, M. K.; Field, K.W. *Chem. Rev*. **1970**, *70*, 639.
13. Coleman, G. H.; Hauser, C. R. *J. Am. Chem. Soc*. **1928**,*50*, 1193.
14. (a) Sheradsky, T.; Salemnick, G.; Nir, Z. *Tetrahedron*, **1972**, *28*, 3833. (b) Sheradsky, T. *Tetrahedron Lett*. **1968**, 909. (c) Sheradsk T. *J. Heterocycl. Chem.* **1967**, *4*, 413.
15. Scopes, D. I. C.; Kluge, A. F.; Edwards, J. A. *J. Org. Chem.* **1977**, *42*, 376.

16. Tayfor, E. C.; Sun, J. H. *Synthesis*, **1980**, 801.
17. Boche, G.; Mayer, N.; Bernheim, M.; Wagner, K. *Angew. Chem., Int. Ed.* **1978**, *17*, 687.
18. Boche, G.; Bernheim, M.; Niedner, M. *Angew. Chem., Int. Ed*. **1983**, *22*, 53.
19. Colvin, E. W.; Kirby, G. W.; Wilson, A. C. *Tetrahedron Lett*. **1982**, *23*, 3835.
20. Boche, G.; Bernheim, M.; Schrott, W. S. *Tetrahedron Lett*. **1982**, *23*, 5399.
21. Boche, G.; Bosold, F.; Niebner, M. *Tetrahedron Lett*. **1982**, *23*, 3255.
22. Boche, G.; Schrodt, W. *Tetrahedron Lett.* **1982**, *23*, 5403.
23. (a) Reed, J. N.; Snieckus, V. *Tetrahedron Lett*. **1983**, *24*, 3795. (b) Reed, J. N.; Snieckus, V. *Tetrahedron Lett*. **1984**, *25*, 5505.
24. Itauno, *S.;* Miyanaki, K.; Ito, K. *Tetrahedron Lett.* **1986**, *27*, 3033.
25. Yamamoto, H.; Maruoka, K. *J. Org. Chem*. **1980**, *45*, 2739.
26. (a) Casarini, A.; Dembech, P.; Lazzari, D.; Marini, E.; Reginato, G.; Ricci, A.; Seconi, G. *J. Org. Chem*. **1993**, *58*, 5620. (b) Genet, J. P.; Mallart, S.; Greck, C.; Piveteau, E. *Tetrahedron Lett.* **1991**, *32*, 2359. (c) Greck, C.; Bischoff, L.; Ferreira, F.; Genet, J.P. *J. Org. Chem*. **1995**, *60*, 7010. (d) Zheng, N.; Armstong III, J. D.; McWilliams, J. C.; Volante, R. P. *Tetrahedron Lett.* **1997**, *38*, 2817. (e) Mitchell, H.; Leblanc, Y.; *J. Org. Chem*. **1994**, *59*, 682. (f) Beak, P.; Selling, G. W.; *J. Org. Chem*. **1989**, *54*, 5574. (g) Alberti, A.; Cane, F.; Dembech, P.; Lazzari, D.; Ricci, A.; Seconi, G. *J. Org. Chem*. **1996**, *61*, 1677.
27. (a) Tsutsui, H.; Hayashi, Y.; Narasaka, K. *Chem. Lett.* **1997**, 317. (b) Tsutsui, H.; Narasaka, K. *Chem. Lett*. **1999**, 45. (c) Tsutsui, H.; Narasaka, K. *Chem. Lett.* **2001**, 526. (d) Koganemaru, K.; Kitamura, M.; Narasaka, K. *Chem. Lett*. **2002**, 784. (e) Kitamura, M.; Narasaka, K. *Chem. Rec.* **2002**, *2*, 268.
28. (a) Berman, A. M.; Johnson, J. S. *J. Am. Chem. Soc.* **2004**, *126*, 5680. (b) Berman, A. M.; Johnson, J. S. *J. Org. Chem.* **2005**, *70*, 364. (c) Berman, A. M.; Johnson J. S. *J. Org. Chem.* **2006**, *71*, 219. (d) Campbell, M. J.; Johnson, J. S. *Org. Lett.* **2007**, *9*, 1521
29. (a) Heuger, G.; Kalsow, S.; Göttlich, R. *Eur. J. Org. Chem*. **2002**, 1848. (b) Göttlich, R. *Synthesis* **2000**, 1561.
30. (a) Liu, S.; Yu, Y.; Liebeskind, L. S.; *Org. Lett.* **2007**, *9*, 1947. (b) Liu, S.; Liebeskind, L. S. *J. Am. Chem. Soc.* **2008**, *130*, 6918.
31. He, C.; Chen, C.; Cheng, J.; Liu, C.; Liu, W.; Li, Q.; Lei, A. *Angew. Chem. Int. Ed.*

2008, *47*, 6414.

32. Ferreira, C.M.P.; Guedes da Silva, M.F.C.; Kukushkin, V.Y.; Fraústo da Silva, J.J.R.; Pombeiro, A.J.L. *J Chem Soc, Dalton Trans.* **1998**, 325.
33. (a) Zaman, S.; Mitsuru, K.; Abell, A. D. *Org. Lett.* **2005**, *7*, 609. (b) Zaman, S.; Mitsuru, K.; Abell, A. D. *Aust. J. Chem*. **2007**, *60*, 624.
34. Gerfaud, T.; Neuville, L.; Zhu, J. *Angew. Chem. Int. Ed*. **2009**, *48*, 572.
35. Berman, A. M.; Johnson, J. S. *Synlett* **2005**, 1799.
36. (a) Barker, T. J.; Jarbo, E. R. *J. Am. Chem. Soc.* **2009**, *131*, 15598.
37. Feng, C.; Loh, T. P. *Org. Lett.* **2014**, *16*, 3444.
38. Louillat, M. L.; Patureau, F. W. *Chem. Soc. Rev*. **2014**, *43*, 901.
39. (a) Kawano, T.; Hirano, K.; Satoh, T.; Miura, M. *J. Am. Chem. Soc.* **2010**, *132*, 6900. (b) Matsuda, N.; Hirano, K.; Satoh, T.; Miura, M. *Org. Lett.* **2011**, *13*, 2860.
40. Tan, Y.; Hartwig, J. F. *J. Am. Chem. Soc.* **2010**, *132*, 3676.
41. Yoo, E. J.; Ma, S.; Mei, T. S.; Chan, K. S. L.; Yu, J. Q. *J. Am. Chem. Soc.* **2011**, *133*, 7652.
42. Sun, K.; Li, Y.; Xiong, T.; Zhang, J.; Zhang, Q. *J. Am. Chem. Soc.* **2011**, *133*, 1694.
43. (a) Ng, K. H.; Chan, A. S. C.; Yu, W. Y. *J. Am. Chem. Soc.* **2010**, *132*, 12862. (b) Ng, K. H.; Ng, F. N.; Yu, W. Y; *Chem. Commun*. **2012**, *48*, 11680.
44. (a) Ng, K. H.; Zhou, Z.; Yu, W. Y. *Org. Lett.* **2012**, *14*, 272. (b) Ng, K. H.; Zhou, Z.; Yu, W. Y. *Chem. Commun*. **2013**, *49*, 7031.
45. (a) Grohmann, C.; Wang, H.; Glorius, F. *Org. Lett.* **2012**, *14*, 656. (b) Grohmann, H.; Wang, H.; Glorius, F. *Org. Lett.* **2013**, *15*, 3014.
46. (a) Kim, J. Y.; Park, S. H.; Ryu, J.; Cho, S. H.; Kim, S. H.; Chang, S. *J. Am. Chem. Soc.* **2012**, *134*, 9110. (b) Ryu, J.; Shin, K.; Park, S. H.; Kim, J. Y.; Chang, S. *Angew. Chem. Int. Ed*. **2012**, *51*, 9904. (c) Shin, K.; Baek, Y.; Chang, S. *Angew. Chem. Int. Ed*. **2013**, *52*, 8031.
47. Guimond, N.; Gorelsky, S. I.; Fagnou, K. *J. Am. Chem. Soc.* **2011**, 133, 6449.
48. (a) Rakshit, S.; Grohmann, C.; Besset, T.; Glorius, F. *J. Am. Chem. Soc.* **2011**, *133*, 2350. (b) Wang, H.; Grohamann, C; Nimphius, C.; Glorius, F. *J. Am. Chem. Soc.* **2012**, *134*, 19592
49. Yu, D.G.; Suri, M.; Glorius, F. *J. Am. Chem. Soc.* **2013**, *135*, 8802.
50. Hyster, T. K.; Ruhl, K. E.; Rovis, T. *J. Am. Chem. Soc.* **2013**, *135*, 5364.

51. Zhou, T.; Guo, W.; Xia, Y. *Chem. Eur. J.* **2015**, *21*, 1.
52. Thirunavukkarasu, V. S.; Raghuvanshi, K.; Ackermann, L. *Org. Lett.* **2013**, *15*, 3286.
53. Shang, M.; Zeng, S. H.; Sun, S. Z.; Dai, H. X.; Yu, J. Q. *Org. Lett.* **2013**, 15, 5286.
54. Ryu, J.; Kwak, J.; Shin, K.; Lee, D.; Chang, S. *J. Am. Chem. Soc.* **2013**, *135*, 12861.

Chapter 2

55. Shimpukade, B.; Hudson, B. D.; Hovgaard, C. K.; Milligan, G. *J. Med. Chem.* **2012**, *55*, 4511.
56. Katrtzky, A. R.; Pozharskii, A. F. *Handbook of Heterocyclic Chemistry*. 2nd *Ed.*; Academic Press, 2000.
57. Guram, A. S.; Rennels, R. A.; Buchward, S. *Angew. Chem. Int. Ed*. **1995**, *34*, 1348.
58. Referenced from the synthetic procedures of [Ru(p-cymene)Cl(Ph)]: Farrington, E. J.; Barnard, C. F. J.; Rowsell, E.; Brown, J. M. *Adv. Synth. Catal*. **2005**, *347*, 185.
59. Phanstiel, IV, O.; Wang, Q. X.; Powell, D. H.; Ospina, M. P.; Leeson, B. A. *J. Org. Chem.* **1999,** *64*, 803.
60. (a) He, C.; Chen, C.; Cheng, J.; Liu, C.; Liu, W.; Li, Q.; Lei, A. *Angew. Chem. Int. Ed*. **2008**, *47*, 6414. (b) Zhang, Z.; Yu, Y.; Liebeskind, L. S. *Org. Lett.* **2008**, *10*, 3005. (c) Matsuda, N.; Hirano, K.; Satoh, T.; Miura, M. *Angew. Chem. Int. Ed*. **2012**, *51*, 3642. (d) Rucker, R. P.; Whittaker, A. M.; Dang, H.; Lalic, G. *Angew. Chem. Int. Ed*. **2012**, *51*, 3953.
61. For selected transition metal catalyzed aminating/amidation reactions which are not cited in chapter: (a) Matsuda, N.; Hirano, K.; Satoh, T.; Miura, M. *J. Org. Chem.* **2012**, *77*, 617. (b) Hirano, K.; Satoh, T.; Miura, M. *Org. Lett.* **201**, *13*, 2395. (c) Matsuda, N.; Hirano, K.; Satoh, T.; Miura, M. *Angew. Chem. Int. Ed*. **2012**, *51*, 11827. (d) Rucker, R. P.; Whittaker, A. M.; Dang, H.; Lalic, G. *J. Am. Chem. Soc.* **2012**, *134*, 6571. (e) Miki, Y.; Hirano, K.; Satoh, T.; Miura, M. *Org. Lett.* **2013**, *15*, 172.

Chapter 3

62. Chan, W. W; Lo, S. F.; Zhou, Z.; Yu, W. Y. *J. Am. Chem. Soc.* **2012**, *134*, 13565.
63. For selected publications, please see: (a) Chen, Y.; Wang, F.; Zhen, W.; Li, X. *Adv. Synth. Catal*. **2013**, *355*, 353. (b) Wang, N.; Li, B.; Song, H.; Xu, S.; Wang, B. *Chem. – Eur. J.* **2013**, *19*, 358. (c) Presset, M.; Oehlrich, D.; Rombouts, F.; Molander, G. A. *Org. Lett.* **2013**, *15*, 1528. (d) Quiñones, N.; Seoane, A.; García-Fandiño, R.; Mascareñas, J. L.; Gulías, M. *Chem. Sci.* **2013**, *4*, 2874. (e) Li, B.-J.; Wang, H.-Y.; Zhu, Q.-L.; Shi, Z.-J. *Angew. Chem., Int. Ed.* **2012**, *51*, 3948. (f) Zhu, C.; Falck, F. R. *Chem. Commun.* **2012**, *48*, 1674. (g) Tan, X.; Liu, B.; Li, X.; Li, B.; Xu, S.; Song, H.; Wang, B. *J. Am. Chem. Soc.* **2012**, *134*, 16163. (h) Wang, Y.-F.; Toh, K. K.; Lee, J.-Y.; Chiba, S. *Angew. Chem., Int. Ed.* **2011**, *50*, 5927. (i) Muralirajan, K.; Parthasarathy, K.; Cheng, C.-H. *Angew. Chem., Int. Ed.* **2011**, *50*, 4169. (j) Patureau, F. W.; Besset, T.; Kuhl, N.; Glorius, F. *J. Am. Chem. Soc.* **2011**, *133*, 2154. (k) Li, X.; Zhao, M. *J. Org. Chem.* **2011**, *76*, 8530. (l) Zhang, X.; Chen, D.; Zhao, M.; Zhao, J.; Jia, A.; Li, X. *Adv. Synth. Catal.* **2011**, *353*, 719; (m) Too, P. C.; Wang, Y.-F.; Chiba, S. *Org. Lett.* **2010**, *12*, 5688. (n) Hyster, T. K.; Rovis, T. *J. Am. Chem. Soc.* **2010**, *132*, 10565.
64. For pioneer work from Miura and Satoh: (a) Ueura, K.; Satoh, T.; Miura, M. *Org. Lett.* **2007**, *9*, 1407. (b) Ueura, K.; Satoh, T.; Miura, M. *J. Org. Chem.* **2007**, *72*, 5362.
65. For selected works from Fagnou and co-workers: (a) Guimond, N.; Gouliaras, C.; Fagnou, K. *J. Am. Chem. Soc.* **2010**, *132*, 6908. (b) Stuart, D. R.; Alsabeh, P.; Kuhn. M.; Fagnou, K. *J. Am. Chem. Soc.* **2010**, *312*, 18326.
66. For examples of Rh(III)-catalyzed carbenoid cycloadditions to afford six- and seven-membered heterocycles, see: (a) Cui, S.; Zhang, Y.; Wang D.; Wu, Q. *Chem. Sci.* **2013**, *4*, 3912. (b) Shi, Z.; Koester, D. C.; BoultadakisArapinis, M.; Glorius, F. *J. Am. Chem. Soc.* **2013**, *135*, 12204.
67. During our investigation, Rovis and co-workers reported a similar cycloaddition reaction: (a) Hyster, T. K.; Ruhl, K. E.; Rovis, T. *J. Am. Chem. Soc.* **2013**, *135*, 5364. Cramer and co-workers also reported the synthesis of chiral isoindolones through a chiral cyclopentadienyl-rhodium(III)-catalyzed cycloaddition reaction: (b) Yu, B.; Cramer, M.; *Angew. Chem., Int. Ed.* **2014**, *53*, 7896.

68. For example of Rh(II)-catalyzed cyclopropanation of allyl phenyldiazoacetates, see: Doyle, M. P.; Hu, W.; Weathers Jr, T. M.; *Chirality*, **2003**, *15*, 369.
69. Our previous report on Pd(II)-catalyzed coupling of arylboronic acids and diazoesters proposed that β-H elimination was the key step to form alkene products and the Pd^{II}-hydride complex. See: Tsoi, Y.-T.; Zhou, Z.; Chan, A. S. C.; Yu, W.-Y. *Org. Lett.* **2010**, *12*, 4506.
70. (a) Li, L.; Jiao, Y.; Brennessel, W. W.; Jones, W. D. *Organometallics*, **2010**, *29*, 4593. (b) Li, L.; Brennessel, W. W.; Jones, W. D. *Organometallics*, **2009**, *28*, 3492. (c) Boutadla, Y.; Al-Duaij, O.; Davies, D. L.; Griffith, G. A.; Singh, K. *Organometallics*, **2009**, *28*, 433. (d) Sortais, J.-B.; Pannetier, N.; Holuigue, A.; Barloy, L.; Sirlin, C.; Pfeffer, M. *Organometallics*, **2007**, *26*, 1856.
71. Davies and co-workers reported the synthesis of a five-membered rhodacycle [Cp*Rh(C_6H_4-2-C_5H_4N-κ-C,N)Cl] in which the distance of Rh–C(aryl) was determined to be 2.305(3). (see ref. 70d).
72. Xu, L.; Zhu, Q.; Huang, G.; Cheng, B.; Xia, Y. *J. Org. Chem.* **2012**, *77*, 3017.

Chapter 4

73. For recent development, see: Patureau, F. W.; Glorius, F. *Angew. Chem., Int. Ed.* **2011**, *50*, 1977 and the references therein.
74. For Rh-catalyzed C-H activation using N-N bond as internal oxidant, see: (a) Liu, B.; Song, C.; Sun, C.; Zhou, S.; Zhu, J. *J. Am. Chem. Soc.* **2013**, *135*, 16625. (b) Sun, H.; Wang, C.; Yang, Y. –F.; Chen, P.; Wu, Y. –D.; Zhang, X.; Huang, Y. *J. Org. Chem.* **2014**, *79*, 11863. (c) Han, W.; Zhang, G.; Li, G.; Huang, H. *Org. Lett.* **2014**, *16*, 3532. (d) Chen, W. –J.; Lin, Z. *Organometallics*, **2015**, *34*, 309. (e) Fan, Z.; Song, S.; Li, W.; Geng, K.; Xu, Y.; Miao, Z- H.; Zhang, A. *Org. Lett.* **2015**, *17*, 310. (f) Wu, W.; Liu, Y.; Bi, S. *Org. Biomol. Chem*. **2015**, asap
75. For Ru-catalyzed C-H activation using N-N bond as internal oxidant, see fZardi, P.; Savoldelli, A.; Carminati, D. M.; Caselli, A.; Ragaini, F.; Gallo, E. *ACS catal*. **2014**, *4*, 3820.
76. Selected examples on the Rh-catalyzed oxidative C−H activation using stoichiometric extenal oxidant: (a) Umeda, N.; Tsurugi, H.; Satoh, T.; Miura, M. *Angew. Chem., Int. Ed*. **2008**, *47*, 4019. (b) Mochida, S.; Hirano, K.; Satoh, T.;

Miura, M. *J. Org. Chem*. **2011**, *76*, 3024. (c) Park, S. H.; Kim, J. Y.; Chang, S. *Org. Lett*. **2011**, *13*, 2372. (d) Tsai, A. S.; Brasse, M.; Bergman, R. G.; Ellman, J. A. *Org. Lett*. **2011**, *13*, 540. (e) Umeda, N.; Hirano, K.; Satoh, T.; Shibata, N.; Sato, H.; Miura, M. *J. Org. Chem*. **2011**, *76*, 13. (f) Fukuyani, T.; Hirano, K.; Satoh, T.; Miura, M. *J. Org. Chem*. **2011**, *76*, 2867. (g) Wang, C.; Sun, H.; Fang, Y.; Huang, Y. *Angew. Chem., Int. Ed*. **2013**, *52*, 5795. (h) Shang, Y.; Jie, X.; Zhao, H.; Hu, P.; Su, W. *Org. Lett*. **2014**, *16*, 416.

77. Heugebaert, T. S. A.; Roman, B. I.; Stevens, C. V. *Chem. Soc. Rev*. **2012**, *41*, 5626.